Bioactive Secondary Metabolites from Endophytic and Marine Fungi

Inaugural dissertation

for the attainment of the title of doctor
in the Faculty of Mathematics and Natural Sciences
at the Heinrich Heine University Düsseldorf

presented by

Marian Frank
from Neuss, Germany

Düsseldorf, 01. 2019

From the Institute for Pharmaceutical Biology and Biotechnology at the Heinrich Heine University Düsseldorf

Published by permission of the
Faculty of Mathematics and Natural Sciences at

Heinrich Heine University Düsseldorf

Supervisor: Prof. Dr. Dres. h.c. Peter Proksch
Co-supervisor: Prof. Dr. Matthias U. Kassack

Date of the oral examination: 18.03.2019

Devoted to my grandfather

Karl Frank †2018

and

my wife

Annika Frank

Table of Contents

Abstract

The emergence of therapy-resistant cancer and infectious diseases fuels the demand for novel therapeutic agents. Bioactive compounds from nature have always met that demand or inspired optimized synthetic analogs in the past. Marine derived fungi and other microorganisms are still relatively underexplored concerning their secondary metabolites, when compared to terrestrial microorganisms. The inherit potential of marine derived fungi can further be expanded by unlocking silent biogenetic gene clusters using OSMAC (One Strain Many Compounds) and co-cultivation experiments or by producing semisynthetic analogs. This makes them an invaluable resource for bioprospecting and a worthy target for investigation. This doctoral thesis includes three major projects desribed in manuscript form. The first project deals with the stability, mode of action and structure-activity-relation (SAR) of the mycotoxin phomoxanthone A (PXA), which was isolated from *Phomopsis longicolla*, an endophyte of the Chinese mangroveplant *Sonneratia caseolaris*. The second and third project deal with the investigation of the fungal strains *Penicillium canescens* and *Aspergillus ochraceus* respectively, which were both derived from the inner tissue of the Mediterranean sponges *Agelas oroides*. For those projects, the main work revolved around fermentation with modification of culture parameters (OSMAC, co-culture and feeding experiments) to increase the discovery rate of novel fungal metabolites. The structures of all isolated secondary metabolites were unequivocally elucidated by 1D and 2D NMR (nuclear magnetic resonance) experiments and high resolution electrospray ionisation mass spectrometry (HRESIMS), whereas their stereochemical configurations were elucidated by optical rotation measurements, Marfeys's method or electronic circular dichroism (ECD) calculations.

First Project: Investigation of the mycotoxin phomoxanthone A:

The results of the first project are published and included in **chapters 2** (Phomoxanthone A - From Mangrove Forests to Anticancer Therapy) and to a minor degree in **chapter 3** (The Mycotoxin Phomoxanthone A Disturbs the Form and Function of the Inner Mitochondrial Membrane). The work of Rönsberg *et al.* (Rönsberg *et al.* 2013) was continued to investigate the mode of action of PXA. PXA was produced at multigram scale through solid rice fermentation and ethyl acetate extraction of *P. longicolla* to meet the demand for indepth target finding studies during our cooperation with the working group of Sebastian Wesselborg (Böhler *et al.* 2018). The stability of

PXA in several solvent systems was investigated to explain the activity decline in frozen stock solutions and a rearrangement of PXA to dicerandrol C was discovered (discussed in **chapter 6.5**). A protocol for proper handling of PXA was established and made further mechanistic studies possible. The SAR were investigated by preparation of six semisynthetic derivatives that were tested for their cytotoxic activity against Ramos B- and Jurkat T-lymphocytes. All synthesized compounds were considerably less active than PXA, but the magnitude of activity loss allowed for general SAR predictions. Further SARs were established by extensive bioactivity-data literature comparison of PXA and structurally related compounds.

Second Project: Investigation of the sponge derived fungus *Penicillium canescens*

The results of the second project are ready to be submitted for publication and are included in **chapter 4** (Brominated Azaphilones from the Sponge-Associated Fungus *Penicillium canescens*). The fungus *P. canescens* was isolated from the inner tissue of the Mediterranean sponge *Agelas oroides*. Initial solid rice fermentation showed promising cytotoxic and antitubercular activity of the ethyl acetate (EtOAc) crude extract. Chromatographic investigation of the extract yielded one new chlorinated diphenylether (penicanether) and thirteen known compounds. The majority of isolated compounds were intermediates or byproducts of griseofulvin biosynthesis. Adding 5% sodium bromide (NaBr) to rice medium changed the secondary metabolite pattern and strongly increased the amount of unchlorinated benzophenone intermediates and xanthones, including the previously absent 1,3,5,6 tetrahydroxy-8-methylxanthone. While the amount of griseofulvin sharply decreased and no bromo analogs were detected, two novel brominated azaphilones, bromophilones A and B, were isolated. All new compounds were unequivocally elucidated by 1D and 2D NMR experiments and HRESIMS data. The relative configuration of bromophilones A and B was assigned by nuclear Overhauser effect (NOE) experiments and detailed ^{13}C-chemical shift analysis and literature comparison and they were identified as epimers. Bromophilone B exhibited cytotoxicity against the mouse lymphoma cell line L5178Y (IC$_{50}$ 8.9 µM), as well as against the human ovarian cancer cell line A2780 (IC$_{50}$ 2.7 µM), whereas the epimer bromophilone A was considerably less active.

Third Project: Investigation of the sponge derived fungus *Aspergillus ochraceus*

The results of the third project were submitted to *Marine Drugs* in 12/2018 and are included in **chapter 5** (Cryptic Secondary Metabolites from the Sponge-Associated Fungus *Aspergillus ochraceus*). The fungus *A. ochraceus* was isolated from the inner tissue of the Mediterranean sponge *Agelas oroides*. The initial solid rice fermentation EtOAc extract showed promising cytotoxic and antitubercular activity and an interesting chromatographic profile. The investigation of the large-scale extract yielded sixteen known compounds, which were mainly comprised of ochratoxin A (OTA), penicillic acid (PA) derivatives, tryptophan-derived alkaloids (circumdatins) and polyketide pigments (e.g. viomellein). The accumulation of these metabolites was influenced by addition of several inorganic halide and nitrogen salts. Fermentation on solid beans medium yielded the new diketopiperazine alkaloid waspergillamide B, which features a highly unusual *p*-nitrobenzoic acid subunit. Co-cultivation with *Bacillus subtilis* yielded two new PA-derivatives, ochraspergillic acids A and B, which seem to be of mixed fungal-bacterial biosynthesis. Ochraspergillic acid A was also produced in axenic fungal culture following feeding of tryptophan or anthranilic acid. The structures of new compounds were elucidated based on 1D and 2D NMR experiments as well as from their HRESIMS data. The absolute configuration of waspergillamide B was established by hydrolysis and conversion of the amino acids using Marfey's reagent. The compounds viomellein and ochratoxin B exhibited strong cytotoxicity against the human ovarian carcinoma cell line A2780 with IC_{50} values of 5.0 and 3.0 μM, respectively.

Zusammenfassung

Das Aufkommen therapieresistenter Krebs- und Infektionskrankheiten heizt den Bedarf an neuartigen Arzneistoffen an. Bioaktive Naturstoffe haben in der Vergangenheit diesen Bedarf stets gedeckt oder zur Entwicklung verbesserter, halbsynthetischer Analoga geführt. Marine Pilze und andere Mikroorganismen stellen eine, bezüglich ihrer Sekundärmetaboliten, immer noch relativ unerforschte Gruppe dar, im Vergleich zu an Land lebenden Mikroorganismen. Das den marinen Pilzen innewohnende Potential kann noch erweitert werden, indem schlafende Biosynthese-Gencluster durch den Einsatz von OSMAC- oder Co-Kultivierungsexperimenten induziert werden. Dies macht sie zu einer unverzichtbaren Quelle auf der Suche nach bioaktiven Naturstoffen. Diese Dissertation gliedert sich in drei Hauptprojekte, die in Manuskriptform präsentiert werden. Das erste Projekt befasst sich mit Untersuchungen zur Stabilität, dem Wirkmechanismus und den Struktur-Wirkungs-Beziehungen (SWB) des Mykotoxins Phomoxanthon A (PXA), das aus *Phomopsis longicolla*, einem Endophyten der chinesischen Mangrovenpflanze *Sonneratia caseolaris*, isoliert wurde. Das zweite und dritte Projekt befassen sich jeweils mit einem der beiden Pilze *Penicillium canescens* und *Aspergillus ochraceus*, welche aus dem inneren Gewebe des Mittelmeerschwammes *Agelas oroides* isoliert wurden. Der Schwerpunkt in diesen Projekten liegt darauf Variationen der Fermentationbedingungen zu finden (OSMAC, Co-Kultivierung, Fütterungsversuche). Das Ziel hierbei ist es, die Akkumulation neuer Sekundärmetabolite zu induzieren. Die Strukturen aller isolierten Sekundärmetaboliten wurden durch den Einsatz von ein- und zweidimensionaler Kernspinresonanzspektroskopie (NMR) und Massenspektrometrie (MS) aufgeklärt. Die absolute Konfiguration einiger Substanzen wurde mithilfe von Messungen der optischen Aktivität, Marfey Analyse und elektronischer Circular Dichroismus Berechnungen (ECD) bestimmt.

Erstes Projekt: Untersuchungen zum Mykotoxin Phomoxanthon A

Die Ergebnisse zum ersten Projekt wurden bereits veröffentlicht und umfassen **Kapitel 2** (Phomoxanthon A - Aus dem Mangrovenwald zur Krebstherapie) und in einem geringeren Umfang **Kapitel 3** (Das Mykotoxin Phomoxanthon A stört die Form und Funktion der inneren Mitochondrienmembran). Die Arbeit von Rönsberg *et al.* (Rönsberg *et al.* 2013) wurde fortgeführt um den Wirkmechanismus von PXA zu untersuchen.

Um die Mengenanforderungen an PXA für vertiefende Targetfindungsstudien der kooperierenden Arbeitsgruppe von Sebastian Wesselborg zu decken (Böhler *et al.* 2018), wurde die Substanz durch Ethylacetat (EtOAc) Extraktion der Reismedium-Fermentation des Pilzes *Phomopsis longicolla* im Multigramm-Maßstab produziert. Da die gefrorenen PXA-Stammlösungen über die Zeit einen Aktivitätsverlust zeigten, wurde die Stabilität von PXA in verschiedenen Lösungsmitteln untersucht und eine Umlagerungsreaktion zu Dicerandrol C beobachtet (beschrieben in **Kapitel 6.5**). Es wurde ein Protokoll zur korrekten PXA-Handhabung entwickelt, welches weitere mechanistische Untersuchungen ermöglichte. Die SWB wurden durch die Synthese von sechs halbsynthetischen Derivaten untersucht, indem ihre Zytotoxizität gegenüber Ramos B- und Jurkat T-Lymphozyten ermittelt wurde. Alle hergestellten Substanzen waren weniger aktiv als PXA, allerdings konnten anhand des Umfangs des Aktivitätsverlustes allgemein gültige SWB Aussagen getroffen werden. Weitere SWB wurden ermittelt indem die Bioaktivitäten von PXA und strukturell ähnlichen Substanzen anhand von zahlreichen Literaturquellen miteinander verglichen wurden.

Zweites Projekt: Untersuchung zum schwamm-assoziierten Pilz *Penicillium canescens*

Die Ergebnisse des zweiten Projekts liegen als veröffentlichungsfertiges Manuskript vor und umfassen **Kapitel 4** (Bromierte Azaphilone aus dem schwamm-assoziierten Pilz *Penicillium canescens*). Der Pilz *P. canescens* wurde aus dem inneren Gewebe des Mittelmeerschwammes *Agelas oroides* isoliert. Der EtOAc Extrakt der initialen Fermentation auf festem Reismedium zeigte vielversprechende zytotoxische und anti-Tuberkulose Aktivität. Chromatographische Untersuchungen des Extraktes führten zur Isolierung eines neuen, chlorierten Diphenylether (Penicanether) und von dreizehn bekannten Verbindungen. Die meisten isolierten Verbindungen waren als Zwischenprodukte der Griseofulvin Biosynthese einzuordnen. Das Hinzufügen von 5% NaBr zum Reismedium veränderte das Sekundärmetabolitmuster und führte zu einer starken Akkumulation von nicht-chlorierten Benzophenonen und Xanthonen, einschließlich des zuvor nicht nachgewiesenen 1,3,5,6-Tetrahydroxy-8-methylxanthons. Obwohl die Griseofulvinmenge stark reduziert war und keine Bromo-Analoga des Griseofulvins nachgewiesen wurden, konnten zwei neuartige bromierte Azaphilone (Bromophilone A und B) isoliert werden. Die Strukturen aller neuen Verbindungen wurden durch den Einsatz von 1D und 2D NMR Experimenten und Hochauflösungsmassenspektrometrie (HRMS) eindeutig aufgeklärt und die relativen

Konfigurationen von Bromophilon A und B wurden durch Kern-Overhauser-Effekt (NOE) Experimente und den detaillierten Vergleich der ^{13}C chemischen Verschiebungen mit Literatur bestimmt. Hierbei stellte sich heraus, dass es sich bei Bromophilon A und B um Epimere handelt. Bromophilon B zeigte Zytotoxizität gegenüber der Maus Lymphom Zelllinie L5178Y (IC$_{50}$ 8.9 µM) und der menschlichen Ovarialkarzinom Zelllinie A2780 (IC$_{50}$ 2.7 µM), während das Epimer Bromophilon A deutlich weniger aktiv war.

Drittes Projekt: Untersuchungen zum schwamm-assoziierten Pilz *Aspergillus ochraceus*

Die Ergebnisse des dritten Projektes wurden 12/2018 bei *Marine Drugs* eingereicht und umfassen **Kapitel 5** (Kryptische Sekundärmetaboliten des schwamm-assoziierten Pilzes *Aspergillus ochraceus*). Der Pilz *A. ochraceus* wurde aus dem inneren Gewebe des Mittelmeerschwammes *Agelas oroides* isoliert. Der EtOAc Extrakt der initialen Reismediumsfermentation zeigte vielversprechende zytotoxische und anti-Tuberkulose Aktivität und ein interessantes chromatographisches Profil. Die Untersuchungen des Hauptextraktes führte zur Isolation von sechzehn bekannten Verbindungen, welche sich hauptsächlich aus Ochratoxin A, Penicillinsäure (PS) Derivaten, Tryptophan-basierten Alkaloiden (Circumdatine) und Polyketid Pigmenten (z.B. Viomellein) zusammensetzen. Die Akkumulation dieser Metaboliten ließ sich durch die Zugabe von diversen anorganischen Halogenid- und Stickstoff-Salzen beeinflussen. Eine Fermentation auf Bohnen statt auf Reis führte zur Entdeckung des neuen Diketopiperazin-Alkaloids Waspergillamid B, welches sich durch seinen ungewöhnlichen *p*-Nitrobenzoesäurebaustein auszeichnet. Co-Kultivierung mit *Bacillus subtilis* ergab die zwei neuen PS-Derivate Ochraspergillsäuren A und B, welche augenscheinlich Produkte einer bakteriell-pilzlich gemischten Biosynthese sind. Ochraspergillsäure A wurde ebenfalls in axenischer Pilzkultur produziert, nachdem Tryptophan oder Anthranilsäure zugefüttert wurden. Die Strukturen der neuen Verbindungen wurden durch 1D und 2D NMR Experimente und HRMS aufgeklärt. Die absolute Konfiguration von Waspergillamid B wurde durch Hydrolyse und anschließende Umsetzung der resultierenden Aminosäuren mit Marfey Reagenz ermittelt. Die Verbindungen Viomellein und Ochratoxin B zeigten starke Zytotoxizität gegenüber der menschlichen Ovarialkarzinom Zelllinie A2780 mit IC$_{50}$ Werten von jeweils 5.0 und 3.0 µM.

Chapter 1 - General Introduction

„Die höchste Form der Hoffnung ist die überwundene Verzweiflung.“

-Albert Camus

1.1.1 Microbial fermentation in history and modern times

The word *fermentation* is most commonly understood as the process of microbes growing on nutrient rich media to produce desired small molecules from sugars, such as ethanol in beer and wine production or acetic acid in vinegar or just CO_2 during the baking process. This process includes anaerobic and the more common aerobic processes and is applied to the production of secondary metabolites such as antibiotics (Junker 2000). Long before the discovery of microbes in 1675 by Antonie van Leeuwenhoek (Ralston, Alma Payne, 1900- 1970), humans have utilized microbial fermentation for food and medicinal purposes. The fermentation of sugars by the yeast *Saccharomyces cerevisiae* into ethanol has been utilized for millenia in the production of beer and can be traced back to 3,500–3,100 BC in ancient Iran (Wilkins and Hill 2006) and to 7000 BC ancient China (McGovern *et al.* 2004). Fermentation products were also used for medicinal purposes since ancient times. Red rice is a fermentation product of solid rice and the fungus *Monascus purpureus*, which was found to contain the cholesterol-lowering agent Lovastatin in relevant amounts. It was widely used in East Asia throughout history and was noted for its health benefits in Traditional Chinese Medicine 2,000 years ago (Erdoğrul and Azirak 2004). The use of moulds and their antibacterial properties to treat infections was discovered independently by several cultures throughout history and is well documented. The English herbalist John Parkington recommended mouldy bread for the treatment of wounds in 1640, but the oldest written records of its therapeutic effects are from 1,500 BC ancient Egypt (Wainwright 1989).

Today fermentation is still used for foodproduction processes in the same way; additionally defined compounds such as vitamins (Vandamme 1992) are produced through fermentation for supplementation purposes. A new significant role in drug production must be added. A major part of industrial scale fermentation is used for the production of antibacterial, antiviral, antifungal, anticancer, immunosuppressant, cholesterol lowering and antiparasitic low molecular drugs (Jozala *et al.* 2016; Rahman 2013), while the production of recombinant peptides such as human insulin is

also achieved through microbial fermentation today (Johnson 1983). While most fungal antibiotics are semisynthetic in nature, the fermentation of fungi is extensively used for the production of stereochemicaly complex precursors. Fungal products such as penicillin G and cephalosporin C are the starting materials for modern semisynthetic derivatives and are mass produced using industrial scale fermentations. The antifungal drug griseofulvin is also produced by fungal fermentation (Najafpour 2007). The production of most other antibiotic classes, such as macrolides, aminoglycosides, glycopeptides, bacitracin, polymyxins and the antifungal amphotericin is achieved through bacterial fermentation, mostly of *Streptomyces sp.* (Najafpour 2007), while the production of low molecular weight anticancer drugs through fermentation is not common today. Efforts have been made to produce drugs such as camptothecin (Amna *et al.* 2006) or paclitaxel (Gangadevi and Muthumary 2007) through fermentation of endophytes or paclitaxel through fermentation of recombinant production strains (Biggs *et al.* 2016). As the field of biotechnology advances fast for the production of recombinant proteins (Kunert and Casanova 2013), it is feasible to assume, that stereochemically challenging low molecular weight natural products with identified gene clusters can be produced through the fermentation of recombinant production strains in an industrial scale in the future (Huttanus *et al.* 2016).

1.1.2 Drugs from fungi

The modern age of medicine arguably started with the discovery of antimicrobial drugs such as penicillin in 1928 (Fleming 1929) and griseofulvin in 1939 (Oxford *et al.* 1939). Their discovery opened, for the first time in history, the ability to treat infectious diseases effectively (Aminov 2010). The occurrence of these first antiinfective compounds sparked an increased interest in microbial secondary metabolites. All around the world scientist began to analyze culture broths of fungi and bacteria for new antimicrobial natural products. Since then a steady stream of bacterial and fungal secondary metabolites has regularly entered the drug market and has put forward effective lead structures for semisynthetic or synthetic drugs. While new synthetic compounds started entering the drug market, natural products, being shaped by millions of years of evolutionary arms races, still provide excellent templates for the development of future drugs. While natural product discovery from bacteria (especially *Streptomyces species*) has led to the discovery of a plethora of new classes of antibiotics, such as the aminoglycosides (streptomycin)

in 1940 (Schatz *et al.* 1944), tetracyclin in 1945 (Nelson and Levy 2011), chloramphenicol in 1948 (Aminov 2017), macrolides (erythromycin) in 1949 (Jelić and Antolović 2016), glycopeptides (vancomycin) in 1952 (Anderson *et al.* 1961), rifampicin in 1958 (Sensi *et al.* 1959), carbapenems (thienamycin) in 1976 (Kahan *et al.* 1979) and monobactams in 1985 (Sykes and Bonner 1985), fungal metabolites have produced only two major classes of commonly used antibiotics, the penicillins in 1928 and the cephalosporins in 1948.

Fungal metabolites have also branched out into various other areas of therapy. The ergot alkaloids isolated from *Claviceps purpurea* were discovered in 1918 and their derivatives bromocriptin and pergolide are still relevant in the the treatment of Parkinson's disease today (Montastruc *et al.* 1993). The developement of vitamin K antagonists of the coumarine type was started from the discovery of dicumarol from *Aspergillus fumigatus* (Bye and King 1970), which was initially used as ratpoison, but is used today in the form of the derivatives phenprocoumon and warfarin as a standard therapy for the prevention of cardiavascular bloodclots (Husted *et al.* 2006).
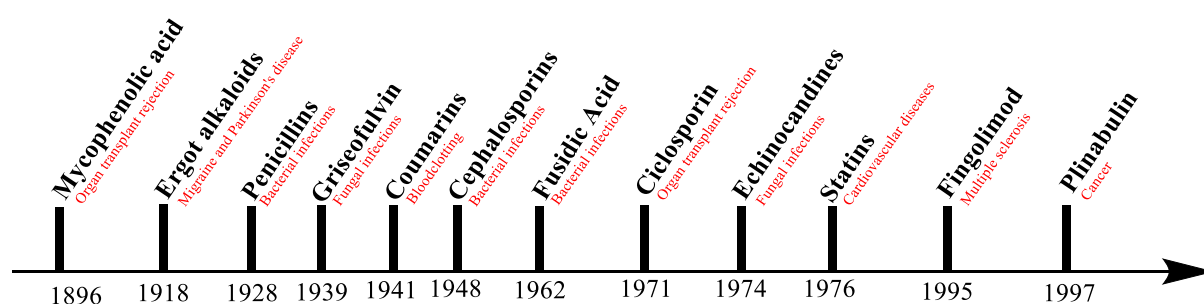
Figure 1: Emergence of new compound classes from fungi (modified after Beekman and Barrow 2014).

The remaining fungal drug classes are antibacterial, antifungal, anticancer, immunosuppressant and antilipemic compounds and are discussed in detail in the following **chapters 1.2.1- 1.2.5**.

1.2.1 Antibacterial agents of fungal origin

Today the majority of antibacterial drugs is derived from natural products. The original compound penicillin G was discovered by Alexander Fleming in 1928 from a strain of *Penicillium notatum*

and was made available for the treatment of bacterial infections by 1941, where it provided a major relief to allied soldiers and battleground infections during World War II. Further development on the field of penicillins made them more suitable through chemical modification of their core 6-aminopenicillanic acid core structure. While the first generation penicillins (the natural products penicillin G and V) were active against gram-positive bacteria, the occurence of betalactamase producing *Staphilococci* called for chemically stabilized derivatives. Second generation penicillins such as oxacillin and methicillin were developed improving the betalactamase stability through steric shielding of the pharmacophor, but they possessed no activity against gram-negative bacteria. The third generation of penicillins (aminoacylpenicillins) improved oral bioavailability and broadened the effectiveness against some gram-negative bacteria (amoxicillin and ampicillin), but lost betalactamase stability. This can be remedied by combination with betalactamase inhibitors such as clavulanic acid (e.g. Augmentin® = amoxicillin + clavulanic acid). The fourth generation of penicillins (ureidopenicillins and carboxypenicillins) continue from the aminoacylbasestructure and further broadens the spectrum by incorporating it into an ureidogroup or replacing it by a carboxygroup. Piperacillin is the penicillin with the broadest activity, which includes *Pseudomonas sp.* and *Enterobacter sp.* (Lobanovska and Pilla 2017). The general mode of action stayed largely the same for all penicillin derivatives: By structurally mimicking the *D*-ala-*D*-ala-terminus of the peptidoglycan, betalactam antibiotics (penicillins, cephalosporins, monobactams and carbapenems) bind to the transpeptidase (PBS = penicillin-binding protein) and irreversible acylate a serine residue in the catalytic binding site. This way the crosslinking of bacterial cell walls is inhibited, resulting in a bactericidal effect on growing bacteria (Yocum *et al.* 1979). Even though numerous resistances have arisen, the penicillins are still one of the most prescribed and essential anbiotic classes today. From 2013 - 2015 penicillins accounted for 50% of the antibiotic prescription in primary care in England (Dolk *et al.* 2018).

The second class of natural product derived betalactams are the cephalosporines, which are derived from cephalosporine C, which was first discovered from the marine fungus *Acremonium chrysogenum* by Giuseppe Brotzu in 1948 (Brotzu 1948). While very similar to the penicillines, cephalosporins are almost exclusively semisynthetic derivatives of the naturally occuring cephalosporine C. Modification of the sidechain leads to a classification systems which currently includes five generations of cephalosporines. First generation cephalosporines are available in oral

or parenteral form, are active primarily against gram-positive bacteria and do not have additional betalactamase stability (e.g. cefalexin). Second generation cephalosporins possess increased betalactamase stability and have some activity against gram-negative bacteria (e.g. cefaclor). Third generation cephalosporines are broadspectrum cephalosporines with a zwitterionic structure to help cross gram-negative cell membranes and a high betalacamase stability (e.g. cefixim). Fourth generation cephalosporines have additional acitivity against *Pseudomonas aeruginosa* (e.g. cefepim) and fifth generation cephalosporines are broad spectrum antibiotics which are specifically designed with increased activity against multiresistant gram-negative bacteria (e.g. ceftaroline (Duplessis and Crum-Cianflone 2011)).
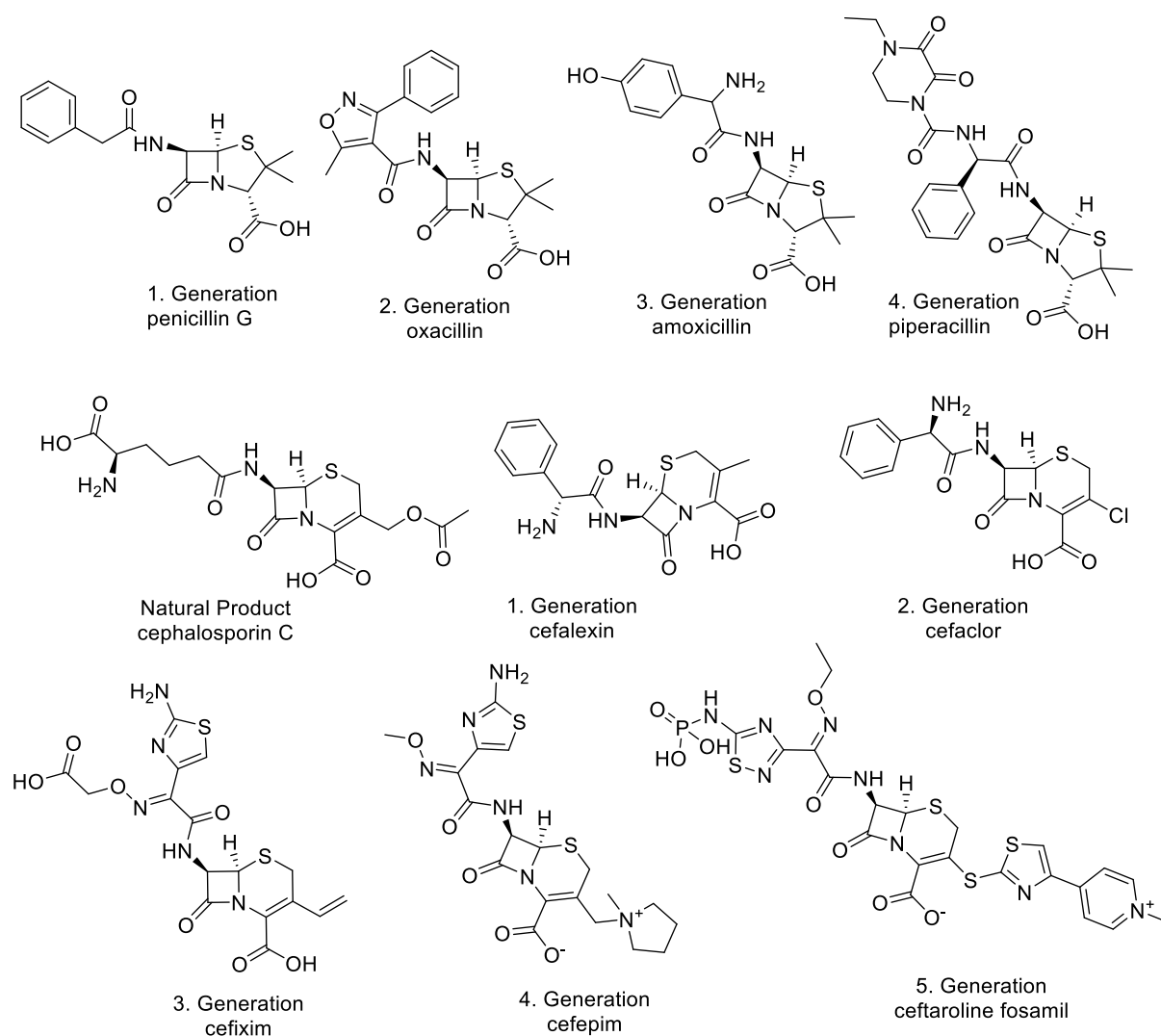
Figure 2: Different generations of betalactam antibiotics.

1.2.2 Antifungal agents of fungal origin

The systematic therapy of fungal infections during history was difficult due to the nonavailability of effective oral drugs and was limited to the topical treatment with weak acids or phenols until the 1940s (Smith 1990). The discovery of griseofulvine from the fungus *Penicillium griseofulvum* in 1939 by Oxford *et al.* (Oxford *et al.* 1939) led to the first orally available antifungal drug against dermatophytes and marked a major breakthrough in antifungal therapy when it was approved in 1959. While the development of antifungal drugs was dominated by the synthetic azole-antimycotics from the 1960s to the 1980s (Maertens 2004), the development has recently shifted towards fungal natural products again, with the discovery of echinocandine antimycotics in 1974 by Benz *et al.* (Nyfeler and Keller-Schierlein 1974). The first echinocandine entering the drug market was caspofungin (Cancidas®) in 2001, which is a derivative of the natural fungal lipopeptide pneumocandin B_0, first isolated from *Glarea lozoyensis* in 1985 (Balkovec *et al.* 2014). Echinocandins block the synthesis of $\beta(1,3)$-D-glucan, by inhibiting the enzyme $\beta(1,3)$-*D*-glucan synthase noncompetetively and thus disrupt the formation of the fungal cell wall (Letscher-Bru 2003). Even though echinocandines are new to antifungal therapy regime, they have proven themselves to be cost effective and equivalent or superiour to established standard therapeutics amphotericin B and fluconazol for invasive mycosis (Patil and Majumdar 2017).

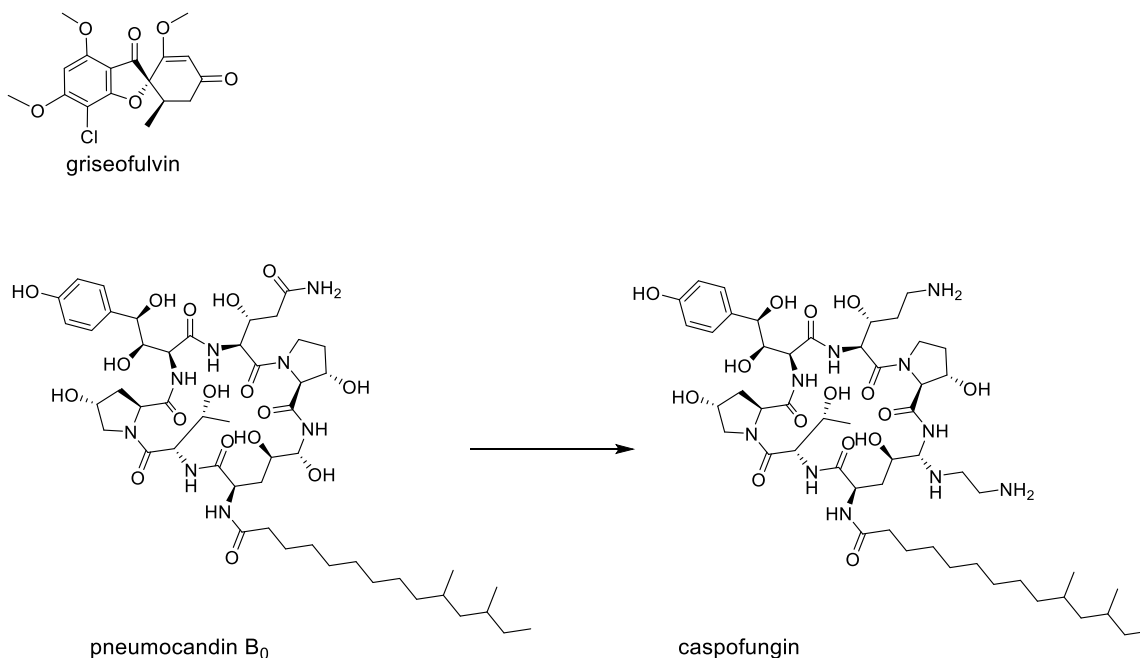griseofulvin

pneumocandin B_0 caspofungin

Figure 3: Antifungal drugs of fungal origin.

1.2.3 Anticancer agents of fungal origin

The importance of natural products for the development of anticancer drugs cannot be understated. From 1930 to 2014 worldwide there were 207 approved small molecule anticancer drugs, of which 160 (77%) were natural products, natural product derived or natural product inspired (Newman and Cragg 2016). While most of these therapeutics are derived from plants or bacteria (especially *Streptomyces sp.*) (Kornienko *et al.* 2015), fungal anticancer metabolites are underrepresented, even though a large number of cytotoxic fungal metabolites has been investigated and are expected to enter clinical trials in the future (Evidente *et al.* 2014; Gomes *et al.* 2015). The first fungal metabolite to become an approved anticancer drug is likely going to be plinabulin. It is currently in clinical trial stage III (ClinicalTrials.gov Identifier: NCT02504489) as a combination therapy with docetaxel for the treatment of non-small cell lung cancer and in clinical stage II (ClinicalTrials.gov Identifier: NCT02846792) in combination with the immune checkpoint inhibitor nivolumab for recurrent or metastatic non-small cell lung cancer. Plinabulin (Singh *et al.* 2011) is a structurally optimized synthetic analog of the fungal metabolite (-)-phenylahistin (Yamazaki *et al.* 2012), which was isolated from the marine fungus *Aspergillus ustus* by Kanoh *et al* in 1997 (Kanoh *et al.* 1997). Plinabulin acts as a tubuline inhibitor during cell division by binding to the colchicine-binding site (Kanoh *et al.* 1997) and additionally inhibits tumor vascularization (Singh *et al.* 2011), while simultaneously decreasing the severity of docetaxel-related neutropeny through activation of dendritic cell maturation (Blayney *et al.* 2016). Other relevant examples of fungal anticancer drugs include paclitaxel (Taxol[®]) and vinblastine (Velbe[®]), which while they were originally isolated from the plants *Taxus brevifolia* and *Catharanthus roseus*, were also discovered as secondary metabolites of their respective endophytic fungi *Taxomyces andreanae (Stierle et al. 1993)* and *Alternaria sp. (Guo et al. 1998)*. Paclitaxel stabilizes microtubuli by binding to a unique bindig site, which inhibits their depolymerization and leads to G2/M phase cell cycle arrest (Horwitz 1994). Vinblastine also binds to a binding site on tubuline, but instead leads to its depolymerization and cell cycle arrest (Cormier *et al.* 2010; Wilson *et al.* 1975). These examples clarify the importance of research in the area of fungal anticancer drugs.
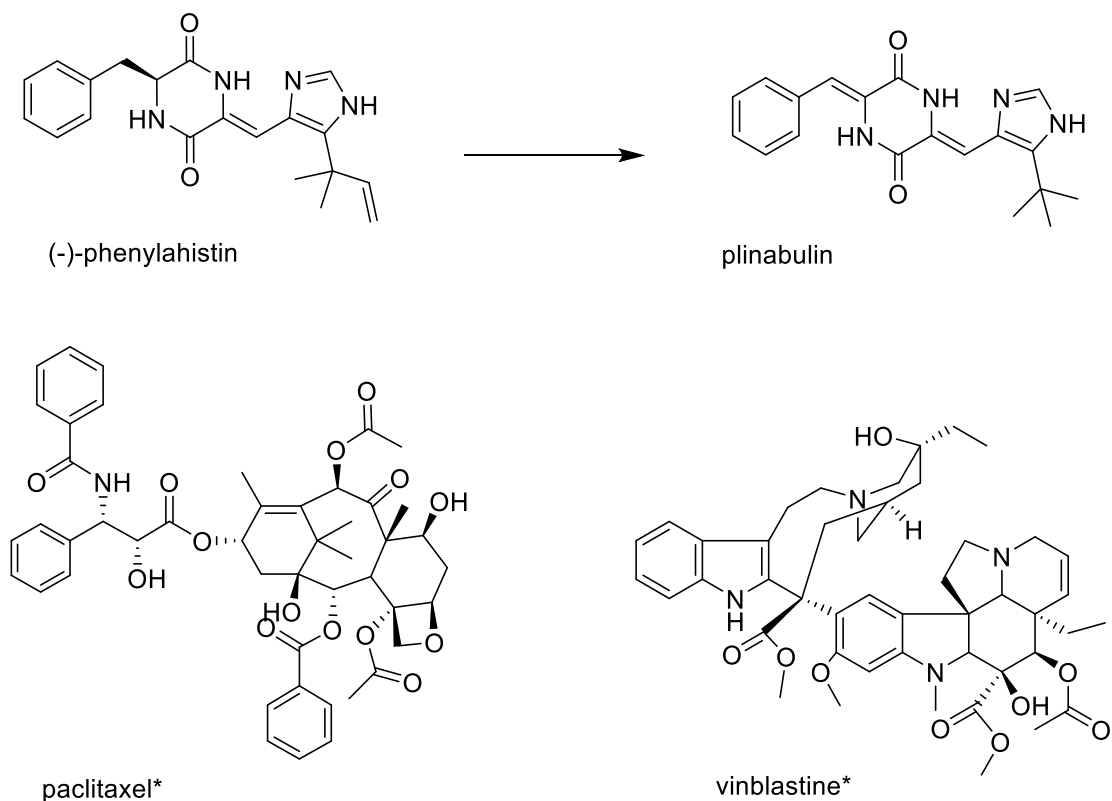
(-)-phenylahistin   plinabulin

paclitaxel*   vinblastine*

Figure 4. Anticancer drugs of fungal origin and *suspected fungal origin.

1.2.4 Antilipemic agents of fungal origin

When the lipidhypothesis was formed in 1976 (Ahrens 1976), high blood levels of low-density lipopreotein cholesterol (LDL) were linked to an increased risk of fatal cardiovascular diseases. During this time, the therapeutic measures were limited to low compliance drugs such as bile sequestrants, which only showed minor improvements to the LDL levels. Ischaemic heart disease and stroke were the global top two causes of human death in 2016 (WHO statistic). One of the five major risk factors for these diseases is LDL-cholesterol, which can be significantly reduced using statins (Law *et al.* 2003). The first discovered statin was mevastatin, which is a fungal natural product, initially isolated from a culturing broth of *Penicillium citrinum* and recognized for its cholesterol-lowering potential by Akira Endo in 1976 (Endo *et al.* 1976). The first statin entering the market in 1987 was lovastatin (Mevacor®), which was isolated from *Aspergillus terreus* in 1978 by Alberts *et al.* (Alberts *et al.* 1980). Statins competitively inhibit the key-enzyme 3-hydroxy-3-methylglutaryl coenzyme A (HMG-CoA) reductase in nanomolar concentrations (Stancu and Sima 2001), blocking the mammalian cholesterol *de-novo* synthesis at an early stage and leaving the

degradable HMG-CoA as a non-accumulating, non-toxic waste product (Tobert 2003). The relative deficite of cholesterol in the hepatocytes leads to the activation of a protease, which slices sterol regulatory element binding proteins (SREBPs) from the endoplasmatic reticulum. The SREBPs then translocate into the nucleus and increase the transcription rate of their respective responsive elements, including the upregulation of LDL-receptors. Hepatic LDL receptors reduce the level of circulating blood LDL-cholesterol and risk of ischaemic heart disease and stroke in the process (Castilla-Guerra *et al.* 2016; Law *et al.* 2003; Stancu and Sima 2001). After the initial success of lovastatin, the two more potent drugs simvastatin (semisynthetic) and pravastatin (biotransformation) were derived from lovastatin and mevastatin respectively and are still in wide use today. When it was discovered, that the chiral lactone ring was merely a prodrug and would be hydrolyzed into its active acid form *in vivo* and the bicyclic core was not crucial to the target binding, new ways to design statins with more desirable traits were opened up. Since then fluvastatin (1994), atorvastatin (1997) and rosuvastatin (2003) were developed as synthetic analogs of the naturally occurring statins. Cerivastatin, which was developed in 1998, was withdrawn from the market after a high number of fatal adverse side effects were reported, which occurred when the drug was administered in combination with gemfibrozil (Tobert 2003). The synthetic statins have similar efficacy as the natural products but improved pharmacokinetic effects. Examples include cytochrome P450 3A4 (CYP3A4) independent metabolism in the case of fluvastatin and pravastatin, resulting in a more predictable pattern of adverse side effects or a much longer half life time in the case of atorvastatin, resulting in a smoother time-plasma concentration and a more cost effective dose regime (Chong *et al.* 2001).
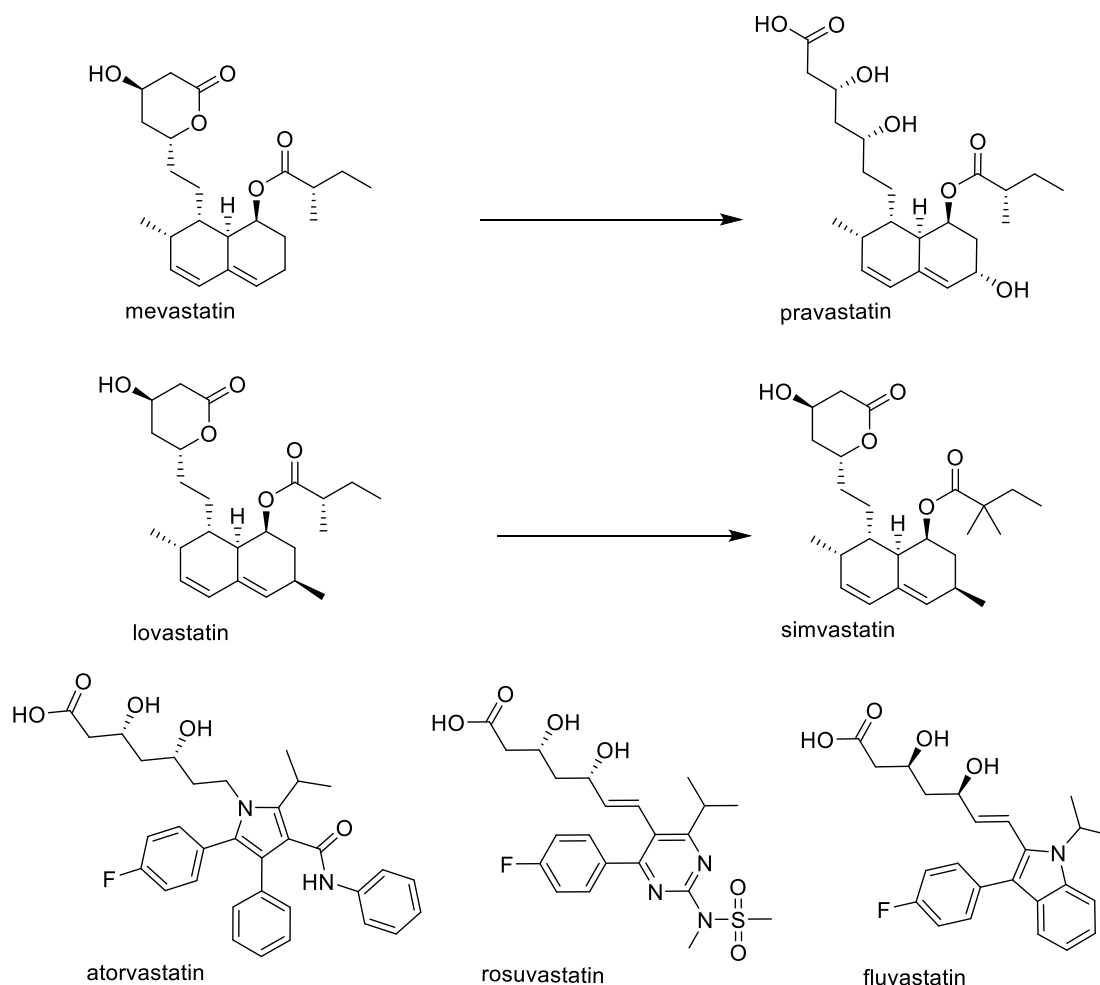
Figure 5: Naturally occuring, semisynthetic and synthetic statins currently on the drug market.

1.2.5 Immunosuppressant agents of fungal origin

Today there are several drugs on the market for the treatment of autoimmune diseases or the prevention of organ transplant rejection. This is a major area for fungal secondary metabolites. Mycophenolic acid was discovered from .the fungus *Penicillium brevicompactum* (originally *P. glaucum*) in 1893 by Bartolomeo Gosio (Gosio 1893) during his investigation of the disease pellagra. It was first recognized for its ability to fight anthrax, but was also recognized for its antifungal, antiviral and immunosuppresant properties, and was used in the 1970s to treat severe cases of psoriasis (Silverman Kitchin *et al.* 1997). In 1998, the semisynthetic prodrug mycophenolate mofetil (Cellcept®) was approved by the US Food and Drug Administration (FDA) for the treatment of organ-transplant patients to prevent organ rejection. Mycophenolate inhibits

the inosine monophosphate dehydrogenase and thereby blocks the *de novo* synthesis of guanosine nucleotides, leading to a decline of activated T-cells and reduced rate and a reduction in lymphocyte recrutement alongside the graft area of organ transplants (Allison and Eugui 2000). Ciclosporin A (CsA) is an immunosuppresant cyclic undecapeptide, which was first isolated from the Norwegian soil fungus *Tolypocladium inflatum* (misidentified as *Trichoderma polysporum*) in 1976 by Dreyfuss *et al.* (Dreyfuss *et al.* 1976). CsA is a highly selective inhibitor of T-cell activation that forms a complex with cyclophilin and thus inhibits the phosphatatse calcineurin as well as the dephosphorylation of NF-AT (nuclear factor of activated T-cells). The transcription factor is thus unable to translocate into the nucleus in its phosphorylated form and thus cannot activate the expression of related responsive elements such as nuclear factor kappa-light-chain-enhancer of activated B cells (NFκB). This leads to a decrease in interleukine 2 etc., which keeps the T-cells inactive (Matsuda and Koyasu 2000). CsA (Sandimmune®) was approved by the FDA in 1983 for the prevention of organ-transplant rejection. Another important immunosuppressant drug is fingolimod (Gilenya®), which was synthesized based on the fungal natural product myriocin (Adachi and Chiba 2007), first isolated from the entomopathogenic fungus *Isaria sinclairii* by Fujita *et. al.* (Fujita *et al.* 1994), which by itself was reported to be 10-100 times more immunosuppressant than CsA. Fingolimod was approved by the FDA in 2010 for the treatment of adult humans with relapsing multiple sclerosis (MS) and in May 2018 for the treatment of children (>10 years of age) with the same indication. Fingolimod decreases the increased activity of the immune system by interfering with the sphingosine-1-phosphat (S1P) pathway. Orally taken fingolimod is phophorylated to fingolimodphosphat and binds with high affinity to several S1P receptors, which are expressed on the cell membrane of numerous immune cells. After initial activation of $S1P_1$-receptor, the receptor is downregulated, which leads to a reduced autoaggresive lymphocyte infiltration (Chun and Hartung 2010).
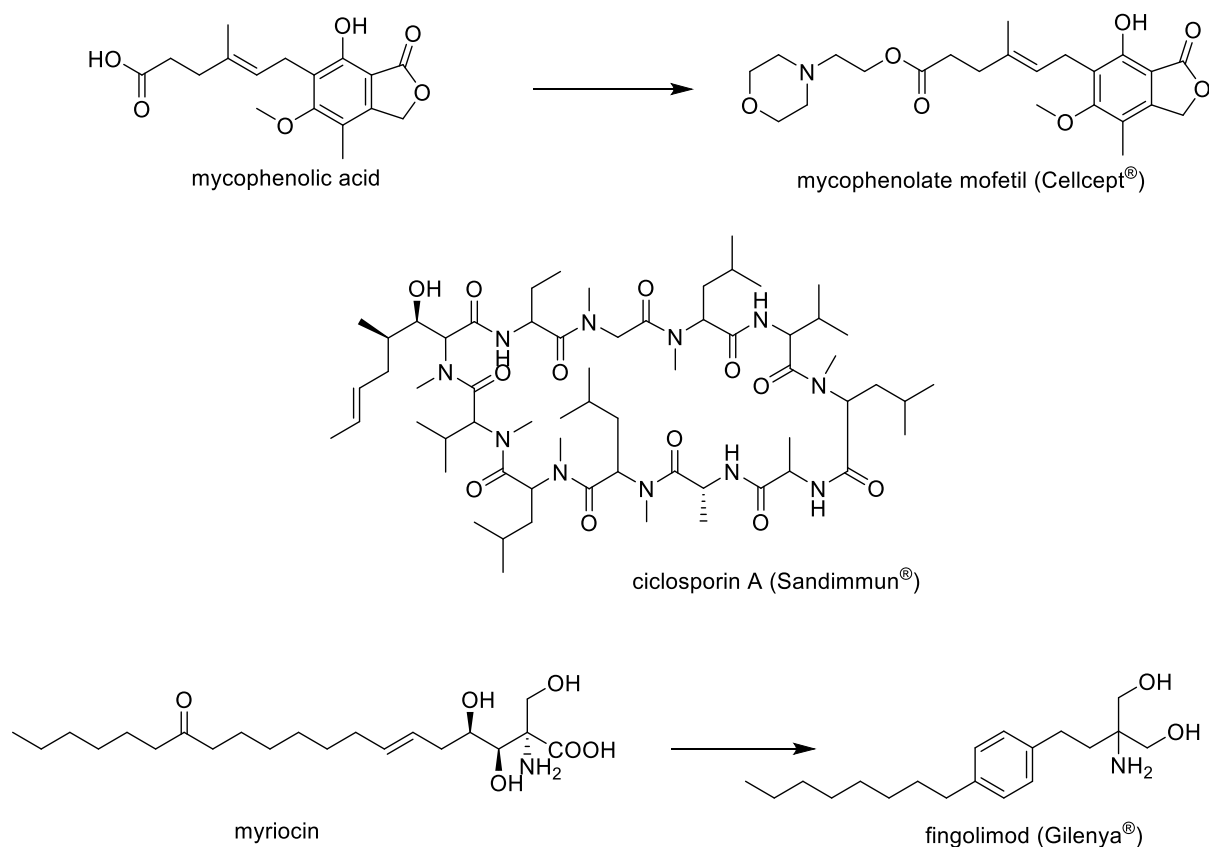
Figure 6. Immunosuppressant drugs of fungal origin.

1.3.1 Modern natural product discovery

As discussed in **Chapter 1.2**, the most prolific age of natural product discovery and drug approvement was in the middle of the 20th century (1950-1970) (Patridge *et al.* 2016). Since bioactive natural compounds can be extremely complex with regard to their stereochemistry, they are sometimes undesirable for chemical synthesis and thus must be obtained by other means, such as fermentation or aquaculture of aquatic (marine) organisms. Sometimes the pharmacophore can be reduced to a smaller but better manageable unit and be chemically synthesized, as shown for erybulin (Halaven®), an anticancer drug derived from the structurally complex sponge compound halichondrin B (Dabydeen *et al.* 2006). As such, natural products are important for finding lead compounds and should not be underestimated or brushed aside. Taking semisynthetic compounds that have been derived from natural products and natural products into consideration, 63% of all compounds approved by the FDA between 1981 and 2006 have a natural product origin (Barreiro *et al.* 2012; Newman and Cragg 2007). Today one of the most important aspects of natural product

discovery is the formation of compound libraries for bioactivity screening processes either *in vitro* (Bugni *et al.* 2008) or *in silico* (Gu *et al.* 2013) to discover new lead compounds. Organisms spend resources and energy to produce secondary metabolites, as they are not waste products, but usually provide an ecological benefit, e.g. for chemical defense, to the producer. Due to their higher structural diversity, natural product libraries have inherently higher hit rates in high throughput screenings compared to purely combinatorial chemistry libraries (Lahlou 2013) and should not be underestimated. Many pharmaceutical companies have reduced their efforts in natural product discovery during the late 20th century, which has resulted in a decline of FDA approved natural products in the last two decades (Patridge *et al.* 2016). Despite of this, natural product discovery has reached a resurgence in recent years with the Nobel price awarded in medicine in 2015 for the discovery of the antihelmintic avermectins and the antimalaria drug artemisinin (Shen 2015). Even though natural product research has been pushed into the backround by large-scale combinatorial chemistry screening, the number of drugs of natural origin entering the market between 1981 and 2014 is still staggeringly high in certain subgroups. For example, the small molecule anticancer drugs or antibacterial drugs that are natural products, natural product derived or inspired by natural products still make up 83 % and 73% respectively of total FDA approved drugs (Newman and Cragg 2016). Considering all this, there seems to be a discrepancy between the perceived usefulness of natural product research in the industry and the actual success rate during drug discovery.

1.3.2 Natural product discovery from marine fungi

Marine organisms have proven themselves as prominent producers of novel bioactive compounds in the history of drug discovery. Marine sponges, tunicates, slugs, snails, fish, sea hares, algae, soft coral, bryozoans, ascidians, fungi and bacteria have already led to the development of drugs that have entered the market or clinical trials (Martins *et al.* 2014). In the last few years, marine fungi have proven themselves a fruitful source of new natural products leading to the development of the first strictly fungal anticancer drug plinabulin (covered in **chapter 1.2.3**). Marine fungi are not defined by their taxonomy, but rather from their isolation source, because their metabolism can vary greatly in dependance of their original habitat. Until 2011, most fungal strains were isolated as symbionts of mangroves (16%), algae (21%) or sponges (19%) as these host organisms seem to

yield the most complex microbial communities (Rateb and Ebel 2011). Regarding the total number of reported new marine natural products, marine fungi provide 328 of 1,277 new compounds in 2016 and 369 of 1,340 new compounds published in 2015. Mangrove associated fungi provided 142 of 1,277 new compounds in 2016 and 126 of 1340 new compounds in 2015 (Blunt *et al.* 2018). These findings indicate that marine fungi are important organisms for natural product bioprospecting.

1.3.3 Sponge-derived fungi

Marine sponges are filter feeding sessile animals that consist of soft tissue encasing a spicule-based sceleton. While all macroogranisms live in symbiosis with microorganisms, sponges are a special case, because up to 40% of their body mass is made up by associated microorgansims. Sponges have proven themselves as prolific producers of bioactive metabolites that have entered the drug market over the last few decades. Examples are the anticancer drugs cytarabin (Cytosar-U®), an analog of spongothymidin, isolated in 1950 from the Carribean sea sponge *Crypotothetia crypta (Bergmann and Feeney 1950)* and eribulin (Halaven®), an analog of halichondrin B, isolated in 1986 from *Halichondria okadai* (Hirata and Uemura 1986). While the discovery of bioactive compounds with unprecendeted core structures from sponges is continuing until today (Ancheeva *et al.* 2017), the production of sponge metabolites proves to be problematic, because laboratory cultivation of sponges usually proves to be difficult and the optimal conditions for secondary metabolite production are difficult to imitate in aquaculture (Osinga *et al.* 1999). Luckily, a great number of symbiotic microbes can be isolated from sponge tissue, which when cultivated under laboratory conditions can produce metabolites with potent bioactivites (Proksch *et al.* 2008). Examples for bioactive secondary metabolites from sponge associated fungi from recent years include the cytotoxic compound isopropylchaetominine (Özkaya *et al.* 2018) from *Aspergillus carneus*, the cytotoxic metabolite cyclohexapeptide similanamide from *Aspergillus similanensis* (Prompanya *et al.* 2015) and the antioxidant compound angupyrone A from *Truncatella angustata* (Zhao *et al.* 2017). Sponge associated fungi seem to be a promising resource, which is relatively easy to handle (compared to macroorganisms) with regard to the discovery of bioactive secondary metabolites.
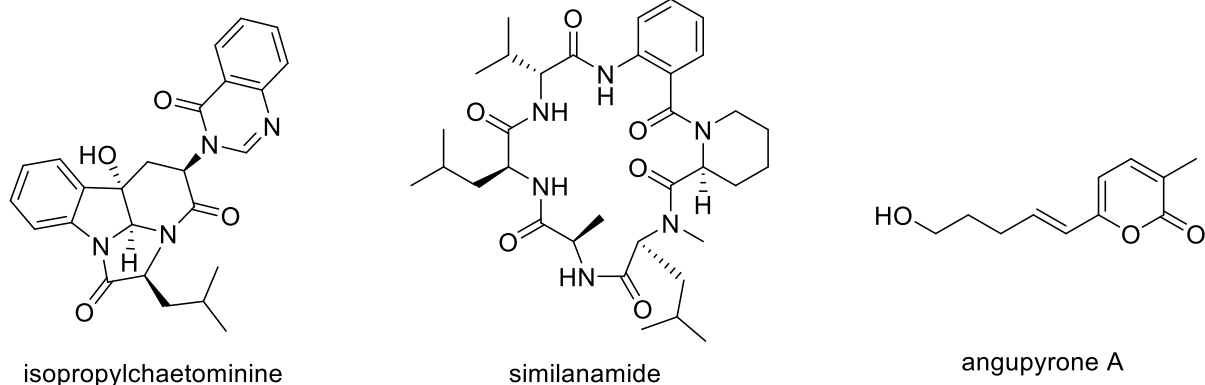
| isopropylchaetominine | similanamide | angupyrone A |

Figure 7: Recently discovered bioactive secondary metabolites from sponge associated fungi.

1.3.4 Mangrove endophytes

Endophytes are microorganisms that live inside the tissue of hostplants without causing any apparent harm to the healthy plant, but the relationship can vary from mutualism to parasitism (Hardoim *et al.* 2015). Almost every plant that has been investigated so far hosts endophytes (Stone *et al.* 2000) and the close intertwinement of plant and endophyte is mirrored in their secondary metabolism. Many endophytic fungi have been found to produce plant growth promoting phytohormons such as indol-3-acetic acid (Zhang *et al.* 2006) or antimicrobial agents (Ratnaweera *et al.* 2015) under laboratory conditions, suggesting an evolutionary symbiotic relationship in which the plant supplies water, nutrients and shelter and the fungi increases the plants overall growth speed and resistance to pathogens. These claims are supported be studies showing that mangrove endophytes can be transferred to different plant species to increase seedling growth under laboratory conditions (Deivanai *et al.* 2014). Mangroves are extremophilic plants, which grow in tropical and subtropical environments in brackish water with a high salinity, high UV-light exposure, tidal draught and floods and low oxygen environments. These challenges are partially overcome by the development of special plant organs such as saltexcreting glands and long, aerial oxygenabsorbing roots (Tomlinson 2016). It is also believed that some metabolic challenges are overcome by the symbiotic relationship of mangroves with special endophytes that are also adapted to the extreme environment (Chávez *et al.* 2015). Endophytic fungi from mangroves are also subjected to these harsh enviromental conditions and can be seen as extremophiles as well. They have been shown to produce diverse bioactive secondary metabolites and are still underexplored because of the limited access that laboratories around the world have to them and because fungal

endophyte communities are complex, plant- and tissue specific (Li *et al.* 2016). Relevant examples for bioactive secondary metabolites from mangrove endophytes include the immune stimulating, antineoplastic phomoxanthone A from *Phomopsis longicolla* (Rönsberg *et al.* 2013), the α-glucosidase inhibtor aspergifuranone from *Aspergillus sp.* 16-5B (Liu *et al.* 2015) and the antineoplastic autophagy inhibitor daldinone I from *Annulohypoxylon sp.* (Liu *et al.* 2017b). Mangrove endophytes have proven themselves as a rich resource for bioactive secondary metabolites and are still heavily underexplored and worthy of further investigation.
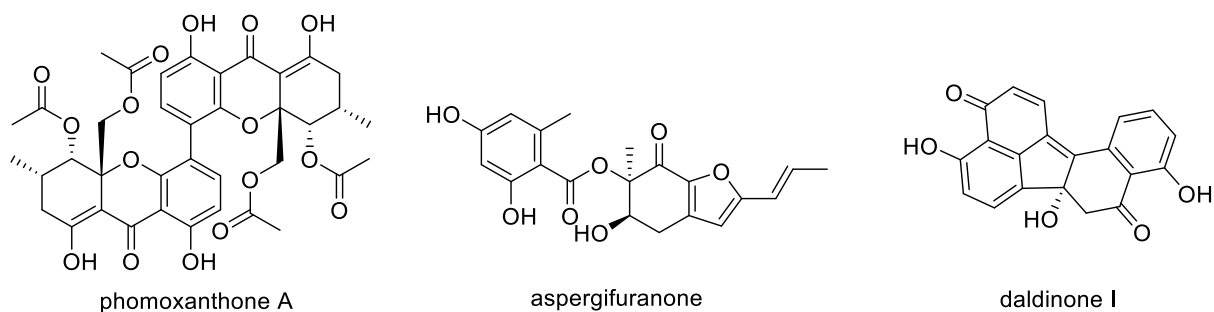

phomoxanthone A   aspergifuranone   daldinone I

Figure 8: Recently discovered bioactive secondary metabolites from fungal mangrove endophytes

1.3.5 Activation of silent gene clusters

The classical approach of natural product discovery in fungi is severely limited by the silencing of biogenetic genes under standard laboratory conditions. Full genome and transcriptome analysis have discovered many inactive gene clusters which house the potential for a multitude of additional fungal natural products, should these gene clusters be unlocked (Wang *et al.* 2015). As an example of highly regulated genes, the polyketide synthase (PKS) genes has been investigated extensively (Bergmann *et al.* 2010; Schroeckh *et al.* 2009; Zabala *et al.* 2012). Several strategies have been developed in the last few years, to trigger a metabolic response in fungi, in order to increase the yield of or induce new secondary metabolites. These methods include OSMAC (One strain many compounds), co-cultivation and the use of epigenetic modifiers. All three strategies have their merits and will be discussed briefly.
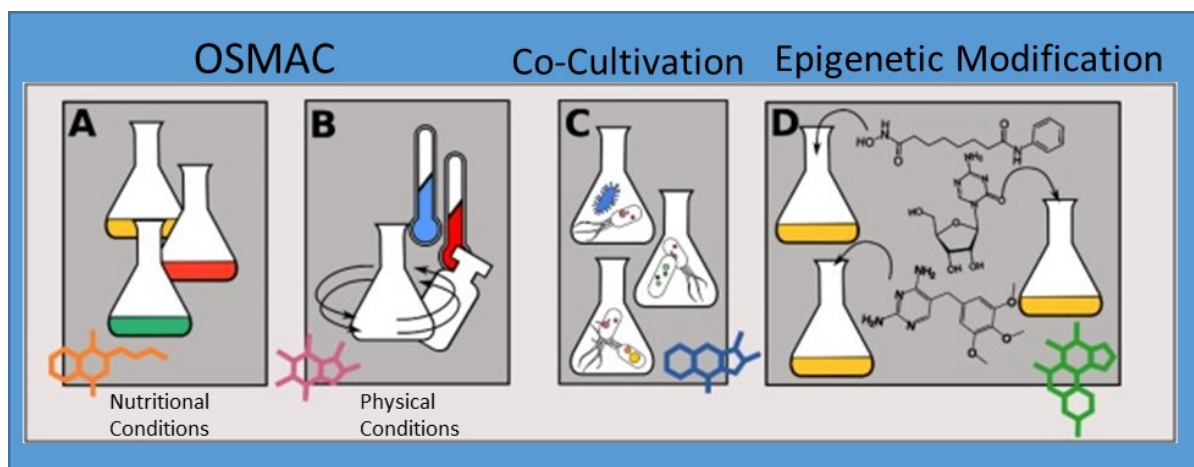
Figure 9: Approaches of unlocking silent gene clusters (modified after Romano *et al.* 2018).

OSMAC

The OSMAC approach employs axenic cultivation of fungal strains under varying nutritional or physical culturing conditions to invoke a metabolic response. The OSMAC approach is empirical in nature and as such a vast amount of experiments have been performed that yielded metabolic responses. Examples for nutritional factors include the type of carbon and nitrogen sources. Changing from solid rice medium to Czapek medium (Wang *et al.* 2013), or solid beans medium (El-Neketi *et al.* 2013) can have profound effects on the secondary metabolite pattern. Furthermore, the addition of trace elements, inorganic salts (Wang *et al.* 2018; Wijesekera *et al.* 2017) and sugars (Zain *et al.* 2011) and feeding experiments with precursor molecules such as amino acids (Wang *et al.* 2011a) have all proven to be effective in enhancing the secondary metabolite patterns of fungal cultures. Physical parameters influence the metabolite patterns as well. Parameters such as high salt stress (Wang *et al.* 2011b), different cultivation temperature (Hussain *et al.* 2017), light conditions (Fanelli *et al.* 2017), shape of the culturing vessel and aeration (Bode *et al.* 2002) all have been shown to influence the secondary metabolite patterns. The OSMAC approach is effective in stimulating the synthesis of new metabolites, but it is inherently empirical and as such can be impractical due to its unpredictability when figuring out obscure culturing strategies (Zhang *et al.* 2017).

Co-cultivation

The interactions of fungi and bacteria in a mixed biofilm are numerous and range between growth support, metabolite exchange, antibiosis, influence of chemotaxis and genetic exchange (Frey-Klett *et al.* 2011). The co-cultivation of two or more different microorganisms aims to mimic a natural environment for microbes in which they compete for space and resources and ideally enhance the production of cryptic bioactive compounds through interspecies crosstalk (Netzker *et al.* 2015). Though the mechanisms of induction are until today not fully understood, studies with *Aspergillus nidulans* have shown that the contact between fungal cells and the bacterial cell wall is a determining factor in order to induce the transcription of PKS gene clusters, such as orsA and increase the accumulation of secondary metabolites (Schroeckh *et al.* 2009). These silent fungal genes are locked through the process of chromatin modelling under the recruitment of histone-deacetylases (HDACs) (Bok *et al.* 2009) and can be unlocked by the recruitment of histone-acetyltransferases (HATs), such as Saga/Ada. Experiments with *A. nidulans* and *Streptomyces sp.* demonstrated that the bacteria were able to activate the fungal chromatine modelling systems through direct contact and significantly increased the transcription of orsA and polyketide metabolites (Nützmann *et al.* 2011). These effects can be observed even with dead bacteria, as long as the direct contact of fungal and bacterial cells is established (Ancheeva *et al.* 2018; Oh *et al.* 2005). Another byproduct of co-cultivation is the potential for fungal-bacterial biotransformation products. *Bacillus subtilis* has been reported to produce anthranilic acid (Cooper *et al.* 1995), which can be incorporated into the fungal metabolism during co-cultivation to yield hybrid metabolites such as *N*-(carboxymethyl)anthranilic acid (Ola *et al.* 2013), expanding the possibilites for natural product discovery even more. Co-cultivation is a powerful tool, which can be used to increase the discovery rate of new natural products or increase the accumulation of constitute natural products (Marmann *et al.* 2014)

Chromatin Remodeling by Epigenetic Modifiers

As previously stated, fungi use chromatin modification as a method for silencing unused genes. The principle method which fungal cells use for gene silencing are the histone deacetylation (HDAC) (Nützmann *et al.* 2011) and DNA methylation (DNA-methyltransferase = DNMT) (Jeon *et al.* 2015). Enzyme inhibitors such as the HDAC inhibitor suberoylanilide hydroxamic acid (SAHA, Vorinostat[®]) and the DNMT-inhibitor 5-azacytidin (5AC, Vidaza[®]) can directly influence

both pathways and have both resulted in the isolation of cryptic metabolites from fungi (Okada and Seyedsayamdost 2017). Epigenetic modifiers provide a straightforward approach by directly targeting two major gene-silencing mechanisms and as such are always a good first approach when empirically investigating fungi for cryptic metabolites.

1.4 Aims and significance of the study

As clarified in **chapter 1.2**, fungal metabolites have historically led to the development of numerous drugs for the treatment of various diseases. The emerging resistances of pathogenic microbes and tumors against conventional chemotherapy drastically increased the demand for new lead structures. Fungi have been underutilized for the discovery of anticancer drugs, even though large amounts of compounds have shown promising *in vitro* activity (Evidente *et al.* 2014; Gomes *et al.* 2015; Kharwar *et al.* 2011). The primary aim of this study was to explore fungal metabolites in order to find new lead structures for antibacterial or antineoplastic therapy. To achieve this aim, several endophytic or sponge derived fungal strains were isolated, purified and cultivated on solid rice medium. After initial characterization of the EtOAc extracts, pure secondary metabolites were isolated and identified. To expand the secondary metabolites beyond the standard laboratory patterns, OSMAC and co-cultivation experiments were performed to activate silent biosynthetic gene clusters. Semisynthetic derivatives were produced as well. The molecular structures of new compounds were unequivocally determined by 1D and 2D NMR spectroscopy, mass-spectrometry, optical rotation measurements, Marfey's analysis and ECD calculations. The biological activity of all isolated or synthesized compounds was tested against mouse lymphoma cell line L5178Y and against human ovarian cancer cell line A2780. Significant results include the structures of new natural products and semisynthetic compounds and their cytotoxic activities, regulatory effects on secondary metabolite patterns during OSMAC and co-cultivation experiments, as well as biosynthetic relationships. Structure-activity-relation- and stability-investigations of PXA were performed to enable detailed mode of action studies. The most noticeable results were either published or submitted as manuscripts as shown in **chapters 2-5**.

Chapter 2 - Phomoxanthone A - From Mangrove Forests to Anticancer Therapy

Overall contribution to this publication: 70%, first author, production of phomoxanthone A, synthesis and purification of new derivatives, structure elucidation, interpretation of SAR data and preparation of the manuscript.

2.1 Publication Manuscript

Phomoxanthone A - From Mangrove Forests to Anticancer Therapy

Marian Frank[1], Hendrik Niemann[1], Philip Böhler[2], Björn Stork[2], Sebastian Wesselborg[2], Wenhan Lin[3] and Peter Proksch[1,*]

[1]*Institute of Pharmaceutical Biology and Biotechnology, Heinrich-Heine University, 40225 Duesseldorf, Germany;* [2]*Institute of Molecular Medicine, University Hospital, 40225 Duesseldorf, Germany;* [3]*National Research Laboratories of Natural and Biomimetic Drugs, Peking University, Health Science Center, 100083 Beijing, People's Republic of China*

Abstract: Mangrove associated endophytes are treasure chests for bioprospecting especially in light of the need for new anticancer leads that are necessary to overcome drug resistance of cancer cells. This review highlights the potent anti-tumour compound phomoxanthone A (PXA), which represents a tetrahydroxanthone atropisomer derived from the mangrove-associated fungus *Phomopsis longicolla*. PXA displayed strong anti-tumour activity when tested against a panel of solid (including cisplatin resistant) tumour cell lines or of blood cancer cell lines with IC_{50} values in the submicromolar range whereas it was up to 100 folds less active against peripheral blood mononuclear cells (PBMC) from healthy donors. The anti-tumour activity of PXA was demonstrated to be due to an induction of caspase 3 dependent apoptosis. At the same time PXA was shown to activate immune cells such as murine T-lymphocytes, NK cells and macrophages which might help in fighting resistance during cancer chemotherapy. Structure activity studies that involved several naturally occurring as well as semisynthetic derivatives of PXA indicated the position of the biaryl linkage and the acetyl substituents as structural features that are important for the activity of this natural product.

Keywords: Anticancer therapy, apoptosis, atropisomerism, endophytic fungi, immunostimulation, mangroves, polyketide, tetrahydroxanthone.

1. INTRODUCTION

1.1. Mangrove Forests - A Unique Stress Prone Habitat

Mangroves are swamps of the intertidal zone in (sub)tropical coastal regions that are predominantly colonized by trees [1]. By definition five characteristics determine a *true mangrove tree*: (i) exclusive occurrence in the intertidal zone; (ii) taxonomic isolation from terrestrial relatives (at least to the generic level); (iii) populations composed of individuals with insular stands; (iv) morphological adaptation, e.g. aerial roots or vivipary; and (v) physiological adaptation mechanisms such as salt exclusion, secretion and accumulation [2]. Salt exclusion is established by salt-excreting glands in the leaves, which are indispensable for the

plant as the typical seawater salinity of mangrove habitats ranges from 17.0 - 36.4% [3]. The latter properties affiliate mangrove trees to the group of halophytes. Temperature forms another extreme of the mangrove habitat. Commonly, the average air temperature of the coldest month is found higher than 20 °C with an amplitude of maximum 10 °C [4, 5] whereas temperatures of the warm season may exceed 40 °C. Limitations in oxygen and nutrient supply, a high tidal range alternated with periods of drought and excessively high light exposure are further stress factors that typically confront mangrove trees [6]. In these harsh habitats mangroves play a crucial role in coastal stabilization and nutrient fixation. Additionally, they provide nurseries for juvenile fish [7]. In their warm and moist habitat mangrove plants are confronted with a plethora of invasive microbial plant pathogens. In order to guarantee survival Mangrove plants have evolved highly effective antimicrobial chemical defense mechanisms [3]. It is remarkable that opportunistic plant endophytes such as fungi, which inhabit these plants in often complex

*Address correspondence to this author at the Department of Pharmaceutical Biology and Biotechnology, Faculty of Pharmacy, Heinrich-Heine University, 40225 Duesseldorf, Germany;
Tel: +49-221-81-14173; Fax: +49-221-81-11923;
E-mail: proksch@uni-duesseldorf.de

communities [8], withstand this effective chemical barrier. Structurally diverse defense metabolites apparently have yielded a selection of unique endophytes that have evolved effective escape mechanisms against the plants' chemical defense. On the other hand it may be assumed that endophytes contribute to the ecological success of Mangrove plants as frequently shown for other plant-endophyte associations [9-11]. The highly active and diverse microbial communities living in association with the host plant [8] which have been shaped by co-evolution strongly contribute to the evolutionary success of mangrove trees, which is essential for their survival in this extreme habitat. Both, Mangrove plants and their associated endophytes represent treasure chests for bioprospecting due to the occurrence of structurally unusual bioactive metabolites [12-14].

1.2. Chemistry of the Mangrove Microbiome

Mangrove associated endophytes are highly diverse and include actinomycetes, bacteria, fungi, cyanobacteria, microalgae and protozoa [8]. Among these different phylogenetic groups bacteria and fungi are by far the most abundant phyla contributing approximately 91% of the total microbial biomass known from mangrove trees [15]. Nevertheless recent estimations state that more than 95% of the endophyte community of Mangroves remains unknown [15] leaving a broad spectrum of metabolites and producing endophytes undiscovered for future investigations. Among the above mentioned groups of Mangrove endophytes, fungi are not only the most abundant ones with regard to biomass production, but also with regard to their secondary metabolites that have so far shown the highest hit rate during bioprospecting [16].

Geographical hotspots of Mangrove habitats are found along the coastlines of the Indian, Pacific and Atlantic Oceans [17]. The South China Sea e.g. and in particular the mangrove forests at the coastline of the Chinese Island Hainan represent an exceptional fruitful source for bioprospecting as indicated by the rise of publications devoted to this topic that have appeared in the recent years [18-22]. Investigations of Mangrove derived endophytic fungi from this region have so far yielded numerous active natural products such as cytotoxic terpenoids [20, 23] and peptides [18], antibacterial fatty acid glycosides [19], protein kinase inhibiting decalactones [21] and polyphenols with anti-HCV activities isolated from a mangrove plant [22]. In addition, cytotoxic furanocumarins [24] and naphtopyrones [25] have been found in Mangrove endophytes from this most southern Chinese province. Interest-

ingly, also flavonoids, which are rarely described as fungal secondary metabolites, have been reported from an endophytic *Fusarium* strain [26]. In spite of the various groups of compounds encountered in these endophytes polyketides are by far the most dominant class of natural products. Out of 464 new metabolites reported between January 2011-December 2013 from Mangrove endophytes 258 compounds represent polyketides [8]. A major group of bioactive polyketides from these fungal endophytes are xanthones [27]. Various fungal xanthones have been reported to possess pronounced biological activities including anti-tumour [28-30] activity. Among these compounds phomoxanthone A (PXA) can be pointed out as a putative lead structure for future anticancer therapy due to its potent, rapid and selective activity against tumour cells [31].

2. STRUCTURAL CHARACTERISTICS OF PHOMOXANTHONE A AND RELATED TETRAHYDROXANTHONE DIMERS

PXA is the dominating metabolite of *Phomopsis longicolla* being a fungal endophyte derived from the mangrove plant *Sonneratia caesolaris* (Lythraceae), which typically occurs in the intertidal zones of South China including the island of Hainan [31]. *P. longicolla* was first described in 1985, when Hobbs *et al.* isolated this fungus from soybeans where it is the causative agent of the so-called Phomopsis seed decay that is a major cause for poor-quality soybeen seed [32]. Fungi of the genus *Phomopsis* occur also in other Mangrove plants such as in *Excoecaria agallocha* (Euphorbiaceae), which is likewise typical for the South China Sea coast [33]. Several further reports on the occurrence of PXA in *Phomopsis* sp. from non Mangrove sources include the Costa Rican rain forest plant *Costus* sp. (Costaceae) [34], the teak plant *Tectona grandis* (Lamiaceae) [35] and the tropical plant *Garcinia dulcis* (Clusiaceae) [36]. The taxonomically closely related fungus *Phoma* sp., an endophyte inhabiting the African plant *Aizoon canariense* [37] (Aizoaceae) was likewise reported to accumulate this natural product. Structurally, PXA is a symmetrical atropisomer consisting of two tetrahydroxanthone monomers that are linked via an unsual 4,4'-biaryl linkage, which distinguishes this compound from other closely related natural products such as the dicerandrols, which show a 2,2'-biaryl linkage [8] or the eumitrins, the latter being xanthone dimers from lichens such as *Usnea baileyi*, which feature the biaryl linkage in positions 4,2' [34]. In addition to PXA talaroxanthone, a metabolite isolated from *Talaromyces* sp., an endophyte present in the Amazonian rainforest medicinal plant *Duguetia stelechantha* (An-

nonaceae) also exhibits the unusual 4,4'-biaryl linkage [38] (Fig. **1**). A further structural difference of PXA compared to other tetrahydroxanthone dimers lies in the substitution pattern at positions 10a and 10a' which either carry acetoxymethyl acids (PXA) or methoxycarbonyl groups (eumitrins and talaroxanthone) [35]. In PXA and other related xanthone dimers featured in this report all non-chelated hydroxyl groups are present in the acetylated form [34].

Both structural features, the unusual 4,4'-biaryl linkage as well as the bulky acetyl substituents contribute to a hindered rotation along the biaryl axis, leading to axial chirality of PXA [31, 34]. Interestingly, the methoxycarbonyls in 4,4'-linked talaroxanthone apparently do not lead to atropisomerism as Koolen *et al.* did not report atropisomerism for this PXA relative [38].

Several efforts have been undertaken to elucidate the absolute configuration of PXA. In an initial report on the structure of this intriguing metabolite Isaka *et al.* [35] determined the relative configuration of the six stereogenic centers based on NMR experiments and stated that the absolute configuration of the compound should be either 5*R*, 6*R*, 10a*R*, 5'*R*, 6'*R*, 10a'*R* or 5*S*, 6*S*, 10a*S*, 5'*S*, 6'*S*, 10a'*S*. Later, Elsässer *et al.* [34] reported the absolute configuration of PXA utilizing single-crystal X-ray analysis and comparison of quantum-mechanically calculated and experimentally measured

CD spectra. The CD spectrum of PXA is dominated by the axial chirality of the compound, which enabled the authors to determine it as (*aS*). With the knowledge of the configuration of the biaryl axis, the absolute configurations of the stereogenic centers were determined by X-ray as 5*R*, 6*R*, 10a*R*, 5'*R*, 6'*R*, 10a'*R*. Recently, the absolute configuration of PXA was revised by X-ray analysis as being *aR*, 5*S*, 6*S*, 10a*S*, 5'*S*, 6'*S*, 10a'*S* [31] which is the enantiomer of the original structure proposed by Elsässer *et al.*

Taking into consideration several further structurally closely related polyketide derivatives that are likewise accumulated by *P. longicolla* such as the dicerandrols and a benzophenone intermediate (monodictyphenone) Rönsberg *et al.* proposed a plausible biosynthetic pathway leading to PXA (Scheme **1**). The initial step transforms eight acetate units into an octaketide (C-16 polyketide), a pathway which was discovered for polyphenols through ^{14}C-labelled acetate feeding experiments by Birch *et al.* already back in the 1950s [39]. The enzyme complex which is responsible for this decarboxylating Claisen condensation present in fungal metabolism is well understood today and belongs to the class of polyketide synthases (PKS) [40]. Subsequently this open-chain polyketide undergoes cyclization reactions affording the monomeric anthranoide congener emodin. *Via* oxidative ring-scission
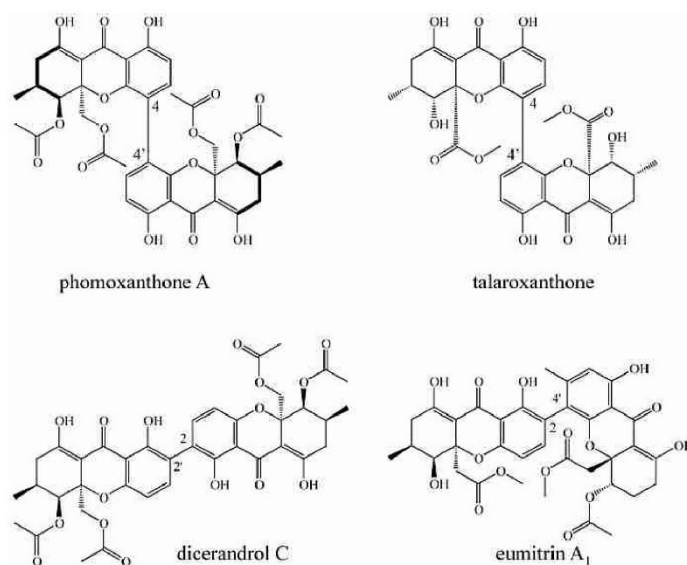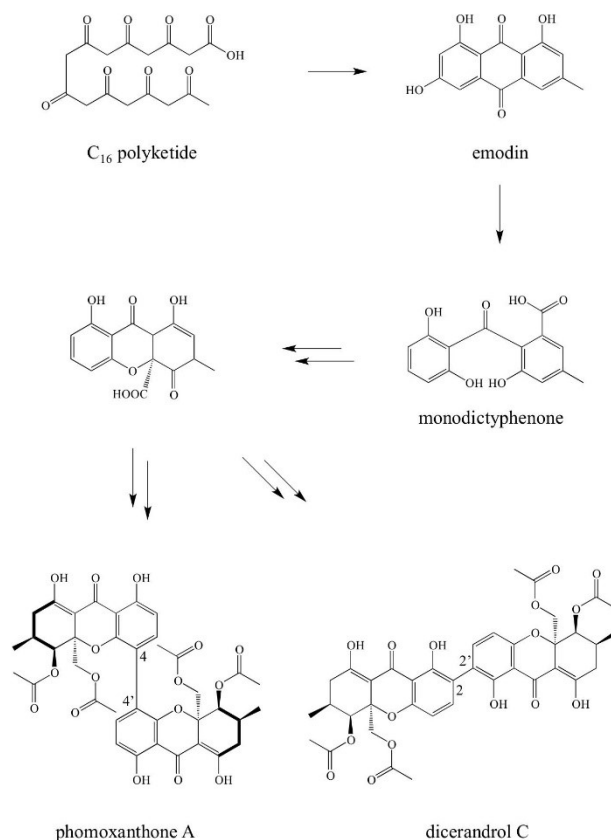

phomoxanthone A

talaroxanthone

dicerandrol C

eumitrin A₁

Fig. (1). Phomoxanthone A and further structurally related tetrahydroxanthone dimers.

C_{16} polyketide

emodin

monodictyphenone

4

4'

phomoxanthone A

2'

2

dicerandrol C

Scheme 1. Putative biosynthetic pathway of polyketides leading to 4,4'-linked phomoxanthone A and 2,2'-linked dicerandrols. Modified from Rönsberg *et al.* [31].

emodin is converted into monodictyphenone, which through subsequent decarboxylative cyclisation leads to the first xanthone indermediate [27]. The exact mechanism of dimerisation of xanthone monomers is so far not fully understood [27]. In this class of compounds linkages are found either as biaryl ether C-O-C linkages or as rotatable or atropisomeric biaryl C-C-bonds [27], the latter being present in PXA. In these dimeric xanthone C-C-bonds between monomers typically occur in positions 2 or 4 of ring A. A putative oxidative dimerisation mechanism proposed by Wezeman *et al.* (2015) postulated the occurrence of a xanthonyl radical that can be formed in either of these two positions by single-electron-transfer. Resonance contributors of the delocalised aryl radical can then couple to a second xanthone moiety that acts as an electron-donor [27]. The fact that identical xanthone monomers, as in the case of PXA and dicerandrol C, condense at different positions strongly suggests an enzymatic dimerisation mechanism, as was recently shown for dimeric fungal coumarins such as the *Aspergillus niger* derived kotanin [41]. In the respective study Girol *et al.* identified the cytochrome P450 monooxygenase KtnC as being responsible for the regio- and stereoselective C-C coupling of coumarin moieties.
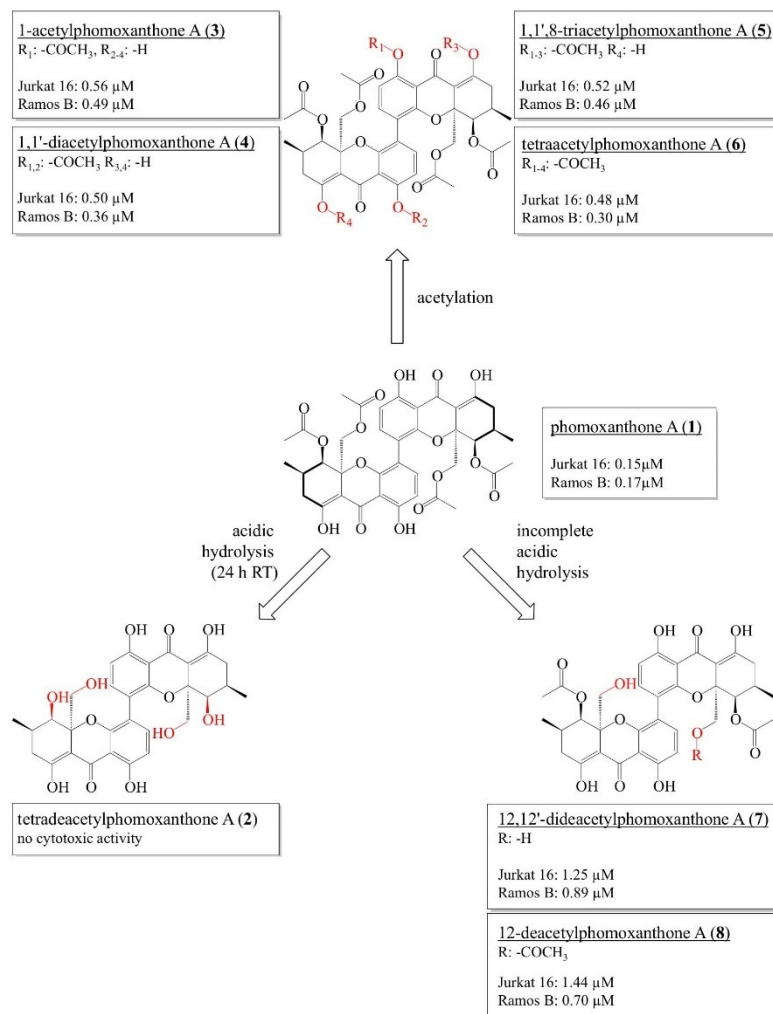
3. ANTI-TUMOUR ACTIVITY OF PXA

A recent report indicated the pronounced anti-tumour activity of phomoxanthone A against a panel of

human and other cancer cell lines. PXA showed for example a remarkable activity against human epidermoid carcinoma KB cells (IC$_{50}$ 1.32 μM), the human breast cancer cell line BC-1 (IC$_{50}$ 0.68 μM), African monkey kidney fibroblast Vero cells (IC$_{50}$ 1.87 μM) [36], and the L5178Y mouse lymphoma cell line (IC$_{50}$ 0.3 μM) [31]. In addition PXA demonstrated strong growth inhibition against several cisplatin-sensitive (sens) and -resistant (CisR) solid tumour cells, e.g. human ovarian carcinoma cells A2780 (IC$_{50}$ sens 0.7 μM; CisR 0.9 μM), human tongue carcinoma cells Cal27 (IC$_{50}$ sens 5.2 μM; CisR 5.6 μM), and human esophagus cells Kyse510 (IC$_{50}$ sens 0.8 μM; CisR 0.8 μM) [31]. Considering the clinical importance of cisplatin as a cytostatic drug in chemotherapy of cancer the fact that cancer cells which have become resistant and do no longer respond to this anti-cancer drug still succumb to PXA is a remarkable finding. Since selectivity of an anti-tumour drug compared to its effect against healthy cells is of utmost importance for potential future use in chemotherapy the selectivity of PXA was investigated against two human cancer cell lines including Jurkat J16 cells (T cell lymphoma) and DG75 cells (Burkitt's lymphoma) as well as against healthy human peripheral blood mononuclear cells (PBMCs). The selectivity index of PXA against the investigated cancer cells *vs.* PBMCs amounted to more than two orders of magnitude, suggesting a highly selective mode of action against cancer cells, which highlights PXA as an interesting candidate for further investigations.

When reporting on PXA for the first time Isaka *et al.* generated a semisynthetic derivative of this natural product through acidic hydrolysis thus generating tetradeacetylphomoxanthone A [35]. The latter proved to be inactive in all biological assays conducted such as cytotoxic [31], antibiotic [34, 35], antimalarial [35] and antifungal [34] assays. The naturally occurring 12-deacetylphomoxanthone A (12-dPXA) that was isolated from *P. longicolla* in addition to PXA was found to be about ten times less active than PXA with regard to growth inhibition of the mouse lymphoma cell line L5178 (PXA: IC$_{50}$ 0.3 μM *vs.* 12-dPXA: IC$_{50}$ 2.8 μM) [31]. This observance led to the hypothesis, that the acetate substituents modulate the anti-tumour activity of PXA. To further investigate the structure activity relationships of PXA and derivatives seven semisynthetic congeners of PXA (**2-8**) were prepared of which five (**3-7**) are new compounds and are described in this review for the first time (Scheme **2**, unpublished data). Acetylated compounds **3-6** were obtained by partial or complete acetylation of PXA, while compound **7** was generated through partial acidic hydrolysis of the par-

ent compound. The anti-tumour activity of the various derivatives was evaluated against Jurkat 16 T lymphocytes and Ramos B lymphocytes. Hydrolysis of all acetate functions lead to a total loss of activity as previously reported for tetradeacetylphomoxanthone A (**2**). When comparing the IC$_{50}$ values of all seven compounds (**2-8**) *vs.* the parent compound PXA (**1**) the latter turned out to be the most active congener. Acetylation of the phenolic and enolic hydroxyl-groups of the PXA core structure was found to decrease the anti-tumour activity even though the resulting derivatives still retained a certain level of activity. There was no clear trend with regard to the activity of the different congeners in relation to the positions of acetate substituents or to the number of free hydroxyl-groups. When comparing the deacetylation products 12-dPXA and 12,12'-dPXA (Jurkat T IC$_{50}$ 1.25-1.44 μM; Ramos B IC$_{50}$ 0.70-0.89 μM) to PXA the loss of activity was stronger than that caused by acetylation (**3-6**) (Jurkat T IC$_{50}$ 0.48-0.56 μM; Ramos B IC$_{50}$ 0.30-0.49 μM). The difference in activity between 12-dPXA (Jurkat T IC$_{50}$ 1.44 μM; Ramos B IC$_{50}$ 0.70 μM) and 12,12'-dPXA was negligible (Jurkat T IC$_{50}$ 1.25 μM; Ramos B IC$_{50}$ 0.89 μM), which lead to the conclusion that the acetyl-moiety at C-12 is not crucial for the anti-tumour activity of PXA. In conclusion, all structural alterations of the hydroxyl or acetyl ester moieties of PXA that were obtained by acetylation or by acidic hydrolysis of the parent compound lead to a decreased anti-tumour activity when compared to PXA. Hydrolysis of the ester moieties at C-12 resulted in a stronger decrease of activity compared to acetylation of free hydroxyl moieties.

The position of the biaryl axis linking the two tetrahydroxanthone monomers seems to be likewise important for the anti-tumour activity. Considering the structural similarity of PXA and dicerandrol C that differ with regard to the position of their biaryl axis the more than three fold higher activity of PXA *vs.* dicerandrol C against murine L5178Y lymphoma cells (PXA: IC$_{50}$ 0.3 μM; dicerandrol C: IC$_{50}$ 1.1 μM) can be clearly linked to the different positions of their biaryl axis (Scheme **3**). Since both compounds induce apoptosis in tumour cells as shown by Rönsberg *et al.* (2013) it is safe to assume that PXA and dicerandrol share a similar mode of action [31]. Hydrolysis of one ester moiety at C-12 of dicerandrol C leads to dicerandrol B, which exhibits a nearly ten-fold weaker cytotoxicity when compared with dicerandrol C against the mouse lymphoma cell line L5178Y (dicerandrol B: IC$_{50}$ 10 μM; dicerandrol C: IC$_{50}$ 1.1 μM) [31]. In contrast, a stronger effect of dicerandrol B in comparison to dicerandrol C

Frank et al.

1-acetylphomoxanthone A (**3**)
R_1: -COCH$_3$, R_{2-4}: -H

Jurkat 16: 0.56 µM
Ramos B: 0.49 µM

1,1'-diacetylphomoxanthone A (**4**)
$R_{1,2}$: -COCH$_3$ $R_{3,4}$: -H

Jurkat 16: 0.50 µM
Ramos B: 0.36 µM

1,1',8-triacetylphomoxanthone A (**5**)
R_{1-3}: -COCH$_3$ R_4: -H

Jurkat 16: 0.52 µM
Ramos B: 0.46 µM

tetraacetylphomoxanthone A (**6**)
R_{1-4}: -COCH$_3$

Jurkat 16: 0.48 µM
Ramos B: 0.30 µM

acetylation

phomoxanthone A (**1**)

Jurkat 16: 0.15µM
Ramos B: 0.17µM

acidic
hydrolysis
(24 h RT)

incomplete
acidic
hydrolysis

tetradeacetylphomoxanthone A (**2**)
no cytotoxic activity

12,12'-dideacetylphomoxanthone A (**7**)
R: -H

Jurkat 16: 1.25 µM
Ramos B: 0.89 µM

12-deacetylphomoxanthone A (**8**)
R: -COCH$_3$

Jurkat 16: 1.44 µM
Ramos B: 0.70 µM

Scheme 2. SAR study on the influence of acetyl substituents on the anti-tumour activity of PXA against Jurkat 16 and Ramos B cells as evident from IC$_{50}$ values after 72 h exposure (unpublished data).

was observed when tested against Dox40, H929, KMS34, L363, MM1S, OCIMY5, OPM2, RPMI8226 myeloma cell lines (IC$_{50}$ 2.2-16.7 µM) [42], making a coherent statement on the influence of acetylation with regard to the cytotoxic potential of dicerandrols difficult. Interestingly, penexanthone B, which is the monomeric building block of PXA and of dicerandrol C alike showed only moderate to negligible activity in

cytotoxicity assays against above mentioned myeloma cells (IC$_{50}$ 11.6-464.2 µM) when compared to considerably active dicerandrol C (IC$_{50}$ 4.8-14.7 µM) [42].

All structure-activity studies on PXA and congeners strongly suggest that the linkage of two xanthone monomers is important for the anti-tumour activity with a 4-4'-biaryl linkage as in PXA being favourable to a 2-2'-biaryl linkage as in the dicerandrols.
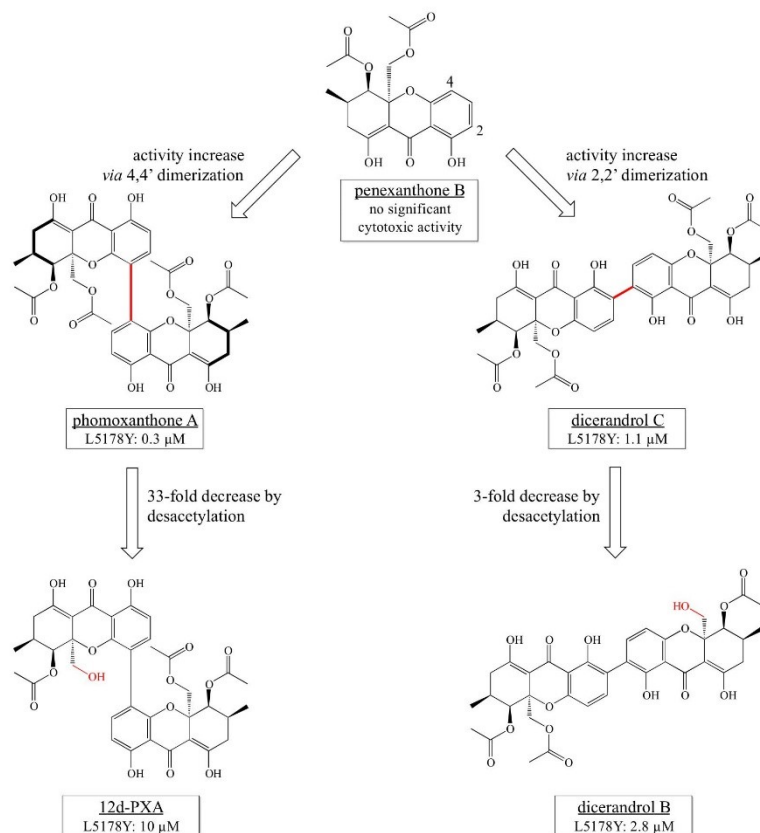
Scheme 3. Comparative SAR on the anti-tumour activity of monomeric penexanthone B against myeloma cells [42] and 4,4'-linked PXA and 2,2'-linked dicerandrols against murine L5178Y lymphoma cells [31] based on the respective IC$_{50}$ values.

However, since only one atropisomer (the *aR* enantiomer) of PXA was isolated so far the influence of atropisomerism on the biological activity of PXA remains unknown. For other atropisomers such as for tetrahydroanthraquinones it was shown earlier that the nature of the biaryl axis has a profound influence on the biological activity as the (*aR*) acetylalterporriol E showed a remarkable activity against the L5178Y lymphoma cell line (IC$_{50}$ 10.4 µM) while (*aS*) acetylalterporriol D exhibited no cytotoxicity [43].

4. INDUCTION OF APOPTOSIS AS A PLAUSIBLE MODE OF ACTION OF PXA

Even though detailed mechanistic studies on the exact molecular target and mode of action of PXA are still underway experimental evidence supports the induction of apoptosis in tumour cells by this natural product. The fragmentation of DNA through activation of caspases after treatment of tumour cells with PXA was used as an indicator for induction of apoptosis, since this effect could be blocked almost completely by addition of a caspase inhibitor (Q-VD-OPh). In addition to PXA, 12-dPXA and dicerandrol C significantly increased the number of apoptotic Jurkat T lymphocytes and DG75 B lymphocytes when the latter were treated with a concentration of 1 µM of either compound for 24 hours. This effect was strongest for PXA followed by 12-dPXA and dicerandrol C. Additionally, the cleavage of the caspase substrate poly(ADP-ribose)-polymerase (PARP) was investigated through

immunoblotting after treatment of Jurkat and DG75 cells with 1 µM and 10 µM PXA which in both cases showed cleavage of PARP which could be inhibited by addition of caspase inhibitors [31]. Further experiments compared the apoptosis inducing properties of PXA to its semisynthetic derivate 1,1'-diacetylphomoxanthone A (PXA-DA). The induction of apoptosis was investigated using Jurkat T lymphocytes and Ramos B lymphocytes which were treated with increasing concentrations of either PXA or PXA-DA for 24 and 48 hours. The percentage of apoptotic sub-G1 nuclei as a marker for apoptosis was assessed using propidium iodide staining and flow cytometry. The activities observed for the different compounds as indicated by the percentages of sub-G1-nuclei detected after 24 hours in Jurkat T lymphocytes were in accordance with their anti-tumour activities detected in the cellular assays, where PXA-DA showed slightly lower activity than PXA (PXA: EC_{50} 5.17 µM; PXA-DA: 8.26 µM). The results of these assays strongly suggest, that the acetyl-derivatives of PXA retain their apoptosis inducing properties even though their overall anti-tumour activity is reduced compared to the parent compound (unpublished results).

To further investigate the caspase dependent induction of apoptosis by PXA, the compound was compared to mitomycin C (a DNA-damaging anticancer drug) and with the broad range kinase inhibitor staurosporine in a time dependent caspase-3 activity assay. The activity of caspase-3 was measured using fluorescence detection methods utilising DEVD-AMC as a caspase-3 substrate fluorescence indicator (Fig. **2**). When comparing the time course of caspase induction it became apparent that PXA acts slower than staurosporine (STS) but in considerably faster kinetics than mitomycin C (MITO) which makes it unlikely for PXA to possess a mode of action involving direct DNA-damage. These findings suggest that the apoptotic sub-G1 nuclei observed after treament of cells with PXA [31] are in fact a result of the activation of caspases and not the effect of a direct DNA-damage.

5. PXA ACTIVATES IMMUNE CELLS

As tumour stem cells are known to persist and may cause recrudescence even after an effective chemotherapy, an activation of immune cells such as natural killer (NK) cells that specifically recognize cancer stem cells and trigger apoptosis is highly favourable for the overall success of an anticancer therapy. Therefore Roensberg *et al.* investigated the cell-type specific activation markers in murine immune cell subpopulations following treatment with PXA, 12d-PXA or dicerandrols B and C [31]. The population of $CD69^+$ T cells was most prominently enhanced by the treatment of the two 4-4'-
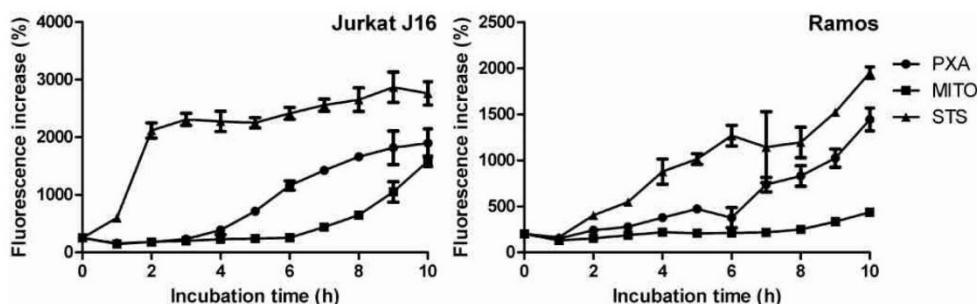
Fig. (2). Comparison of Caspase-3 induction by phomoxanthone A, mitomycin C, and staurosporine. Jurkat J16 cells (T lymphocytes; from DSMZ #ACC-282) or Ramos cells (Burkitt's lymphoma B lymphocytes; from Michael Engelke, University of Göttingen) were seeded at a density of 10^6 cells / mL and incubated with either 10 µM phomoxanthone A (PXA), 25 µg / mL mitomycin C (MITO), or 2.5 µM staurosporine (STS) for up to 10 h. Cells treated with DMSO (0.1% v/v) for 10 h were used as negative control. An amount of 100,000 cells per sample was harvested by centrifugation at 600 rcf and 4 °C for 5 min. The supernatant was removed and the cells were quick-frozen in liquid nitrogen. The cells were then thawed on ice, incubated with 150 µL of ice-cold lysis buffer (20 mM HEPES, 84 mM KCl, 10 mM MgCl2, 200 µM EDTA, 200 µM EGTA, 0.5% NP-40, 1 µg / mL leupeptin, 1 µg / mL pepstatin, 5 µg / mL aprotinin) for 10 min, and transferred to a clear flat-bottom 96-well plate. To each well, 150 µL of ice-cold reaction buffer (50 mM HEPES, 100 mM NaCl, 10% Sucrose, 0.1% CHAPS, 2 mM CaCl2, 13.35 mM DTT, 70 µM DEVD-AMC) were added and the fluorescence (Ex 360 nm, Em 450 nm) was measured at 37 °C over a time course of 150 min using a multiplate reader (Synergy Mx, BioTek). The ratio of the highest to the lowest value of the linear range of the fluorescence curve was calculated. Data points shown are the mean of triplicates, error bars = SD.

linked dimeric xanthones with a 1.8-fold (PXA) and 1.4-fold (12d-PXA) increase when treated with 1 μM of either of the respective compounds. In accordance to the cytotoxicity data the activation of CD69$^+$ T cells was antagonised by hydrolysis of the acetyl groups as tetradeacetylphomoxanthone showed no effect even at the highest concentration investigated. The authors hypothesised that the reduction in the T cell recruiting potential might correlate with reduced cellular uptake as total desacetylation of PXA leads to a significant loss in lipophilicity. Therefore an intracellular target rather than a cell-surface interaction was proposed as a potential target structure for PXA. For dicerandrol C an activation of the same T cell population was likewise observed albeit only at a higher concentration of 10 μM while dicerandrol B completely lacked activity. Similarly, an activation was observed in primary murine NK cells and macrophages as indicated by an upregulation of CD69 and MHC class II, respectively. Nevertheless murine B lymphocytes were not activated by the tested dimeric xanthones as there was no significant induction of CD86. This immune and in particular T and NK cell stimulatory effect of PXA in combination with the strong pro-apoptotic properties of the compound represents a synergistic mechanism towards tumour elimination that could be valuable for tumour chemotherapy.

CONCLUSION

Mangrove plants that thrive in stress prone habitats harbour unique endophytes that accumulate structurally unusual and highly active natural products such as phomoxanthone A (PXA) that is highlighted in this review. PXA shows powerful anti-tumour activities against different human cancer cells that even include cells that have become resistant against the cytostatic drug cisplatin. The mode of action of PXA was shown to be due to an induction of caspase 3 dependent apoptosis. Remarkably, PXA is up to 100 folds less active against PBMC that were used as a control for healthy blood cells. The immune stimulatory activity of PXA that was demonstrated for murine T-lymphocytes, NK cells and for macrophages could be important during cancer chemotherapy in order to eradicate any surviving cancer cells. Further studies on the target and on the mechanism of this interesting anti-tumour drug are highly warranted.

CONFLICT OF INTEREST

The authors confirm that this article content has no conflict of interest.

REFERENCES

[1]   Twilley, R.R.; Day, J.W. Mangrove Wetlands. In: *Estuarine Ecology,* 2nd ed.; Wiley-Blackwell: New York, **2012**.

[2]   Tomlinson, P.B. *The Botany of Mangroves;* Cambridge University Press: New York, **1994**.

[3]   Wu, J.; Xiao, Q.; Xu, J.; Li, M.Y.; Pan, J.Y.; Yang, M.H. Natural products from true mangrove flora: source, chemistry and bioactivities. *Nat. Prod. Rep.,* **2008**, *25*(5), 955-981.

[4]   Walsh, G.E. Mangroves: A Review. In: *Ecology of Halophytes*; Academic Press, Inc.: New York, **1974**.

[5]   Chapman, V.J. *Mangrove Vegetation;* J. Cramer: Vaduz, **1976**, p. 581.

[6]   Feller, I.; Lovelock, C.; Berger, U.; McKee, K.; Joye, S.; Ball, M. Biocomplexity in mangrove ecosystems. *Ann. Rev. Mar. Sci.,* **2010**, *2*, 395-417.

[7]   Valiela, I.; Bowen, J.L.; York, J.K. Mangrove forests: one of the world's threatened major tropical environments. *Bioscience*, **2001**, *51*(10), 807-815.

[8]   Xu, J. Bioactive natural products derived from mangrove-associated microbes. *R. Soc. Chem. Adv.,* **2015**, *5*(2), 841-892.

[9]   Arnold, A.E.; Mejía, L.C.; Kyllo, D.; Rojas, E.I.; Maynard, Z.; Robbins, N.; Herre, E.A. Fungal endophytes limit pathogen damage in a tropical tree. *Proc. Natl. Acad. Sci. USA*, **2003**, *100*(26), 15649-15654.

[10] Reinhold-Hurek, B.; Hurek, T. Living inside plants: bacterial endophytes. *Curr. Opin. Plant Biol.,* **2011**, *14*(4), 435-443.

[11] Aly, A.H.; Debbab, A.; Proksch, P. Fungal endophytes: unique plant inhabitants with great promises. *Appl. Microbiol. Biotechnol.*, **2011**, *90*(6), 1829-1845.

[12] Aly, A.H.; Debbab, A.; Kjer, J.; Proksch, P. Fungal endophytes from higher plants: a prolific source of phytochemicals and other bioactive natural products. *Fungal Divers.,* **2010**, *41*(1), 1-16.

[13] Strobel, G.; Daisy, B. Bioprospecting for microbial endophytes and their natural products. *Microbiol. Mol. Biol. Rev.,* **2003**, *67*(4), 491-502.

[14] Strobel, G.A. Endophytes as sources of bioactive products. *Microbes Infect.*, **2003**, *5*(6), 535-544.

[15] Thatoi, H.; Behera, B.C.; Mishra, R.R.; Dutta, S.K. Biodiversity and biotechnological potential of microorganisms from mangrove ecosystems: a review. *Ann. Microbiol.,* **2013**, *63*(1), 1-19.

[16] Xu, J. Biomolecules produced by mangrove-associated microbes. *Curr. Med. Chem.,* **2011**, *18*(34), 5224-5266.

[17] Salini, G. Pharmacological profile of mangrove endophytes - a review. *Int. J. Pharm. Pharm. Sci.*, **2014**, *7*(1), 6-15.

[18] Ebrahim, W.; Kjer, J.; El Amrani, M.; Wray, V.; Lin, W.; Ebel, R.; Lai, D.; Proksch, P. Pullularins E and F, two new peptides from the endophytic fungus *Bionectria ochroleuca* isolated from the mangrove plant *Sonneratia caseolaris*. *Mar. Drugs,* **2012**, *10*(5), 1081-1091.

[19] Zeng, Y.B.; Wang, H.; Zuo, W.J.; Zheng, B.; Yang, T.; Dai, H.F.; Mei, W.L. A fatty acid glycoside from a marine-derived fungus isolated from mangrove plant *Scyphiphora hydrophyllacea*. *Mar. Drugs*, **2012**, *10*(3), 598-603.

[20] Mei, W.L.; Zheng, B.; Zhao, Y.X.; Zhong, H.M.; Chen, X.L. W.; Zeng, Y.B.; Dong, W.H.; Huang, J.L.; Proksch, P.; Dai, H.F. Meroterpenes from endophytic fungus A1 of mangrove plant *Scyphiphora hydrophyllacea*. *Mar.* Drugs, **2012**, *10*(9), 1993-2001.

[21] Ebrahim, W.; Aly, A.H.; Mándi, A.; Totzke, F.; Kubbutat, M. H.; Wray, V.; Lin, W. H.; Dai, H.; Proksch, P.; Kurtán, T.; Debbab, A. Decalactone derivatives from *Corynespora cassiicola*, an endophytic fungus of the mangrove plant *Laguncularia racemosa*. *Eur. J. Org. Chem.*, **2012**, *18*, 3476- 3484.

[22] Li, Y.; Yu, S.; Liu, D.; Proksch, P.; Lin, W. Inhibitory effects of polyphenols toward HCV from the mangrove plant *Excoecaria agallocha* L. *Bioorg. Med. Chem. Lett.*, **2012**, *22*(2), 1099-1102.

[23] Zeng, Y.B.; Gu, H.G.; Zuo, W.J.; Zhang, L.L.; Bai, H.J.; Guo, Z.K.; Proksch, P.; Mei, W.L.; Dai, H.F. Two new sesquiterpenoids from endophytic fungus J3 isolated from mangrove plant *Ceriops tagal*. *Arch. Pharm. Res.*, **2015**, *38*(5), 673-676.

[24] Huang, Z.; Yang, J.; Cai, X.; She, Z.; Lin, Y. A new furanocoumarin from the mangrove endophytic fungus *Penicillium* sp.(ZH16). *Nat. Prod. Res.*, **2012**, *26*(14), 1291-1295.

[25] Huang, Z.; Yang, R.; Guo, Z.; She, Z.; Lin, Y. A new naphtho-γ- pyrone from mangrove endophytic fungus ZSU-H26. *Chem. Nat. Compd.*, **2010**, *1*(46), 15-18.

[26] Huang, Z.; Yang, J.; She, Z.; Lin, Y. A new isoflavone from the mangrove endophytic fungus Fusarium sp.(ZZF60). *Nat. Prod. Res.*, **2012**, *26*(1), 11-15.

[27] Wezeman, T.; Brase, S.; Masters, K.S. Xanthone dimers: a compound family which is both common and privileged. *Nat. Prod. Rep.*, **2015**, *32*(1), 6-28.

[28] Na, Y. Recent cancer drug development with xanthone structures. *J. Pharm. Pharmacol.*, **2009**, *61* (6), 707-712.

[29] Pinto, M.; Sousa, M.; Nascimento, M. Xanthone derivatives: new insights in biological activities. *Curr. Med. Chem.*, **2005**, *12*(21), 2517-2538.

[30] Pouli, N.; Marakos, P. Fused xanthone derivatives as antiproliferative agents. *Anticancer Agents Med. Chem.,* **2009**, *9*(1), 77-98.

[31] Rönsberg, D.; Debbab, A.; Mándi, A.; Vasylyeva, V.; Böhler, P.; Stork, B.R.; Engelke, L.; Hamacher, A.; Sawadogo, R.; Diederich, M.; Wray, V.; Lin, W., Kassack, M.U.; Janiak, C.; Scheu, S.; Wesselborg, S.; Kurtán, T.; Aly, A.H.; Proksch, P. Pro-apoptotic and immunostimulatory tetrahydroxanthone dimers from the endophytic fungus *Phomopsis longicolla*. *J. Org. Chem.*, **2013**, *78*(24), 12409-12425.

[32] Li, S.; Hartman, G.L.; Boykin, D.L., Aggressiveness of *Phomopsis longicolla* and other *Phomopsis* spp. on soybean. *Plant Dis.*, **2010**, *94*(8), 1035-1040.

[33] Yang, J.; Xu, F.; Huang, C.; Li, J.; She, Z.; Pei, Z.; Lin, Y. Metabolites from the mangrove endophytic fungus Pho-

mopsis sp. (# zsu-H76). *Eur. J. Org. Chem.*, **2010**, *19*, 3692-3695.

[34] Elsässer, B.; Krohn, K.; Flörke, U.; Root, N.; Aust, H.J.; Draeger, S.; Schulz, B.; Antus, S.; Kurtán, T. X-ray structure determination, absolute configuration and biological activity of phomoxanthone A. *Eur. J. Org. Chem.*, **2005**, *21*, 4563-4570.

[35] Isaka, M.; Jaturapat, A.; Rukseree, K.; Danwisetkanjana, K.; Tanticharoen, M.; Thebtaranonth, Y. Phomoxanthones A and B, novel xanthone dimers from the endophytic fungus *Phomopsis* species. *J. Nat. Prod.*, **2001**, *64*(8), 1015-1018.

[36] Rukachaisirikul, V.; Sommart, U.; Phongpaichit, S.; Sakayaroj, J.; Kirtikara, K. Metabolites from the endophytic fungus *Phomopsis* sp. PSU-D15. *Phytochemistry*, **2008**, *69*(3), 783-787.

[37] Dai, J.; Hussain, H.; Draeger, S.; Schulz, B.; Kurtán, T.; Pescitelli, G.; Floerke, U.; Krohn, K. Metabolites from the fungus *Phoma* sp. 7210, associated with *Aizoon canariense*. *Nat. Prod. Commun.*, **2010**, *5*(8), 1175-1180.

[38] Koolen, H.H.; Menezes, L.S.; Souza, M.P.; Silva, F.; Almeida, F.G.; de Souza, A.Q.; Nepel, A.; Barison, A.; Silva, F.H.D.; Evangelista, D. E. Talaroxanthone, a novel xanthone dimer from the endophytic fungus *Talaromyces* sp. associated with *Duguetia stelechantha* (Diels) RE Fries. *J. Braz. Chem. Soc.*, **2013**, *24*(5), 880-883.

[39] Birch, A.; Massy-Westropp, R.; Moye, C. Studies in relation to biosynthesis. VII. 2-Hydroxy-6-methylbenzoic acid in *Penicillium griseofulvum* Dierckx. *Aust. J. Chem.*, **1955**, *8*(4), 539-544.

[40] Simpson, T. J. Genetic and biosynthetic studies of the fungal prenylated xanthone shamixanthone and related metabolites in *Aspergillus* spp. revisited. *Chembiochem*, **2012**, *13*(11), 1680-1688.

[41] Gil Girol, C.; Fisch, K.M.; Heinekamp, T.; Günther, S.; Hüttel, W.; Piel, J.; Brakhage, A.A.; Müller, M. Regio- and stereoselective oxidative phenol coupling in *Aspergillus niger*. *Angew. Chem.*, **2012**, *124*(39), 9926-9929.

[42] Cao, S.; McMillin, D.W.; Tamayo, G.; Delmore, J.; Mitsiades, C.S.; Clardy, J. Inhibition of tumor cells interacting with stromal cells by xanthones isolated from a Costa Rican *Penicillium* sp. *J. Nat. Prod.*, **2012**, *75*(4), 793-797.

[43] Liu, Y.; Marmann, A.; Abdel-Aziz, M.S.; Wang, C.Y.; Müller, W.E.; Lin, W.H.; Mándi, A.; Kurtán, T.; Daletos, G.; Proksch, P. Tetrahydroanthraquinone derivatives from the endophytic fungus stemphylium globuliferum. *Eur. J. Org. Chem.*, **2015**, *12*, 2646-2653.

2.2 Supporting Information

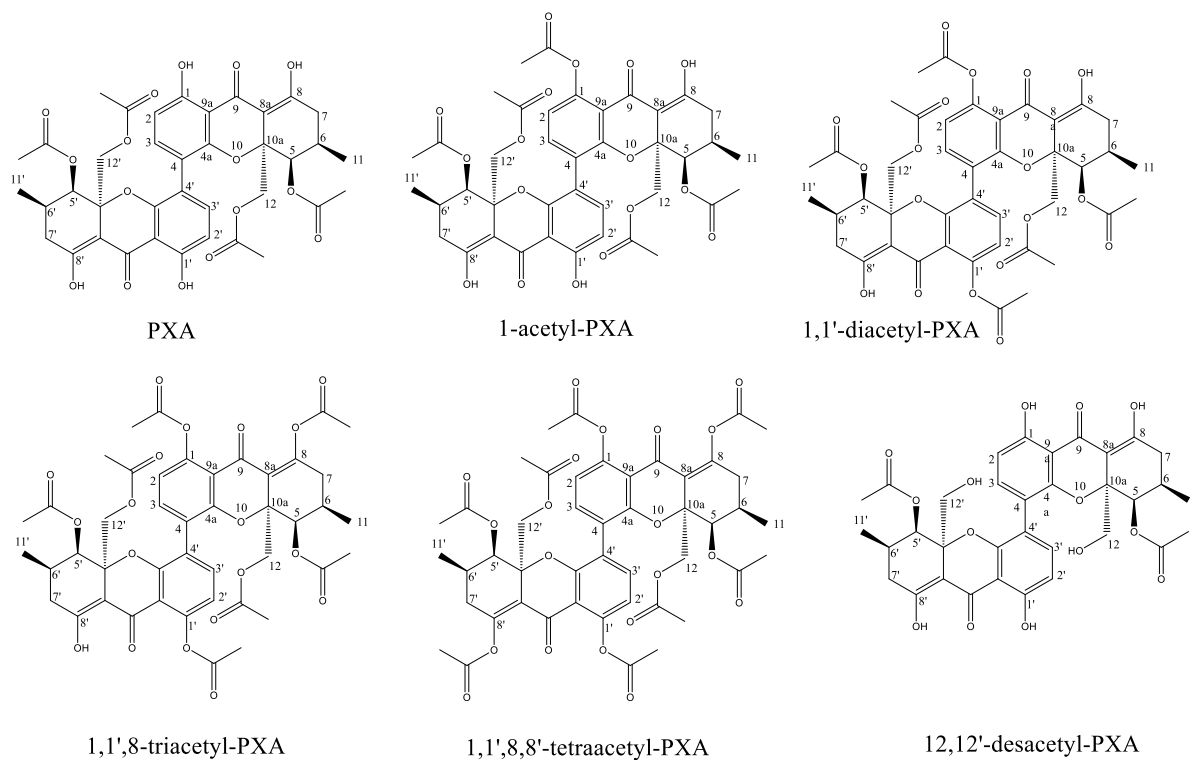# Phomoxanthone A - From Mangrove Forests to Anticancer Therapy

Author(s):[1]Marian Frank,[1]Hendrik Niemann,[2]Philip Böhler,[2]Björn Stork,[2]Sebastian Wesselborg,[3]Wenhan Lin,[1]Peter Proksch.

1. Institute of Pharmaceutical Biology and Biotechnology, Heinrich-Heine University, 40225 Duesseldorf, Germany;
2. Institute of Molecular Medicine, University Hospital, 40225 Duesseldorf, Germany;
3. National Research Laboratories of Natural and Biomimetic Drugs, Peking University, Health Science Center, 100083 Beijing, People's Republic of China

The following supporting information was added to this dissertation and is not available online.

Table of Content

Table 1: ^{1}H-NMR Data of new PXA Derivatives

PXA

1-acetyl-PXA

1,1'-diacetyl-PXA

1,1',8-triacetyl-PXA

1,1',8,8'-tetraacetyl-PXA

12,12'-desacetyl-PXA

| Position	^{1}H-NMR chemical shifts at 600MHz in CDCl$_3$					
	PXA	**1-acetyl PXA**	**1,1'-diacetyl PXA**	**1,1',8-triacetyl PXA**	**1,1',8,8'-tetraacetyl PXA**	**12,12'-didesacetyl PXA**
2/2'	6.58 (d)	6.76 (d) 6.60 (d)	6.77 (d)	6.76 (d) 6.74 (d)	6.73 (d)	6.54 (d)
3/3'	7.38 (d)	7.42 (d) 7.47 (d)	7.48 (d)	7.46 (d)	7.41 (d)	7.09 (d)
5/5'	5.40 (s)	5.39 (s)	5.34 (s)	5.32 (s) 5.28 (s)	5.28 (s)	5.45 (s)
6/6'	2.37 (m)	2.33 (m)	2.33 (m)	2.27 (m)	2.27 (m)	2.23 (m)
7/7'	2.46 (m), 2.33 (m)	2.43 (m) 2.31 (m)	2.41 (m) 2,30 (m)	2.25 (m)	2.41 (m) 2.30 (m)	2.36 (m)
11/11'	1.01 (d, 5.8)	0.99 (d) 0.97 (d)	0.94 (d)	0.93 (m)	0.91 (d)	0.98 (d)
12/12'	4.28(d) 4.17 (d)	4.27 (d) 4.14 (d) 4.24 (d) 4.20 (d)	4.20 (d) 4.17 (d)	4.28 (br m)	4.29 (d) 4.27 (d)	3.83 (d) 3.39 (d)
5/5'-OC(O)CH3	2.07 (s)	2.07 (s) 2,06 (s)	2.04 (s)	1.99 (s) 1.98 (s)	2.04 (s)	2.10 (s)
12/12'-OC(O)CH3	1.89 (s)	1.87 (s) 1,84 (s)	1.82 (s)	1.90 (s) 1.88 (s)	1.92 (s)	-
12/12'-OH	-	-	-	-	-	3.45 (s)
1/1'-OC(O)CH3	-	2,35 (s)	2.34 (s)	2.34 (s)	2.34 (s)	-
1/1'-OH	11.52 (s)	11,53 (s)	-	-	-	11.39 (s)
8/8'-OH	14.09 (s)	14,08 (s) 15,86 (s)	15.83 (s)	15.80 (s)	-	13.96 (s)

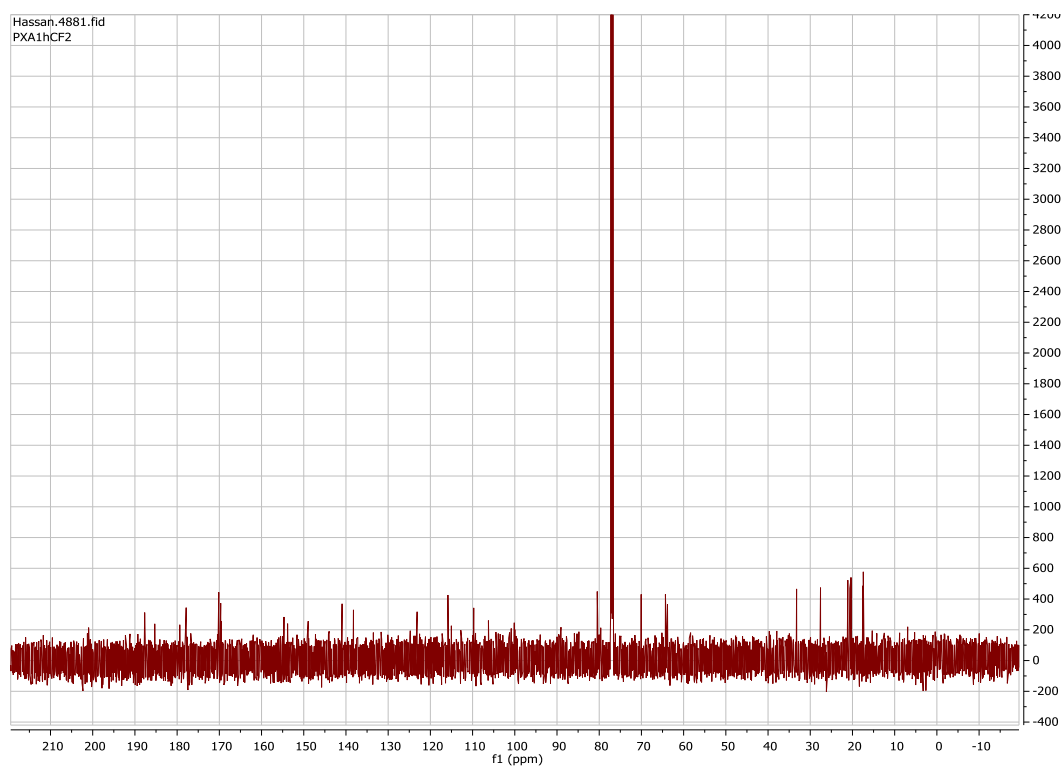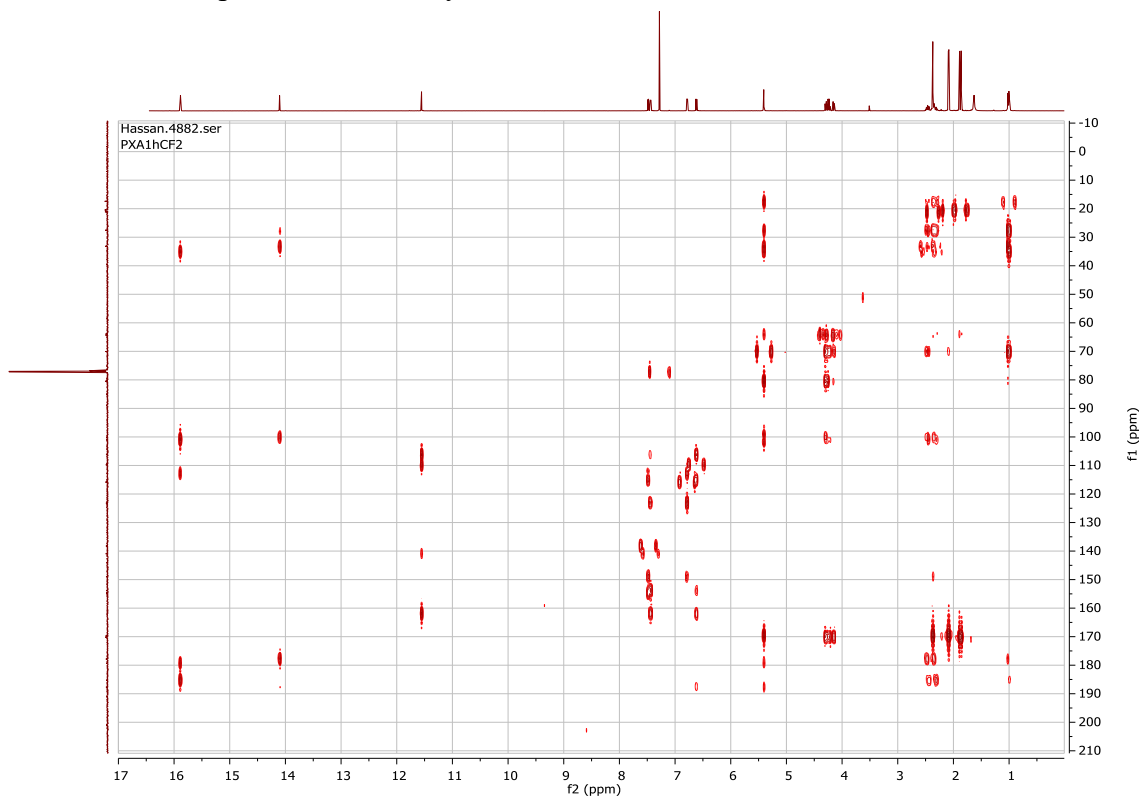## S1 UV-spectrum of 1-acetyl-PXA
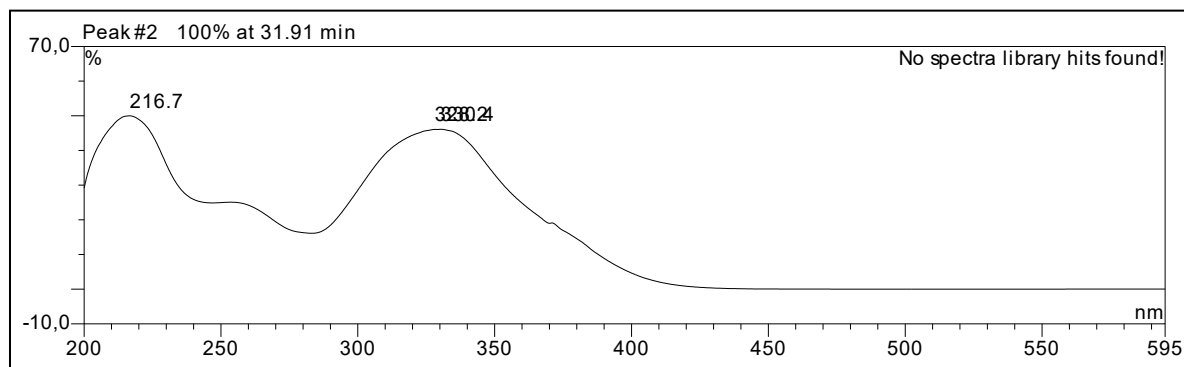
S2 HRESIMS signals for 1-acetyl-PXA

793.2339 (M+H), calc. for $C_{40}H_{41}O_{17}$ (793.2338)

S3 Specific Optical Rotation of 1-acetyl-PXA

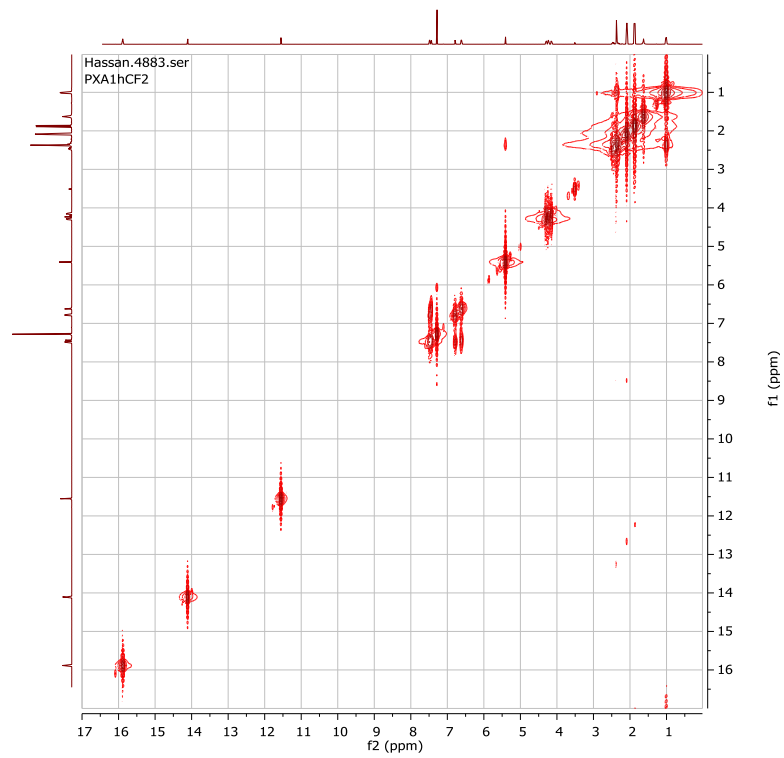$[\alpha]_D^{25}$ -88.3 (c 1.0, MeOH)
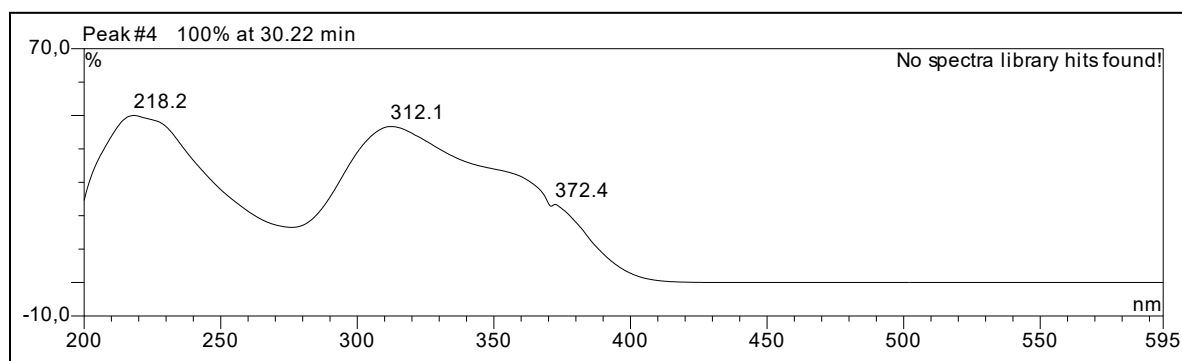
S4 ^{1}H-NMR spectrum of 1-acetyl-PXA
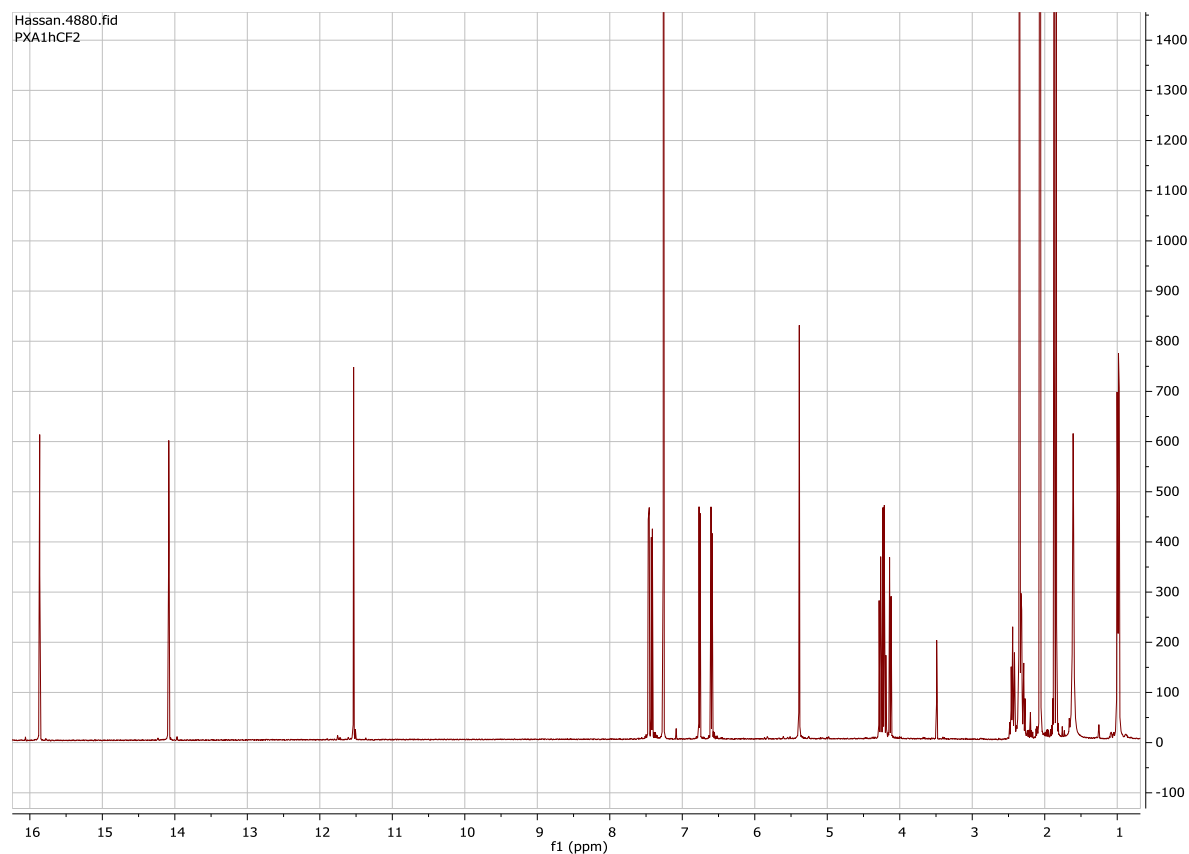
S5 ^{13}C-NMR spectrum of 1-acetyl-PXA

S6 ^{1}H-^{13}C-HMBC spectrum of 1-acetyl-PXA

S7 ^{1}H-^{1}H-COSY spectrum of 1-acetyl-PXA

S8 UV-spectrum of 1,1'-diacetyl-PXA

S9 HRESIMS signals for 1,1'-diacetyl-PXA

835.2447 (M+H), calc. for $C_{42}H_{43}O_{18}$ (835.245)

S10 Specific Optical Rotation of 1,1'-diacetyl-PXA

$[\alpha]_D^{25}$ -106.1 (c 1.0, MeOH)

S11 CD spectrum of 1,1'-diacetyl PXA (c: 0.215 mM)
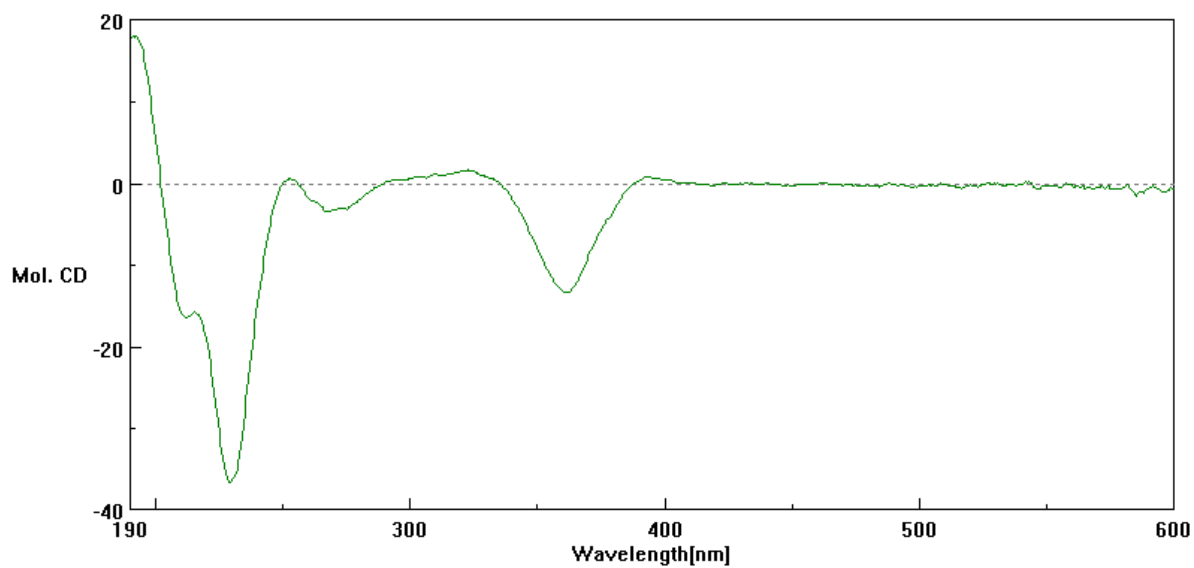
S12 Comparison of CD spectra of 1,1'-diacetyl PXA and PXA

Blue: PXA (0.11 mM)   Green: 1,1'-diacetyl-PXA (0.215 mM)
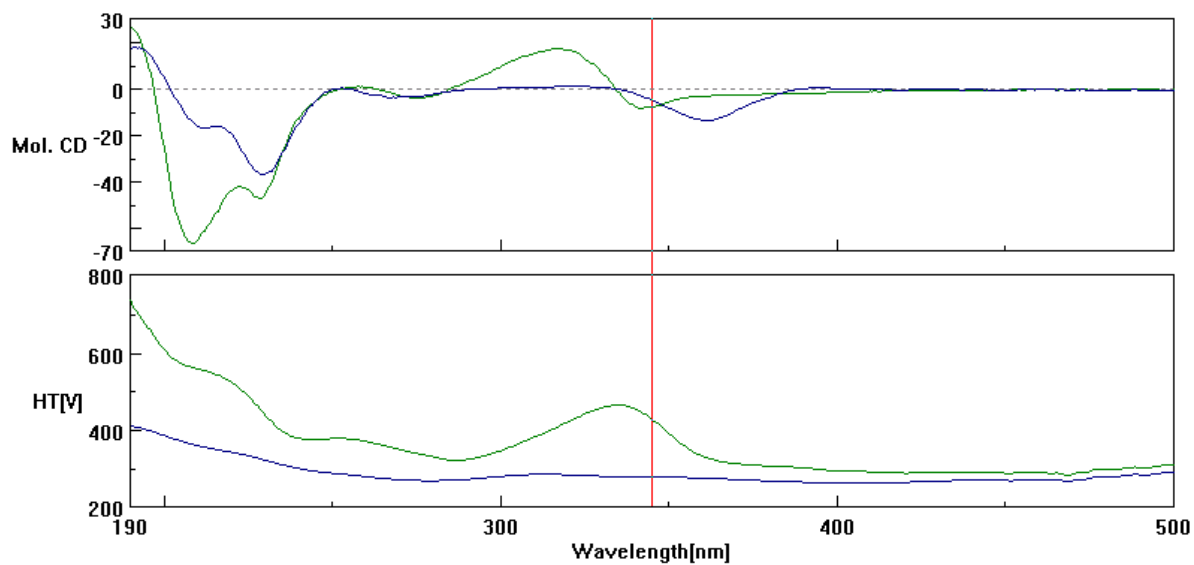
S13 ^{1}H-NMR spectrum of 1,1'-diacetyl-PXA
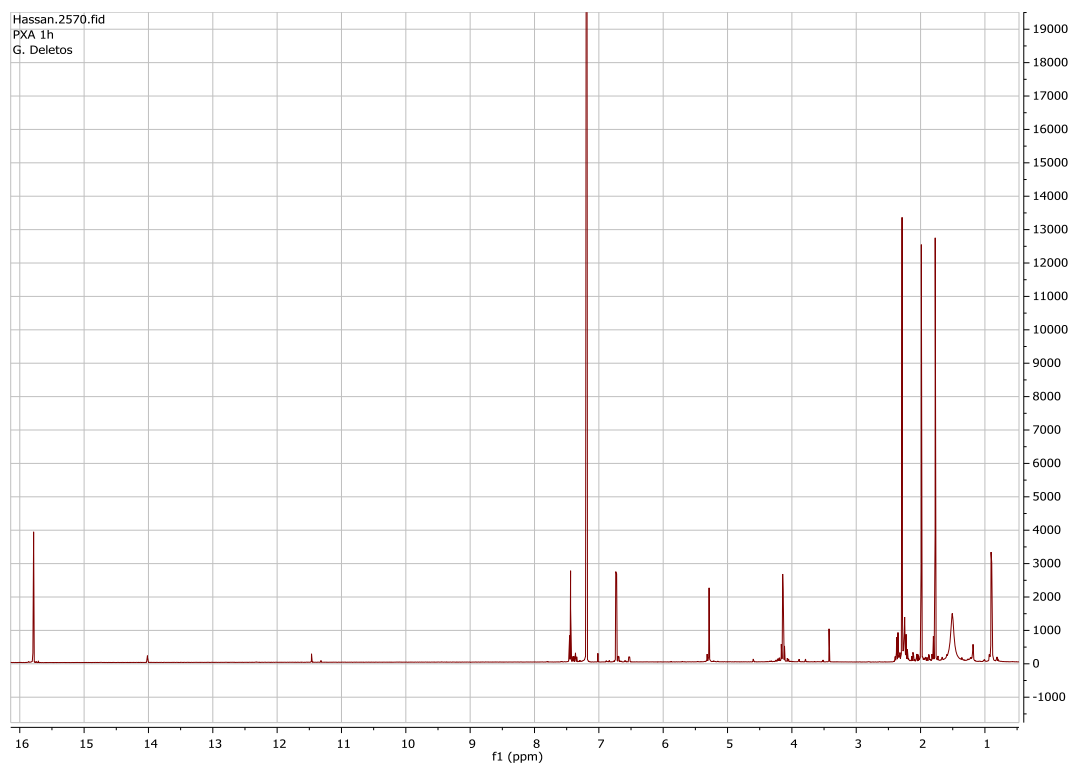
S14 ^{1}H-^{1}H-COSY spectrum of 1,1'-diacetyl-PXA
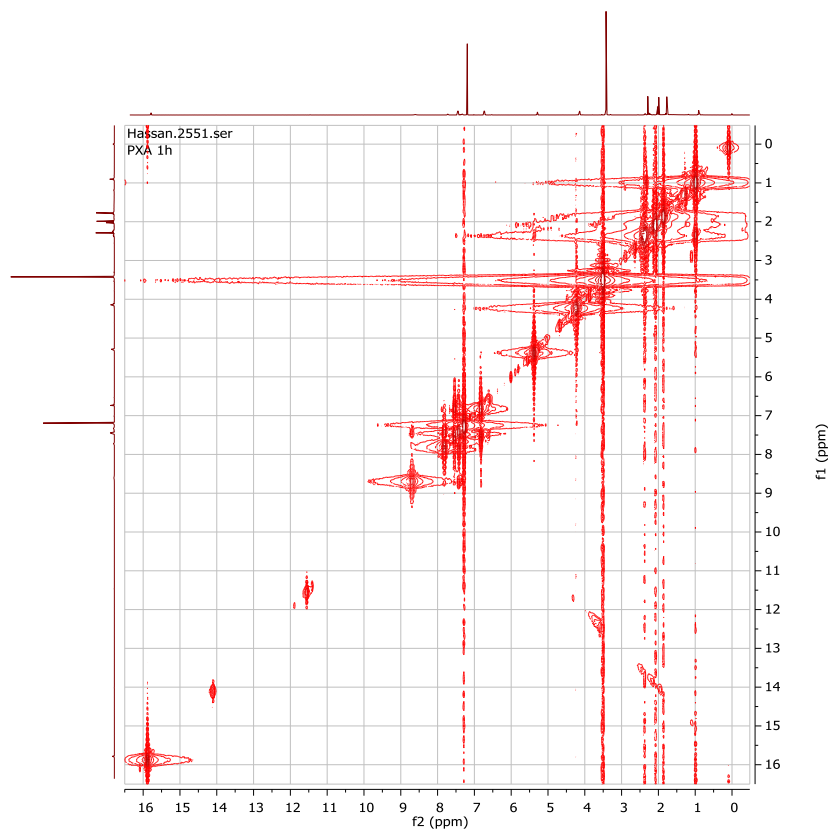
S15 UV-spectrum of 1,1',8 –triacetyl-PXA
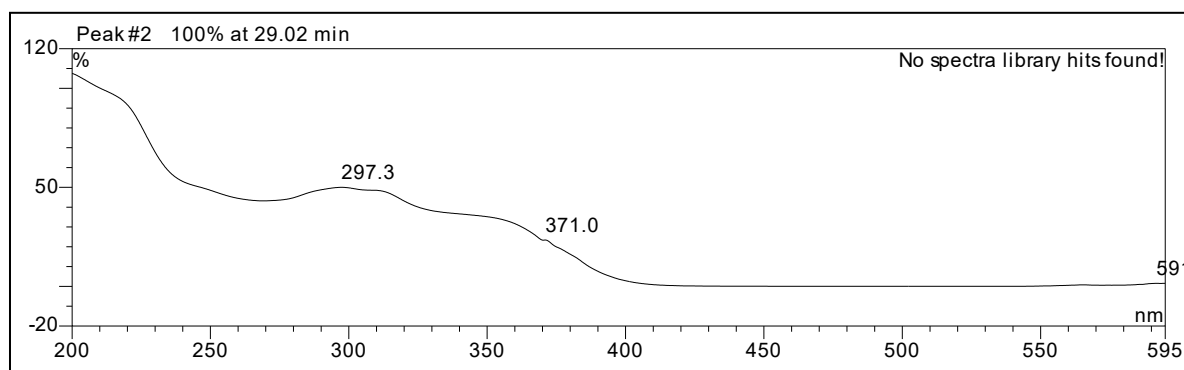
S16 HRESIMS signals for 1,1',8, -triacetyl-PXA

877.2549 (M+H), calc. for $C_{44}H_{45}O_{19}$ (877.256)

S17 Specific Optical Rotation of 1,1',8, -triacetyl-PXA

$[\alpha]_D^{25}$ -55.2 (c 1.0, MeOH)

S18 ^{1}H-NMR spectrum of 1,1',8-triaacetyl-PXA
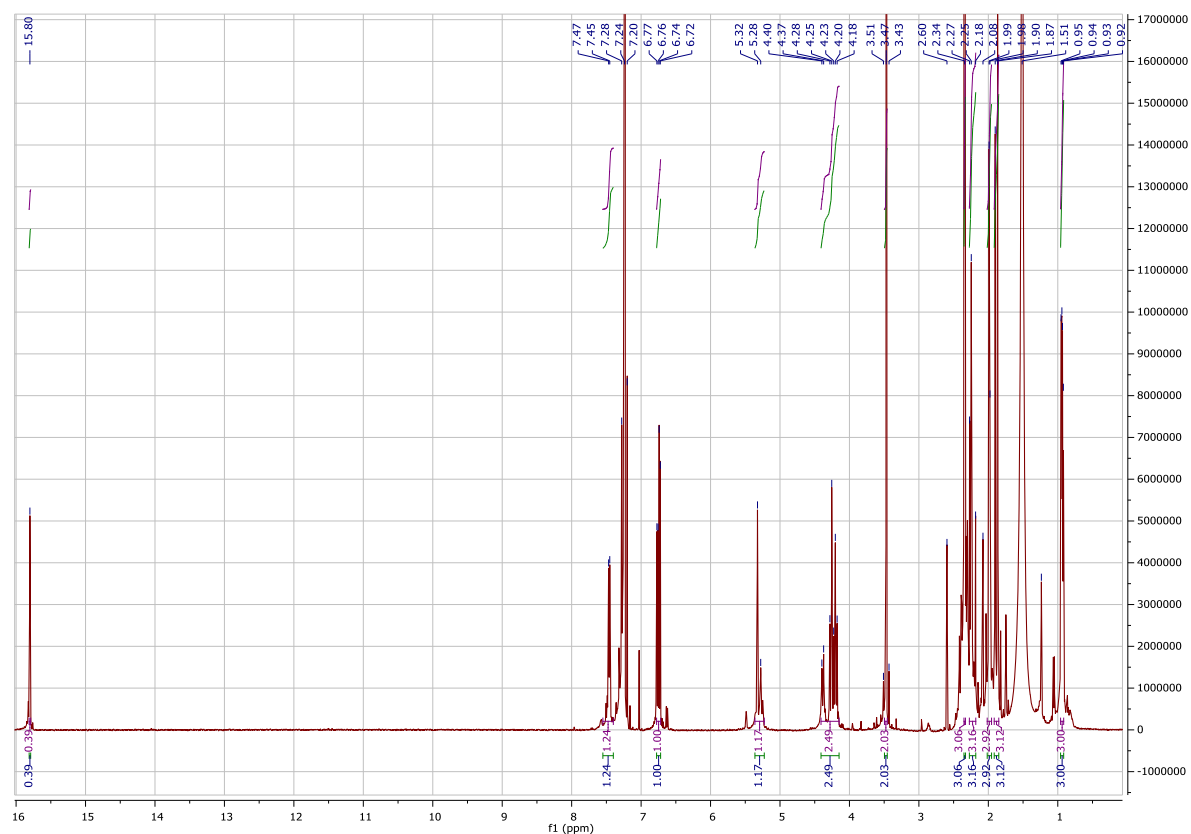
S19 UV-spectrum of 1,1',8,8'-tetraacetyl-PXA
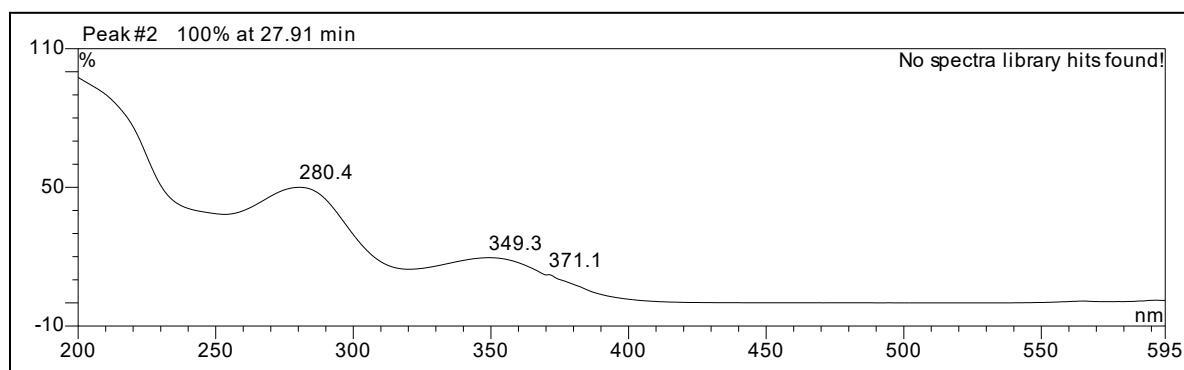
S20 HRESIMS signals for 1,1',8,8'-tetraacetyl-PXA

919.2650 (M+H), calc. for $C_{46}H_{47}O_{20}$ (919.266)

S21 Specific Optical Rotation of 1,1',8,8'-tetraacetyl-PXA

$[\alpha]_D^{25}$ -13.7 (c 1.0, MeOH)

S22 ^{1}H-NMR spectrum of 1,1',8,8'-tetraacetyl-PXA
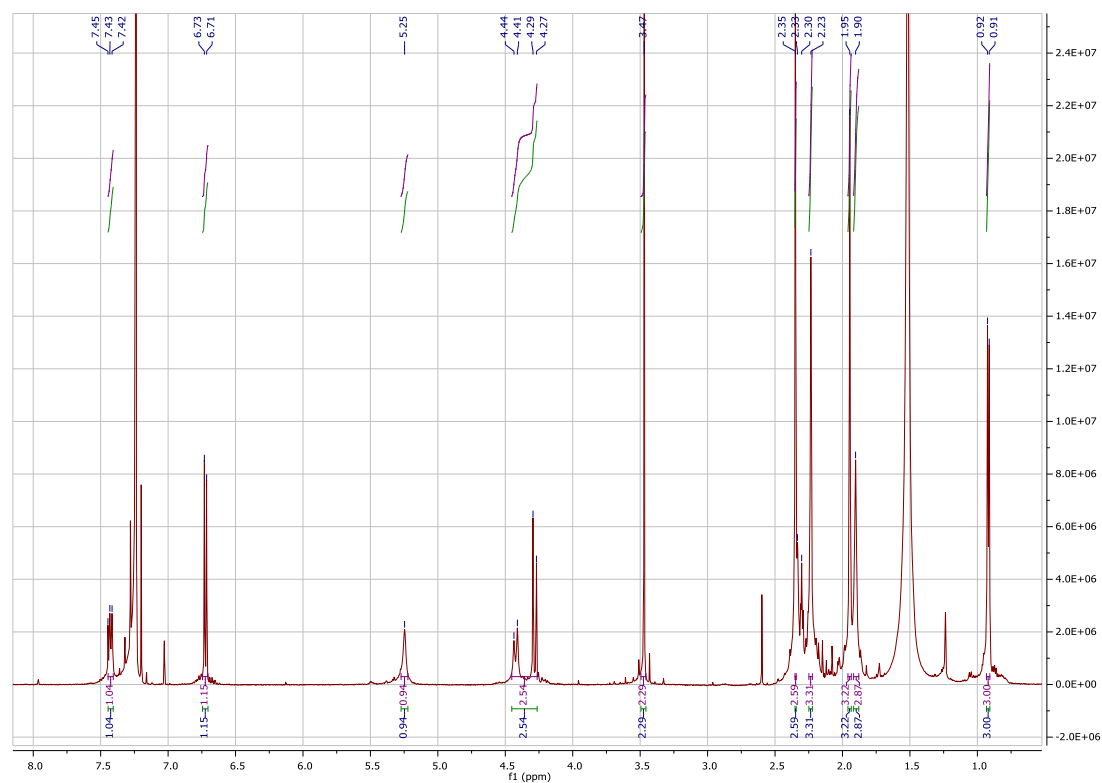
S23 ^{1}H-^{1}H-COSY spectrum of 1,1',8,8'-tetraacetyl-PXA
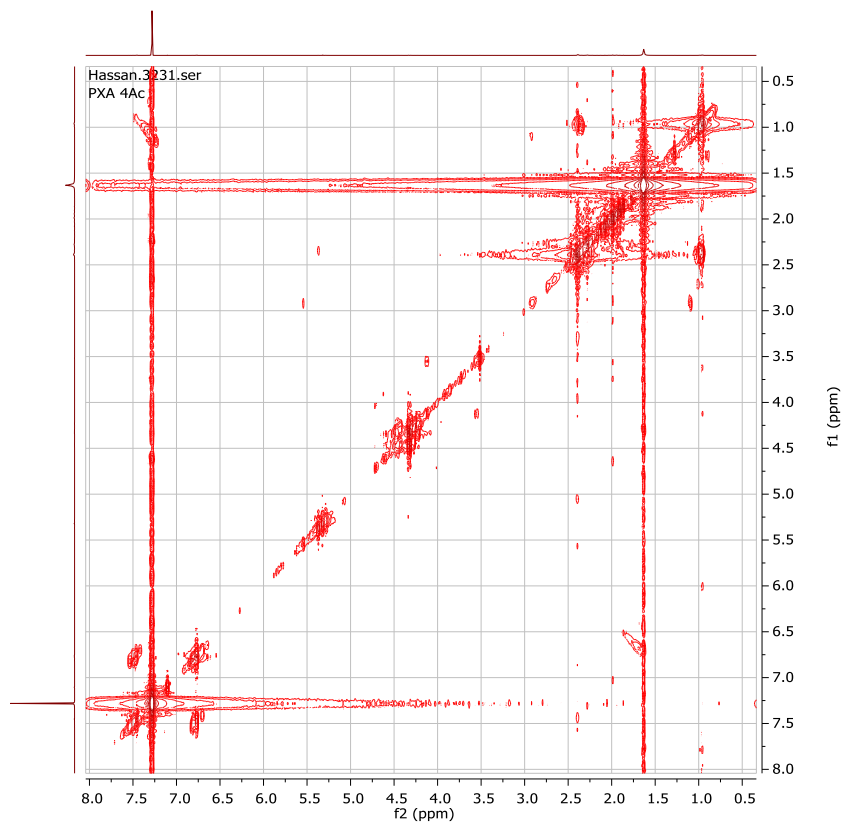
S24 UV-spectrum of 12, 12'-didesacetyl-PXA
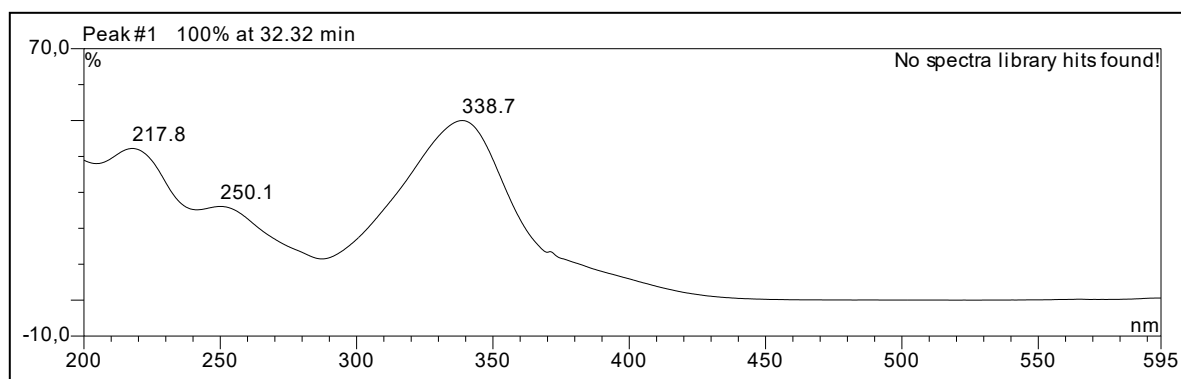
S25 HRESIMS signals for 12, 12'-didesacetyl-PXA

667.2023(M+H), calc. for $C_{34}H_{35}O_{14}$ (667.203)

S26 Specific Optical Rotation of 12,12'-didesacetyl-PXA

$[\alpha]_D^{25}$ +190.3 (c 1.0, MeOH)

S27 ^{1}H-NMR spectrum of 12, 12'-didesacetyl-PXA
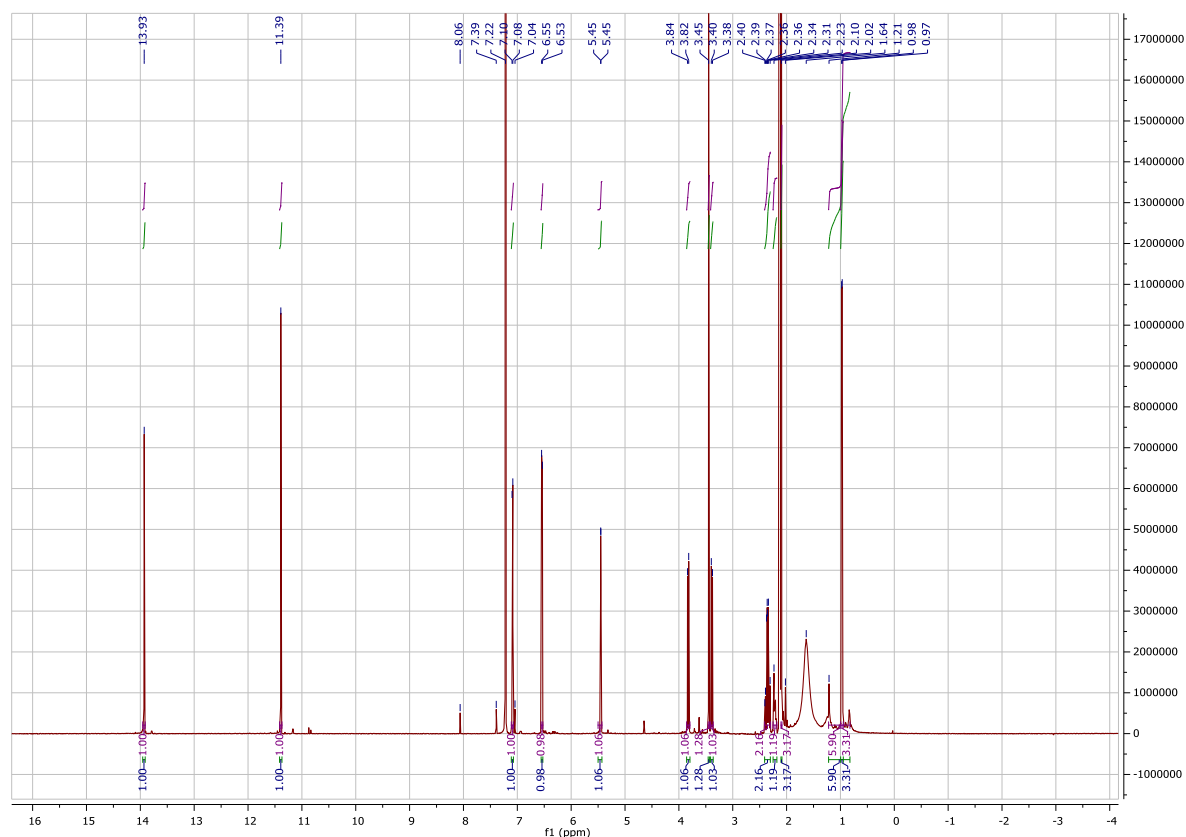
Chapter 3 - The Mycotoxin Phomoxanthone A Disturbs the Form and Function of the Inner Mitochondrial Membrane

Overall contribution to this publication: 10%, tenth author, producer and supplier of phomoxanthone A (PXA), analytical investigation of PXA instability and development of PXA handling protocol.

3.1 Publication Manuscript

Cell Death & Disease

ARTICLE　　　　　　　　　　　　　　　　　　　　　**Open Access**

The mycotoxin phomoxanthone A disturbs the form and function of the inner mitochondrial membrane

Philip Böhler[1], Fabian Stuhldreier[1], Ruchika Anand[2], Arun Kumar Kondadi[2], David Schlütermann[1], Niklas Berleth[1], Jana Deitersen[1], Nora Wallot-Hieke[1], Wenxian Wu[1], Marian Frank[3], Hendrik Niemann[3], Elisabeth Wesbuer[4], Andreas Barbian[4], Tomas Luyten[5], Jan B. Parys[5], Stefanie Weidtkamp-Peters[6], Andrea Borchardt[2], Andreas S. Reichert[2], Aida Peña-Blanco[7], Ana J. García-Sáez[7], Samuel Itskanov[8], Alexander M. van der Bliek[8], Peter Proksch[3], Sebastian Wesselborg[1] and Björn Stork[1]

Abstract

Mitochondria are cellular organelles with crucial functions in the generation and distribution of ATP, the buffering of cytosolic Ca^{2+} and the initiation of apoptosis. Compounds that interfere with these functions are termed mitochondrial toxins, many of which are derived from microbes, such as antimycin A, oligomycin A, and ionomycin. Here, we identify the mycotoxin phomoxanthone A (PXA), derived from the endophytic fungus *Phomopsis longicolla*, as a mitochondrial toxin. We show that PXA elicits a strong release of Ca^{2+} from the mitochondria but not from the ER. In addition, PXA depolarises the mitochondria similarly to protonophoric uncouplers such as CCCP, yet unlike these, it does not increase but rather inhibits cellular respiration and electron transport chain activity. The respiration-dependent mitochondrial network structure rapidly collapses into fragments upon PXA treatment. Surprisingly, this fragmentation is independent from the canonical mitochondrial fission and fusion mediators DRP1 and OPA1, and exclusively affects the inner mitochondrial membrane, leading to cristae disruption, release of pro-apoptotic proteins, and apoptosis. Taken together, our results suggest that PXA is a mitochondrial toxin with a novel mode of action that might prove a useful tool for the study of mitochondrial ion homoeostasis and membrane dynamics.

Introduction

Mitochondria are cellular organelles that are crucial to almost all eukaryotic organisms. Among their most important functions are generation and distribution of ATP, buffering of cytosolic Ca^{2+} and, in animal cells, initiation of apoptosis. Disturbance of these or other functions by mitochondrial toxins can lead to cellular stress and cell death[1,2].

Mitochondria produce ATP through oxidative phosphorylation (OXPHOS), which depends on the electron transport chain (ETC) embedded in the inner mitochondrial membrane (IMM). The ETC pumps protons out of the mitochondrial matrix and into the mitochondrial intermembrane space. This generates a proton gradient (ΔpH_m) and, consequently, a membrane potential ($\Delta\Psi_m$) across the IMM. The $\Delta\Psi_m$ is then used to drive the mitochondrial ATP synthase[3].

To provide all regions within the cell with sufficient ATP, mitochondria often form a network that constantly undergoes balanced fission and fusion. This allows

Correspondence: Sebastian Wesselborg (sebastian.wesselborg@uni-duesseldorf.de) or Björn Stork (bjoern.stork@uni-duesseldorf.de)
[1]Institute of Molecular Medicine I, Medical Faculty, Heinrich Heine University Düsseldorf, 40225 Düsseldorf, Germany
[2]Institute of Biochemistry and Molecular Biology I, Medical Faculty, Heinrich Heine University Düsseldorf, 40225 Düsseldorf, Germany
Full list of author information is available at the end of the article
Philip Böhler, Fabian Stuhldreier, Sebastian Wesselborg, Björn Stork contributed equally to this work.
Edited by G. Raschellà

SPRINGER NATURE
CDDpress

remodelling of the network as well as removal and recycling of damaged mitochondria through mitophagy[1,4,5]. Excessive fission can be triggered by mitochondrial toxins that cause loss of $\Delta\Psi_m$, such as the protonophore carbonyl cyanide *m*-chlorophenyl hydrazone (CCCP)[6].

The $\Delta\Psi_m$ also plays a role in the mitochondrial buffering of cytosolic Ca^{2+}. Normally, the cytosol of a typical animal cell contains only a very low Ca^{2+} concentration ($[Ca^{2+}]_{cyt}$, ~0.1 µM), whereas the concentration of Ca^{2+} within the endoplasmic reticulum ($[Ca^{2+}]_{ER}$, > 100 µM) or outside the cell ($[Ca^{2+}]_{ext}$, > 1000 µM) is up to 10,000-fold higher[2]. In response to certain stimuli, Ca^{2+} channels in the ER and/or the plasma membrane open to release Ca^{2+} into the cytosol as a second messenger. Mitochondria contribute to removal of cytosolic Ca^{2+} by uptake into their matrix via $\Delta\Psi_m$-driven Ca^{2+} transporters. After that, a slow, regulated efflux moves the Ca^{2+} out of the matrix and into the cristae, which are folds in the IMM, from where it is slowly released and shuttled back to the ER[2,7–9]. A separate mechanism through which Ca^{2+} can cross the IMM is the mitochondrial permeability transition pore (mPTP), which can open irreversibly in response to severe mitochondrial stress. The mPTP directly connects the mitochondrial matrix with the cytosol to allow the free exchange of molecules up to 1.5 kDa in size, including Ca^{2+}. Irreversible mPTP opening leads to release of mitochondrial Ca^{2+}, loss of $\Delta\Psi_m$, swelling of the matrix and eventually mitochondrial outer membrane permeabilisation (MOMP)[10,11].

In animal cells, MOMP initiates apoptosis. Several proteins normally contained in the cristae attain a pro-apoptotic function if they pass the outer mitochondrial membrane (OMM) and are released into the cytosol. Among these proteins are cytochrome c (CYCS), SMAC (DIABLO) and OMI (HTRA2). Cytosolic CYCS becomes part of the caspase-activating apoptosome complex, while DIABLO and HTRA2 bind and inhibit the inhibitor of apoptosis proteins (IAPs), thus attenuating their inhibition of caspases[1]. MOMP can be caused either passively through rupture of the OMM, such as triggered by the mPTP, or actively through the formation of pores in the OMM by the pro-apoptotic proteins BAK and BAX, which can be induced in response to severe cellular stress[12].

A variety of mitochondrial toxins with different effects and molecular targets is known today[13]. Several of these toxins are natural products, such as the *Streptomyces*-derived ETC inhibitor antimycin A and the ATP synthase inhibitor oligomycin A.

Phomoxanthone A and B (PXA and PXB) are natural products named after the fungus *Phomopsis*, from which they were first isolated, and after their xanthonoid structure (Fig. S1). PXA is a homodimer of two acetylated tetrahydroxanthones symmetrically linked at C-4,4′,

whereas PXB is structurally almost identical but asymmetrically linked at C-2,4′. Both possess antibiotic activity against diverse organisms from all biological kingdoms. Originally described in 2001, PXA and PXB were tested against the protozoan *Plasmodium falciparum*, the Gram-positive *Mycobacterium tuberculosis*, and three animal cell lines. In all of these organisms, both PXA and PXB showed significant cytotoxic activity, with PXA being more toxic in every case[14]. A later study in different organisms produced similar results, showing that PXA inhibits the growth of the Gram-positive *Bacillus megaterium*, the alga *Chlorella fusca*, and the fungus *Ustilago violacea*[15].

We previously showed that PXA induces apoptosis in human cancer cell lines. Signs of apoptosis were observed as early as after 4 h of treatment with low micromolar doses of PXA[16,17]. However, the mechanism by which PXA causes apoptosis or cytotoxicity in general has never before been investigated.

The aim of this study was to elucidate the mechanism through which PXA exerts its toxicity. Following our initial results, we hypothesised that PXA directly affects the mitochondria and thus investigated its effects on the ETC, $\Delta\Psi_m$, ATP production, Ca^{2+} buffering, and mitochondrial morphology. It appears that PXA is a mitochondrial toxin that specifically affects the IMM, leading to loss of $\Delta\Psi_m$, ETC inhibition, Ca^{2+} efflux, mitochondrial fragmentation, cristae disruption, and finally to the release of mitochondrial pro-apoptotic factors.

Results

PXA induces Ca^{2+} release from an intracellular store

To determine how PXA induces apoptosis, we analysed its effect on cellular Ca^{2+} levels since ionic imbalance can be an apoptotic trigger. Treatment of Ramos cells with PXA resulted in a strong, steady increase of $[Ca^{2+}]_{cyt}$ (Fig. 1a). Interestingly, there was a delay of about 2–5 min between addition of PXA and increase in $[Ca^{2+}]_{cyt}$. Since this pattern of Ca^{2+} release is similar to that caused by the tyrosine phosphatase inhibitor pervanadate (VO_4^{3-}) (Fig. S2a), and since tyrosine phosphatase inhibition can induce apoptosis, we tested the effect of PXA on tyrosine phosphorylation. However, in contrast to pervanadate, we could not detect any effect (Fig. S2b). In a broader picture, PXA had no inhibitory effect on any of 141 protein kinases against which we tested it (Table S1).

We next tried to determine the origin of the released Ca^{2+}. Since PXA increases $[Ca^{2+}]_{cyt}$ even in the absence of extracellular Ca^{2+}, we tested if it releases Ca^{2+} from the ER. Using thapsigargin, which causes a net efflux of Ca^{2+} from the ER, we could induce an increase in $[Ca^{2+}]_{cyt}$ even after PXA-inducible Ca^{2+} stores were depleted
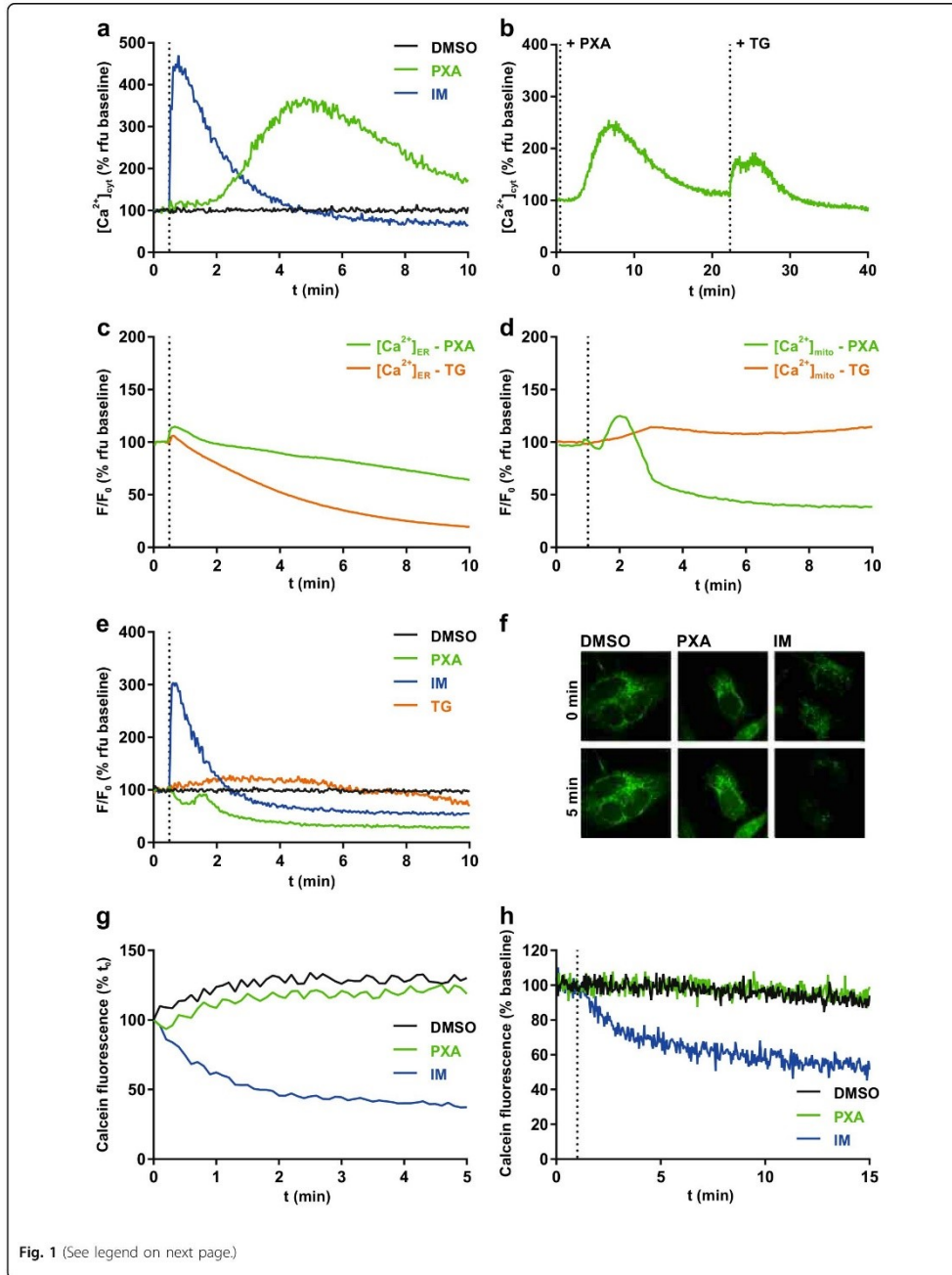
Fig. 1 (See legend on next page.)

Fig. 1 PXA causes an increase of [Ca^{2+}]$_{cyt}$ and a release of [Ca^{2+}]$_{mito}$ but not [Ca^{2+}]$_{ER}$. a Live measurement of the effect of PXA (10 μM) on [Ca^{2+}]$_{cyt}$ in Ramos cells, where DMSO (0.1% v/v) was used as vehicle control and ionomycin (IM; 2 μM) was used as positive control, and **b** live measurement of [Ca^{2+}]$_{cyt}$ after PXA followed by thapsigargin (TG; 10 μM). Measurements were performed by flow cytometry using the Ca^{2+}-sensitive fluorescent probe Fluo-4-AM (Ex 488 nm, Em 530 ± 30 nm) in the absence of extracellular Ca^{2+} by maintaining the cells in Krebs-Ringer buffer containing 0.5 mM EGTA during measurement. **c, d** Comparison of the effect of PXA (10 μM) and thapsigargin (TG; 1 μM) on either [Ca^{2+}]$_{ER}$ or [Ca^{2+}]$_{mito}$ as measured by the Ca^{2+}-sensitive fluorescent protein CEPIA targeted to the respective organelle in HeLa cells. All traces were normalised (F/F$_0$) where F$_0$ is the starting fluorescence of each trace. **e** Comparison of the effect of PXA (10 μM), ionomycin (IM; 2 μM), and thapsigargin (TG; 1 μM) on [Ca^{2+}]$_{mito}$ in Ramos cells stably transfected with the Ca^{2+}-sensitive ratiometric fluorescent protein mito-Pericam. DMSO (0.1% v/v) was used as vehicle control. F/F$_0$ is the ratio of fluorescence with excitation at 488 nm (high [Ca^{2+}]) to 405 nm (low Ca^{2+}). **f, g** Live imaging and quantification of the effect of PXA (10 μM) on mPTP opening in HeLa cells as measured by mitochondrial calcein fluorescence using the calcein/cobalt quenching method. DMSO (0.1% v/v) was used as vehicle control and ionomycin (IM; 2 μM) was used as positive control. Mitochondrial calcein fluorescence was quantified. **h** Additional live measurement of the effect of PXA on mPTP opening in Ramos cells by the calcein/cobalt quenching method using flow cytometry

(Fig. 1b), suggesting that the Ca^{2+} released by PXA at least partially originates from a source other than the ER.

PXA induces Ca^{2+} release mainly from the mitochondria

To quantify the effect of PXA on Ca^{2+} stores, we used HeLa cells expressing CEPIA Ca^{2+} probes targeted to either the ER or the mitochondria. Although PXA provoked some Ca^{2+} release from the ER, it was much slower and weaker than that evoked by thapsigargin (Fig. 1c). Mitochondria, however, were quickly and severely depleted (Fig. 1d). This effect of PXA on mitochondrial Ca^{2+} was confirmed in Ramos cells, making use of the Ca^{2+} probe Pericam (Fig. 1e).

Mitochondrial Ca^{2+} release caused by PXA is independent from the mPTP

Large-scale Ca^{2+} efflux from the mitochondria can result from persistent opening of the mPTP. We thus tested whether PXA induces mPTP opening by using the cobalt/calcein method, comparing PXA to the mPTP inducer ionomycin (IM). While IM caused a strong decrease in mitochondrial calcein fluorescence as expected, PXA had no observable effect (Fig. 1f, g; Supplementary Movies S1–S3). Similar results were obtained by further live measurement using flow cytometry (Fig. 1h). In addition, we tested whether the mPTP inhibitor cyclosporin A (CsA) can prevent the mitochondrial Ca^{2+} release caused by PXA. We measured mitochondrial Ca^{2+} retention capacity in isolated mitochondria, comparing PXA to IM and CCCP. This was done in either normal isolated mitochondria or mitochondria loaded with Ca^{2+}, and in the presence of either CsA or its derivative cyclosporin H (CsH), which does not affect the mPTP (Fig. 2)[18]. While PXA caused a decrease in calcium green fluorescence, indicating Ca^{2+} release, under every condition, i.e., regardless of Ca^{2+} loading and also in the presence of CsA, IM had an observable effect only in loaded mitochondria, but also regardless of CsA. On the other hand, CCCP caused a release of Ca^{2+} only in the presence of CsH but not CsA, indicating that CCCP-induced Ca^{2+} release does indeed depend on the mPTP, unlike that

induced by PXA. Taken together, these results indicate that PXA causes mitochondrial Ca^{2+} release largely independent from the mPTP.

PXA depolarises the mitochondria but does not uncouple cellular respiration

A change in [Ca^{2+}]$_{mito}$ likely correlates with changes in other mitochondrial ion gradients. Uptake of Ca^{2+} into the mitochondrial matrix is driven by ΔΨ$_m$. We thus analysed the effect of PXA on ΔΨ$_m$. Indeed, PXA caused immediate mitochondrial depolarisation similar to CCCP, both in whole cells and isolated mitochondria (Fig. 3a, b). The EC$_{50}$ for PXA-induced loss of ΔΨ$_m$ in Ramos cells was determined to be 1.1 ± 0.3 μM (Fig. S3). The key contributor to ΔΨ$_m$ is ΔpH$_m$, which is maintained via cellular respiration by consumption of O$_2$. If the PXA-induced loss of ΔΨ$_m$ was caused by loss of ΔpH$_m$ downstream of the ETC, as in case of CCCP, it would be accompanied by an increase in respiration to compensate for the loss. Therefore, we measured cellular O$_2$ consumption upon increasing concentrations of either PXA or CCCP. As expected, CCCP caused a dose-dependent increase in O$_2$ consumption. However, in contrast to CCCP, PXA caused no increase but rather a slight decrease in O$_2$ consumption (Fig. 3c). An overview of the kinetics of the effects of PXA on [Ca^{2+}]$_{cyt}$, [Ca^{2+}]$_{mito}$, O$_2$ consumption and ΔΨ$_m$ is presented in Fig. 3d.

PXA inhibits cellular respiration by disrupting the electron transport chain

Since PXA had a moderate inhibitory effect on cellular O$_2$ consumption under basal conditions, we next measured O$_2$ consumption after the respiration rate was first increased by CCCP. Here, treatment with PXA caused a strong decrease in O$_2$ consumption to levels below baseline (Fig. 4a). It thus appeared likely that PXA, unlike CCCP, is not an inducer but rather an inhibitor of cellular respiration and of the ETC. We, therefore, compared PXA to known ETC inhibitors: rotenone (complex I), thenoyltrifluoroacetone (TTFA; complex II), antimycin A (complex III), sodium azide (NaN$_3$; complex IV) and

Fig. 2 Live measurement of the effect of PXA on mitochondrial Ca^{2+} retention capacity. Isolated mitochondria were stained with calcium green AM and maintained in the presence of either (**a**, **c**) CsH or (**b**, **d**) CsA, and fluorescence was measured either (**a**, **b**) directly after staining or (**c**, **d**) after first loading the mitochondria with 150 μM Ca^{2+}
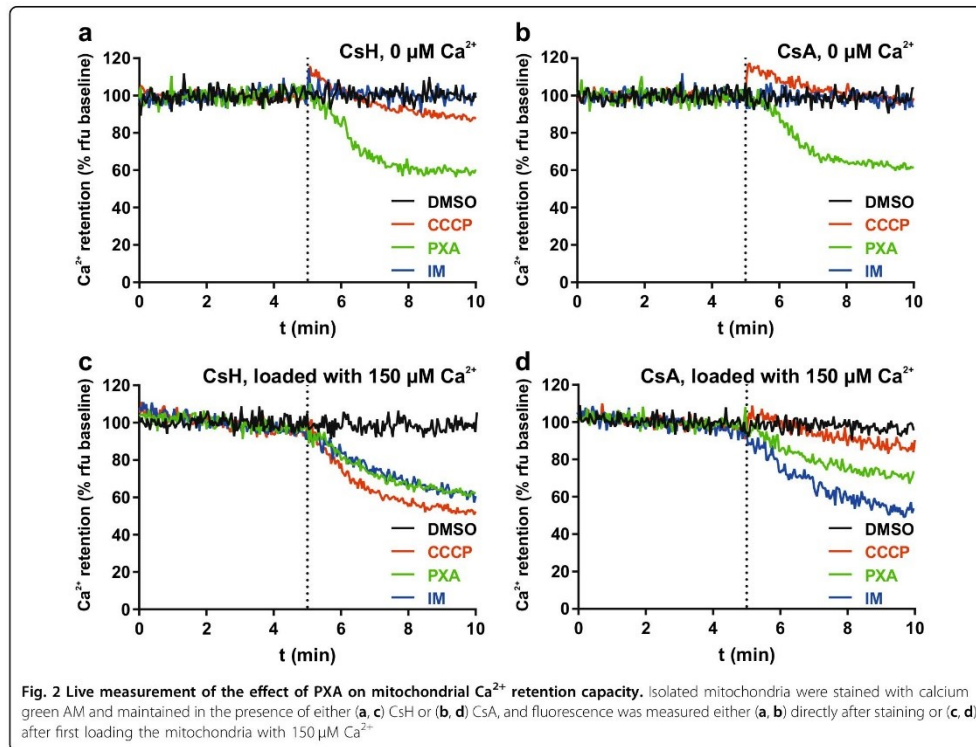
oligomycin A (complex V / ATP synthase). In an O$_2$ consumption assay, PXA caused a strong decrease in cellular respiration, both after CCCP treatment and under basal conditions, similar to that caused by rotenone, antimycin A and azide (Fig. 4b). Oligomycin A expectedly inhibited respiration under basal conditions but not after CCCP treatment since CCCP uncouples respiration from ATP synthesis. TTFA did not have a significant effect, probably because complex II is not involved in respiration if complex I substrates are available[19].

Since a functional ETC is required for ATP synthesis by OXPHOS, we also compared PXA to known ETC inhibitors in this context. Indeed, PXA as well as all tested ETC inhibitors strongly reduced cellular ATP levels if galactose was the only available sugar and ATP had to be synthesised via OXPHOS instead of glycolysis (Fig. 4c). Thus assuming that PXA targets the ETC, we tried to determine if it specifically inhibits one of the ETC complexes. This experiment was performed in permeabilized cells, comparing PXA to rotenone. Succinate, which induces complex II-dependent respiration only if complex I is inhibited, alleviated rotenone-induced inhibition of O$_2$

consumption but had only a marginal effect in PXA-treated cells. In contrast, duroquinol, which induces complex III-dependent respiration, increased O$_2$ consumption in both PXA-treated as well as rotenone-treated cells back to levels before inhibition (Fig. 4d). These data suggest that PXA might either affect both complex I and II or the shuttling of electrons between complex I/II and III.

Comparison of PXA with other ETC inhibitors

While PXA inhibits the ETC as well as ATP synthesis, it differs from the other ETC inhibitors used in this study concerning its effects on Ca^{2+} and ΔΨ$_m$. Unlike PXA, neither CCCP nor any of the tested ETC inhibitors with the exception of antimycin A caused a noticeable release of Ca^{2+} (Fig. S4a), and that caused by antimycin A was much weaker and had an earlier but slower onset than the one caused by PXA. Similarly, while both CCCP and PXA induced a strong and immediate decrease in ΔΨ$_m$, none of the other ETC inhibitors except antimycin A had any effect on ΔΨ$_m$, and that of antimycin A was much slower and weaker (Fig. S4b). Since we previously

Fig. 3 PXA dissipates the mitochondrial membrane potential ($\Delta\Psi_m$) but does not increase cellular respiration. a Live measurement of the effect of PXA (10 μM) on $\Delta\Psi_m$ in Ramos cells. Measurements were performed by flow cytometry using the $\Delta\Psi_m$-sensitive fluorescent probe TMRE (Ex 488 nm, Em 575 ± 26 nm). A decrease in TMRE fluorescence corresponds to a decrease in $\Delta\Psi_m$. The protonophore carbonyl cyanide *m*-chlorophenyl hydrazone (CCCP; 10 μM) was used as positive control for mitochondrial depolarization. **b** Live measurement of the effect of PXA (10 μM) $\Delta\Psi_m$ in isolated mitochondria. Measurements were performed by flow cytometry using the $\Delta\Psi_m$-sensitive fluorescent probe TMRM (Ex 488 nm, Em 575 ± 26 nm). The mitochondria were maintained in the presence of 1.6 μM CsH to prevent passive TMRM leakage. **c** Titration of PXA to determine the effect on cellular respiration in Ramos cells as measured by oxygen consumption. CCCP was used as positive control for increase of respiration. Measurement of extracellular [O$_2$] was performed using an oxygraph. **d** Comparison of the kinetics of the effects of PXA on [Ca^{2+}]$_{cyt}$ (as measured by Fluo-4-AM fluorescence), [Ca^{2+}]$_{mito}$ (as measured by mito-Pericam fluorescence), O$_2$ consumption (as measured by changes in extracellular [O$_2$]) and $\Delta\Psi_m$ (as measured by TMRE fluorescence). Graphs were partially adapted from other figures

showed that PXA is cytotoxic and induces apoptosis, we also compared it to CCCP, ETC inhibitors, IM (control for Ca^{2+} release) and staurosporine (control for cyto-toxicity/apoptosis) in these regards. PXA, staurosporine and CCCP strongly induced apoptosis, while the ETC inhibitors and IM were much weaker inducers in Ramos cells and did not noticeably induce apoptosis at all in Jurkat cells (Fig. 5a, b). Dependency on OXPHOS for ATP synthesis, which considerably increased the toxicity of the ETC inhibitors, appeared to have no effect on the toxicity of PXA or staurosporine (Fig. 5c, d). These observations indicate that PXA probably causes cyto-toxicity in general and apoptosis in particular not via its effects on the ETC, $\Delta\Psi_m$, or [Ca^{2+}]$_{mito}$, but rather that all of these events might have a common cause further upstream.

PXA causes irreversible cleavage of OPA1 mediated by OMA1 but not YME1L1

Several stress conditions including loss of $\Delta\Psi_m$ and low levels of ATP can induce cleavage of the IMM fusion regulator OPA1 by the protease OMA1 (ref. [20]). Addi-tionally, OPA1 is also cleaved by the protease YME1L1, resulting in fragments of different size. We treated MEF cells deficient for either one or both of these proteases with either PXA or CCCP. We observed that PXA, like CCCP, caused stress-induced OPA1 cleavage that was dependent on OMA1, whereas expression of YME1L1 did not have any visible effect on PXA-induced OPA1 clea-vage (Fig. 6a). Similarly to their effect in MEF cells, PXA and CCCP-induced cleavage of OPA1 in Ramos and Jurkat cells within minutes. Interestingly, and unlike CCCP, removal of PXA did not enable recovery of the

Fig. 4 Effect of PXA on electron transport chain and OXPHOS. a Live measurement of the effect of PXA on uncoupled cellular respiration in intact Ramos cells. Cells were first treated with 1 μM CCCP to uncouple respiration and then with either 10 μM PXA or 0.1% v/v DMSO (vehicle control) to test for inhibition. Measurement of extracellular [O₂] was performed using an oxygraph. **b** Comparative measurements of the effect of PXA and other compounds on basal and uncoupled respiration in Ramos cells. Respiration was uncoupled by CCCP (1 μM). PXA (10 μM) was compared to the complex-specific ETC inhibitors rotenone (Rot; complex I; 10 μM), thenoyltrifluoroacetone (TTFA; complex II; 10 μM), antimycin A (AmA; complex III; 10 μM), azide (NaN₃; complex IV; 1 mM) and oligomycin A (OmA; complex V; 10 μM). Measurement was performed in a microplate reader using the fluorescence-based *MITO-ID® Extracellular O2 Sensor Kit (High Sensitivity)* (Enzo). **c** Comparative measurements of the effect of PXA and other compounds on ATP levels in Ramos cells after 120 min of treatment. PXA (10 μM) was compared to complex-specific ETC inhibitors (see above) as well as CCCP (1 μM). Measurement was performed in a microplate reader using the luminescence-based *Mitochondrial ToxGlo™ Assay* (Promega). Cells were incubated in full growth medium containing either glucose or galactose as the only available sugar. Galactose alone forces the cells to resort exclusively to OXPHOS for ATP synthesis. **d** Live measurement of mitochondrial respiration in Ramos cells permeabilized by digitonin (Digi; 5 μg/ml). The effect of PXA (first 1 μM, then increased to 10 μM as indicated) was compared to that of the known complex I inhibitor rotenone (Rot; 1 μM). To specifically induce complex II and III of the electron transport chain, succinate (Succ; 10 mM) and duroquinol (Duro; 1 mM) were used, respectively. Measurement of extracellular [O₂] was performed using an oxygraph
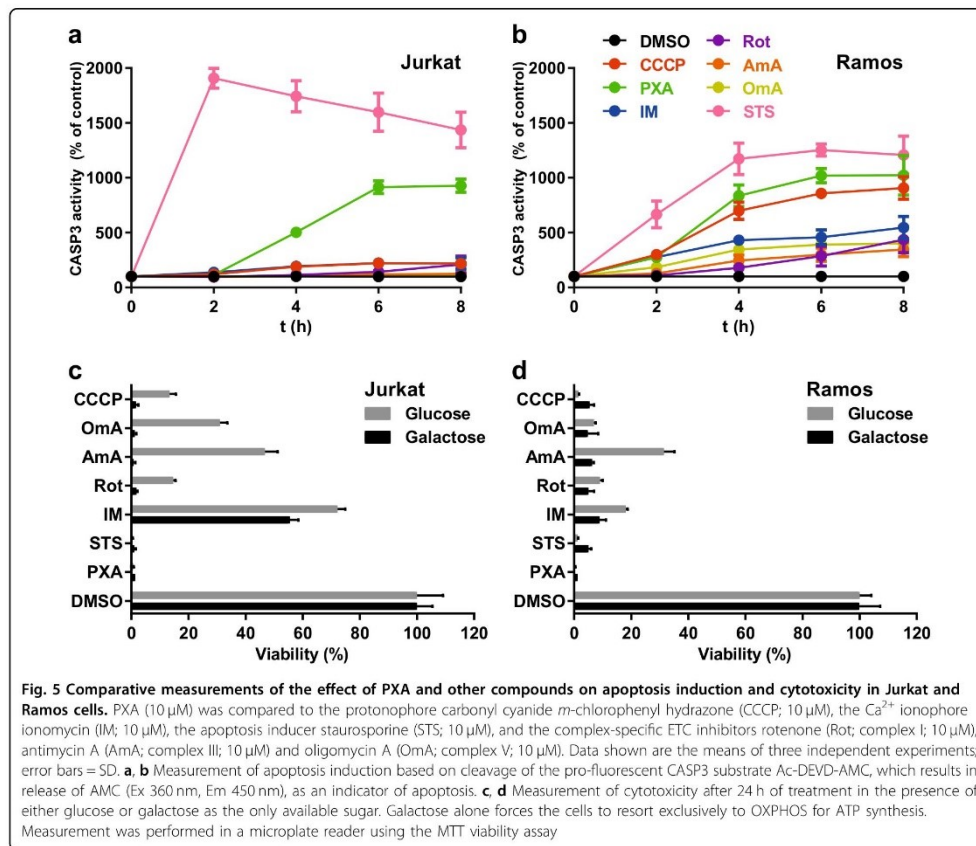
long OPA1 forms (Fig. 6b). This prompted us to also investigate the effects of removal of PXA on cytotoxicity. Indeed, though PXA was about fivefold less toxic if removed after a few minutes, it still irreversibly primed the cells for death (Fig. 6c). It, thus, appears that at least some of the effects of PXA on the cells are irreversible.

PXA induces fragmentation of the inner but not of the outer mitochondrial membrane independently of OMA1, OPA1 and DRP1

Excessive processing of OPA1 by OMA1 changes mitochondrial cristae morphology, resulting in the release of pro-apoptotic factors such as CYCS and SMAC. We,

therefore, investigated the effects of PXA on SMAC localisation and on recruitment of BAX to the OMM. We observed that PXA indeed induced recruitment of GFP-BAX to the mitochondria, with concurrent release of SMAC-mCherry into the cytosol, within about 2–3 h (Fig. 7a and Supplementary Movie S4; quantification shown in Fig. S5). OPA1 processing by OMA1 also prevents IMM fusion and, if excessive, results in mitochondrial fragmentation. Intriguingly, PXA caused rapid fragmentation of the mitochondrial network within minutes (Fig. 7b), and independent of the cells' OMA1 or YME1L1 status (Fig. 7c, left panels; Supplementary Movies S5–S7). The persistence of PXA-induced

Fig. 5 Comparative measurements of the effect of PXA and other compounds on apoptosis induction and cytotoxicity in Jurkat and Ramos cells. PXA (10 μM) was compared to the protonophore carbonyl cyanide *m*-chlorophenyl hydrazone (CCCP; 10 μM), the Ca^{2+} ionophore ionomycin (IM; 10 μM), the apoptosis inducer staurosporine (STS; 10 μM), and the complex-specific ETC inhibitors rotenone (Rot; complex I; 10 μM), antimycin A (AmA; complex III; 10 μM) and oligomycin A (OmA; complex V; 10 μM). Data shown are the means of three independent experiments; error bars = SD. **a**, **b** Measurement of apoptosis induction based on cleavage of the pro-fluorescent CASP3 substrate Ac-DEVD-AMC, which results in release of AMC (Ex 360 nm, Em 450 nm), as an indicator of apoptosis. **c**, **d** Measurement of cytotoxicity after 24 h of treatment in the presence of either glucose or galactose as the only available sugar. Galactose alone forces the cells to resort exclusively to OXPHOS for ATP synthesis. Measurement was performed in a microplate reader using the MTT viability assay
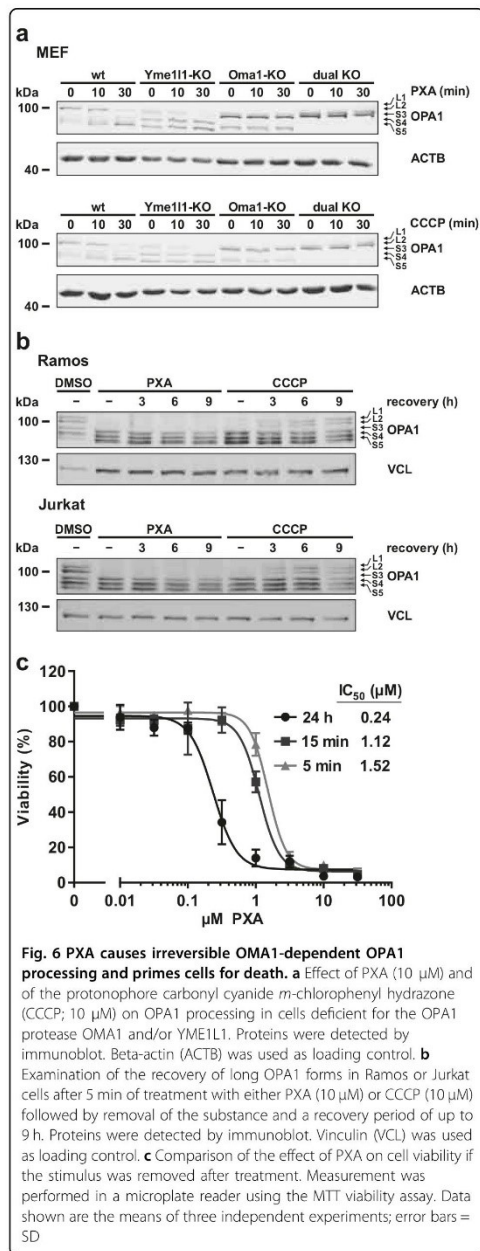
mitochondrial fragmentation in OMA1-YME1L1 DKO cells indicates that this process is independent of OPA1 cleavage.

Mitochondrial fission is also regulated by the dynamin DRP1, which mediates OMM fission. We, thus, tested the effect of PXA on the mitochondrial morphology in DRP1-deficient MEF cells. Again, fragmentation was observed within minutes after treatment (Fig. 7c, right panel; Supplementary Movie S8). We next used dual staining of both the matrix (via HSP60) as well as the OMM (via TOMM20) to determine whether both or only one of these structures are affected by PXA. CCCP was used as a positive control for fragmentation. As expected, CCCP could not induce fragmentation in DRP1-KO cells, and in WT cells it induced fragmentation of both the IMM and OMM together (Fig. 8a, b). In contrast, in the WT cells treated with PXA, fragmentation was much stronger and resulted in smaller fragments. More intriguingly, in

DRP1-KO cells treated with PXA, only the matrix appeared to have fragmented, whereas the OMM appeared to have shrunken around the matrix fragments but otherwise remained connected (Fig. 8a, b). This effect could also be observed in cells deficient for both DRP1 and OPA1 (Fig. S6) demonstrating that PXA acts independently of canonical regulators of mitochondrial fission. Finally, a close examination of the mitochondrial ultrastructure by transmission electron microscopy (TEM) revealed that PXA causes OMA1-independent disruption of mitochondrial matrix morphology, complete loss of cristae, and condensation of IMM structures at the OMM (Fig. 8c).

Taken together, our results show that PXA disturbs mitochondrial form and function in several ways. Some effects, such as the rapid inhibition of both $\Delta\Psi_m$ and the ETC at the same time, the delayed release of mitochondrial Ca^{2+}, and the fragmentation of the inner but not the

Fig. 6 PXA causes irreversible OMA1-dependent OPA1 processing and primes cells for death. a Effect of PXA (10 μM) and of the protonophore carbonyl cyanide *m*-chlorophenyl hydrazone (CCCP; 10 μM) on OPA1 processing in cells deficient for the OPA1 protease OMA1 and/or YME1L1. Proteins were detected by immunoblot. Beta-actin (ACTB) was used as loading control. **b** Examination of the recovery of long OPA1 forms in Ramos or Jurkat cells after 5 min of treatment with either PXA (10 μM) or CCCP (10 μM) followed by removal of the substance and a recovery period of up to 9 h. Proteins were detected by immunoblot. Vinculin (VCL) was used as loading control. **c** Comparison of the effect of PXA on cell viability if the stimulus was removed after treatment. Measurement was performed in a microplate reader using the MTT viability assay. Data shown are the means of three independent experiments; error bars = SD

outer mitochondrial membrane, are unique and indicate a mode of action that is distinct from all other compounds to which it was compared in this study.

Discussion

The mycotoxin PXA is a toxic natural product whose mechanism of action has so far remained elusive. We provide evidence that PXA disrupts mitochondrial function and causes IMM fragmentation and cristae disruption independently of DRP1 and OPA1, leading to the release of pro-apoptotic factors and ultimately to apoptosis.

PXA, just like CCCP, dissipates $\Delta\Psi_m$ within seconds. In the case of CCCP, respiration increases to compensate this, whereas PXA has the opposite effect and blocks respiration. Conversely, respiration is also blocked by ETC inhibitors, yet in contrast to PXA, these do not strongly affect $\Delta\Psi_m$. This suggests an entirely different mode of action for PXA. Additionally, unlike any of these compounds, PXA causes a strong mitochondrial release of Ca^{2+} and rapid fragmentation of the IMM but not the OMM.

Release of mitochondrial Ca^{2+} and loss of $\Delta\Psi_m$ can be results of persistent mPTP opening, yet we showed that PXA does not strongly affect the mPTP. Since mitochondrial ion gradients are interdependent through various antiporters that are generally linked to $\Delta\Psi_m$ (ref. [2]), one might assume that loss of $\Delta\Psi_m$ disturbs these gradients sufficiently to induce a net Ca^{2+} efflux from the mitochondria. For CCCP, contradictory results have been reported—in some cases it caused Ca^{2+} release[21], in some cases it did not[22]. We observed no effect of CCCP and most ETC inhibitors on $[Ca^{2+}]_{cyt}$, and in fact both ETC-deficient (ρ^0) mitochondria[23] and depolarised mitochondria[24] can still facilitate a net uptake of Ca^{2+}. It, thus, appears that the mitochondrial Ca^{2+} release induced by PXA is not necessarily a result of its effects on the ETC and $\Delta\Psi_m$, but rather that all of these effects might have a common cause.

The delay between addition of PXA and the first observable increase in $[Ca^{2+}]_{cyt}$ and decrease in $[Ca^{2+}]_{mito}$ contrasts with the immediate change in $\Delta\Psi_m$ (Fig. 3d). This discrepancy could possibly be explained by the hypothesis that mitochondria release Ca^{2+} mainly into the cristae, and that the cristae junctions may function as bottlenecks for mitochondrial Ca^{2+} transport[8,25]. Cristae junctions are regulated by OPA1, which is cleaved by OMA1 in response to mitochondrial stress, leading to cristae disruption[26]. We not only showed that OPA1 is irreversibly cleaved by OMA1 upon PXA treatment, but that PXA also causes cristae disruption independently of OMA1. Thus, PXA-induced cristae disruption might cause the release of Ca^{2+} from the cristae and thus eventually into the cytosol. In addition, irreversible cristae

Fig. 7 Effects of PXA on mitochondrial integrity and morphology. a Confocal live imaging of a HCT116 cell expressing GFP-BAX (green) and SMAC-mCherry (magenta) after treatment with 10 μM PXA. **b** Confocal live imaging of a HeLa cell stably expressing the fluorescent dye mito-DsRed, which localises to the mitochondrial matrix, after treatment with 10 μM PXA. **c** Confocal live imaging of MEF cells (WT, OMA1-KO, OMA1-YME1L1-DKO and DRP1-KO) before and after treatment with 10 μM PXA. The cells are stably expressing the fluorescent dye mito-DsRed, which localises to the mitochondrial matrix. All scale bars are equivalent to 10 μm

disruption could well be a sufficient condition for the release of pro-apoptotic factors and thus the induction of apoptosis[26–28].

OPA1 also affects the fragmentation of mitochondrial network structures, which can be induced by PXA as well as CCCP. In the case of CCCP, this is commonly explained by the excessive activation of DRP1 after increased OPA1 processing by OMA1, which in turn is a response to several kinds of cellular stress including impaired ATP production and loss of $\Delta\Psi_m$ (ref. [4,6,20,29–32]). Since PXA dissipates $\Delta\Psi_m$, inhibits ATP production and consequently induces OMA1-mediated OPA1 cleavage, one might assume that it induces fragmentation via the same mechanism, yet we observed PXA-induced fragmentation events that were independent of DRP1, OMA1 and even OPA1.

Mitochondrial fragmentation independent of DRP1 is an unusual phenomenon but has been reported in cells undergoing apoptosis after pro-apoptotic factors had already been released[33,34]. In the case of PXA, however, fragmentation occurs within minutes after treatment, whereas pro-apoptotic factors are released only after several hours. In addition, whereas both the OMM and IMM are divided together during DRP1-dependent fragmentation, PXA can cause exclusive fragmentation of the IMM while the OMM remains intact. This is surprising since no active mechanism for exclusive IMM fission is known in higher eukaryotes, and there are only few reports documenting this phenomenon[6,35,36].

The OMA1-processed short OPA1 forms play a role in IMM fission and cristae morphology[5,29,35]. However, since PXA-induced IMM fragmentation and cristae disruption are independent of both OMA1 and OPA1, this implies that OPA1 may well be an IMM fission regulator but not necessarily a fission executor. It has been recently proposed that OPA1 is dispensable for cristae junction biogenesis but may still be required for cristae junction remodelling[37]. Our results suggest that excessive OPA1 processing may be sufficient but not necessary for inner membrane remodelling and cristae disruption and for the consequent release of pro-apoptotic factors.

The independence of PXA-induced IMM fragmentation from DRP1, OMA1 and OPA1, as well as its very fast onset, suggest that it might not depend on the fission/fusion machinery at all, but could work via a completely separate mechanism. Since no such mechanism is known

Fig. 8 Effect of PXA on mitochondrial matrix morphology. a Confocal images of MEF cells (WT and DRP1-KO) at 30 min after treatment with either 0.1% v/v DMSO (vehicle control), 10 μM CCCP (positive control for fragmentation) or 10 μM PXA. HSP60 (green) was stained as a marker for the mitochondrial matrix, and TOMM20 (red) was stained as a marker for the outer mitochondrial membrane (OMM). Scale bars are equivalent to 10 μm. **b** Quantification of mitochondrial morphology by classification of 200 individual cells in each of three independent experiments; error bars = SD. **c** Transmission electron microscopy images of MEF cells (WT or OMA1-KO) after treatment with either 10 μM PXA or with 0.1% v/v DMSO (vehicle control) for 30 min. Scale bars are equivalent to 0.5 μm

in higher eukaryotes, any attempt at explaining this effect remains speculative. One explanation could be a change in IMM fluidity or matrix architecture, causing an immediate and strong retraction of the IMM. This could result from interference with the tethering of IMM and OMM at mitochondrial contact sites. If this is the case, a possible mechanistic target of PXA could be the mitochondrial phospholipid cardiolipin, which is present almost exclusively in the IMM and especially at mitochondrial contact sites[38,39]. Cardiolipin serves as a membrane anchor for many proteins that are implicated in mitochondrial contact site formation, mitochondrial ultrastructure and the ETC, such as MIC27 (APOOL)[40,41], F_1F_O ATP synthase[41,42], CYCS[41], and ETC complexes III and IV[41,43,44]. A disruptive interaction between PXA and either cardiolipin or cardiolipin-binding proteins might thus explain several of the effects induced by PXA.

In summary, we identified PXA as a mitochondrial toxin with a mode of action distinct from known ETC inhibitors, OXPHOS uncouplers, and ionophores. Its effects, such as the rapid inhibition of both ETC and $\Delta\Psi_m$, the release of mitochondrial Ca^{2+}, and the induction of DRP1- and OPA1-independent cristae disruption and fission of the inner but not the outer mitochondrial membrane, might render it a useful tool in studying these phenomena. Further studies may reveal the molecular target of PXA and the mechanisms through which it induces mitochondrial Ca^{2+} release and IMM fission.

Material and methods
Cell lines and cell culture
Jurkat cells were obtained from DSMZ (#ACC-282). Ramos cells were kindly provided by Michael Engelke (Institute of Cellular and Molecular Immunology, University Hospital Göttingen, Göttingen, Germany). HeLa cells stably expressing mito-DsRed were kindly provided by Aviva M. Tolkovsky (Department of Clinical Neurosciences, University of Cambridge, England, UK) and have been described previously[45]. MEF cells deficient for OMA1 and/or YME1L1 as well as the corresponding wild-type cells were generated by Ruchika Anand and kindly provided by Thomas Langer (Institute for Genetics, University of Cologne, Germany) and have been described previously[29]. MEF cells deficient for DRP1 as well as the corresponding wild-type cells used for live imaging were kindly provided by Hiromi Sesaki (Department of Cell Biology, Johns Hopkins University, Baltimore, MD, USA) and have been described previously[33]. MEF cells deficient for DRP1 used for imaging of fixed cells were generated using the CRISPR/Cas9 system as described previously[46]. The DNA target sequence for the guide RNA was 5'-CAGTGGGAAGAGCTCAGTGC-3'. HCT116 cells were kindly provided by Frank Essmann (Interfaculty Institute of Biochemistry, Eberhard Karls University Tübingen,

Germany). Transient expression of SMAC-mCherry and GFP-BAX was achieved by lipofection at 70–80% confluence using Lipofectamine 2000 (Life Technologies, Darmstadt, Germany). Cells were incubated with 0.15 µl Lipofectamine 2000, 50 ng pcDNA3-Smac(1-60)mCherry (Addgene ID 40880; this plasmid was kindly provided by Stephen Tait (Beatson Institute, University of Glasgow, Scotland, UK) and has been described previously[47]), and 50 ng pGFP-Bax (kindly provided by Nathan R. Brady, Department of Molecular Microbiology and Immunology, Johns Hopkins University, Baltimore, MD, USA) per well in glass bottom 8-well chambers (Ibidi, Planegg, Germany) for 16 h. HeLa cells used for Ca^{2+} measurements were cultured in Dulbecco's modified Eagle's medium supplemented with 10% fetal calf serum (FCS) and 4 mM L-glutamine, 100 U/ml penicillin and 100 µg/ml streptomycin at 37 °C and 5% CO_2. They were authenticated using autosomal STR profiling performed by the University of Arizona Genetics Core and they fully matched the DNA fingerprint present in reference databases. Cell lines stably expressing either mito-DsRed (except HeLa; see above) or ratiometric mito-Pericam were generated by retroviral transfection using the Platinum-E (Plat-E) packaging cell line (kindly provided by Toshio Kitamura, Institute of Medical Science, University of Tokyo, Japan) and the retroviral vectors pMSCVpuro-mito-DsRed1 (Addgene ID 87379) or pMSCVpuro-mito-Pericam (Addgene ID 87381). The medium used for the cultivation of Jurkat cells and Ramos cells was RPMI 1640 medium, and the medium used for cultivation of HCT116 cells was McCoy's 5A medium. All other cells were cultivated in high-glucose Dulbecco's Modified Eagle's medium (DMEM). All media were supplemented with 10% FCS, 100 U/ml penicillin, and 100 µg/ml streptomycin. All cell lines were maintained at 37 °C and 5% CO_2 in a humidity-saturated atmosphere.

Reagents
Phomoxanthone A was isolated and purified as described previously[16]. We found that PXA becomes unstable if dissolved in dimethyl sulfoxide (DMSO) and readily isomerises into the essentially non-toxic compound dicerandrol C (data not shown), in a process similar to the one previously described for the structurally related secalonic acids[48]. However, PXA is barely soluble in EtOH and not soluble in H_2O. Therefore, PXA was prepared in small lyophilised aliquots and only dissolved in DMSO immediately before usage.

The tyrosine phosphatase inhibitor pervanadate (VO_4^{3-}) was freshly prepared by mixing 30 mM sodium orthovanadate with 60 mM H_2O_2 in phosphate-buffered saline (PBS) and incubating at room temperature (RT) in the dark for 10 min; sodium orthovanadate was purchased from Sigma (Munich, Germany), #450243; IM from

Sigma, #I9657; thapsigargin (TG) from Sigma, #T9033; carbonyl cyanide *m*-chlorophenyl hydrazone (CCCP) from Sigma, #C2759; rotenone from Sigma, #45656; thenoyltrifluoroacetone (TTFA) from Sigma, #88300; antimycin A from Sigma, #A8674; sodium azide (NaN$_3$) from Sigma, #S2002; oligomycin A from Toronto Research Chemicals (Toronto, Canada), #O532970; staurosporine (STS) from LC Laboratories (Woburn, MA, USA), #9300. All cell culture reagents were purchased from Life Technologies, and all other reagents where no manufacturer is explicitly mentioned were purchased from Carl Roth GmbH (Karlsruhe, Germany).

Replicates and statistical analysis

Experiments were replicated at least three times, and representative data are shown. Error bars indicate standard deviation. All statistical analysis was performed using Prism v7.01 (GraphPad Software, La Jolla, CA, USA).

In vitro kinase activity screening

The effect of PXA on the activity of 141 protein kinases was assessed by the International Centre for Kinase Profiling (Dundee, Scotland, UK) using a radioactive filter binding assay with ^{33}P ATP[49,50].

Live measurement of [Ca^{2+}]$_{cyt}$ by Fluo-4-AM

Cells were stained by incubation in growth medium containing 1 µM Fluo-4-AM (Life Technologies; #F14201), 0.005% w/v Pluronic F-127 (Sigma, #540025), 10 mM HEPES and 5% v/v FCS at 30 °C. After 25 min, an equal volume of full growth medium was added, the temperature was increased to 37 °C, and the cells were incubated for another 10 min. After that, the cells were washed and resuspended in Krebs-Ringer buffer (10 mM HEPES pH 7.0, 140 mM NaCl, 4 mM KCl, 1 mM MgCl$_2$, 10 mM glucose) supplemented with 1 mM CaCl$_2$. The cells were kept at RT in the dark until measurement. Just before measurement, the cells were washed and resuspended in Krebs-Ringer buffer supplemented with 0.5 mM EGTA. Fluo-4-AM fluorescence was measured live using an LSRFortessa flow cytometer (BD, Franklin Lakes, NJ, USA) recording fluorescence in the FITC channel (Ex 488 nm, Em 530 ± 30 nm). For each sample, after at least 30 s of baseline measurement, the stimulus was added and measurement was continued for at least 10 min.

Live measurement of [Ca^{2+}]$_{mito}$ and [Ca^{2+}]$_{ER}$ by CEPIA

Measurements of [Ca^{2+}]$_{mito}$ and [Ca^{2+}]$_{ER}$ in HeLa single cells were performed as described previously[51,52], using the genetically-encoded Ca^{2+} indicators CEPIA3mt (Addgene ID 58219) and G-CEPIA1er (Addgene ID 58215), respectively, which were developed by Dr. M. Iino (The University of Tokyo, Japan)[53]. The constructs were

introduced into HeLa cells utilising the X-tremeGENE HP DNA transfection reagent (Roche, Mannheim, Germany) according to the manufacturer's protocol. The [Ca^{2+}] measurements were performed 48 h after transfection using a Zeiss Axio Observer Z1 Inverted Microscope equipped with a 20 × air objective and a high-speed digital camera (Axiocam Hsm, Zeiss, Jena, Germany). Changes in fluorescence were monitored in the GFP channel (Ex 480 nm, Em 520 nm). Extracellular Ca^{2+} was chelated with 3 mM EGTA, and PXA (10 µM) or thapsigargin (1 µM) were added as indicated on the figures. All traces were normalised (F/F_0) where F_0 is the starting fluorescence of each trace.

Live measurement of [Ca^{2+}]$_{mito}$ by ratiometric mito-Pericam

Ramos cells stably transfected with ratiometric mito-Pericam as described above were used for this measurement. Ratiometric mito-Pericam is a Ca^{2+}-sensitive fluorescent protein and was described previously[54,55]. An increase in [Ca^{2+}] causes a shift of the Pericam excitation maximum from ~410 to ~495 nm while the emission peak remains at ~515 nm. Pericam fluorescence was measured live using an LSRFortessa flow cytometer recording fluorescence in both the FITC channel (Ex 488 nm, Em 530 ± 30 nm) and the AmCyan channel (Ex 405 nm, Em 525 ± 50 nm). For each sample, after at least 30 s of baseline measurement, the stimulus was added and measurement was continued for at least 10 min. The ratio of fluorescence with excitation at 488 to 405 nm was calculated.

Live measurement of mPTP opening by cobalt-calcein assay

This method was adapted from previously published protocols[10,18,56]. The cells were stained by incubation in Krebs-Ringer buffer supplemented with 1 mM CaCl$_2$, 1 mM CoCl$_2$, and 1 µM calcein-AM (Life Technologies, #65-0853-78) at 37 °C for 30 min. After that, the cells were washed and maintained in Krebs-Ringer buffer supplemented with 1 mM CaCl$_2$ and 1.6 µM cyclosporin H (CsH) to prevent passive efflux of calcein. For live measurement by confocal microscopy, imaging and quantification were performed using a Perkin Elmer Spinning Disc microscope with a 60× objective (oil-immersion and NA = 1.49) at an excitation wavelength of 488 nm. The videos were obtained at 1000 × 1000 pixel resolution with a Hamamatsu C9100 camera. Additional live measurement by flow cytometry was performed using an LSRFortessa flow cytometer recording fluorescence in the FITC channel (Ex 488 nm, Em 530 ± 30 nm). For each sample, after at least 30 s of baseline measurement, the stimulus was added and measurement was continued for at least 10 min.

Isolation of live mitochondria

Adherent cells were harvested by a cell scraper. All cells were pelletised by centrifugation at 600 rcf, resuspended in ice-cold mitochondria isolation buffer (210 mM mannitol, 70 mM sucrose, 1 mM K_2EDTA, 20 mM HEPES), and passed through a 23 G needle ten times. The resulting suspension was centrifuged at 600 rcf and the supernatant was transferred to a new tube and centrifuged at 6500 rcf and 4 °C for 15 min. The resulting mitochondrial pellet was resuspended in sodium-free mitochondrial respiration buffer MiR05 (0.5 mM EGTA, 3 mM $MgCl_2$, 60 mM lactobionic acid, 20 mM taurine, 10 mM KH_2PO_4, 20 mM HEPES, 110 mM D-sucrose, 0.1% w/v fatty-acid-free bovine serum albumin [BSA]) supplemented with 10 mM succinate and 5 mM malate.

Live measurement of mitochondrial Ca^{2+} retention capacity by calcium green

Live mitochondria isolated as described above were stained by incubation in MiR05 buffer supplemented with 10 mM succinate, 5 mM malate, and 1 µM calcium green AM (Life Technologies, #C3012) for 20 min on a shaker at 37 °C. Before measurement, the mitochondria were pelletised at 6500 rcf for 5 min, washed and resuspended in MiR05 supplemented with 10 mM succinate, 5 mM malate, and 5 µM of either CsH or CsA. In experiments where the mitochondria were loaded with Ca^{2+} before measurement, this was achieved by incubation in MiR05 additionally supplemented with 150 µM $CaCl_2$ on a shaker at 37 °C for 10 min after the first washing step and followed by a second washing step.

Measurement of mitochondrial membrane potential by TMRE and TMRM

For measurement in whole cells, the cells were stained by incubation in full growth medium containing 100 nM tetramethylrhodamine ethyl ester (TMRE; AAT Bioquest, Sunnyvale, CA, USA; #22220) and 10 mM HEPES at 37 °C in the dark for 15 min. After that, the cells were washed and resuspended in full growth medium containing 10 mM HEPES and were incubated at 37 °C in the dark for another 15 min. The cells were maintained at these conditions until measurement. For measurement in live mitochondria, these were isolated as described above, resuspended in sodium-free mitochondrial respiration buffer MiR05 supplemented with 10 mM succinate, 5 mM malat, and 1 mM ADP, stained with 50 nM tetramethylrhodamine methyl ester (TMRM; Life Technologies, #T668) at 37 °C for 15 min, and washed and resuspended in MiR05 additionally supplemented with 1.6 µM cyclosporin H (CsH) to prevent passive TMRM leakage. For live measurement, TMRE or TMRM fluorescence was measured using an LSRFortessa flow cytometer recording fluorescence in the PE channel (Ex 488 nm, Em 575 ± 26 nm). For each sample, after at least 30 s

of baseline measurement, the stimulus was added and measurement was continued for at least 10 min. For the titration of the EC_{50} for mitochondrial depolarisation, TMRE fluorescence was measured using a Synergy Mx microplate reader (BioTek, Bad Friedrichshall, Germany) recording fluorescence at Ex 549 ± 9 nm, Em 575 ± 9 nm. TMRE fluorescence was measured right before and 10 min after addition of PXA. EC_{50} values were calculated using Prism v7.01.

Live O_2 respirometry measurements

This method was adapted from previously published protocols[19,57]. All measurements were performed using an OROBOROS Oxygraph-2k (Oroboros Instruments, Innsbruck, Austria). For measurement of total cellular respiration, intact cells (2×10^6 cells/ml) were used and maintained in full growth medium supplemented with 20 mM HEPES during measurement. For direct measurement of mitochondrial respiration, digitonin-permeabilised cells (2×10^6 cells/ml) were used and maintained in mitochondrial respiration buffer MiR05 during measurement. To induce respiration, 10 mM glutamate, 5 mM malate, 1 mM ADP, and 5 µg/ml digitonin were added. The following complex-specific ETC inducers were used: For complex II, 10 mM succinate (from Sigma, #S3674); for complex III, 1 mM tetramethylhydroquinone / duroquinol (from TCI Germany, Eschborn, Germany; #T0822); for complex IV, 50 µM tetramethyl-p-phenylenediamine (TMPD; from Sigma, #87890) supplemented with 200 µM ascorbate.

Fluorimetric O_2 consumption assay

This measurement was performed using the *MITO-ID® Extracellular O2 Sensor Kit (High Sensitivity)* (Enzo Life Sciences, Lörrach, Germany; #51045) according to manufacturer's instructions. Fluorescence was measured using a Synergy Mx microplate reader (Ex 340–400 nm, Em 630–680 nm; time-resolved fluorescence, delay time 30 µs, integration time 100 µs).

Measurement of cellular ATP levels

This measurement was performed using the *Mitochondrial ToxGlo™ Assay* (Promega, Mannheim, Germany; #G8000) according to manufacturer's instructions. Since most cancer cells prefer ATP synthesis by glycolysis over OXPHOS if glucose is present, this experiment was conducted in the presence of either glucose or galactose as the only available sugar, the latter of which reduces the net ATP yield of glycolysis to zero and forces the cells to resort to OXPHOS for ATP production[58,59].

Fluorimetric caspase-3 activity assay

Caspase-3 activity was measured as described previously[60]. Briefly, cells were harvested by centrifugation at

600 rcf and lysed with 50 µl of ice-cold lysis buffer (20 mM HEPES, 84 mM KCl, 10 mM, MgCl$_2$, 200 µM EDTA, 200 µM EGTA, 0.5% NP-40, 1 µg/ml leupeptin, 1 µg/ml pepstatin, 5 µg/ml aprotinin) on ice for 10 min. Cell lysates were transferred to a black flat-bottom microplate and mixed with 150 µl of ice-cold reaction buffer (50 mM HEPES, 100 mM NaCl, 10% sucrose, 0.1% CHAPS, 2 mM CaCl$_2$, 13.35 mM DTT, 70 µM Ac-DEVD-AMC). The kinetics of AMC release were monitored by measuring AMC fluorescence intensity (Ex 360 nm, Em 450 nm) at 37 °C in intervals of 2 min over a time course of 150 min, using a Synergy Mx microplate reader. The slope of the linear range of the fluorescence curves (Δrfu/min) was considered as corresponding to caspase-3 activity.

Measurement of cell viability by MTT assay

Cell viability was determined by the ability to convert the yellow MTT substrate (Roth, #4022) into a blue formazan product. MTT solution (5 mg/ml MTT in PBS) was added to cells to a final concentration of 1 mg/ml, and the cells were then incubated at 37 °C for 60 min and pelletised at 600 rcf. The supernatant was discarded and replaced with DMSO. After the formazan crystals were fully dissolved, absorption was measured (test wavelength 570 nm, reference wavelength 650 nm). Reference absorbance was subtracted from test absorbance. Cell-free medium samples were considered as having 0% viability and the average of the control samples was considered as having 100% viability. IC$_{50}$ values were calculated using Prism v7.01.

Immunoblotting

Cells were harvested by centrifugation at 11,000 rcf in 4 °C for 10 s, quick-frozen in liquid nitrogen, thawed on ice, incubated in lysis buffer (20 mM Tris-HCl, 150 mM NaCl, 1% v/v Triton X-100, 0.5 mM EDTA, 1 mM Na$_3$VO$_4$, 10 mM NaF, 2.5 mM Na$_4$P$_2$O$_7$, 0.5% sodium deoxycholate, protease inhibitor (Sigma, #P2714)) for 30 min and vortexed repeatedly. The cell lysates were then cleared from cell debris by centrifugation at 20,000 rcf for 15 min. Sodium dodecyl sulfate-polyacrylamide gel electrophoresis and western blot were performed according to standard protocol. The antibodies used for protein detection were mouse anti-phospho-tyrosine (Merck-Millipore, Darmstadt, Germany; clone 4G10, #05-1050); rabbit anti-OPA1 (described previously[37]); mouse anti-ACTB (Sigma; clone AC-74, #A5316); and mouse anti-VCL (Sigma; clone hVIN-1, #V9131).

Confocal microscopy

Live imaging of HCT116 cells transiently expressing GFP-BAX and SMAC-mCherry was performed using a Zeiss LSM 710 ConfoCor3 microscope (Carl Zeiss, Jena, Germany) with a C-Apochromat × 40 N.A. 1.2 water immersion objective (Zeiss). Excitation light came from argon ion (488 nm) and DPSS (561 nm) lasers. The cells were maintained in full growth medium at 37 °C and 5% CO$_2$ during imaging. Images were recorded every 5 min and were processed with Fiji[61]. For each time frame, the standard deviation (SD) of the fluorescence intensity was measured for each channel. A low SD was considered as corresponding to homogenous distribution, whereas a high SD was considered as corresponding to accumulation.

Live imaging of HeLa cells stably expressing mito-DsRed was performed using a Cell Observer SD Dual Cam spinning disc confocal microscope (Zeiss) equipped with a C-Apochromat 63×, N.A. of 1.45 oil-immersion objective. Excitation light came from an argon ion (488 nm) and DPSS (561 nm) laser. The cells were maintained in full growth medium supplemented with 10 mM HEPES at 37 °C during imaging. Images were recorded every 5 s.

Live imaging of MEF cells stably expressing mito-DsRed was performed using a Perkin Elmer Spinning Disc microscope with a 60 × objective (oil-immersion and NA = 1.49) at an excitation wavelength of 561 nm. The videos were obtained at 1000 × 1000 pixel resolution with a Hamamatsu C9100 camera. The cells were maintained in full growth medium supplemented with 10 mM HEPES at 37 °C during imaging.

For imaging of fixed HeLa and MEF cells, the cells were seeded on glass coverslips and grown to 60–90% confluence prior to experiments. Cells were treated with either 10 µM PXA, 10 µM CCCP or 0.1% v/v DMSO for 30 min, and were fixed by incubation with pre-warmed 4% paraformaldehyde in PBS at 37 °C for 10 min. Coverslips were then washed once with PBS, followed by incubation with PBS supplemented with 0.5% Triton X-100 for 10 min at RT. The coverslips were washed three times for 3–5 min with PBS supplemented with 0.2% Tween-20 (PBS-T). The coverslips were then incubated at RT for 30 min with blocking buffer (PBS-T supplemented with 0.2% fish gelatin and 5% goat serum) in a humidified box, followed by 1 h incubation with primary antibodies (anti-HSP60 clone N-20, #sc-1052 and anti-TOMM20 clone FL-145, #sc-11415 both from Santa Cruz, Dallas, TX, USA) diluted in blocking buffer. The coverslips were then washed three times with PBS-T, and incubated with blocking buffer for 30 min before adding secondary antibodies (Alexa Fluor 488-labelled donkey anti-goat and Alexa Fluor 594-labelled donkey anti-rabbit). Immunofluorescence images were acquired with a Marianas spinning disc confocal microscope (Intelligent Imaging Innovations, Denver, CO, USA).

Transmission electron microscopy

TEM samples were fixed for a minimum of 4 h in 2.5% v/v glutaraldehyde (GA) and 4% w/v paraformaldehyde

(PFA) in 0.1 M cacodylate buffer (pH 7.4) at 4 °C. Then, samples were incubated in 1% osmium tetroxide in 0.1 M cacodylate buffer for 2 h. Dehydration was achieved using acetone (50%, 70%, 90% and 100%) and block contrast was applied (1% phosphotungstic acid/0.5% uranylacetate in 70% acetone). A SPURR embedding kit (Serva, Heidelberg, Germany) was used to embed samples, which were polymerised overnight at 70 °C, before cutting into 80 nm sections using an Ultracut EM UC7 (Leica, Wetzlar, Germany). Images were captured using an H600 TEM (Hitachi, Tokyo, Japan) at 75 kV.

Author details
[1]Institute of Molecular Medicine I, Medical Faculty, Heinrich Heine University Düsseldorf, 40225 Düsseldorf, Germany. [2]Institute of Biochemistry and Molecular Biology I, Medical Faculty, Heinrich Heine University Düsseldorf, 40225 Düsseldorf, Germany. [3]Institute of Pharmaceutical Biology and Biotechnology, Faculty of Mathematics and Natural Sciences, Heinrich Heine University Düsseldorf, 40225 Düsseldorf, Germany. [4]Institute of Anatomy I, Medical Faculty, Heinrich Heine University Düsseldorf, 40225 Düsseldorf, Germany. [5]Laboratory of Molecular and Cellular Signaling, Department of Cellular and Molecular Medicine, KU Leuven, 3000 Leuven, Belgium. [6]Center for Advanced Imaging, Faculty of Mathematics and Natural Sciences, Heinrich Heine University Düsseldorf, 40225 Düsseldorf, Germany. [7]Interfaculty Institute of Biochemistry, Eberhard Karls University Tübingen, 72076 Tübingen, Germany. [8]Department of Biological Chemistry, David Geffen School of Medicine at UCLA, Los Angeles, CA 90095, USA

Conflict of interest
The authors declare that they have no conflict of interest.

References
1. Vyas, S., Zaganjor, E. & Haigis, M. C. Mitochondria and Cancer. *Cell* **166**, 555–566 (2016).
2. Rizzuto, R., De Stefani, D., Raffaello, A. & Mammucari, C. Mitochondria as sensors and regulators of calcium signalling. *Nat. Rev. Mol. Cell Biol.* **13**, 566–578 (2012).
3. Nunnari, J. & Suomalainen, A. Mitochondria: in sickness and in health. *Cell* **148**, 1145–1159 (2012).
4. Mishra, P. & Chan, D. C. Metabolic regulation of mitochondrial dynamics. *J. Cell Biol.* **212**, 379–387 (2016).
5. Youle, R. J. & van der Bliek, A. M. Mitochondrial fission, fusion, and stress. *Science* **337**, 1062–1065 (2012).
6. van der Bliek, A. M., Shen, Q., Kawajiri, S. Mechanisms of mitochondrial fission and fusion. *Cold Spring Harb. Perspect. Biol.* **5**, a011072 (2013).
7. Demaurex, N., Poburko, D. & Frieden, M. Regulation of plasma membrane calcium fluxes by mitochondria. *Biochim. Biophys. Acta* **1787**, 1383–1394 (2009).
8. Palty, R. et al. NCLX is an essential component of mitochondrial Na+/Ca2+ exchange. *Proc. Natl Acad. Sci. USA* **107**, 436–441 (2010).
9. Jiang, D., Zhao, L. & Clapham, D. E. Genome-wide RNAi screen identifies Letm1 as a mitochondrial Ca2+/H+ antiporter. *Science* **326**, 144–147 (2009).
10. Bonora, M. et al. Comprehensive analysis of mitochondrial permeability transition pore activity in living cells using fluorescence-imaging-based techniques. *Nat. Protoc.* **11**, 1067–1080 (2016).
11. Rao, V. K., Carlson, E. A. & Yan, S. S. Mitochondrial permeability transition pore is a potential drug target for neurodegeneration. *Biochim. Biophys. Acta* **1842**, 1267–1272 (2014).
12. Chipuk, J. E. & Green, D. R. Dissecting p53-dependent apoptosis. *Cell Death Differ.* **13**, 994–1002 (2006).
13. Wallace, K. B. & Starkov, A. A. Mitochondrial targets of drug toxicity. *Annu. Rev. Pharmacol. Toxicol.* **40**, 353–388 (2000).
14. Isaka, M. et al. Phomoxanthones A and B, novel xanthone dimers from the endophytic fungus *Phomopsis* Species. *J. Nat. Prod.* **64**, 1015–1018 (2001).
15. Elsässer, B. et al. X-ray structure determination, absolute configuration and biological activity of phomoxanthone A. *Eur. J. Org. Chem.* **2005**, 4563–4570 (2005).
16. Rönsberg, D. et al. Pro-apoptotic and immunostimulatory tetrahydroxanthone dimers from the endophytic fungus *Phomopsis longicolla*. *J. Org. Chem.* **78**, 12409–12425 (2013).
17. Frank, M. et al. Phomoxanthone A - from mangrove forests to anticancer therapy. *Curr. Med. Chem.* **22**, 3523–3532 (2015).
18. Petronilli, V. et al. Transient and long-lasting openings of the mitochondrial permeability transition pore can be monitored directly in intact cells by changes in mitochondrial calcein fluorescence. *Biophys. J.* **76**, 725–734 (1999).
19. Salabei, J. K., Gibb, A. A. & Hill, B. G. Comprehensive measurement of respiratory activity in permeabilized cells using extracellular flux analysis. *Nat. Protoc.* **9**, 421–438 (2014).
20. Baker, M. J. et al. Stress-induced OMA1 activation and autocatalytic turnover regulate OPA1-dependent mitochondrial dynamics. *EMBO J.* **33**, 578–593 (2014).
21. de la Fuente, S., Fonteriz, R. I., de la Cruz, P. J., Montero, M. & Alvarez, J. Mitochondrial free [Ca2+] dynamics measured with a novel low-Ca(2+) affinity aequorin probe. *Biochem. J.* **445**, 371–376 (2012).
22. Hoth, M., Fanger, C. M. & Lewis, R. S. Mitochondrial regulation of store-operated calcium signaling in T lymphocytes. *J. Cell Biol.* **137**, 633–648 (1997).
23. de Andrade, P. B. et al. Diabetes-associated mitochondrial DNA mutation A3243G impairs cellular metabolic pathways necessary for beta cell function. *Diabetologia* **49**, 1816–1826 (2006).
24. Trenker, M., Malli, R., Fertschai, I., Levak-Frank, S. & Graier, W. F. Uncoupling proteins 2 and 3 are fundamental for mitochondrial Ca2+ uniport. *Nat. Cell Biol.* **9**, 445–452 (2007).
25. Fülöp, L., Szanda, G., Enyedi, B., Várnai, P. & Spät, A. The effect of OPA1 on mitochondrial Ca2+ signaling. *PLoS ONE* **6**, e25199 (2011).
26. MacVicar, T. & Langer, T. OPA1 processing in cell death and disease - the long and short of it. *J. Cell Sci.* **129**, 2297–2306 (2016).
27. Zick, M., Rabl, R. & Reichert, A. S. Cristae formation-linking ultrastructure and function of mitochondria. *Biochim. Biophys. Acta* **1793**, 5–19 (2009).
28. Scorrano, L. et al. A distinct pathway remodels mitochondrial cristae and mobilizes cytochrome c during apoptosis. *Dev. Cell* **2**, 55–67 (2002).
29. Anand, R. et al. The i-AAA protease YME1L and OMA1 cleave OPA1 to balance mitochondrial fusion and fission. *J. Cell Biol.* **204**, 919–929 (2014).
30. Head, B., Griparic, L., Amiri, M., Gandre-Babbe, S. & van der Bliek, A. M. Inducible proteolytic inactivation of OPA1 mediated by the OMA1 protease in mammalian cells. *J. Cell Biol.* **187**, 959–966 (2009).
31. Ishihara, N., Fujita, Y., Oka, T. & Mihara, K. Regulation of mitochondrial morphology through proteolytic cleavage of OPA1. *EMBO J.* **25**, 2966–2977 (2006).

32. Duvezin-Caubet, S. et al. Proteolytic processing of OPA1 links mitochondrial dysfunction to alterations in mitochondrial morphology. *J. Biol. Chem.* **281**, 37972–37979 (2006).

33. Wakabayashi, J. et al. The dynamin-related GTPase Drp1 is required for embryonic and brain development in mice. *J. Cell Biol.* **186**, 805–816 (2009).

34. Ishihara, N. et al. Mitochondrial fission factor Drp1 is essential for embryonic development and synapse formation in mice. *Nat. Cell Biol.* **11**, 958–966 (2009).

35. Suen, D. F., Norris, K. L. & Youle, R. J. Mitochondrial dynamics and apoptosis. *Genes Dev.* **22**, 1577–1590 (2008).

36. Labrousse, A. M., Zappaterra, M. D., Rube, D. A. & van der Bliek, A. M. *C. elegans* dynamin-related protein DRP-1 controls severing of the mitochondrial outer membrane. *Mol. Cell* **4**, 815–826 (1999).

37. Barrera, M., Koob, S., Dikov, D., Vogel, F. & Reichert, A. S. OPA1 functionally interacts with MIC60 but is dispensable for crista junction formation. *FEBS Lett.* **590**, 3309–3322 (2016).

38. van Meer, G. & de Kroon, A. I. Lipid map of the mammalian cell. *J. Cell Sci.* **124**, 5–8 (2011). (Pt 1).

39. Ardail, D. et al. Mitochondrial contact sites. Lipid composition and dynamics. *J. Biol. Chem.* **265**, 18797–18802 (1990).

40. Weber, T. A. et al. APOOL is a cardiolipin-binding constituent of the Mitofilin/MINOS protein complex determining cristae morphology in mammalian mitochondria. *PLoS ONE* **8**, e63683 (2013).

41. Planas-Iglesias, J. et al. Cardiolipin interactions with proteins. *Biophys. J.* **109**, 1282–1294 (2015).

42. Acehan, D. et al. Cardiolipin affects the supramolecular organization of ATP synthase in mitochondria. *Biophys. J.* **100**, 2184–2192 (2011).

43. Pfeiffer, K. et al. Cardiolipin stabilizes respiratory chain supercomplexes. *J. Biol. Chem.* **278**, 52873–52880 (2003).

44. Zhang, M., Mileykovskaya, E. & Dowhan, W. Gluing the respiratory chain together. Cardiolipin is required for supercomplex formation in the inner mitochondrial membrane. *J. Biol. Chem.* **277**, 43553–43556 (2002).

45. Bampton, E. T. W., Goemans, C. G., Niranjan, D., Mizushima, N. & Tolkovsky, A. M. The dynamics of autophagy visualised in live cells: from autophagosome formation to fusion with endo/lysosomes. *Autophagy* **1**, 23–36 (2014).

46. Ran, F. A. et al. Genome engineering using the CRISPR-Cas9 system. *Nat. Protoc.* **8**, 2281–2308 (2013).

47. Tait, S. W. et al. Resistance to caspase-independent cell death requires persistence of intact mitochondria. *Dev. Cell* **18**, 802–813 (2010).

48. Qin, T., Iwata, T., Ransom, T. T., Beutler, J. A. & Porco, J. A. Jr. Syntheses of dimeric tetrahydroxanthones with varied linkages: Investigation of "Shapeshifting" properties. *J. Am. Chem. Soc.* **137**, 15225–15233 (2015).

49. Hastie, C. J., McLauchlan, H. J. & Cohen, P. Assay of protein kinases using radiolabeled ATP: a protocol. *Nat. Protoc.* **1**, 968–971 (2006).

50. Bain, J. et al. The selectivity of protein kinase inhibitors: a further update. *Biochem. J.* **408**, 297–315 (2007).

51. Vervloessem, T., Ivanova, H., Luyten, T., Parys, J. B., Bultynck, G. The selective Bcl-2 inhibitor venetoclax, a BH3 mimetic, does not dysregulate intracellular Ca2+ signaling. *Biochim. Biophys. Acta* **1864**, 968–976 (2017).

52. Bittremieux, M. et al. DPB162-AE, an inhibitor of store-operated Ca2+ entry, can deplete the endoplasmic reticulum Ca2+ store. *Cell Calcium* **62**, 60–70 (2017).

53. Suzuki, J. et al. Imaging intraorganellar Ca2+ at subcellular resolution using CEPIA. *Nat. Commun.* **5**, 4153 (2014).

54. Nagai, T., Sawano, A., Park, E. S. & Miyawaki, A. Circularly permuted green fluorescent proteins engineered to sense Ca2+. *Proc. Natl Acad. Sci. USA* **98**, 3197–3202 (2001).

55. Filippin, L. et al. Improved strategies for the delivery of GFP-based Ca2+ sensors into the mitochondrial matrix. *Cell Calcium* **37**, 129–136 (2005).

56. Petronilli, V., Penzo, D., Scorrano, L., Bernardi, P. & Di Lisa, F. The mitochondrial permeability transition, release of cytochrome c and cell death. Correlation with the duration of pore openings in situ. *J. Biol. Chem.* **276**, 12030–12034 (2001).

57. Kuznetsov, A. V. et al. Analysis of mitochondrial function in situ in permeabilized muscle fibers, tissues and cells. *Nat. Protoc.* **3**, 965–976 (2008).

58. Warburg, O. On the origin of cancer cells. *Science* **123**, 309–314 (1956).

59. Marroquin, L. D., Hynes, J., Dykens, J. A., Jamieson, J. D. & Will, Y. Circumventing the Crabtree effect: replacing media glucose with galactose increases susceptibility of HepG2 cells to mitochondrial toxicants. *Toxicol. Sci.* **97**, 539–547 (2007).

60. Czugala, M. et al. Efficient and safe gene delivery to human corneal endothelium using magnetic nanoparticles. *Nanomedicine (Lond.)* **11**, 1787–1800 (2016).

61. Schindelin, J. et al. Fiji: an open-source platform for biological-image analysis. *Nat. Methods* **9**, 676–682 (2012).

3.2 Supporting Information

The mycotoxin phomoxanthone A disturbs the form and function of the inner mitochondrial membrane.

Böhler P[1], Stuhldreier F[1], Anand R[2], Kondadi AK[2], Schlütermann D[1], Berleth N[1], Deitersen J[1], Wallot-Hieke N[1], Wu W[1], Frank M[3], Niemann H[3], Wesbuer E[4], Barbian A[4], Luyten T[5], Parys JB[5], Weidtkamp-Peters S[6], Borchardt A[2], Reichert AS[2], Peña-Blanco A[7], García-Sáez AJ[7], Itskanov S[8], van der Bliek AM[8], Proksch P[3], Wesselborg S[9], Stork B[10].

1. Institute of Molecular Medicine I, Medical Faculty, Heinrich Heine University Düsseldorf, 40225, Düsseldorf, Germany.
2. Institute of Biochemistry and Molecular Biology I, Medical Faculty, Heinrich Heine University Düsseldorf, 40225, Düsseldorf, Germany.
3. Institute of Pharmaceutical Biology and Biotechnology, Faculty of Mathematics and Natural Sciences, Heinrich Heine University Düsseldorf, 40225, Düsseldorf, Germany.
4. Institute of Anatomy I, Medical Faculty, Heinrich Heine University Düsseldorf, 40225, Düsseldorf, Germany.
5. Laboratory of Molecular and Cellular Signaling, Department of Cellular and Molecular Medicine, KU Leuven, 3000, Leuven, Belgium.
6. Center for Advanced Imaging, Faculty of Mathematics and Natural Sciences, Heinrich Heine University Düsseldorf, 40225, Düsseldorf, Germany.
7. Interfaculty Institute of Biochemistry, Eberhard Karls University Tübingen, 72076, Tübingen, Germany.
8. Department of Biological Chemistry, David Geffen School of Medicine at UCLA, Los Angeles, CA, 90095, USA.
9. Institute of Molecular Medicine I, Medical Faculty, Heinrich Heine University Düsseldorf, 40225, Düsseldorf, Germany. sebastian.wesselborg@uni-duesseldorf.de.
10. Institute of Molecular Medicine I, Medical Faculty, Heinrich Heine University Düsseldorf, 40225, Düsseldorf, Germany. bjoern.stork@uni-duesseldorf.de.

The following supporting information was added to this dissertation and is not available online.

Table of Content

S1 HPLC Chromatogram of PXA Stocksolution (DMSO)
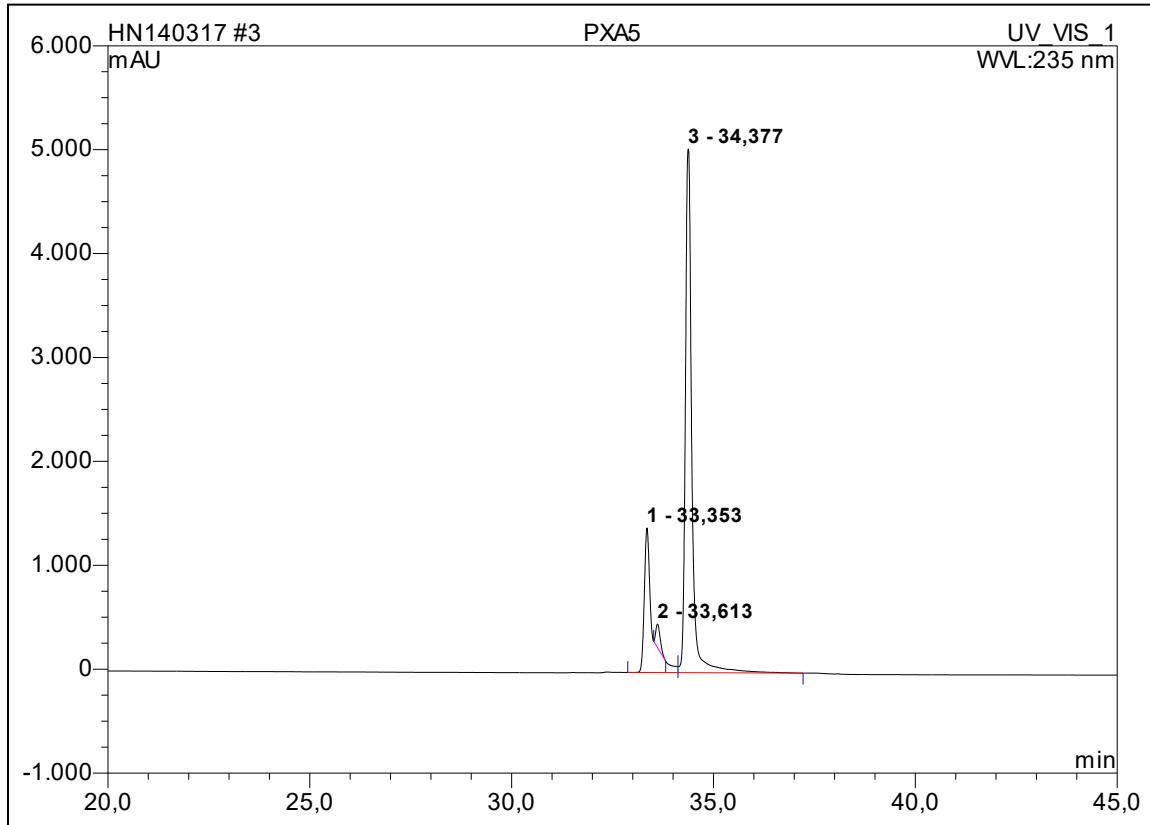
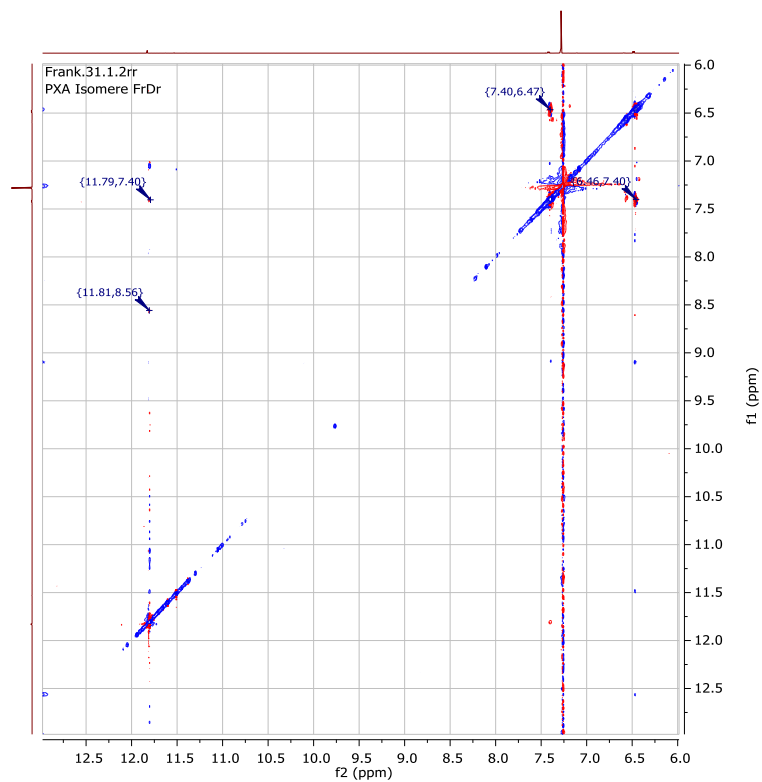PXA: 33.353 min
Dicerandrol C: 34.377 min

S2 UV-spectrum of isolated Dicerandrol C
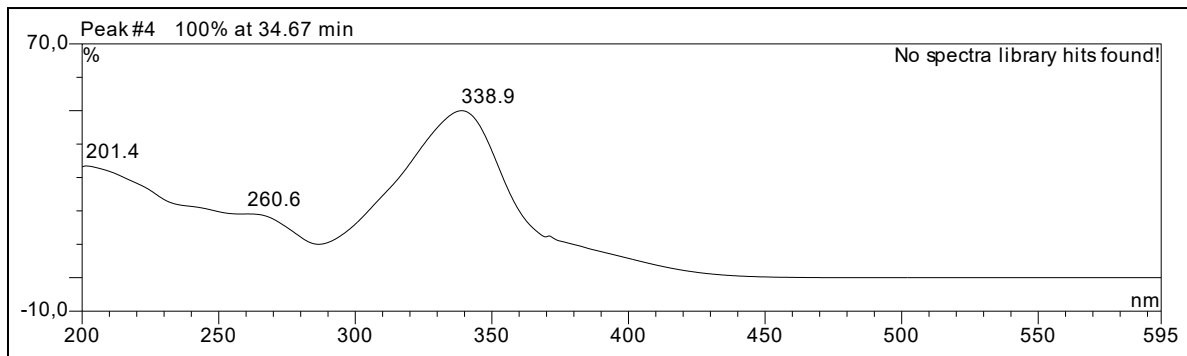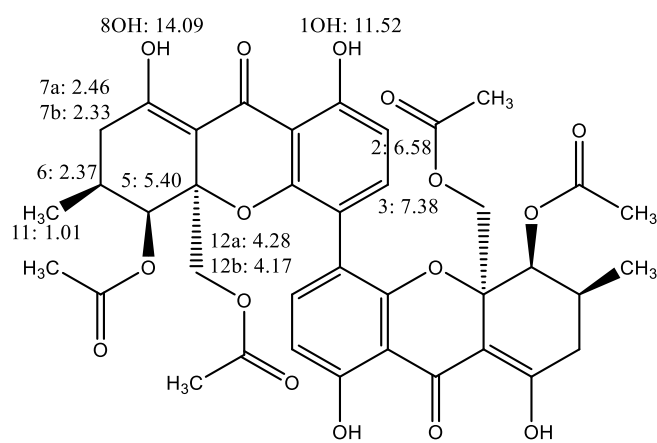
S2 MS of isolated Dicerandrol C

marian102 #1025 RT: 34.50 AV: 1 NL: 1.12E5
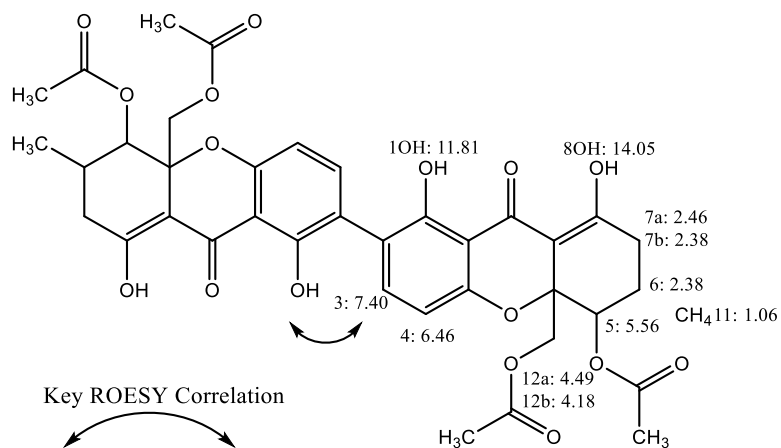F: + c ESI Full ms [100.00-1000.00]
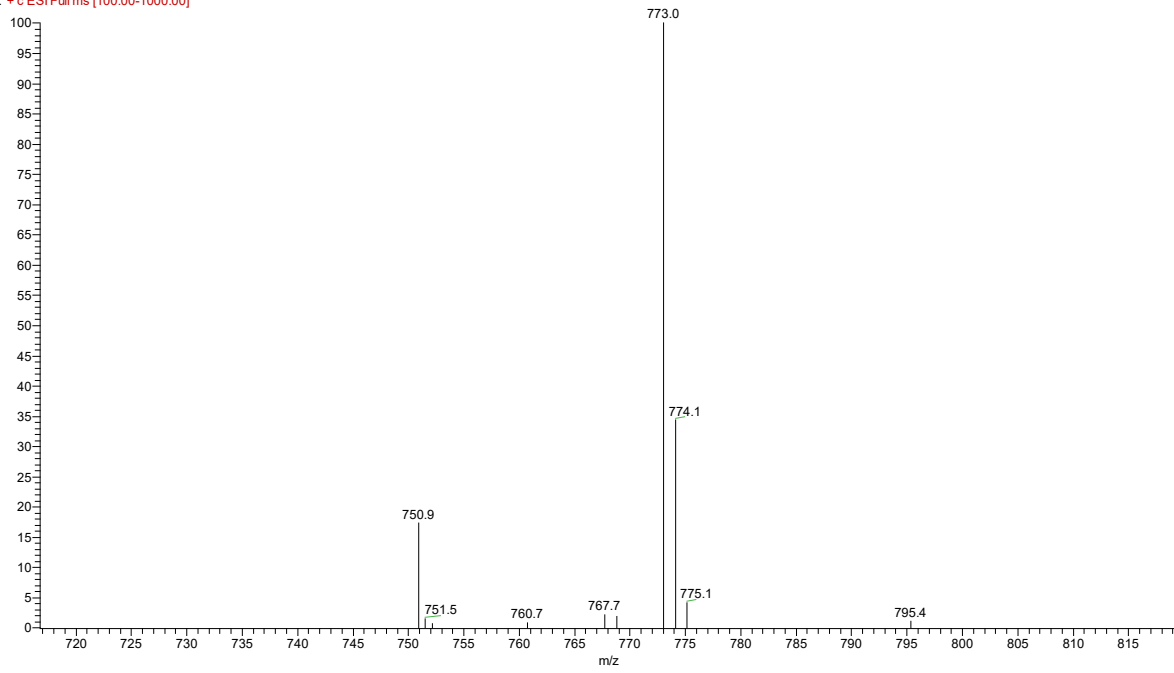
S3 ^{1}H-NMR spectrum of dicerandrol C
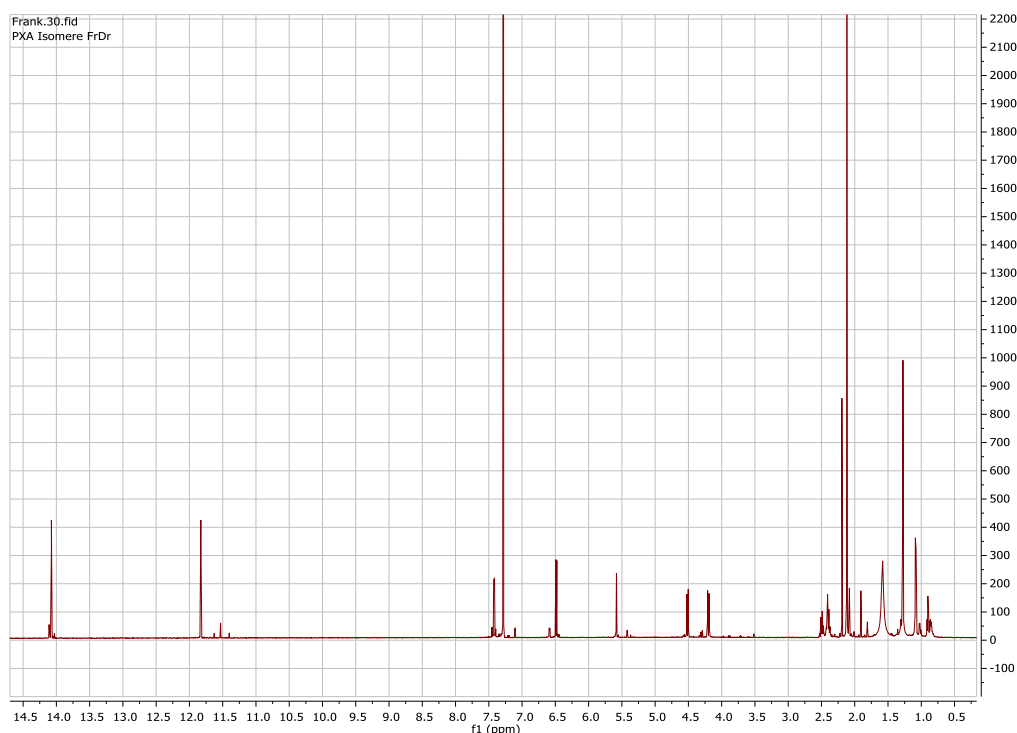
S4 ^{1}H-^{1}H-ROESY spectrum of dicerandrol C

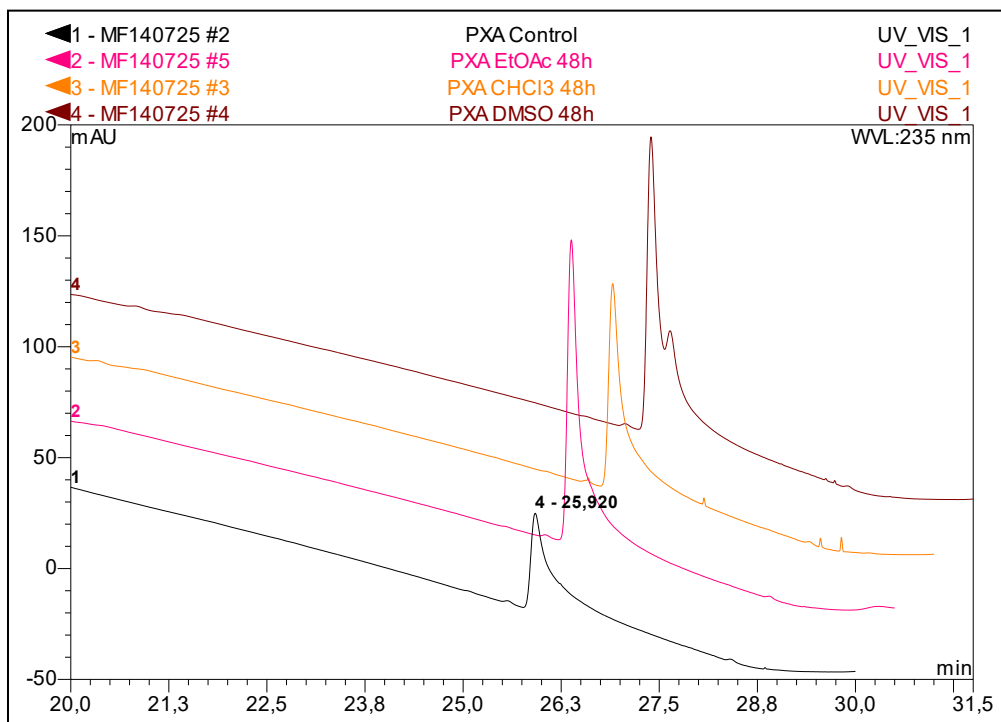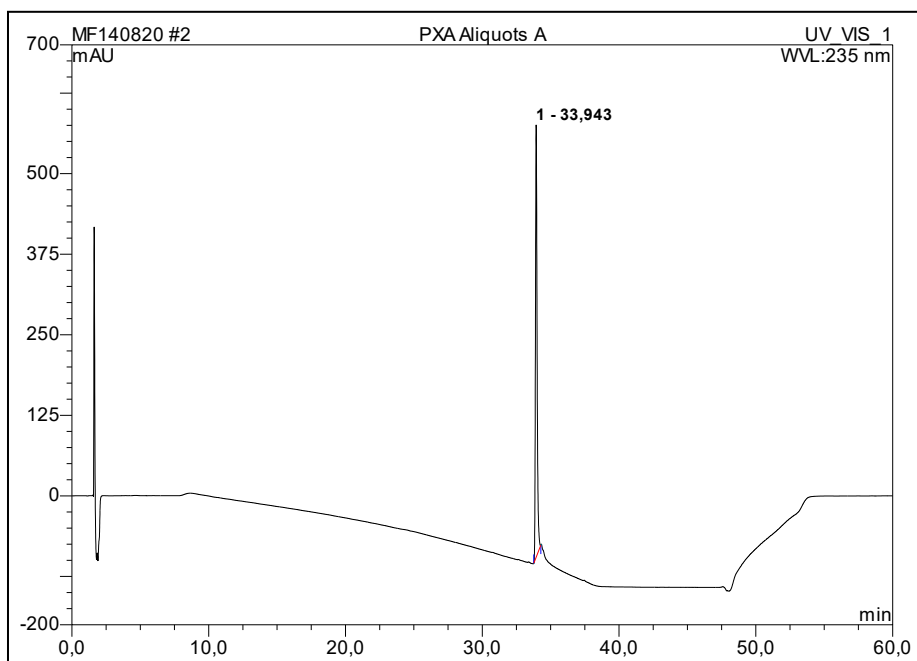S5 Chemical Shifts and Key ROESY Correlation of PXA rearrangement reaction

Phomoxanthone A

Dicerandrol C

Key ROESY Correlation

S6 PXA degradation in DMSO

1. Freshly dissolved in MeOH
2. 48h EtOAc at ambient conditions
3. 48h CHCl3 at ambient conditions
4. 48h DMSO at ambient conditions

S7 Freeze dried PXA aliquot with new handling protocol

Chapter 4 - Brominated Azaphilones from the Sponge-Associated Fungus *Penicillium canescens*

Finished manuscript, ready for submission.

Overall contribution to this manuscript: 70%, first author, laboratory work includes cultivation and extraction, compound isolation and structure elucidation and preparation of the manuscript.

4.1 Publication Manuscript

Brominated Azaphilones from the Sponge-Associated Fungus *Penicillium*

canescens

Marian Frank,[†] Rudolf Hartmann,[‡] Malte Plenker,[‡] Ferhat Can Özkaya,[⊥] Werner E.G.
Müller,[∥] Matthias U. Kassack,[∇] Alexandra Hamacher,[∇] Wenhan Lin,[O] Zhen Liu,[*,†] Peter
Proksch[*,†]

[†]Institute of Pharmaceutical Biology and Biotechnology, Heinrich-Heine-Universität
Düsseldorf, Universitätsstrasse 1, 40225 Düsseldorf, Germany

[‡]Institute of Complex Systems: Strukturbiochemie, Forschungszentrum Juelich, Wilhelm-
Johnen-Strasse, 52428 Juelich, Germany

[⊥]Faculty of Fisheries, İzmir Katip Çelebi University, Çiğli, 35620 İzmir, Turkey

[∥]Institute of Physiological Chemistry, Universitätsmedizin der Johannes Gutenberg-
Universität Mainz, 55128 Mainz, Germany

[∇]Institute for Pharmaceutical and Medicinal Chemistry, Heinrich-Heine-Universität
Düsseldorf, Universitätsstrasse 1, 40225 Düsseldorf, Germany

[O]State Key Laboratory of Natural and Biomimetic Drugs, Peking University, Beijing 100191,
China

1

82

ABSTRACT:

The fungus *Penicillium canescens* was isolated from the inner tissue of the Mediterranian sponge *Agelas oroides*. Fermentation of the fungus on solid rice medium yielded one new diphenyl ether, penicanether (**1**) and thirteen known compounds (**2−14**). Addition of 5% NaBr to the rice medium increased the amounts of **4−6**, while lowering the amounts of **8**, **12** and **14**. Furthermore, it induced the accumulation of **17** and two new brominated azaphilones, bromophilones A and B (**15** and **16**) that feature an unprecedented side chain. The structures of the new compounds were elucidated based on the 1D and 2D NMR spectra as well as on HRESIMS data. The relative configuration of **15** and **16** was determined by NOE and comparing of ^{13}C shifts with literature databases. Compound **16** exhibited pronounced cytotoxicity against the mouse lymphoma cell line L5178Y (IC$_{50}$ 8.9 µM), as well as against the human ovarian cancer cell line A2780 (IC$_{50}$ 2.7 µM), whereas the stereoisomer **15** was considerably less active.

2

Marine-derived microorganisms are prominent producers of novel bioactive compounds as exemplified by the discovery of halimide, which served as a lead structure for plinabulin that is currently in clinical phase III as a new potential anticancer drug.[1,2] Until now hundreds of new compounds have been reported from marine-derived bacteria and fungi, which have been established primarily in the last two decades as a further important source of natural products besides marine invertebrates such as sponges.[1] In spite of this success, bioprospecting of marine-derived fungi (and also of bacteria) meets increasing challenges due to the frequent re-discovery of known natural products.[3,4] Under laboratory conditions fungi often transcribe only a fraction of their biogenetic gene clusters whereas other genes are silent. Thus only a part of the potential chemical diversity of natural products can be obtained from these cultures.[5,6] Numerous strategies aim at the activation of silent biogenetic gene clusters in order to enlarge the diversity of metabolites. One of these strategies is the OSMAC approach which aims at diversifying media and culture conditions in order to generate clues that induce silent biogenetic gene clusters and thus the accumulation of cryptic metabolites.[7]

The OSMAC approach has also been implemented in this study on the sponge-derived fungus *Penicillium canescens* that was isolated from the Mediterranean Sponge *Agelas oroides*. The fungus had previously been isolated from sponge-tissue (*Tethya aurantium*)[8] and is a known producer of several bioactive secondary metabolites, including the antifungal compounds canescin, griseofulvin, curvulinic acid, and several tetrapeptides.[9–11] The crude EtOAc extract of a solid rice medium fermentation of *P. canescens* showed promising cytotoxic activity against the mouse lymphoma cell line L5178Y (100% inhibition at a dose of 10 µg/mL) and was thus further investigated, which resulted in the isolation of fourteen natural products (**1−14**) including a new diphenyl ether (**1**). In an attempt to expand the metabolic profile, the fungus was cultivated on solid rice medium following addition of 5% NaBr. Addition of bromide to solid rice medium had already in the past proved effective for

3

inducing the accumulation of cryptic metabolites in other fungi.[12] Investigation of the fungal extract following fermentation on NaBr spiked rice medium yielded two new brominated azaphilones (**15** and **16**) and a known xanthone derivative (**17**) in addition to the previously isolated compounds (**1−14**) obtained following cultivation on rice lacking NaBr. Compounds **15−17** were not detected when the fungus was cultivated in absence of NaBr. Herein, we describe the structure elucidation of the new metabolites (**1**, **15** and **16**) as well as the biological activities of the isolated compounds against tumor cells.

1 R = Me
2 R = H

3 R_1 = Me, R_2 = H
4 R_1 = R_2 = H
17 R_1 = H, R_2 = OH

5 R_1 = R_2 = H
6 R_1 = Cl, R_2 = H
7 R_1 = R_2 = Cl

8 R = Cl
9 R = H

10 R = H
11 R = Me

12

13

14

15 9α
16 9β
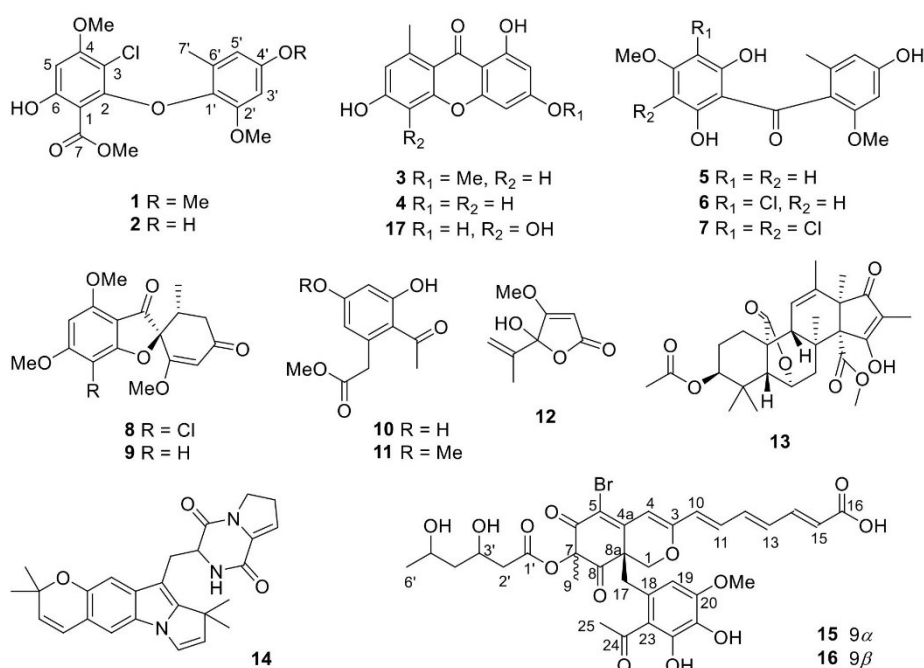
RESULTS AND DISCUSSION

The molecular formula of **1** was established as $C_{18}H_{19}ClO_7$ by HRESIMS data with 9 degrees of unsaturation. The ^{1}H and ^{13}C NMR data of **1** (Table 1) resembled those of **2**, a co-isolated known chlorinated diphenyl ether.[13] The obvious difference was the appearance of an additional methoxy group (δ_C 55.5, δ_H 3.76) and downfield-shifted C-4′ (+4.1 ppm) in **1**. The protons of this additional methoxy group exhibited a HMBC correlation to C-4′ and ROESY

4

correlations to H-3′ (δ_H 6.29) and H-5′ (δ_H 6.35), indicating its location at C-4′. Detailed analysis of the 2D NMR spectra of **1** revealed that the remaining structure of **1** was identical to that of **2**. Thus, compound **1** was elucidated as the 4′-*O*-methyl derivative of **2**, for which the trivial name penicanether is proposed.

Table 1. ^{1}H and ^{13}C NMR data for compound 1.^{a}

position	δ_C	δ_H, m (*J* in Hz)
1	101.2, C	
2	156.4, C	
3	106.7, C	
4	160.1, C	
5	95.6, CH	6.34, s
6	162.2, C	
7	170.8, C	
1′	138.8, C	
2′	149.7, C	
3′	98.6, CH	6.29, d (2.7)
4′	154.9, C	
5′	107.2, CH	6.35, d (2.7)
6′	129.6, C	
7′	17.4, CH₃	2.29, s
4-OMe	56.4, CH₃	3.90, s
6-OH		11.57, s
7-OMe	52.3, CH₃	3.74, s
2′-OMe	56.5, CH₃	3.48, s
4′-OMe	55.5, CH₃	3.76, s

^{a} Measured in CDCl₃ (^{1}H at 600 MHz and ^{13}C at 150 MHz).

Further known compounds that were isolated from the fermentation of *P. cancescens* on solid rice medium included two xanthones griseoxanthone C (**3**)[14] and norlichexanthone (**4**),[15] three benzophenones griseophenones C, B and G (**5−7**),[16] two spirocyclic polyketides griseofulvin (**8**)[16] and dechlorogriseofulvin (**9**)[17], two curvulinic acid derivatives methylcurvulinate (**10**)[18] and 3′-*O*-methylmethylcurvulinate (**11**),[19] the tetraketide mycotoxin penicillic acid (**12**),[20] the meroterpenoid citreohybridonol (**13**),[21] and the diketopiperazine alkaloid piscarinine B (**14**).[22]

In an OSMAC approach, 5% NaBr was added to the solid rice medium. The metabolite profile of *P. cancescens* following fermentation in the presence of NaBr differed markedly from that obtained following cultivation only on rice. The amounts of compounds **4−6**

5

increased strongly in the presence of NaBr, whereas the amounts of **8**, **12** and **14** decreased. In addition, two new brominated azaphilone derivatives (**15** and **16**) as well the known 1,3,5,6-tetrahydroxy-8-methylxanthone (**17**)[23] were obtained from solid rice cultures containing NaBr but were not detected when the fungus was grown only on rice.

Table 2. Concentrations of selected compounds (in mAU*min at 235 nm) in cultures of *P. canescens* grown on solid rice medium (control) vs. cultures grown in the presence of NaBr (n = 5).

Compound	Control (mAU*min)	5% NaBr (mAU*min)
4	n.d. [a]	42.44 ± 2.23
5	3.66 ± 0.04	53.60 ± 2.33
6	n.d.	8.81 ± 0.53
8	145.64 ± 12.52	11.16 ± 1.95
12	408.71 ± 15.24	100.89 ± 10.58
14	59.08 ± 4.88	23.23 ± 1.31
15	n.d.	0.46 ± 0.05
16	n.d.	0.36 ± 0.10
17	n.d.	19.42 ± 5.56

[a] n.d. = not detected.

Compound **15** was isolated as a reddish brown, amorphous powder. The molecular formula was determined as $C_{33}H_{35}O_{13}Br$ with sixteen degrees of unsaturation based on the HRESIMS data. The ^1H NMR data of **15** (Table 3) showed eight olefinic protons at δ_H 7.35 (H-14), 6.98 (H-11), 6.82 (H-12), 6.80 (H-13), 6.40 (H-10), 6.24 (H-4), 6.19 (H-19), and 6.07 (H-15), and a methoxy group at δ_H 3.79 (OMe-20), in addition to three methyl groups at δ_H 2.57 (Me-25), 1.57 (Me-9), and 1.17 (Me-6′). The ^{13}C NMR data of **15** (Table 3) displayed five carbonyls at δ_C 203.2 (C-24), 201.6 (C-8), 186.7 (C-6), 171.0 (C-1′), and 167.6 (C-16), as well as sixteen olefinic carbons at δ_C 162−107, accounting for thirteen degrees of unsaturation. Thus, compound **15** was suggested to be tricyclic. The HMBC correlations from H_{ab}-1 (δ_H 4.49 and 4.12) to C-3 (δ_C 161.2), C-4a (δ_C 150.3), C-8 and C-8a (δ_C 54.7), from H-4 to C-3, C-5 (δ_C 110.9) and C-8a, and from Me-9 to C-6, C-7 (δ_C 81.0) and C-8, as well as the long range ^4J-HMBC correlation from H-4 to C-6 established the pyranoquinone bicyclic core

6

with a methyl group at C-7 and two carbonyls at C-6 and C-8, respectively (Figure 1). The COSY correlations between H-10/H-11/H-12/H-13/H-14/H-15 together with the HMBC correlations from H-15 to C-16, and from H-10 to C-3 and C-4 indicated a hepta-2,4,6-trienoic acid side chain at C-3. The three double bonds are E configured as indicated by the typical coupling constants of the olefinic protons which range from 15.0–15.3 Hz (Table 3). The COSY correlations between H_{ab}-2′/H-3′ (δ_H 4.27)/H_{ab}-4′/H-5′ (δ_H 4.02)/Me-6′ as well as the HMBC correlations from H_{ab}-2′ to C-1′, and the long range ^4J-HMBC correlation from Me-9 to C-1′ indicated the presence of a 3,5-dihydroxyhexanoyl side chain and its attachment at C-7 through an ester bond. In addition, the HMBC correlations from H-19 to C-21 (δ_C 133.2) and C-23 (δ_C 124.0), from Me-25 to C-23 and C-24, and from the methoxy group to C-20 (δ_C 148.5), the weak ^2J-HMBC correlations from H-19 to C-18 (δ_C 125.2) and C-20, the long range ^4J-HMBC correlation from H-19 to C-22 (δ_C 145.5) as well as the ROESY correlation between H-19 and the methoxy group established a benzene moiety with a methoxy group at C-20, two hydroxy groups at C-21 and C-22, and an acetyl group at C-23. Moreover, the HMBC correlations from H_{ab}-17 (δ_H 3.59 and 3.52) to C-1 (δ_C 70.3), C-4a, C-8, C-8a, C-18, C-19 and C-23 indicated the connection of the benzene moiety and the pyranoquinone core through a methylene group (C-17). The bromine substituent is connected to C-5 based on the chemical shift of C-5 (δ_C 110.9) and the molecular formula. Thus, the planar structure of **15** was elucidated as shown, representing a new brominated azaphilone derivative, for which the name bromophilone A is proposed.
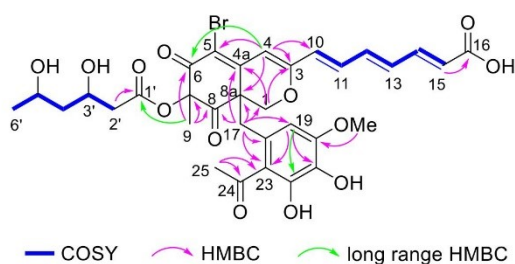
Figure 1. COSY and key HMBC correlations of compound **15**.

In the ROESY spectrum of **15**, the correlation between Me-9 and H_b-1 (δ_H 4.12) indicated that Me-9 and H_b-1 were on the same side of the ring while the C-17 methylene group was on the other side. The relative configuration of the 3,5-diol in the dihydroxyhexanoyl side chain was assigned as *syn* using Kishi's Universal NMR Database (Database 2)[24–26] and by comparison of the chemical shifts of C-3′ (δ_C 68.4) to C-5′ (δ_C 67.2) in **15** with those of (3*R*,5*R*)- and (3*R*,5*S*)-*tert*-butyl 3,5-dihydroxyhexanoate (δ_C 69.2 and 68.3 for 3*R*,5*R*; δ_C 65.9 and 65.1 for 3*R*,5*S*).[27]

Table 3. ^{1}H and ^{13}C NMR Data of Compounds 15 and 16.

position	**15** [a]		**16** [b]	
	δ_C, type	δ_H (*J* in Hz)	δ_C, type	δ_H (*J* in Hz)
1	70.3, CH_2	4.49, d (11.3)	71.4, CH_2	4.64, d (11.4)
		4.12, d (11.3)		3.98, d (11.4)
3	161.2, C		161.1, C	
4	107.3, CH	6.24, s	106.5, CH	6.43, s
4a	150.3, C		150.2, C	
5	110.9, C		115.9, C	
6	186.7, C		185.8, C	
7	85.0, C		82.1, C	
8	201.6, C		203.6, C	
8a	54.7, C		53.2, C	
9	24.0, CH_3	1.57, s	22.2, CH_3	1.34, s
10	129.0, CH	6.40, d (15.1)	128.6, CH	6.52, d (15.2)
11	136.2, CH	6.98, dd (15.1, 10.2)	135.9, CH	7.05, dd (15.2, 10.7)
12	139.4, CH	6.82, dd (15.0, 10.2)	139.2, CH	6.86, dd (14.9, 10.7)
13	136.1, CH	6.80, dd (15.0, 10.2)	136.0, CH	6.81, dd (14.9, 10.7)
14	144.4, CH	7.35, dd (15.3, 10.2)	144.3, CH	7.36, dd (15.2, 10.7)
15	124.5, CH	6.07, d (15.3)	124.3, CH	6.07, d (15.2)
16	167.6, C		167.2, C	
17	40.9, CH_2	3.59, d (14.4)	39.0, CH_2	3.56, d (14.6)
		3.52, d (14.4)		3.29, d (14.6)
18	125.2, C		124.0, C	
19	109.2, CH	6.19, s	107.5, CH	6.24, s
20	148.5, C		148.5, C	
21	133.2, C		133.4, C	
22	145.5, C		145.2, C	
23	124.0, C		124.6, C	
24	203.2, C		202.8, C	
25	33.2, CH_3	2.57, s	32.9, CH_3	2.53, s
1′	171.0, C		171.4, C	
2′	42.6, CH_2	2.64, dd (15.1, 7.1)	41.9, CH_2	2.48, dd (15.4, 7.0)

8

		2.61, dd (15.1, 5.6)		2.43, dd (15.4, 5.9)
3′	68.4, CH	4.27, m	68.1, CH	4.10, m
4′	45.5, CH$_2$	1.73, dt (13.9, 3.7)	45.3, CH$_2$	1.56, dt (14.0, 3.7)
		1.61, dt (13.9, 9.0)		1.50, dt (14.0, 8.9)
5′	67.2, CH	4.02, m	67.1, CH	3.95, m
6′	24.2, CH$_3$	1.17, d (6.1)	24.0, CH$_3$	1.13, d (6.2)
20-OMe	56.3, CH$_3$	3.79, s	56.1, CH$_3$	3.81, s
22-OH				8.19, s

[a] Recorded at 700 MHz (^{1}H) and 175 MHz (^{13}C) in acetone-d_6. [b] Recorded at 750 MHz (^{1}H) and 187.5 MHz (^{13}C) in acetone-d_6;

The UV spectrum and ^{1}H NMR data of bromophilone B (**16**) were comparable to those of **15** (Table 3). The molecular formula of **16** was identical to that of **15** as determined by HRESIMS. Detailed analysis of the 2D NMR spectra of **16** revealed that it shared the same planar structure as **15**. The major changes in the ^{13}C NMR data of **16** were the upfield-shifted signals of C-7 (-2.9 ppm), C-17 (-1.9 ppm), and C-9 (-1.8 ppm), and the downfield-shifted signals of C-5 (+5.0 ppm) and C-8 (+2.0 ppm) when compared to **15**. In the ROESY spectrum of **16**, Me-9 (δ_H 1.34) showed correlations to H$_b$-17 (δ_H 3.29) and H-19 (δ_H 6.24) rather than to H$_b$-1 as observed for **15**, indicating that Me-9 and the C-17 methylene group were on the same side of the ring in **16**. The similar carbon chemical shifts and coupling constants in the 3,5-dihydroxyhexanoyl side chain from C-1′ to C-6′ of compounds **15** and **16** suggested that both compounds shared the same relative configuration at C-3′ and C-5′.

All isolated compounds were evaluated for their cytotoxic activities against the mouse lymphoma cell line L5178Y and the human ovarian cancer cell line A2780. Griseofulvin (**8**), penicillic acid (**12**), and bromophilone B (**16**) showed moderate cytotoxicity against the mouse lymphoma cell line L5178Y with IC$_{50}$ values of 16.4, 8.9, and 8.9 μM, respectively. Bromophilone A (**15**) was less active compared to its epimer **16**, with an IC$_{50}$ value of 13.9 μM. Griseoxanthone C (**3**), griseofulvin (**8**), and bromophilone B (**16**) exhibited weak to moderate cytotoxicity against the human ovarian cancer cell line A2780 with IC$_{50}$ values of 18.3, 11.0, and 2.7 μM, respectively. Bromophilone A (**15**) was again considerably less active

9

with an IC_{50} value of 37.3 µM. All other compounds were inactive ($IC_{50} > 20$ µM).

In summary, fourteen compounds (**1−14**) including a new diphenyl ether, penicanether (**1**) were isolated from the axenic solid rice medium fermentation of the sponge-derived fungus *P. canescens*. Addition of 5% NaBr to the rice medium significantly changed the pattern of metabolites leading to the induction of two new brominated azaphilones (**15** and **16**) and the isolation of one additional known xanthone (**17**). Bromophilone B (**16**) exhibited significant cytotoxicity against the mouse lymphoma cell line L5178Y (IC_{50} 8.9 µM) and the human ovarian cancer cell line A2780 (IC_{50} 2.7 µM) whereas its epimer **15** was considerably less active.

EXPERIMENTAL SECTION

General Experimental Procedures. Specific optical rotation values were measured with a JASCO P-2000 polarimeter. NMR spectra were recorded on Bruker Avance III 600, 700, or 750 spectrometers. HRESIMS was recorded with Bruker Daltonics UHR-QTOF Maxis 4G or Thermo Fisher LTQ FT Ultra mass spectrometers. HPLC-DAD analysis was performed using a Dionex UltiMate-3400SD system (Thermo Fisher) with a LPG-3400SD Pump, a DAD3000RS photodiode array detector and a Knauer Eurospher C_{18} analytical column (125 × 4 mm, 5μm). UV spectra were obtained from the HPLC-DAD chromatograms of this system in concentrations that allowed for absorption in the Lambert-Beer-region. Semi-preparative HPLC was performed using a Lachrom-Merck Hitachi system (an L-7100 pump, an L-7400 UV detector and a 300 × 8 mm Knauer Eurospher C_{18} column) with MeOH and water as eluents. Routine thin layer chromatography (TLC) was performed on pre-coated silica plates (Merck silica gel F254) and spots were detected at 254 or 365 nm or by dipping the plates into anisaldehyde reagent followed by heating at 105°C.

Fungal Material and Identification. The fungus was isolated from the inner tissues of the marine sponge *Agelas oroides*. The specimen was collected at a depth of 10 m at the coast

10

of Sığacık-İzmir, Turkey in 2013 by local fishermen. The identification of the sponge was performed by Prof. Semih Engin in December 2013. The fungus was identified as *Penicillium canescens*, using a molecular biology protocol for the amplification and sequencing of the 5.8S rDNA and the internal transcribed spacer region (18S rDNA) and subsequent BLAST search as described before.[28] The resulting sequence data have been submitted to GenBank under the Acession number MH820167. A deep frozen sample of the fungal strain *P. canescens* (4.14) has been stored at one of the author's laboratory (P.P.).

Fermentation, Extraction, and Isolation. *P. canescens* was cultivated on solid rice medium in 10 Erlenmeyer flasks (1 L each, 100 g rice, 110 mL demineralized water and 3.8 g artificial sea salt per flask). The medium was sterilized by autoclaving it at 121 °C for 20 min prior to fungal inoculation. After seventeen days at 20°C under static conditions, the fermentation was terminated by the addition of 350 mL EtOAc per flask. After an overnight soak, the rice was cut using a scalpel and subsequently shaken at 150 rpm for 8 h. The extract was collected through a paper filter and the residue was washed with 50 mL EtOAc, which was poured through the same filter. The extract was evaporated to dryness at 40°C using the rotary evaporator, to yield around 10 g of crude extract. Liquid–liquid separation between *n*-hexane and 90% MeOH-H$_2$O was performed. 2 g of insoluble griseofulvin (**8**) and 2.4 g of oily phase were removed to give 5.6 g of a MeOH soluble fraction. The latter was separated by vacuum liquid chromatography on a silica gel column using a solvent gradient (from 100% *n*-hexane to 100% EtOAc and subsequently from 100% CH$_2$Cl$_2$ to 100% MeOH), resulting in 14 fractions (V1−V14). Fraction V2 was subjected to a silica gel column (10 × 200 mm) with CH$_2$Cl$_2$-MeOH (99:2), yielding **1** (2.1 mg) and **3** (4.3 mg). Fraction V3 was subjected to a Sephadex LH20 column using MeOH-DCM (1:1) as mobile phase to give **4** (109.0 mg) and three additional subfractions (V3S1−V3S4). Subfraction V3S2 was further separated by a silica gel column (CH$_2$Cl$_2$-MeOH 95:5) to give **12** (11.9 mg). Subfraction V3S3 was purified

11

by semi-preparative HPLC to yield **2** (13.4 mg) while subfraction V3S4 was purified by semi-preparative HPLC to yield **5** (4.1 mg), **6** (15.5 mg), **7** (1.5 mg), **10** (2.5 mg), and **11** (6.4 mg). Fraction V4 was separated by a Sephadex LH20 column (CH$_2$Cl$_2$-MeOH 1:1) followed by purification using semi-preparative HPLC to yield **13** (20.4 mg).

The OSMAC experiment used the same cultivation and extraction parameters as the initial fermentation. It was performed on five flasks (1 L each, 100 g rice, 110 mL demineralized water, 3.8 g artificial sea salt and 5.0 g NaBr per flask). The resulting crude extract (6.3 g) was partitioned between *n*-hexane and 90% MeOH-H$_2$O to give 4.9 g of MeOH soluble extract. The latter was separated by VLC with a gradient solvent system (from 80% *n*-hexane to 100% EtOAc, and subsequently from 100% CH$_2$Cl$_2$ to 100% MeOH) to give seventeen fractions (V1−V17). All fractions were analyzed by HPLC-DAD and the peaks with unidentified UV-spectra were further investigated. Fraction V4 was purified by semi-preparative HPLC to yield **17** (27.3 mg). Fraction V5 was analyzed by co-chromatography with authentic dechlorogriseofulvin standard and identified as such, yielding **9** (200 mg). Fraction V9 was purified by semi-preparative HPLC to yield **14** (31.1 mg). Under the exclusion of light by using brown glass and aluminium foil, fraction V12 was separated by a Sephadex LH20 column (CH$_2$Cl$_2$-MeOH 1:1) followed by purification with semi-preparative HPLC to yield **15** (1.2 mg) and **16** (1.1 mg).

Penicanether (1): white powder; UV (MeOH) λ_{max} 283 and 205 nm; ^{1}H and ^{13}C NMR data, Table 1; HRESIMS *m/z* 383.0892 [M + H]$^+$ (calcd for C$_{18}$H$_{20}$ClO$_7$, 383.0892).

Bromophilone A (15): red powder; $[\alpha]_D^{26}$ -19 (c 0.2, MeOH); UV (CH$_3$OH) λ_{max} 428 and 311 nm; ^{1}H and ^{13}C NMR data, Table 2; HRESIMS *m/z* 719.13398 [M + H]$^+$ (calcd for C$_{33}$H$_{36}$O$_{13}$Br, 719.13338).

12

Bromophilone B (16): red powder; $[\alpha]_D^{26}$ -99 (c 0.2, MeOH); UV (CH$_3$OH) λ_{max} 424 and 306 nm; ^{1}H and ^{13}C NMR data, Table 2; HRESIMS m/z 719.13312 [M + H]$^+$ (calcd for C$_{33}$H$_{36}$O$_{13}$Br, 719.13338).

Cytotoxicity Assay. Cytotoxicity against the mouse lymphoma cell line L5178Y was evaluated by MTT assay as previously described.[29] Kahalalide F (IC$_{50}$ 4.3 μM) and 0.1% ethylene glycol monomethyl ether in DMSO were used as positive and negative controls, respectively. Cytotoxicity against the human ovarian cancer cell line A2780 was carried out as previously described.[30] In brief, A2780 cells were seeded at a density of 9,500 cells/well in 96well plates (Corning, Germany). After 24 h, cells were exposed to 3.6-fold serially diluted concentrations of test compounds. Incubation was ended after 72 h and cell survival was determined by addition of MTT solution (5 mg/mL in phosphate buffered saline). The formazan precipitate was dissolved in DMSO (VWR, Germany). Absorbance was measured at 544 nm and 690 nm in a FLUOstar microplate-reader (BMG LabTech, Germany). Sodium chloride (0.9%) and cisplatin 100 μM were used as negative and positive controls (IC$_{50}$ cisplatin: 1.68 μM).

ACKNOWLEDGMENTS

REFERENCES

1. Blunt, J. W.; Carroll, A. R.; Copp, B. R.; Davis, R. A.; Keyzers, R. A.; Prinsep, M. R. Marine natural products. *Nat. Prod. Rep.* **2018**, *35*, 8–53.

2. Newman, D. J.; Cragg, G. M. Marine natural products and related compounds in clinical and advanced preclinical trials. *J. Nat. Prod.* **2004**, *67*, 1216–1238.

13

3. Kingston, D. G. I. Modern natural products drug discovery and its relevance to biodiversity conservation. *J. Nat. Prod.* **2011**, *74*, 496–511.

4. Hubert, J.; Nuzillard, J.-M.; Renault, J.-H. Dereplication strategies in natural product research: How many tools and methodologies behind the same concept? *Phytochem. Rev.* **2017**, *16*, 55–95.

5. Netzker, T.; Fischer, J.; Weber, J.; Mattern, D. J.; König, C. C.; Valiante, V.; Schroeckh, V.; Brakhage, A. A. Microbial communication leading to the activation of silent fungal secondary metabolite gene clusters. *Front. Microbiol.* **2015**, *6*, 299.

6. Marmann, A.; Aly, A. H.; Lin, W.; Wang, B.; Proksch, P. Co-cultivation—a powerful emerging tool for enhancing the chemical diversity of microorganisms. *Mar. Drugs* **2014**, *12*, 1043–1065.

7. Daletos, G.; Ebrahim, W.; Ancheeva, E.; El-Neketi, M.; Lin, W. H.; Proksch, P. Microbial coculture and OSMAC approach as strategies to induce cryptic fungal biogenetic gene clusters. In: *Chemical biology of natural products*; Newman, D. J.; Cragg, G. M.; Grothaus, P. G.; CRC Press: Boca Raton, FL, USA, **2017**, 233–284. ISBN 9781439841945.

8. Wiese, J.; Ohlendorf, B.; Blümel, M.; Schmaljohann, R.; Imhoff, J. F. Phylogenetic identification of fungi isolated from the marine sponge *Tethya aurantium* and identification of their secondary metabolites. *Mar. Drugs* **2011**, *9*, 561–585.

9. Nicoletti, R.; Lopez-Gresa, M. P.; Manzo, E.; Carella, A.; Ciavatta, M. L. Production and fungitoxic activity of Sch 642305, a secondary metabolite of *Penicillium canescens*. *Mycopathologia* **2007**, *163*, 295–301.

10. Bertinetti, B. V.; Peña, N. I.; Cabrera, G. M. An antifungal tetrapeptide from the culture of *Penicillium canescens*. *Chem. Biodivers.* **2009**, *6*, 1178–1184.

11. Brian, P. W.; Hemming, H. G.; Moffatt, J. S.; Unwin, C. H. Canescin, an antibiotic

14

produced by *Penicillium canescens. Transactions of the British Mycological Society* **1953**, *36*, 243–247.

12. Wang, H.; Dai, H.; Heering, C.; Jankiak, C.; Lin, W.; Orfali, R. S.; Müller, W. E. G.; Liu, Z.; Proksch, P. *RSC Adv.* **2016**, *6*, 81685–81693.

13. Xia, X.; Li, Q.; Li, J.; Shao, C.; Zhang, J.; Zhang, Y.; Liu, X.; Lin, Y.; Liu, C.; She, Z. *Planta Med.* **2011**, *77*, 1735–1738.

14. Mutanyatta, J.; Matapa, B. G.; Shushu, D. D.; Abegaz, B. M. *Phytochemistry* **2003**, *62*, 797–804.

15. Abdel-Lateff, A.; Klemke, C.; König, G. M.; Wright, A. D. *J. Nat. Prod.* **2003**, *66*, 706–708.

16. Cacho, R. A.; Chooi, Y. H.; Zhou, H.; Tang, Y. *ACS Chem. Biol.* **2003**, *8*, 2322–2330.

17. MacMillan, J. Griseofulvin. Part VII. Dechlorogriseofulvin. *J. Chem. Soc.* **1953**, 1697-1702.

18. Varma, G. B.; Fatope, M. O.; Marwah, R. G.; Deadman, M. E.; Al-Rawahi, F. K. *Phytochemistry* **2006**, *67*, 1925–1930.

19. Beekman, A. M.; Martinez, E. C.; Barrow, R. A. *Org. Biomol. Chem.* **2013**, *11*, 1109–1115.

20. Sekiguchi, J.; Katayama, S.; Yamada, Y. 6-Methyl-1,2,4-benzenetriol, a new intermediate in penicillic acid biosynthesis in *Penicillium cyclopium. Appl. Environ. Microbiol.* **1987**, *53*, 1531–1535.

21. Kosemura, S. *Tetrahedron* **2003**, *59*, 5055–5072.

22. Kozlovsky, A.; Vinokurova, N. G.; Adanin, V. M.; Gräfe, U. Piscarinines, New Polycyclic Diketopiperazine Alkaloids from *Penicillium piscarium* NKM F-691. *Nat. Prod. Lett* . **2000**, *14*, 333–340.

23. Belofsky, G. N.; Gloer, K. B.; Gloer, J. B.; Wicklow, D. T.; Dowd, P. F. New *p*-

15

terphenyl and polyketide metabolites from the sclerotia of *Penicillium raistrickii. J. Nat. Prod.* **1998**, *61*, 1115–1119.

24. Kobayashi, Y.; Tan, C.-H.; Kishi, Y. *Helv. Chim. Acta* **2000**, *83*, 2562–2571.

25. Kobayashi, Y.; Tan, C.-H.; Kishi, Y. *Angew. Chem., Int. Ed.* **2000**, *39*, 4279–4281.

26. Kobayashi, Y.; Tan, C.-H.; Kishi, Y. *J. Am. Chem. Soc.* **2001**, *123*, 2076–2078.

27. Bariotaki, A.; Kalaitzakis, D.; Smonou, L. *Org. Lett.* **2012**, *14*, 1792–1795.

28. Kjer, J.; Debbab, A.; Aly, A. H.; Proksch, P. Methods for isolation of marine-derived endophytic fungi and their bioactive secondary products. *Nat. Protoc.***2010**, *5*, 479–490.

29. Ashour, M.; Edrada, R.; Ebel, R.; Wray, V.; Wätjen, W.; Padmakumar, K.; Müller, W. E. G.; Lin, W. H.; Proksch, P. Kahalalide derivatives from the Indian sacoglossan mollusk Elysia grandifolia. *J. Nat. Prod.***2006**, *69*, 1547–1553.

30. Engelke, L. H.; Hamacher, A.; Proksch, P.; Kassack, M. U. Ellagic Acid and Resveratrol Prevent the Development of Cisplatin Resistance in the Epithelial Ovarian Cancer Cell Line A2780. *J. Cancer***2016**, *7*, 353–363.

16

4.2 Supporting Information

Brominated Azaphilones from the Sponge-Associated Fungus *Penicillium canescens*

Marian Frank,[†] Rudolf Hartmann,[‡] Malte Plenker,[‡] Ferhat Can Özkaya,[⊥] Werner E.G. Müller,[‖]

Matthias U. Kassack,[∇] Alexandra Hamacher,[∇] Wenhan Lin,[O] Zhen Liu,[*,†] Peter Proksch[*,†]

[†]Institute of Pharmaceutical Biology and Biotechnology, Heinrich-Heine-Universität Düsseldorf, Universitätsstrasse 1, 40225 Düsseldorf, Germany

[‡]Institute of Complex Systems: Strukturbiochemie, Forschungszentrum Juelich, Wilhelm-Johnen-Strasse, 52428 Juelich, Germany

[⊥]Faculty of Fisheries, İzmir Katip Çelebi University, Çiğli, 35620 İzmir, Turkey

[‖]Institute of Physiological Chemistry, Universitätsmedizin der Johannes Gutenberg-Universität Mainz, 55128 Mainz, Germany

[∇]Institute for Pharmaceutical and Medicinal Chemistry, Heinrich-Heine-Universität Düsseldorf, Universitätsstrasse 1, 40225 Düsseldorf, Germany

[O]State Key Laboratory of Natural and Biomimetic Drugs, Peking University, Beijing 100191, China

Corresponding Authors

[*]Tel: +49 211 81 15979; Fax: +49 211 81 11923; E-mail: zhenfeizi0@sina.com (Z.L.)

[*]Tel: +49 211 81 14163; Fax: +49 211 81 11923; E-mail: proksch@uni-duesseldorf.de (P.P.)

Table of contend

S1. ^{1}H NMR spectrum of compound **(1)** in CDCl$_3$ at 600 MHz

Frank.430.fid
MPC-V2-SI2-SP

1H NMR (600 MHz, Chloroform-*d*) δ 11.57 (s, 1H), 6.35 (*d*, *J* = 2.8 Hz, 1H), 6.34 (s, 1H), 6.29 (*d*, *J* = 2.9 Hz, 1H), 3.90 (s, 3H), 3.76 (s, 3H), 3.74 (s, 3H), 3.48 (s, 2H), 2.29 (s, 3H).

S2. ^{13}C NMR spectrum of compound **(1)** in CDCl$_3$ at 150 MHz

Frank.442.fid
MPC-V2-SI2-SP

13C NMR (151 MHz, CDCl$_3$) δ 170.99, 162.40, 160.22, 156.53, 155.09, 149.90, 138.99, 129.72, 107.35, 106.83, 101.32, 98.73, 95.74, 56.61, 56.57, 55.67, 52.42, 17.52.

17.52
52.42
55.67
56.57
56.61
95.74
98.73
101.32
106.83
107.35
129.72
138.99
149.90
155.09
156.53
160.22
162.40
170.99

f1 (ppm)

S3. ^{1}H-^{13}C HSQC spectrum of compound **(1)** in CDCl$_3$ at 600 MHz/150 MHz

S4. ^{1}H-^{13}C HMBC spectrum of compound **(1)** in CDCl$_3$ at 600 MHz/150 MHz
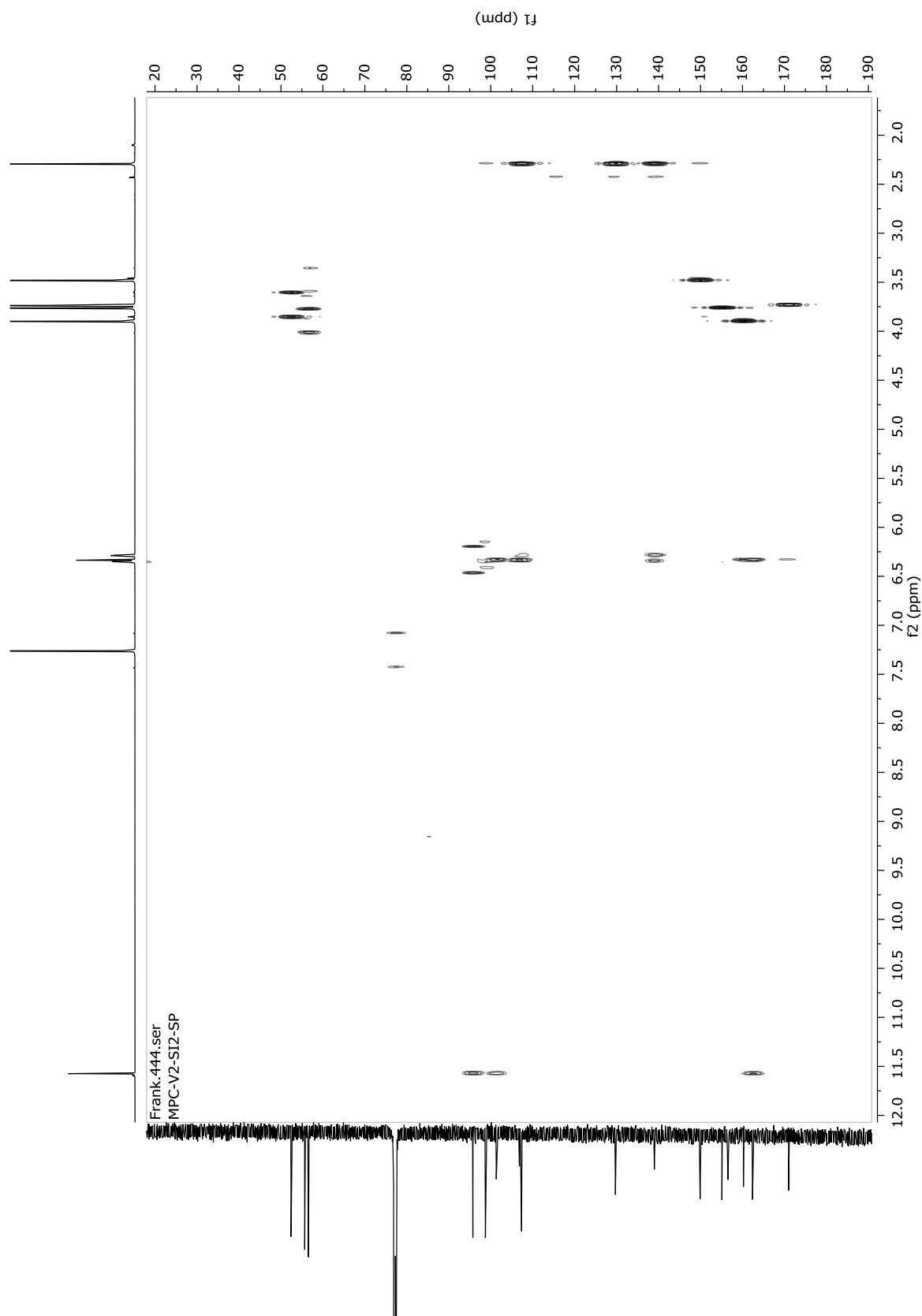
S5. ^{1}H-^{1}H COSY spectrum of compound **(1)** in CDCl$_3$ at 600 MHz

S6. ^{1}H-^{1}H ROESY spectrum of compound **(1)** in CDCl$_3$ at 600 MHz

Frank.445.ser
MPC-V2-SI2-SP
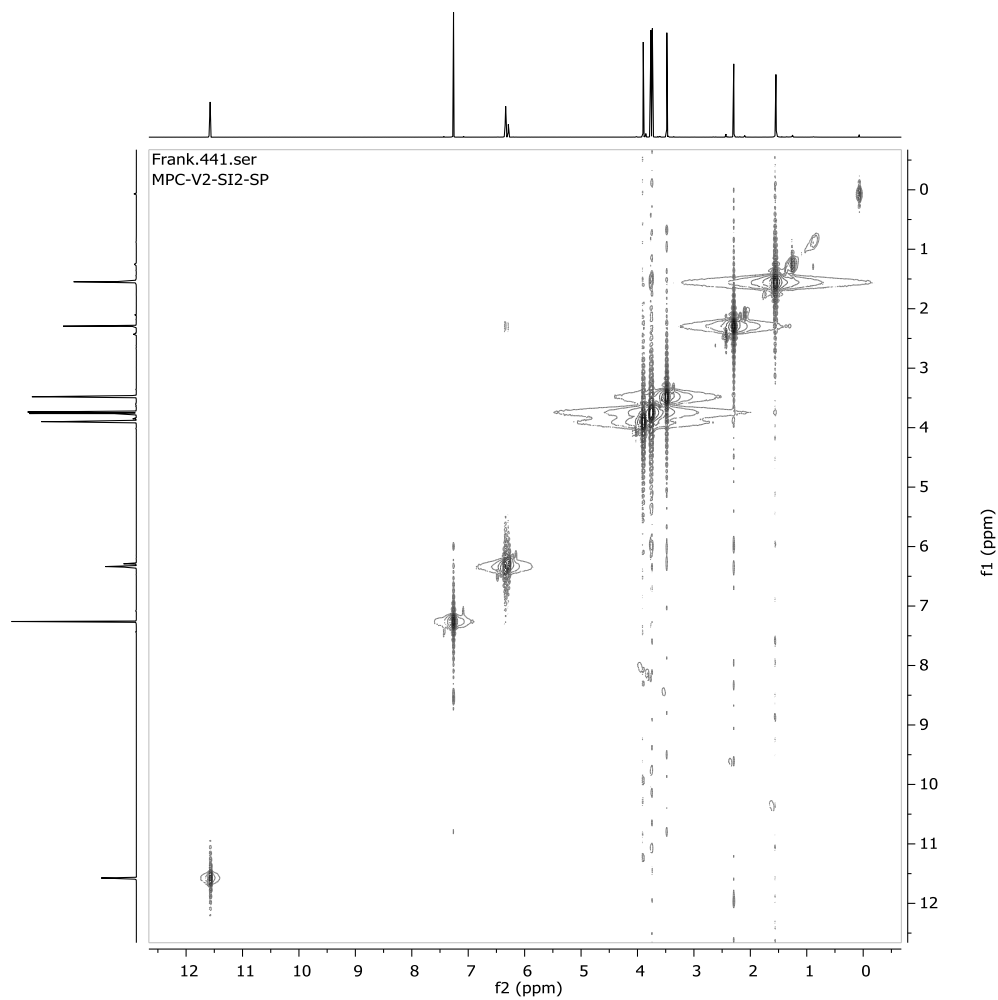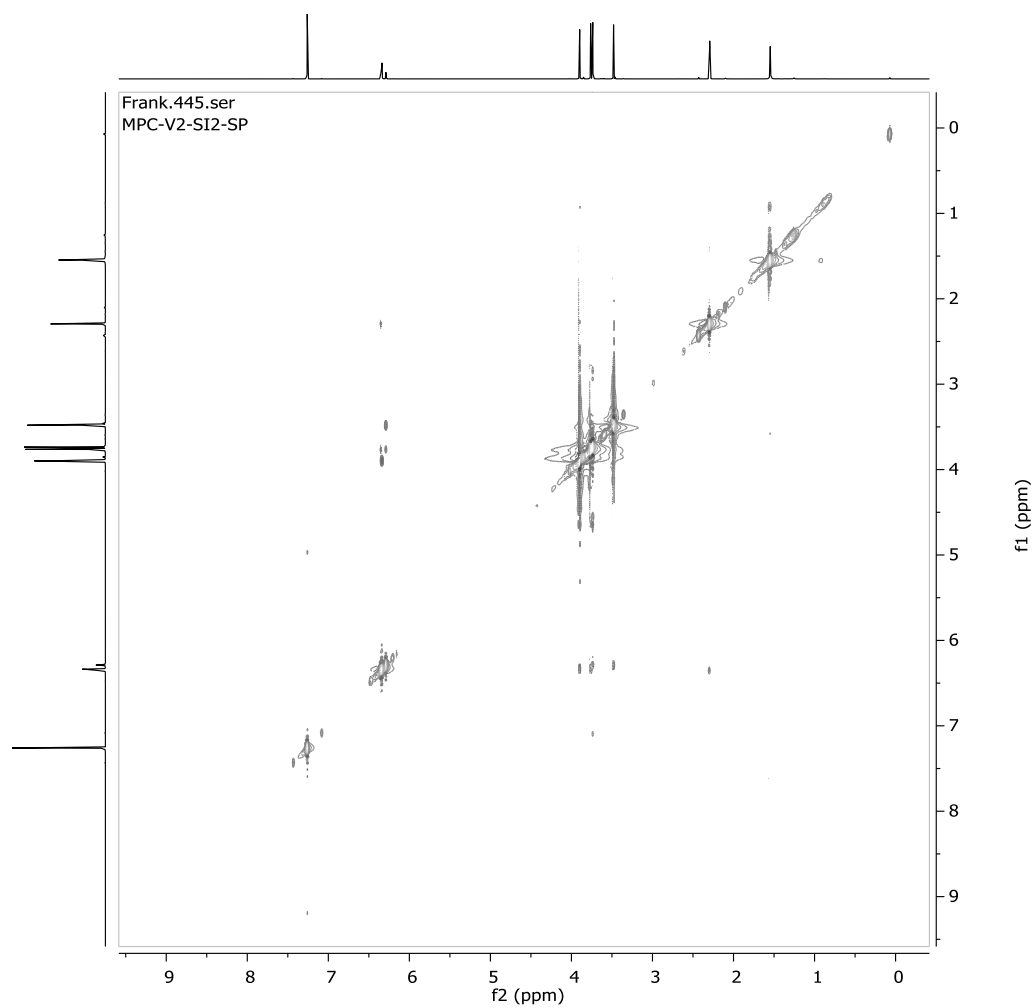
S8. UV-absorption spectrum of compound **(1)** in MeOH
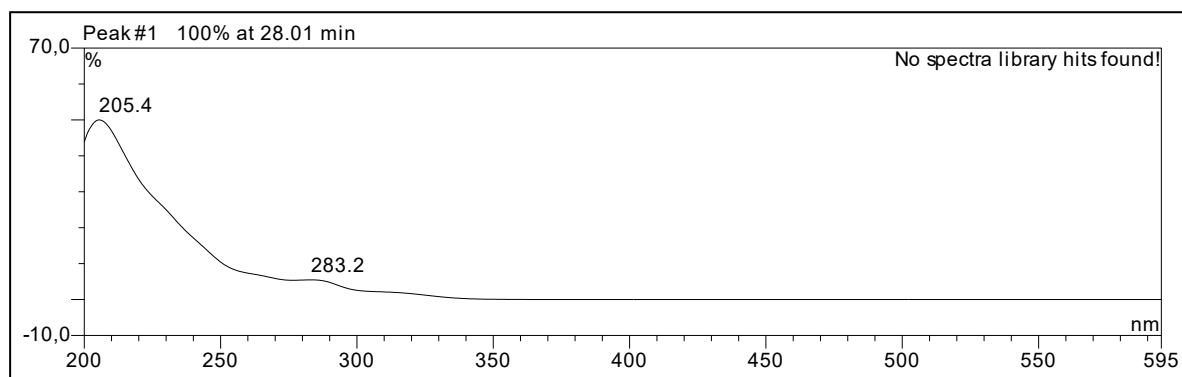
S9. LCMS (ESI+/ESI-) spectrum of compound **(1)**
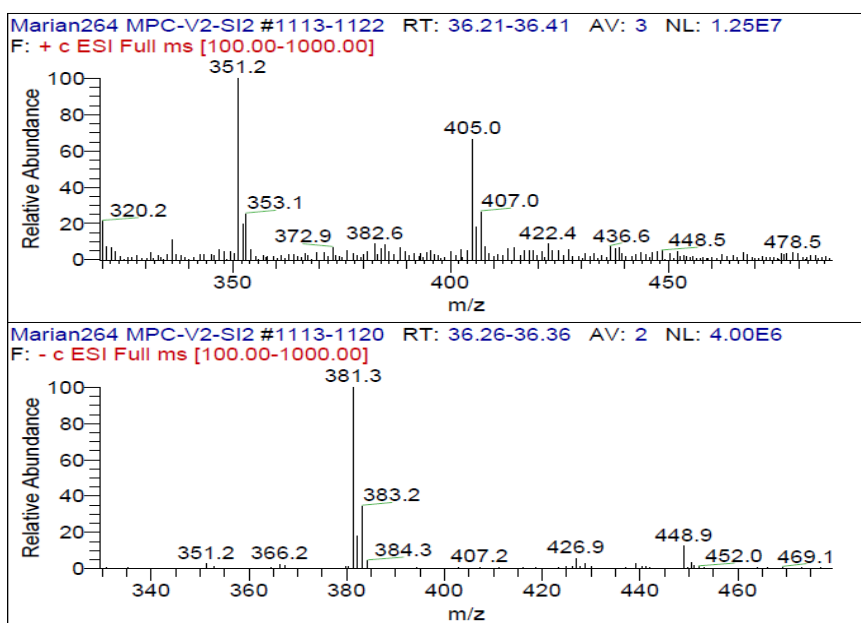
S10. HRMS (ESI+) spectrum of compound **(1)**

Analysis Info

		Acquisition Date	4/11/2018 1:18:31 PM
Analysis Name	D:\Data\Spektren 2018\PRO18HR000025.d		
Method	tune_low_new.m	Operator	Peter Tommes
Sample Name	Frank MPC-V2-Si2-SP 1mg/ml (CH3OH)	Instrument maXis	288882.20213
Comment			

Acquisition Parameter

Source Type	ESI	Ion Polarity	Positive	Set Nebulizer	0.3 Bar
Focus	Not active	Set Capillary	4000 V	Set Dry Heater	180 °C
Scan Begin	50 m/z	Set End Plate Offset	-500 V	Set Dry Gas	4.0 l/min
Scan End	1500 m/z	Set Collision Cell RF	600.0 Vpp	Set Divert Valve	Source

Meas. m/z	#	Ion Formula	m/z	err [ppm]	mSigma	# mSigma	Score	rdb	e⁻ Conf	N-Rule
351.0629	1	C17H16ClO6	351.0630	0.2	19.1	1	100.00	9.5	even	ok
383.0892	1	C18H20ClO7	383.0892	-0.0	11.8	1	100.00	8.5	even	ok

S11. ^{1}H NMR spectrum of compound **(13)** in acetone-d_6 at 750 MHz

MP_20180523_Proksch-MPCBrV12S3H1.1.fid
gereinigt

1H NMR (750 MHz, Acetone-d_6) δ 8.14 (s, 2H), 7.36 (dd, J = 15.3, 10.8 Hz, 1H), 7.05 (dd, J = 15.1, 10.7 Hz, 1H), 6.86 (dd, J = 15.0, 10.7 Hz, 1H), 6.81 (dd, J = 14.9, 10.8 Hz, 1H), 6.52 (d, J = 15.2 Hz, 1H), 6.43 (s, 1H), 6.24 (s, 1H), 6.07 (d, J = 15.3 Hz, 1H), 4.64 (d, J = 11.4 Hz, 1H), 4.12 – 4.08 (m, 1H), 3.98 (d, J = 11.4 Hz, 1H), 3.95 (td, J = 6.1, 5.3, 3.1 Hz, 1H), 3.81 (s, 3H), 3.56 (d, J = 4.7 Hz, 1H), 3.29 (d, J = 14.7 Hz, 1H), 2.53 (s, 3H), 2.48 (dd, J = 15.4, 7.0 Hz, 1H), 2.43 (dd, J = 15.4, 5.9 Hz, 1H), 1.56 (dt, J = 13.9, 3.7 Hz, 1H), 1.50 (dt, J = 14.0, 8.9 Hz, 1H), 1.34 (s, 3H), 1.13 (d, J = 6.2 Hz, 3H).

S12. ^{13}C NMR spectrum of compound **(13)** in acetone-d_6 at 200 MHz

S13. ^{1}H-^{13}C HSQC spectrum of compound **(13)** in acetone-d_6 at 750 MHz/200 MHz

S13. ^{1}H-^{13}C HSQC spectrum of compound **(13)** in acetone-d_6 at 750 MHz/200 MHz
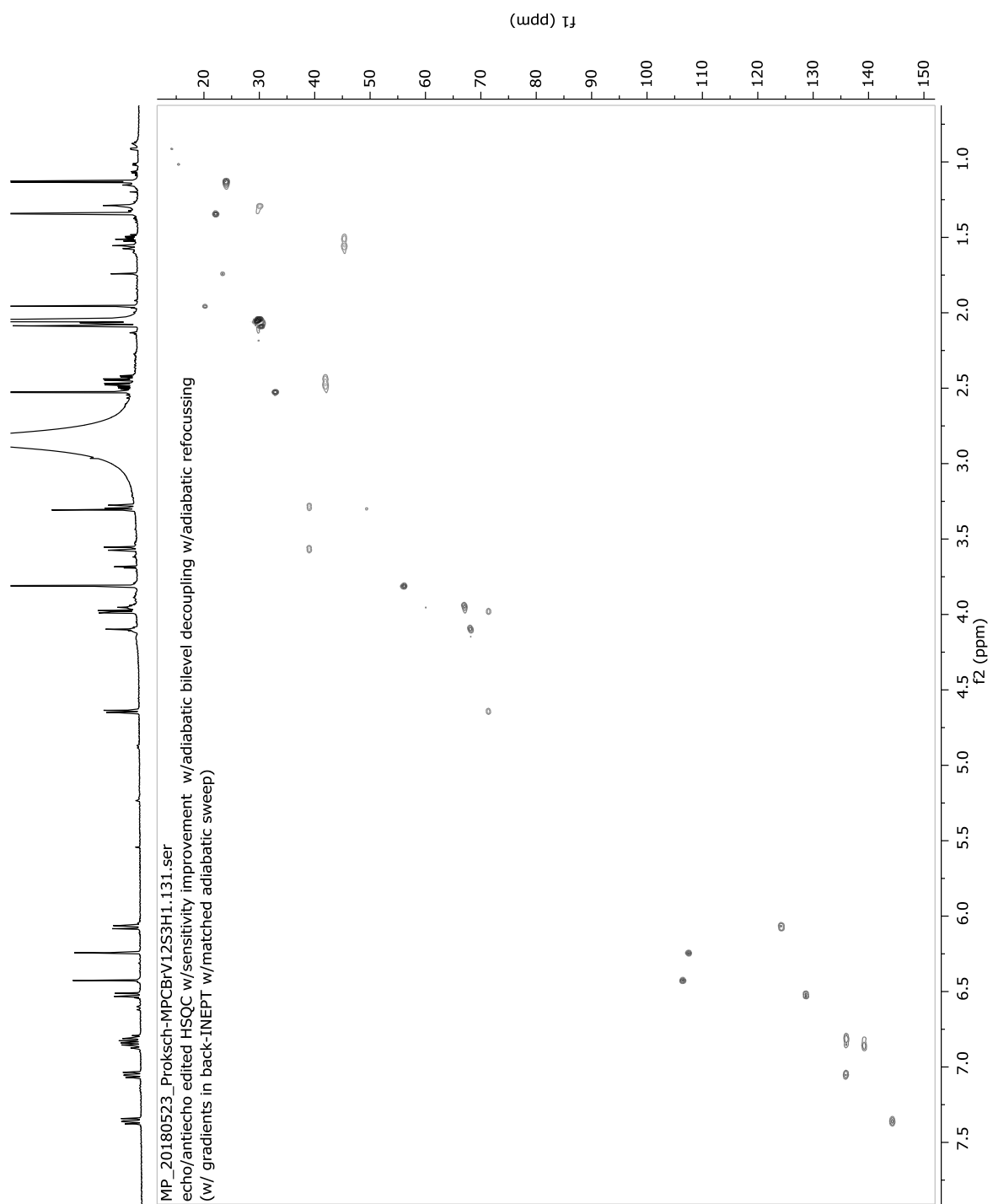
S14. ^{1}H-^{13}C HMBC spectrum of compound **(13)** in acetone-d_6 at 750 MHz/200 MHz
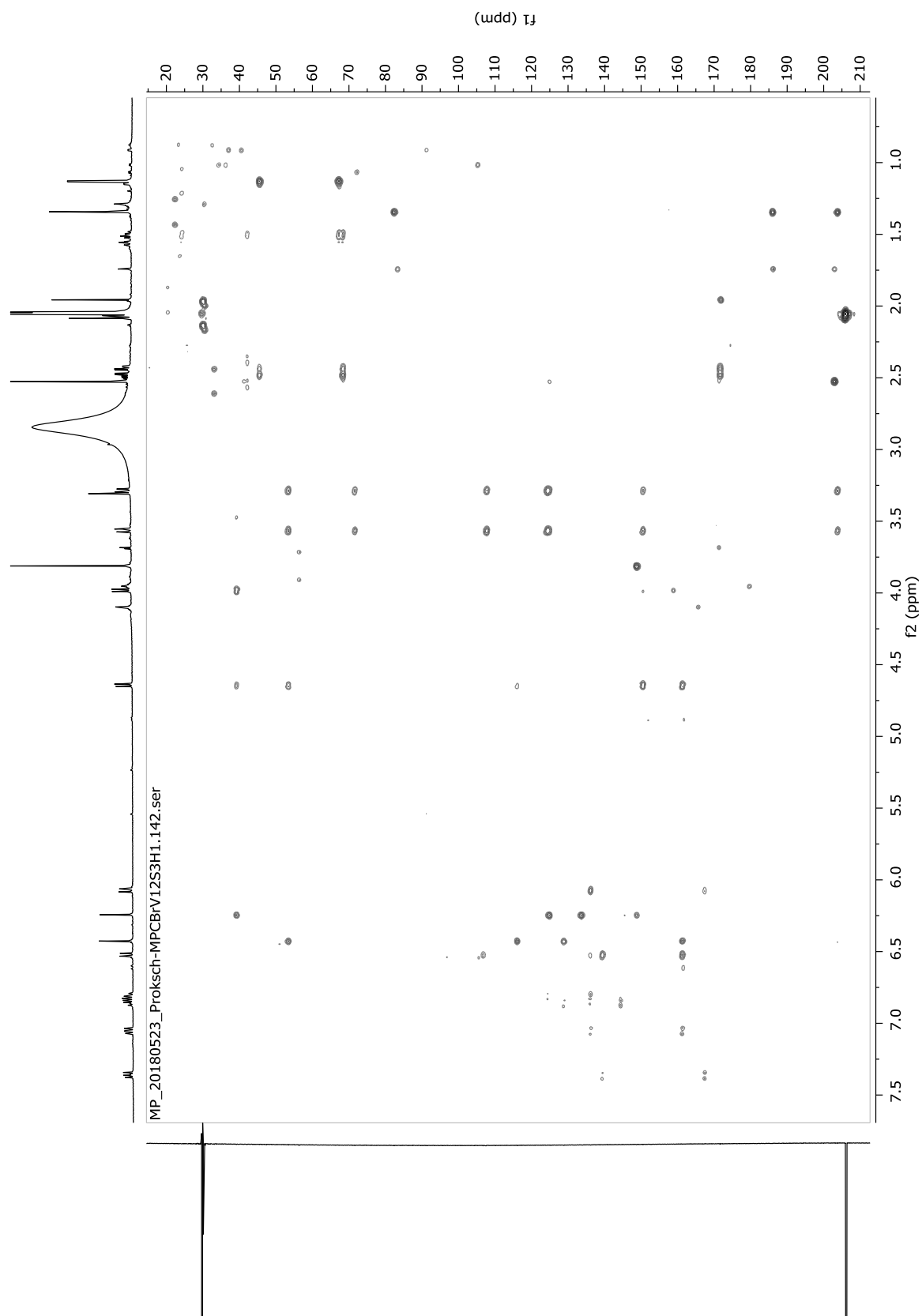
S15. ^{1}H-^{13}C HMBC spectrum of compound **(13)** in acetone-d_6 at 750 MHz/200 MHz
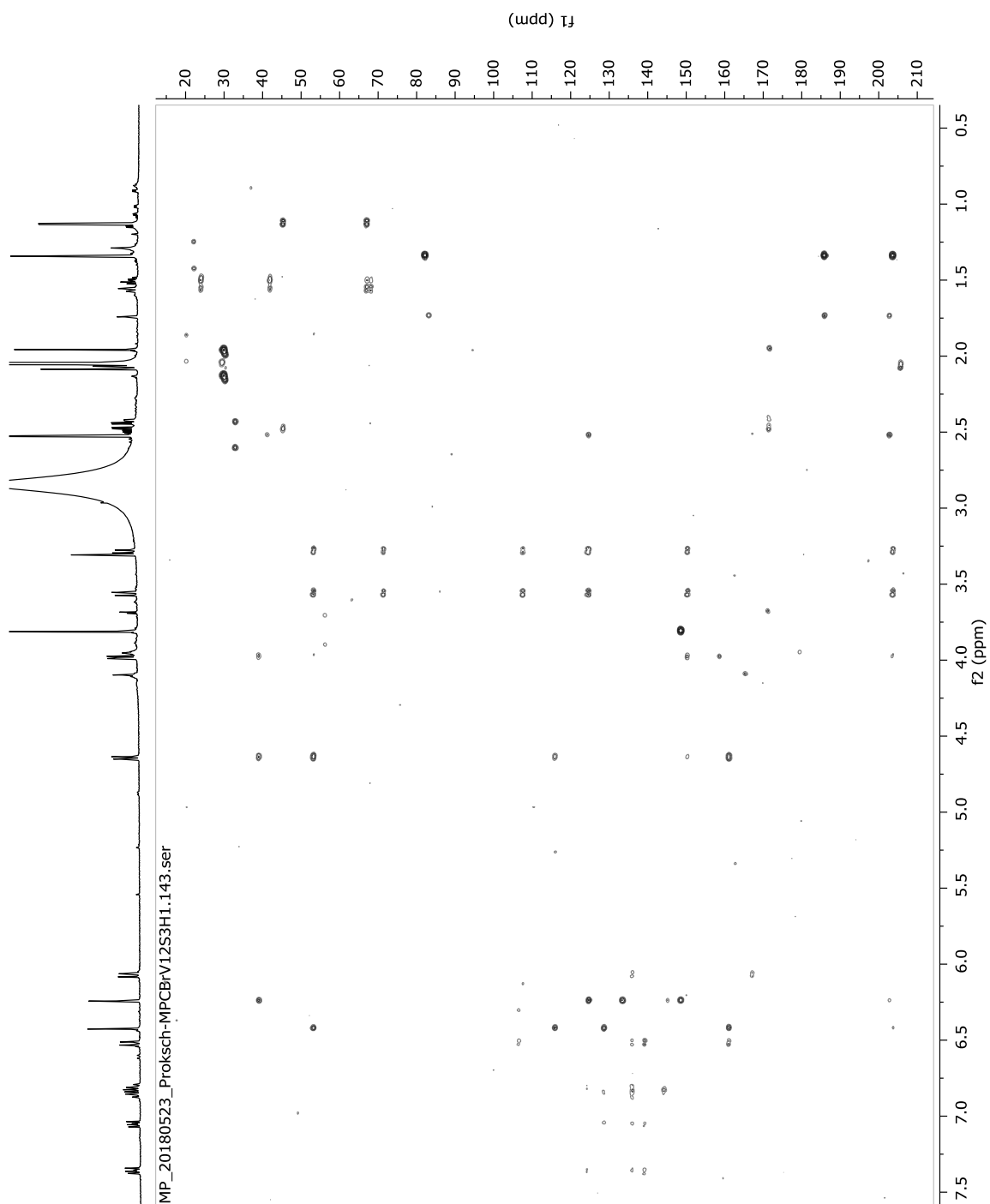
S16. ^{1}H-^{1}H TOCSY spectrum of compound **(13)** in acetone-d_6 at 750 MHz
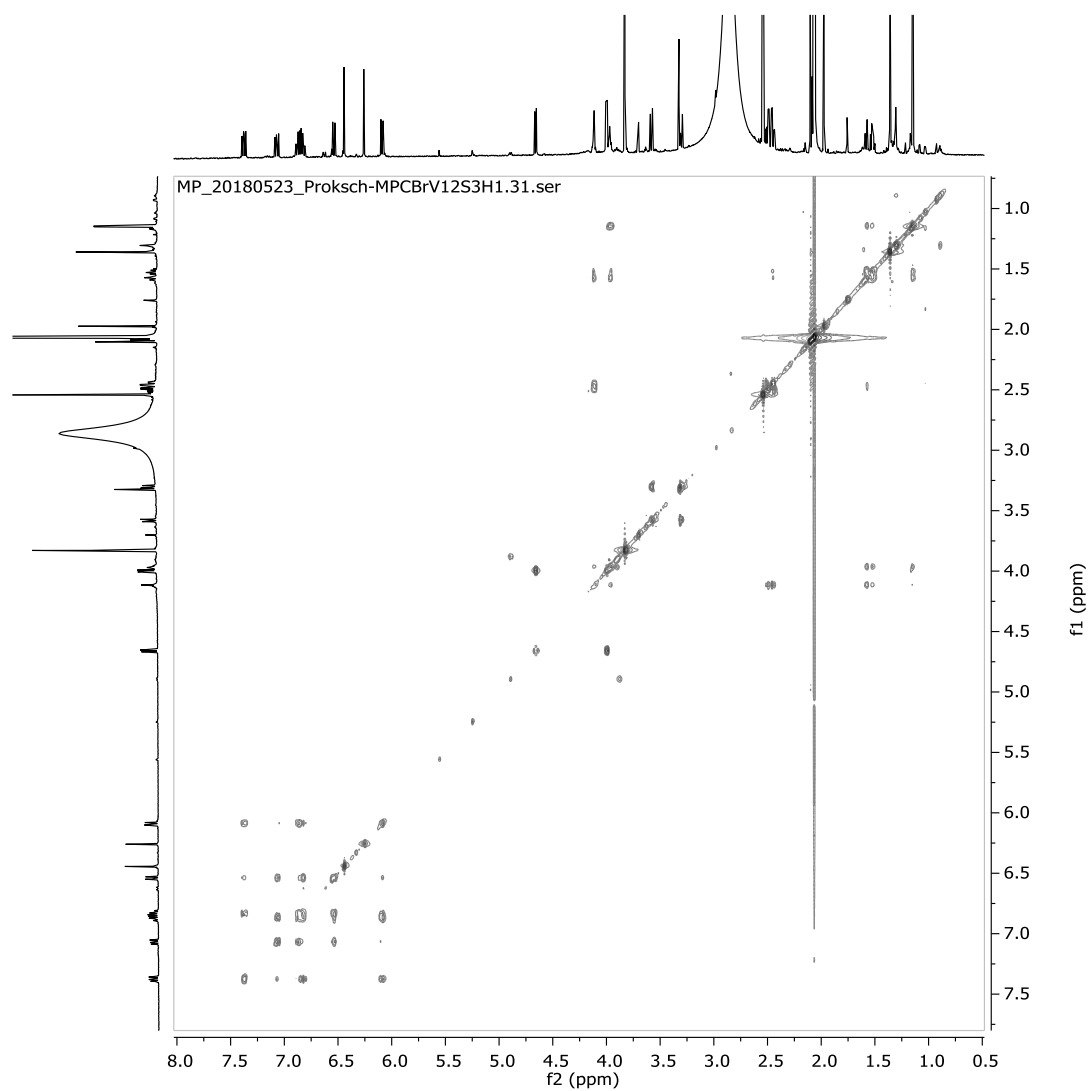
S17. ¹H-¹H COSY spectrum of compound **(13)** in acetone-*d₆* at 750 MHz
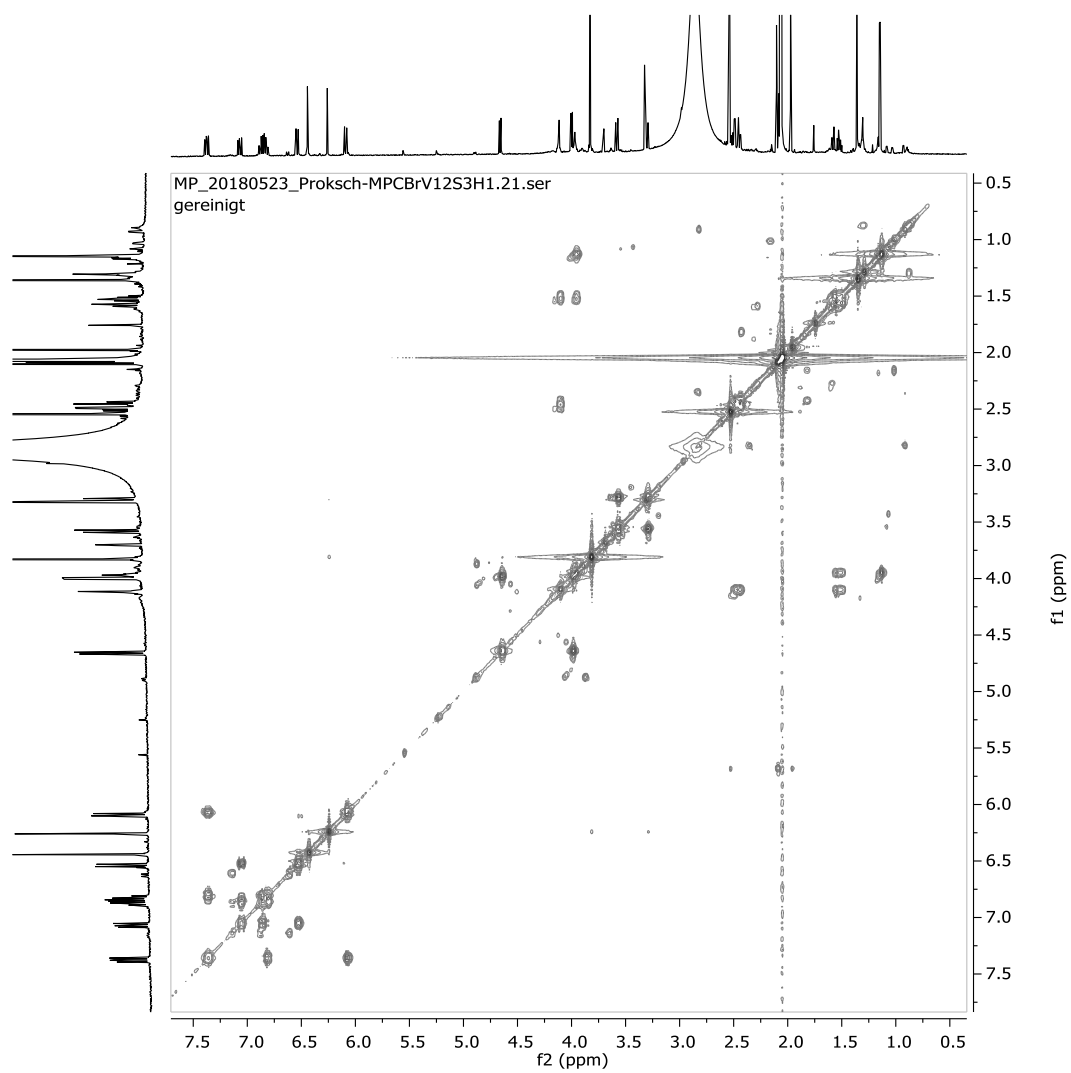
S18. ^{1}H-^{1}H ROESY spectrum of compound **(13)** in acetone-d_6 at 750 MHz
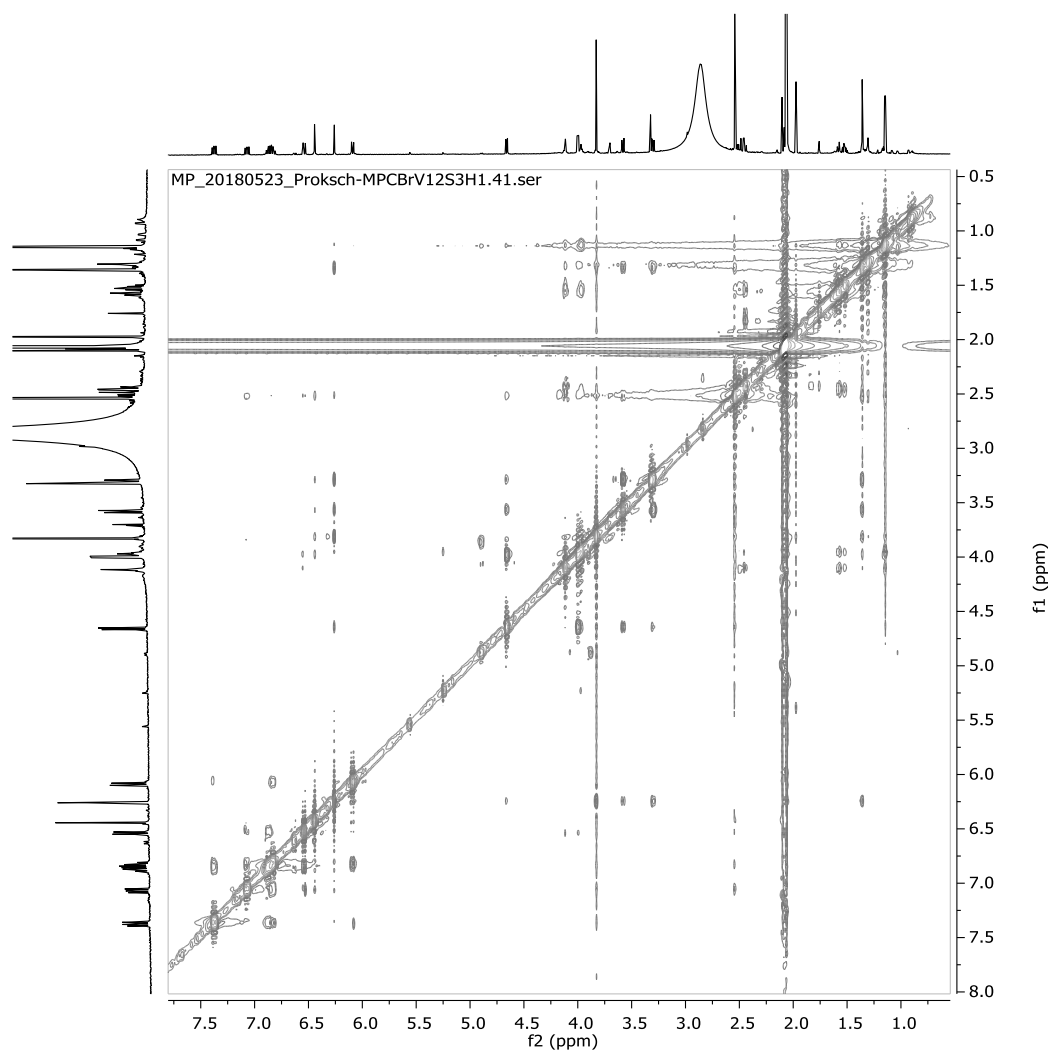
S19. UV-absorption spectrum of compound **(13)** in MeOH

Peak #1   100% at 25.85 min

No spectra library hits found!

423.4

305.7

370.3
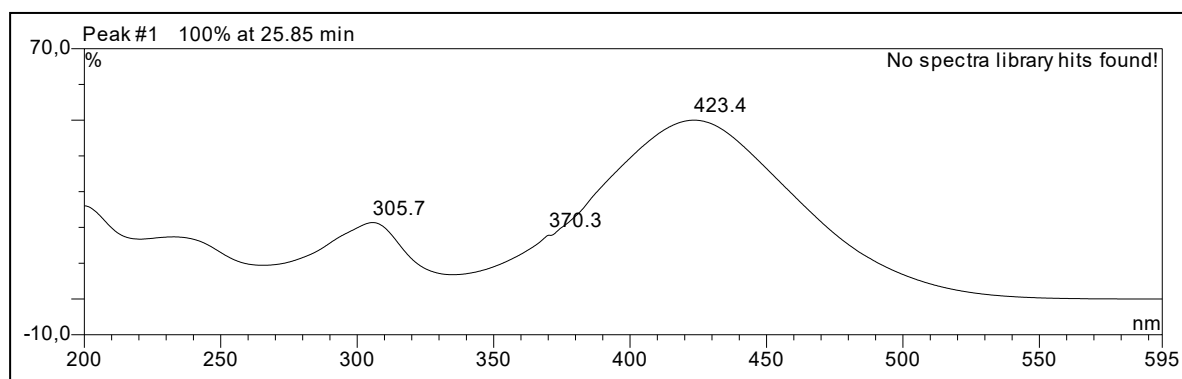
S20. ESI+/ESI- spectrum of compound **(13)**

MPCBR_V1253H1_5mgml #930   RT: 31.17   AV: 1   NL: 1.10E7
F: + c ESI Full ms [100.00-1000.00]

721.2
718.9
511.6
421.6
420.7
419.3 422.6
739.2
205.9
226.2
544.3
740.0
695.3
510.7 512.6
545.4
667.5
741.0
167.1
194.8
247.3
249.2 295.4 312.0
344.4
378.5
409.6
443.7 479.9
509.6 513.5
546.0
580.5 595.1
634.4 666.8 684.1
746.3
765.2 796.5
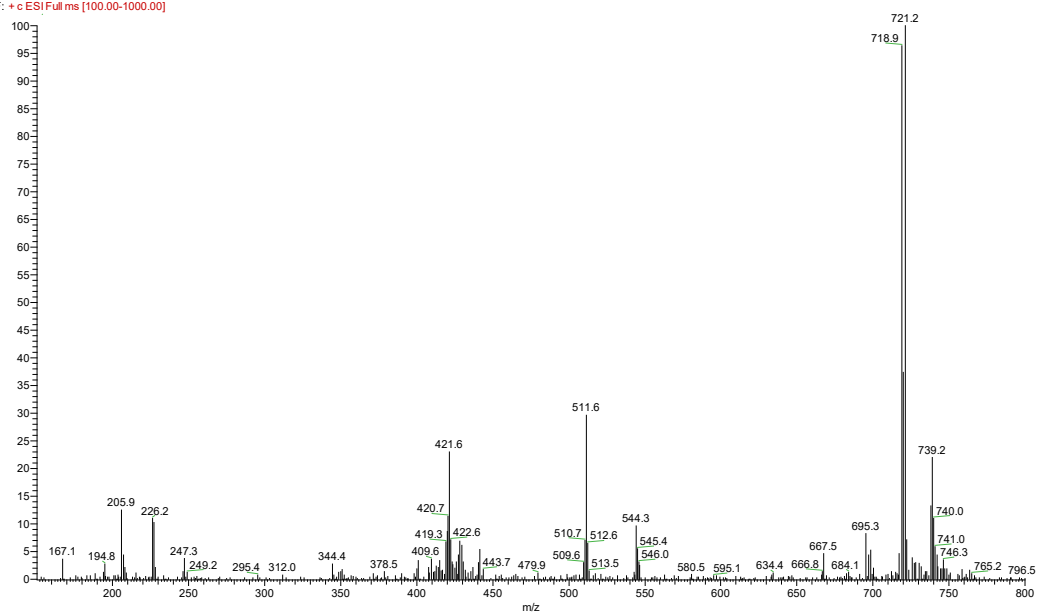
MPCBR_V1253H1_5mgml #928   RT: 31.12   AV: 1   NL: 4.12E6
F: - c ESI Full ms [100.00-1000.00]

525.0
523.2
509.9
526.5
527.4
147.6
193.0
313.5
371.5 378.4
377.5
559.1
598.9
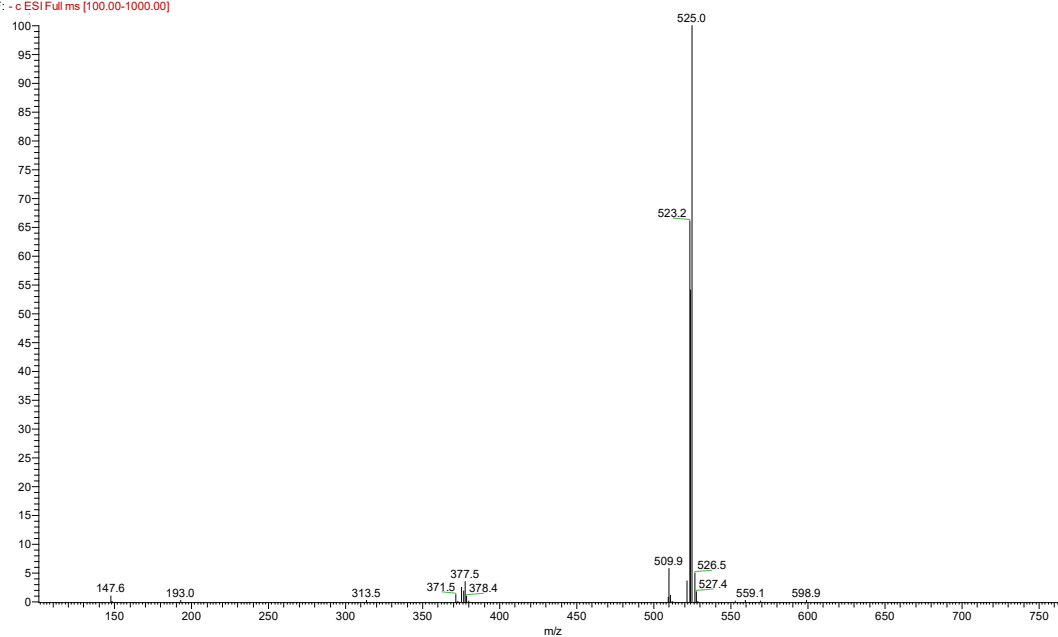
S21. HRMS (FTICR) (ESI+) spectrum of compound **(13)**

#180582_FTICRMS_MPCBrV12S3H1 #7-12   RT: 0.19-0.36   AV: 6   NL: 3.98E6
T: FTMS + p ESI Full ms [150.00-1000.00]
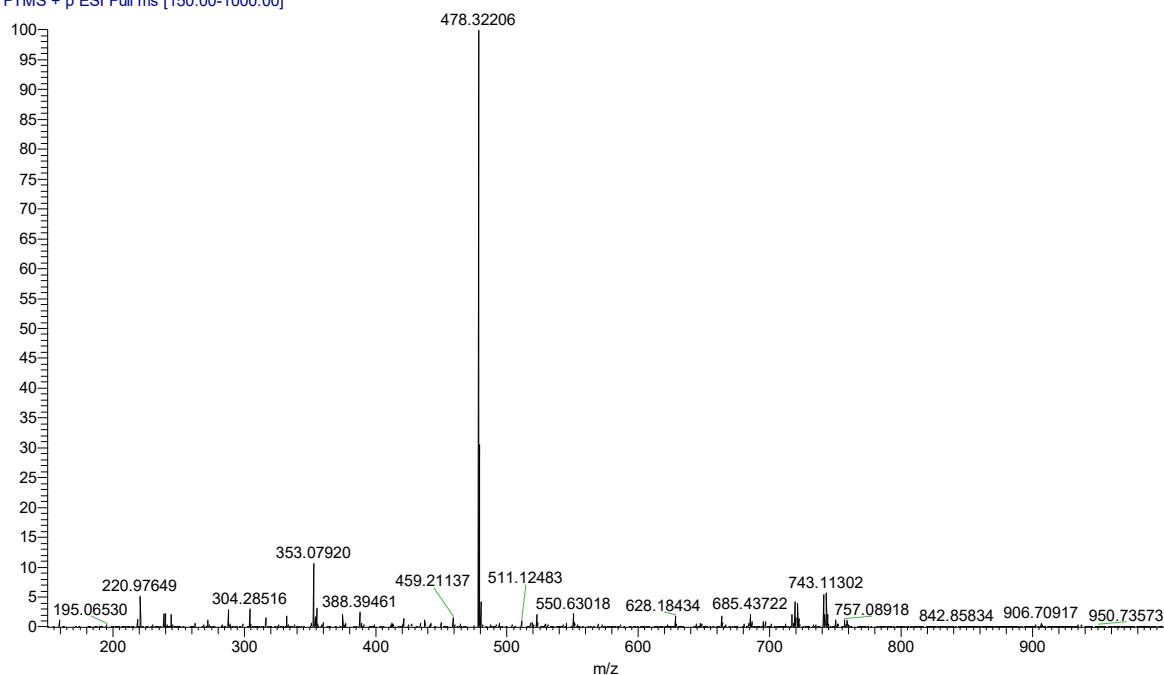
#180582_FTICRMS_MPCBrV12S3H1 #7-12   RT: 0.19-0.36   AV: 6   NL: 2.25E5
T: FTMS + p ESI Full ms [150.00-1000.00]
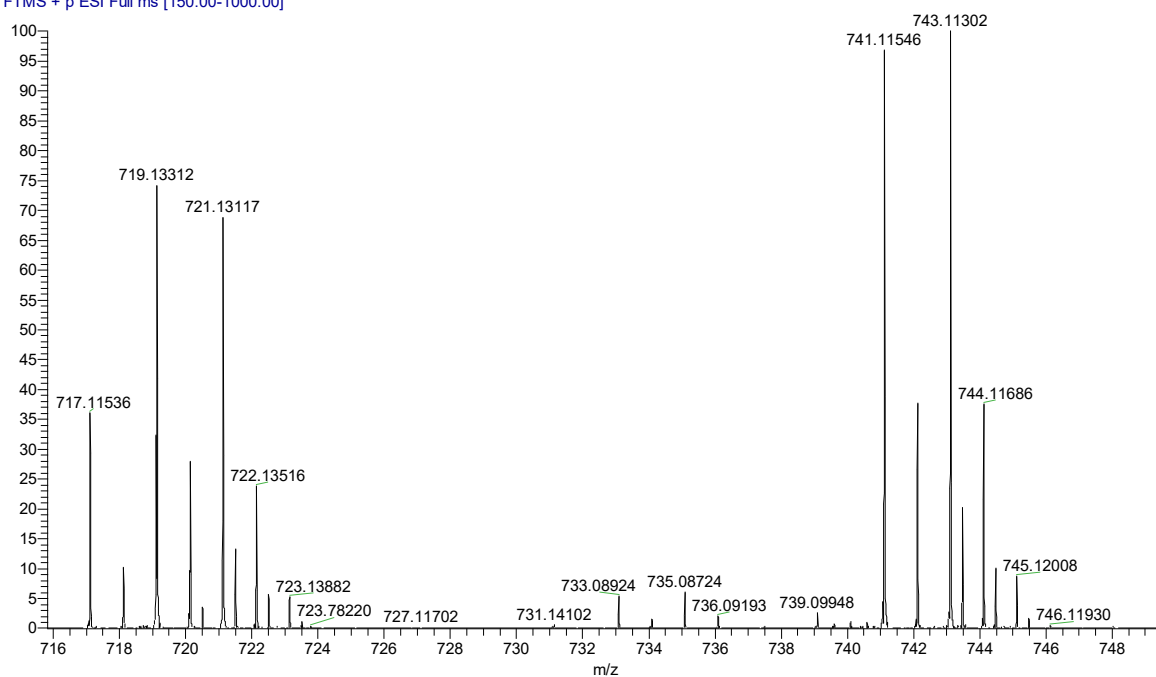
Measured m/z	Calculated m/z	Delta (ppm)	Molecular Formular
719.13312	719.13338	0.08	C33 H36 O13 Br
721.13117	721.13133	0.27	C33 H36 O13 [81]Br
741.11546	741.11532	0.64	C33 H35 O13 Br Na
743.11302	743.11328	0.16	C33 H35 O13 [81]Br Na

S22. ¹H NMR spectrum of compound **(14)** in acetone-d_6 at 700 MHz

S23. ^{13}C NMR spectrum of compound **(14)** in acetone-d_6 at 200 MHz

MP_20180423_MPCBrV12S3H2.31.fid

13C NMR (201 MHz, Acetone) δ 203.20, 201.59, 186.70, 171.05, 167.60, 161.12, 150.34, 148.40, 145.45, 144.45, 139.44, 136.18, 136.15, 133.13, 129.00, 124.53, 124.08, 110.88, 109.10, 107.37, 84.94, 70.23, 68.38, 67.18, 56.25, 54.68, 45.50, 42.59, 40.80, 33.21, 23.98.
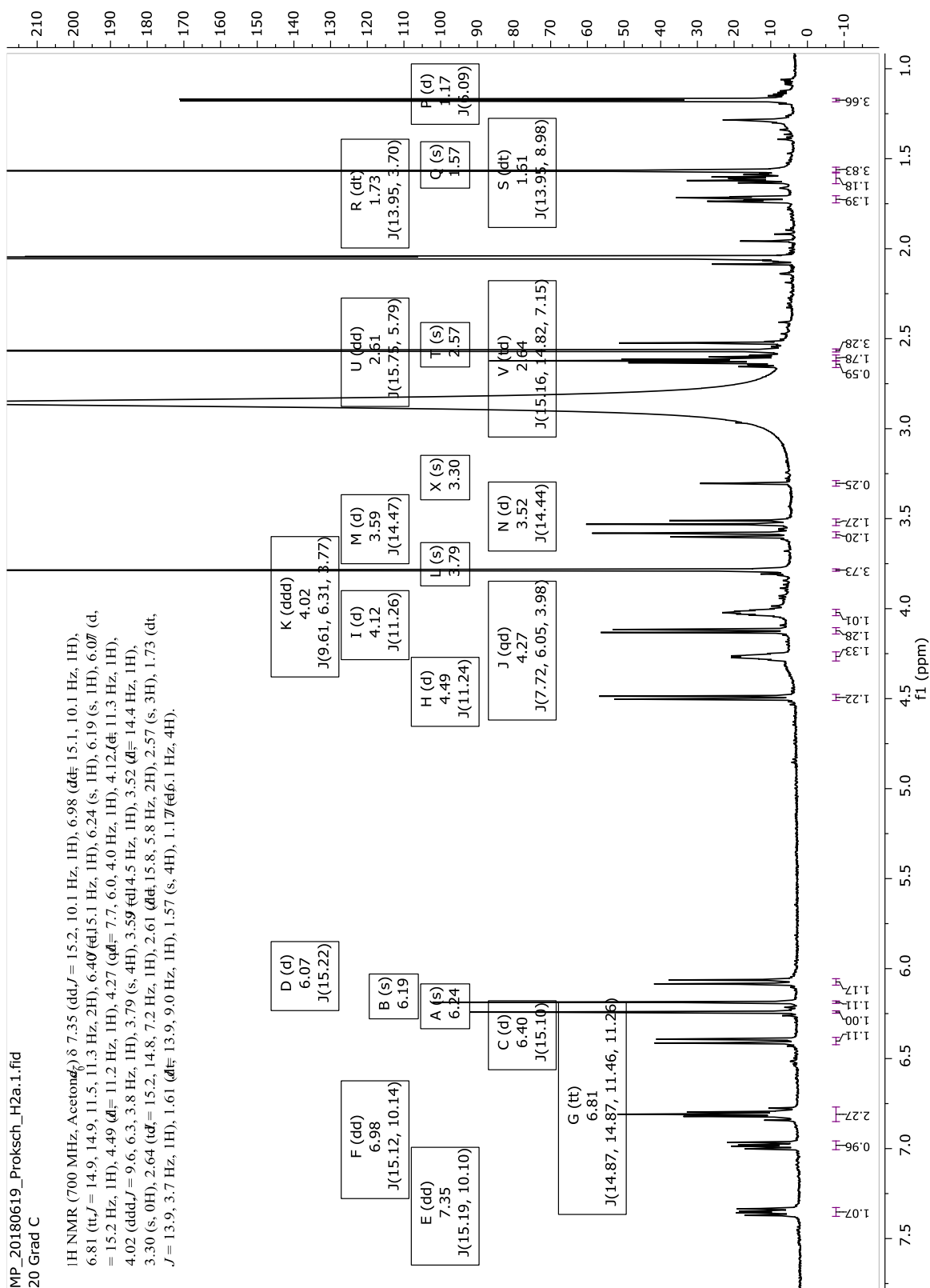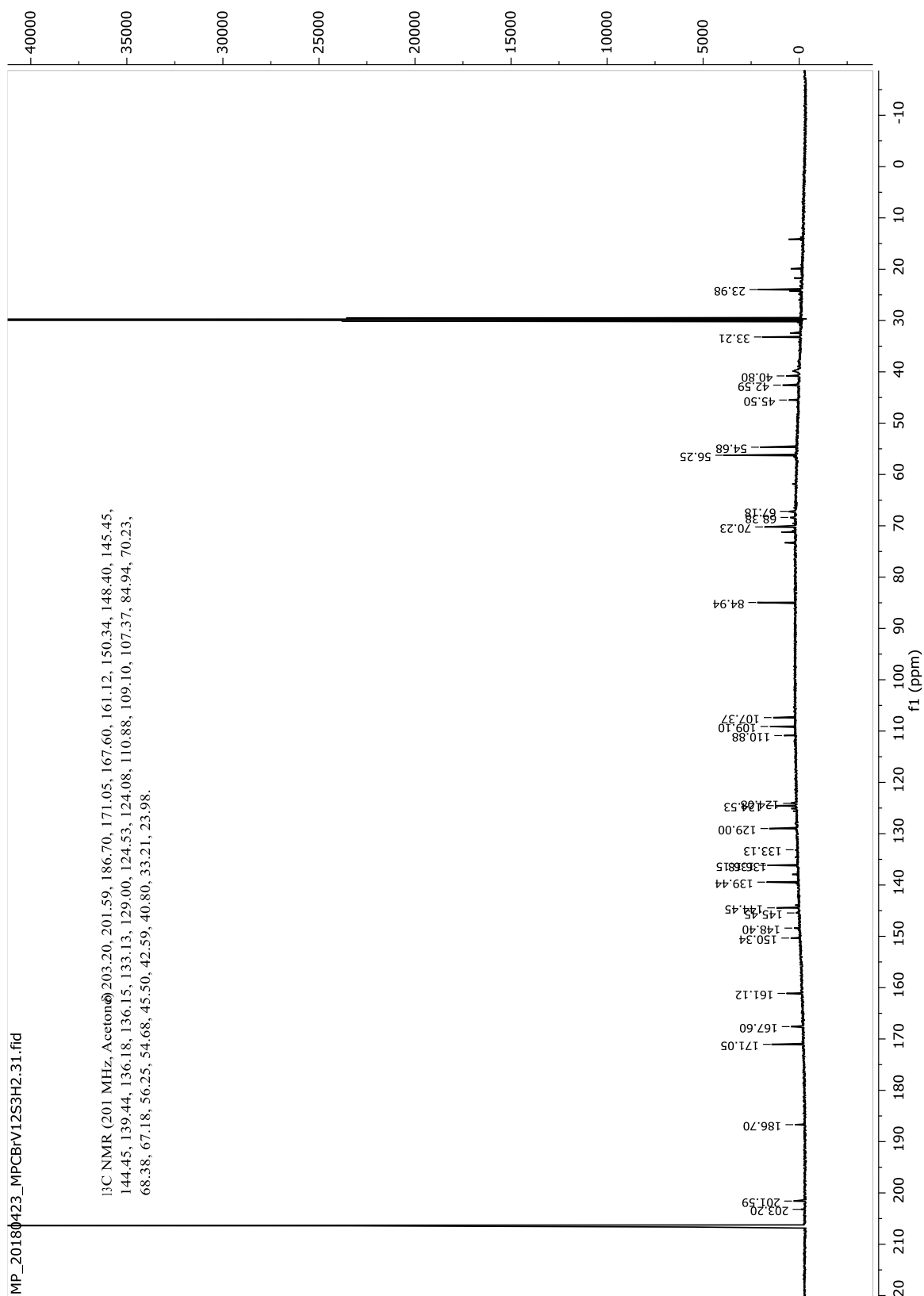
S24. ^{1}H-^{13}C HSQC spectrum of compound **(14)** in acetone-d_6 at 700 MHz/175 MHz
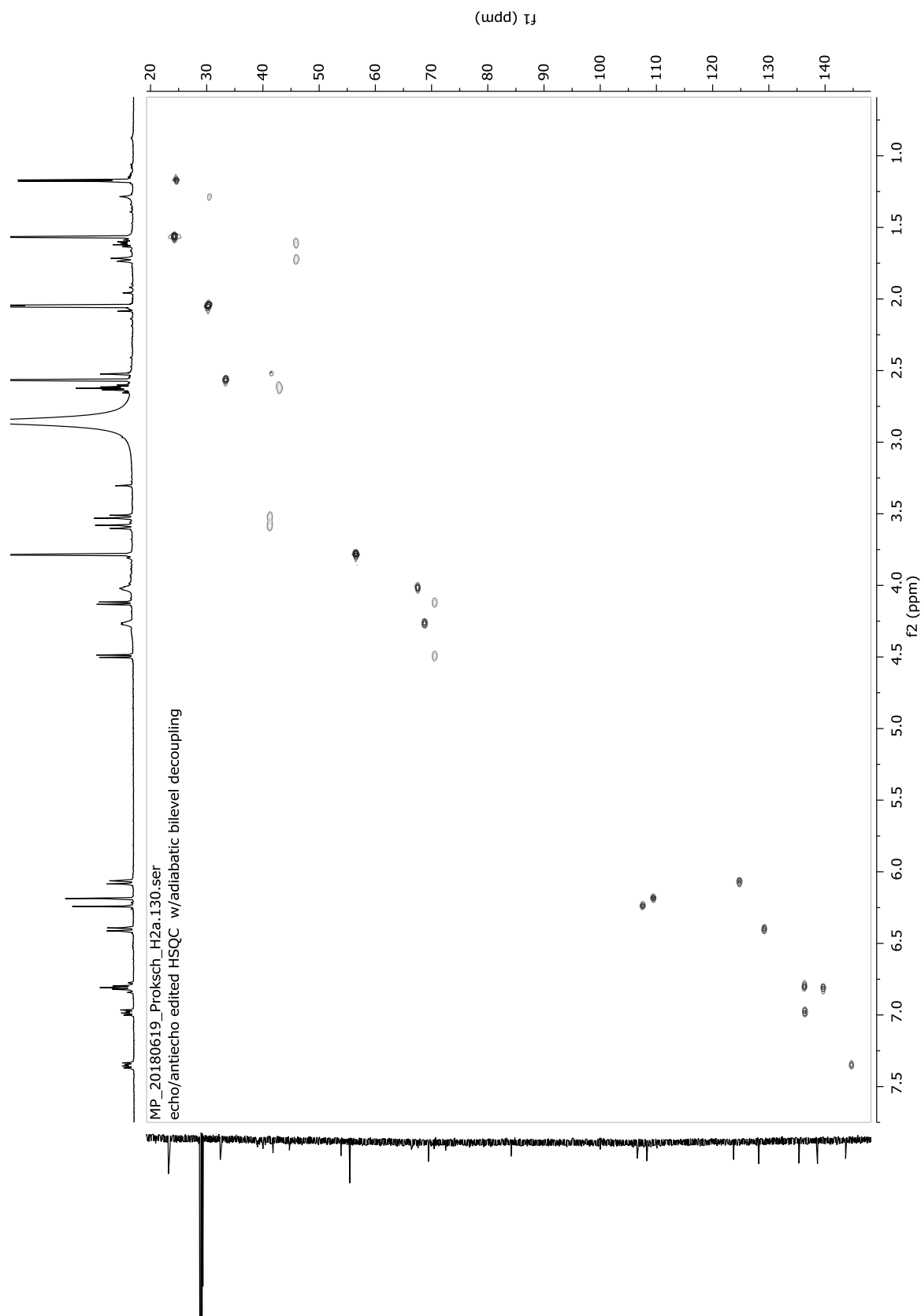
S25. ^{1}H-^{13}C HMBC spectrum of compound **(14)** in acetone-d_6 at 700 MHz/175 MHz (3Hz, 20°C)
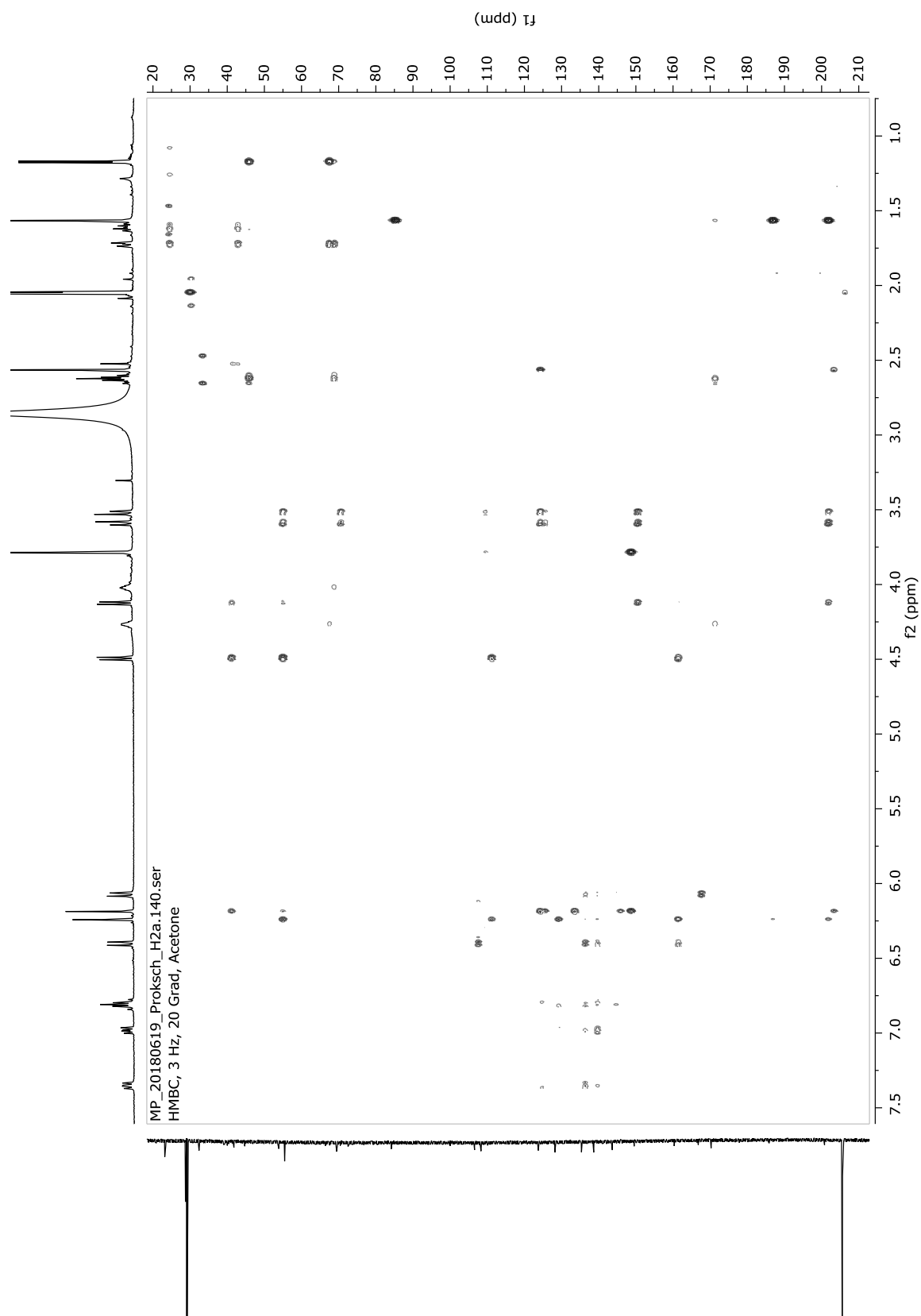
S26. ^{1}H-^{13}C HMBC spectrum of compound **(14)** in acetone-d_6 at 700 MHz/175 MHz (7Hz, 20°C)
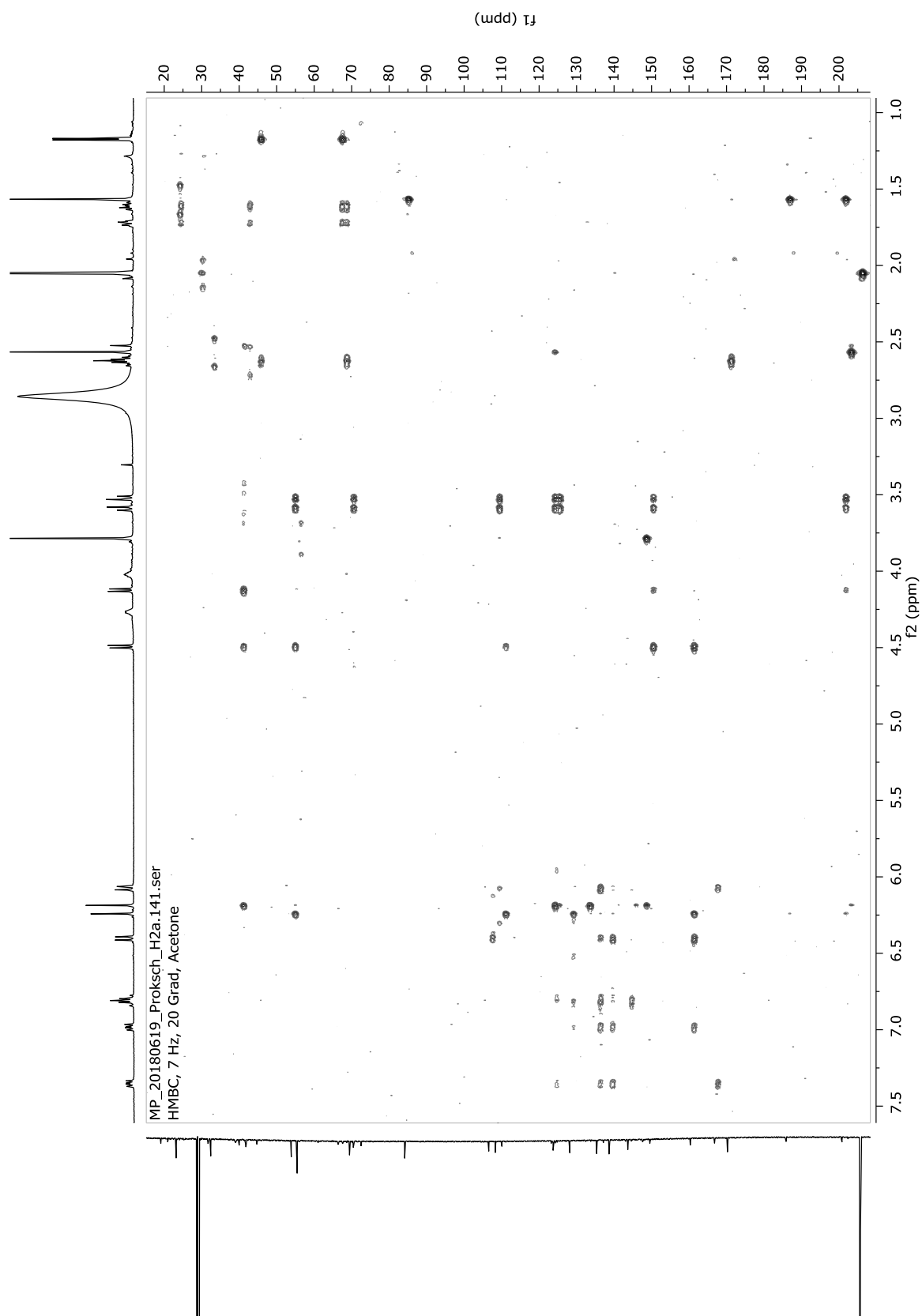
S27. ^{1}H-^{1}H TOCSY spectrum of compound **(14)** in acetone-d_6 at 700 MHz
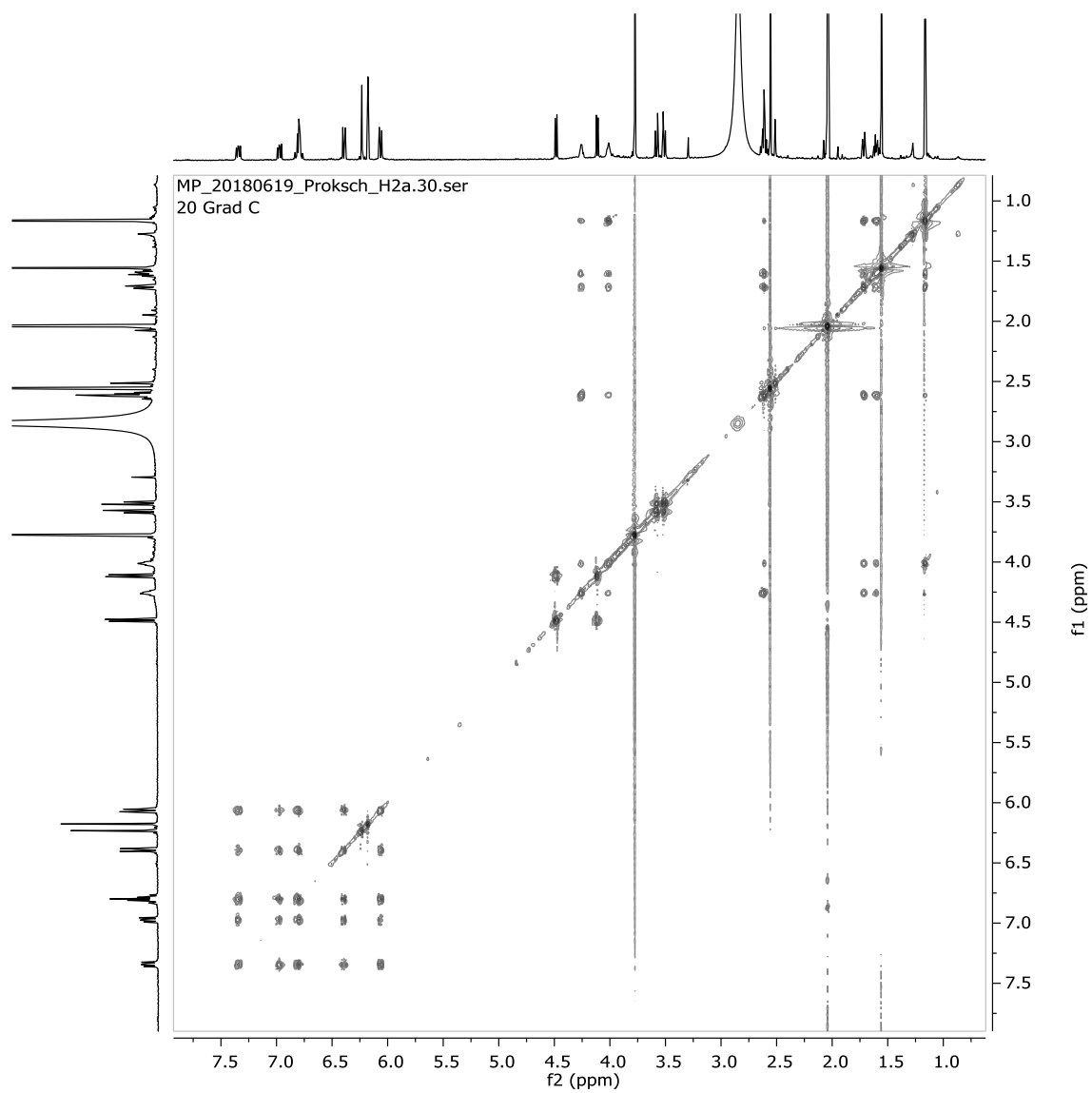
S28. ^{1}H-^{1}H COSY spectrum of compound **(14)** in acetone-d_6 at 300 MHz

Frank.961.ser
MPCBr-V12-S3-H2
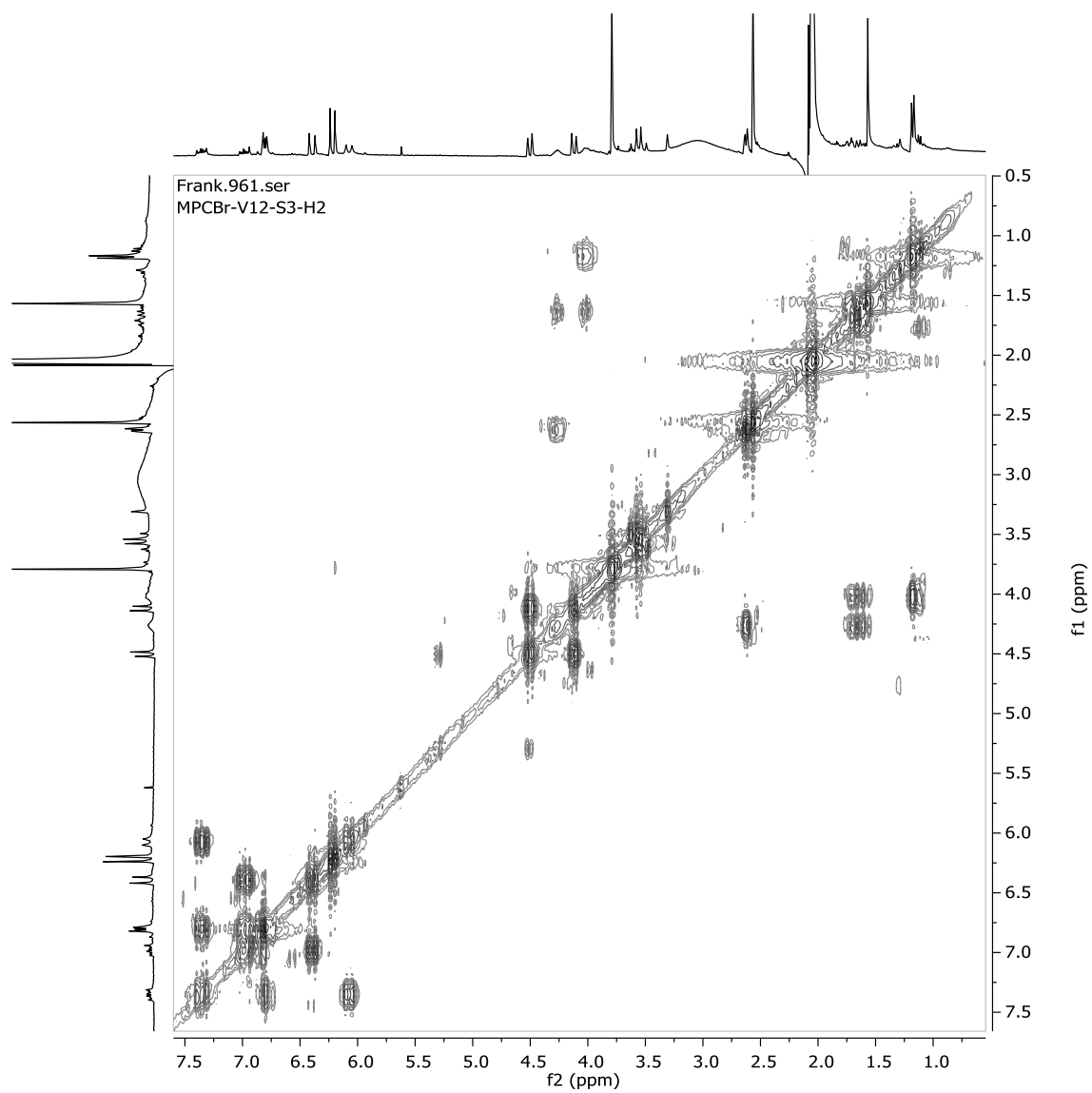
S29. ^{1}H-^{1}H ROESY spectrum of compound **(14)** in acetone-d_6 at 700 MHz
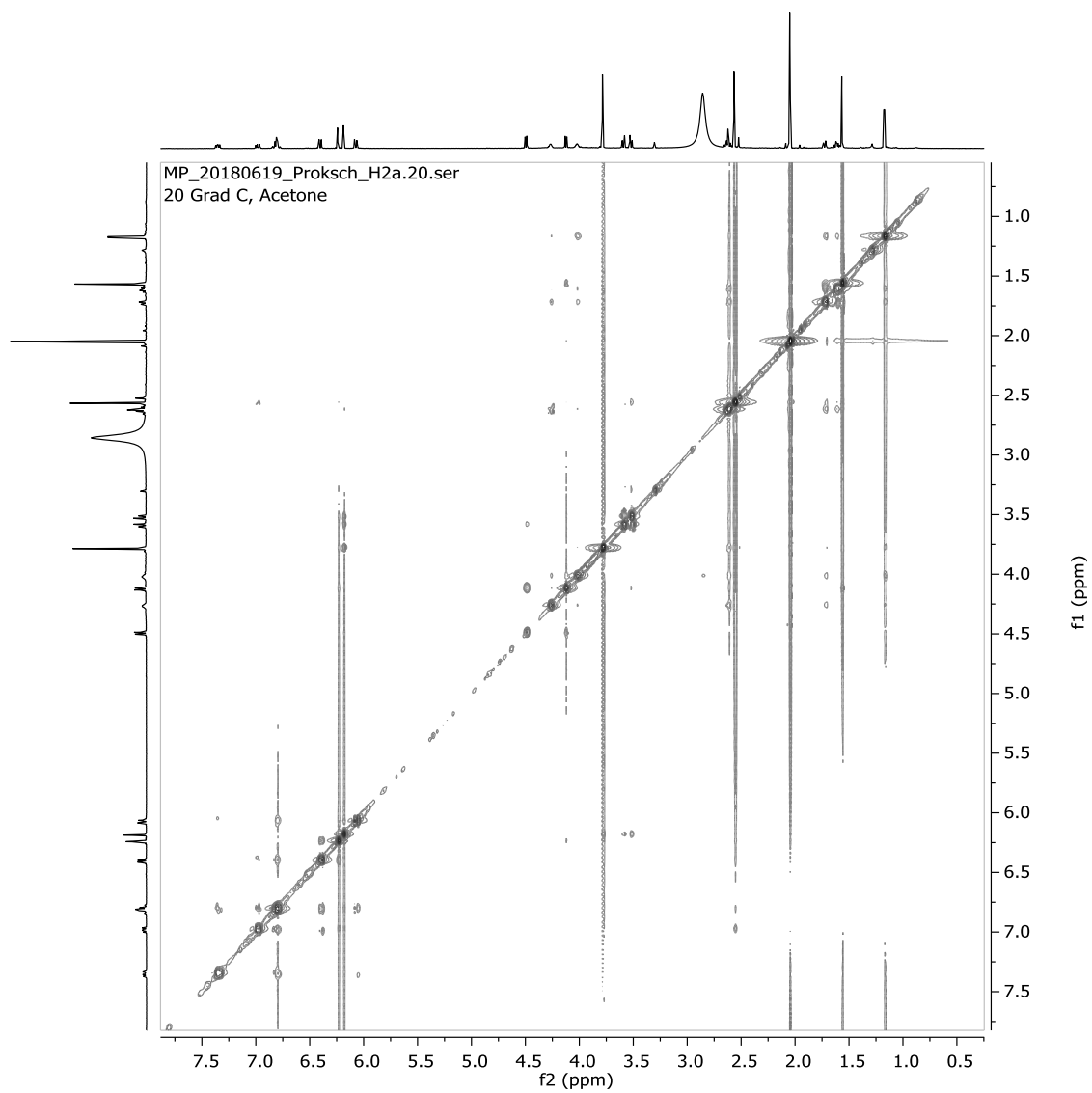
S30. UV-absorption spectrum of compound **(14)** in MeOH

Peak #1   100% at 26.12 min

70,0 %

No spectra library hits found!

428.4

310.7

237.5

-10,0

nm

200   250   300   350   400   450   500   550   595
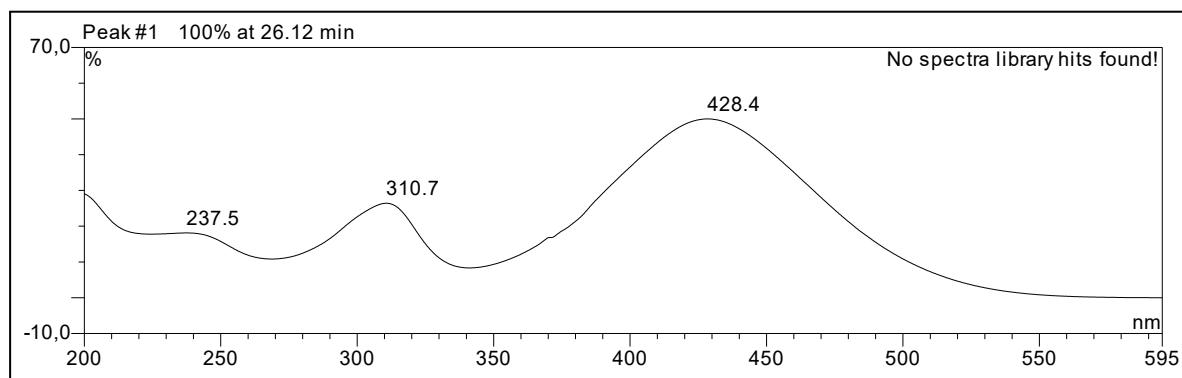
S31. ESI+/ESI spectrum of compound **(14)**

MPCBrV12S3H2pos #30   RT: 0.43   AV: 1   NL: 5.20E7
T: + c ESI Full ms [150.00-1000.00]
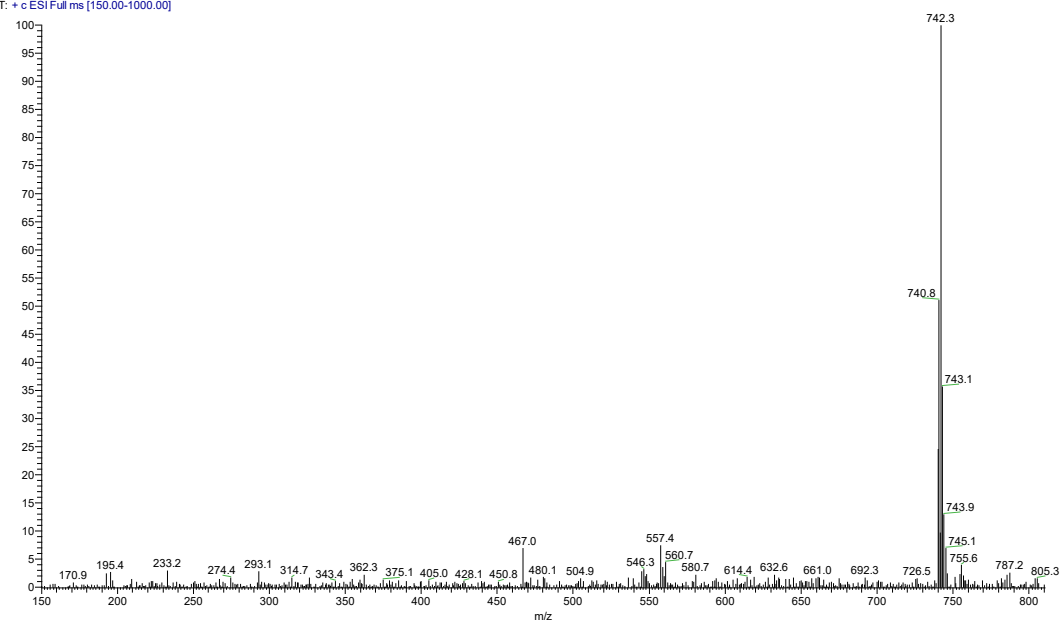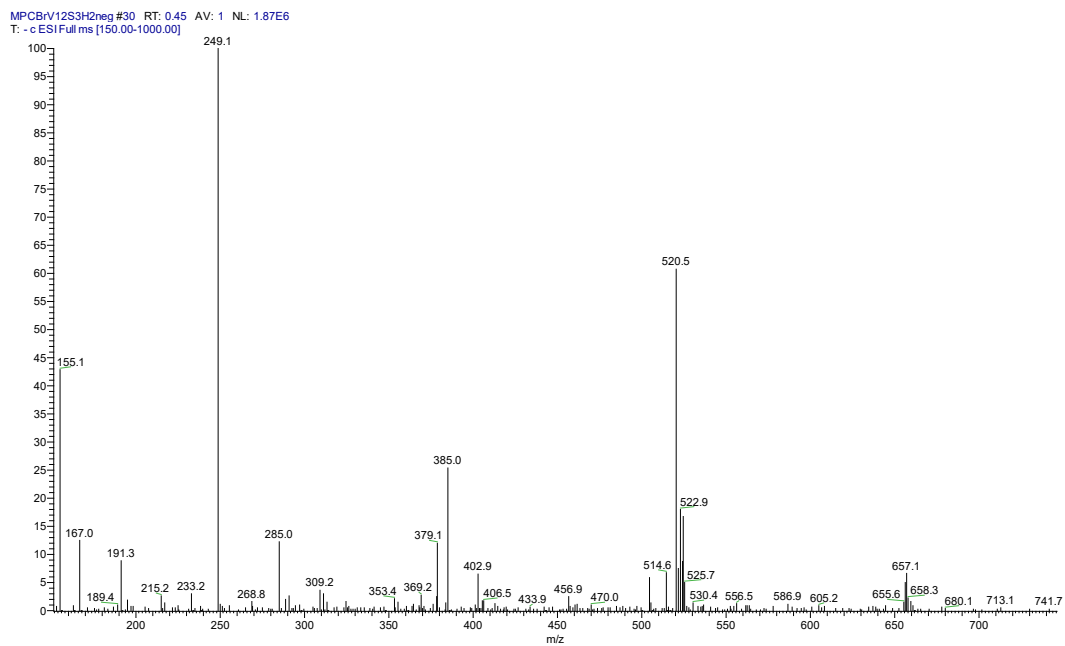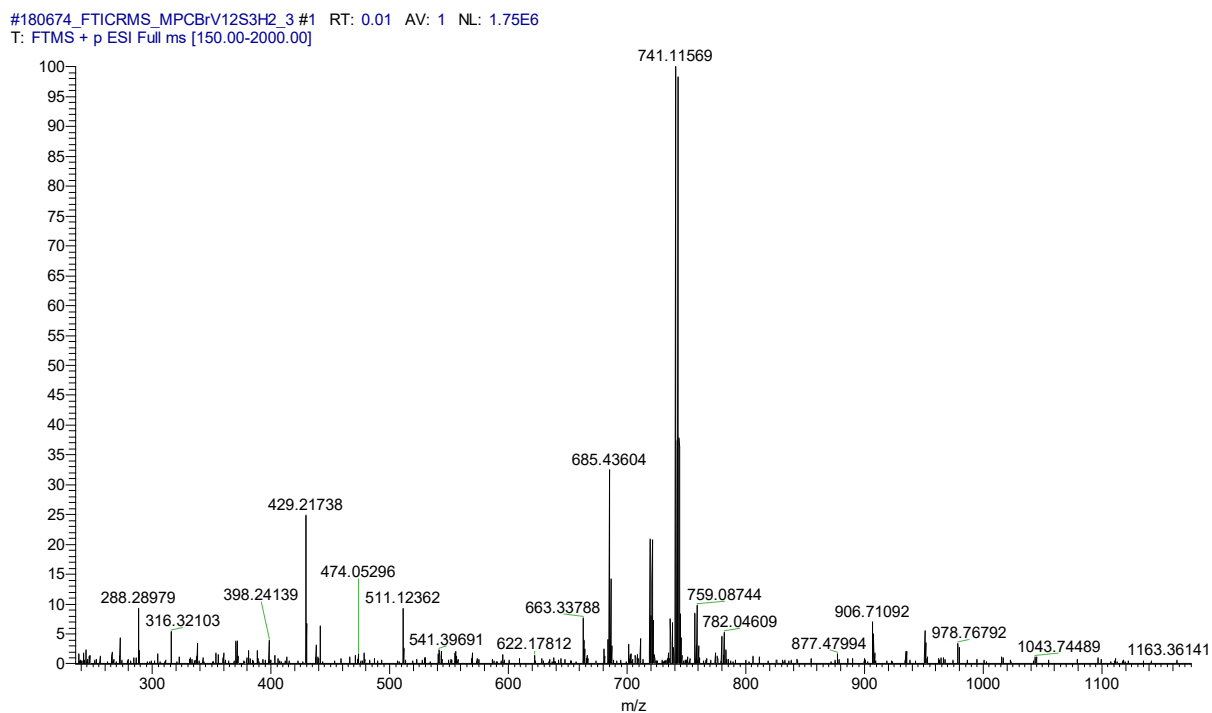
742.3

740.8

743.1

743.9

745.1

755.6

557.4

560.7

467.0

170.9   195.4   233.2   274.4   293.1   314.7   343.4   362.3   375.1   405.0   428.1   450.8   480.1   504.9   546.3   580.7   614.4   632.6   661.0   692.3   726.5   787.2   805.3

m/z

150   200   250   300   350   400   450   500   550   600   650   700   750   800

S32. HRMS (FTICR) (ESI+) spectrum of compound **(14)**
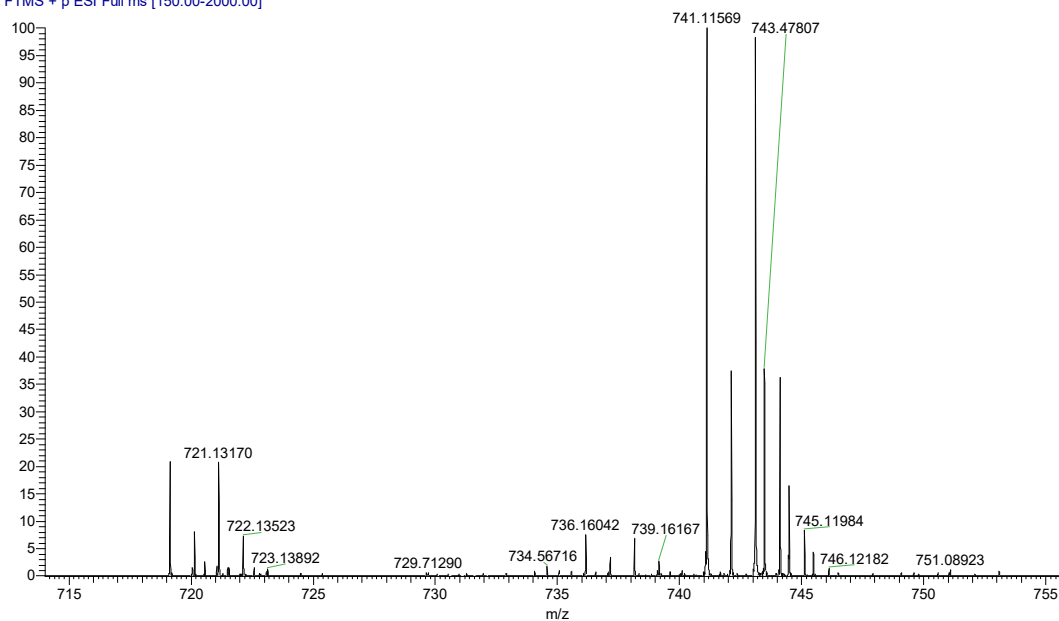
Measured m/z	Calculated m/z	Delta (ppm)	Molecular Formular
719.13398	719.13338	0.83	C33 H36 O13 Br
721.13170	721.13133	0.51	C33 H36 O13 [81]Br
741.11569	741.11532	0.49	C33 H35 O13 Br Na
743.11349	743.11328	0.29	C33 H35 O13 [81]Br Na

Chapter 5 - Cryptic Secondary Metabolites from the Sponge-Associated Fungus *Aspergillus ochraceus*

Submitted to "Marine Drugs" in 12/2018.

Impact Factor: 4.379

Overall contribution to this manuscript: 70%, first author, laboratory work includes cultivation and extraction, compound isolation and structure elucidation, preparation of the manuscript.

5.1 Publication Manuscript

Cryptic Secondary Metabolites from the Sponge-Associated Fungus *Aspergillus ochraceus*

Marian Frank [1], Ferhat Can Özkaya [2], Werner E. G. Müller [3], Alexandra Hamacher [4], Matthias U. Kassack [4], Wenhan Lin [5], Zhen Liu [1,*] and Peter Proksch [1,*]

[1] Institute of Pharmaceutical Biology and Biotechnology, Heinrich-Heine-Universität Düsseldorf, 40225 Düsseldorf, Germany; marian.frank@hhu.de (M.F.)
[2] Faculty of Fisheries, İzmir Katip Çelebi University, Çiğli, 35620 İzmir, Turkey; fcanozkaya@gmail.com (F.C.Ö.)
[3] Institute of Physiological Chemistry, Universitätsmedizin der Johannes Gutenberg-Universität Mainz, 55128 Mainz, Germany; wmueller@uni-mainz.de (W.E.G.M.)
[4] Institute of Pharmaceutical and Medicinal Chemistry, Heinrich-Heine-Universität Düsseldorf, 40225 Düsseldorf, Germany; alexandra.hamacher@hhu.de (A.H.); matthias.kassack@hhu.de (M.U.K.)
[5] State Key Laboratory of Natural and Biomimetic Drugs, Peking University, Beijing 100191, People's Republic of China; whlin@bjmu.edu.cn (W.L.)
* Correspondence: zhenfeizi0@sina.com (Z.L.); proksch@uni-duesseldorf.de (P.P.); Tel.: +49-211-81-14163

Abstract: The fungus *Aspergillus ochraceus* was isolated from the Mediterranean sponge *Agelas oroides*. Initial fermentation of the fungus on solid rice medium yielded 16 known compounds (**4–19**). Addition of several inorganic salts to the rice medium mainly influenced the accumulation of these secondary metabolites. Fermentation of the fungus on white beans medium yielded the new waspergillamide B (**1**) featuring an unusual *p*-nitrobenzoic acid as partial structure. Moreover, two new compounds, ochraspergillic acids A and B (**2** and **3**), which are both adducts of dihydropenicillic acid and *o*- or *p*-aminobenzoic acid, were isolated from co-culture of the fungus with *Bacillus subtilis*. Compound **2** was also detected in axenic fungal cultures following addition of either anthranilic acid or tryptophan to the rice medium. The structures of the new compounds were established by 1D- and 2D-NMR experiments as well as from the HRMS data. The absolute configuration of **1** was elucidated following hydrolysis and conversion of the amino acids using Marfey's reagent. Viomellein (**9**) and ochratoxin B (**18**) exhibited strong cytotoxicity against the A2780 human ovarian carcinoma cells with IC$_{50}$ values of 5.0 and 3.0 μM, respectively.

Keywords: *Aspergillus ochraceus*; OSMAC; co-cultivation; cytotoxicity

1. Introduction

Sponge-associated fungi are known for their production of structurally diverse secondary metabolites, many of which exhibit pharmacological activities such as antibiotic, antiviral, antifungal and anticancer properties [1,2]. Examples include cephalosporin C which was first isolated and described from the marine-derived fungus *Acremonium chrysogenum* as well as the potential anticancer drug plinabulin which is derived from the fungal metabolite halimide obtained from a marine *Aspergillus* sp. [3,4]. Up till now several hundred bioactive compounds have been isolated from marine-derived fungi [5,6]. However, under standard laboratory conditions, fungi will only express a fraction of their biosynthetic potential while expression of genes that are not directly involved in growth or differentiation such as those responsible for biosynthesis of natural products are often kept silent to conserve resources [7]. To increase the chances of discovering novel compounds both the OSMAC (One Strain MAny Compounds) approach and microbial

co-cultivation techniques are frequently employed in order to induce silent biogenetic gene clusters [8]. These strategies were also adopted in the present study on *Aspergillus ochraceus*.

    A. ochraceus was isolated from the inner tissue of the Mediterranean sponge *Agelas oroides*. The fungus was previously reported from the marine environment but is also known as an important food pathogen which is responsible for production of the carcinogenic mycotoxin ochratoxin A (OTA, **17**) [9,10], as well as of other important mycotoxins such as penicillic acid (PA, **5**) [11], dihydropenicillic acid (DHPA, **6**) [12] and viomellein (**9**) [13]. The toxicological importance of this fungus is highlighted by a disease known as "balcan nephropathy", which has been linked to the consumption of food products contaminated with PA (**5**) and OTA (**17**) [14,15].
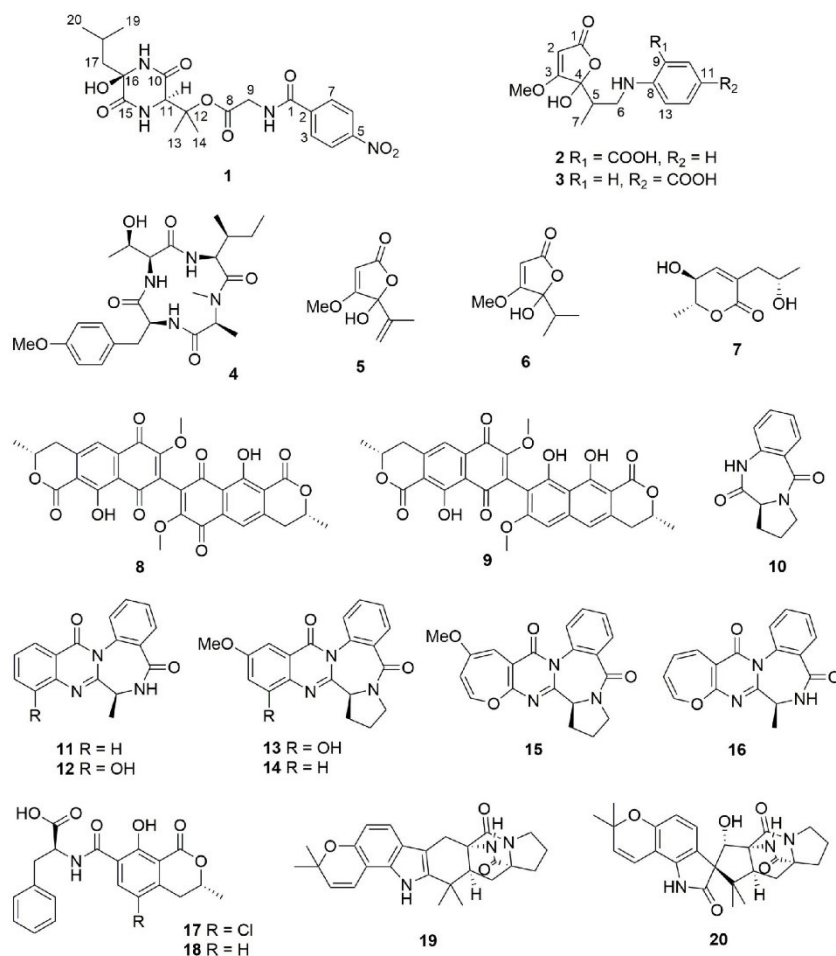
Figure 1. Structures of compounds isolated from *A. ochraceus*.

    In this study, initial fermentation of marine-derived *A. ochraceus* on solid rice medium containing 3.5% sea salt yielded 16 known metabolites (**4–19**). In an attempt to diversify the secondary metabolite pattern, several OSMAC experiments employing different inorganic salts or nitrogen sources were performed. Cultivation of *A. ochraceus* on white beans instead of rice yielded a known alkaloid (**20**) and a new diketopiperazine (**1**), the latter featuring an unusual nitrobenzoic

acid moiety. Moreover, co-cultivation experiments with *Bacillus subtilis* were performed, yielding two new penicillic acid/aminobenzoic acid hybrids (**2** and **3**). Interestingly, accumulation of **2** could also be provoked by addition of either anthanilic acid or of tryptophan to axenic fungal cultures, suggesting that bacteria are perhaps the source of the aminobenzoic acid partial structures of **2** obtained during fungal-bacterial co-cultivation. All isolated metabolites (Figure 1) were tested for their cytotoxicity against the mouse lymphoma cell line L5178Y and the human ovarian carcinoma cell line A2780. Only viomellein (**9**) and ochratoxin B (**18**) exhibited strong cytotoxicity whereas the other compounds proved to be inactive when assayed at an initial dose of 10 μM.

2. Results

The fungus *A. ochraceus* was initially cultivated for 14 days on solid rice media with addition of 3.5% artificial sea salt. Chromatographic separation of the EtOAc extract of the fugal culture led to the isolation of several known compounds including violaceotide A (**4**) [16], penicillic acid (**5**) [17], dihydropenicillic acid (**6**) [18], dihydroaspyrone (**7**) [19], xanthomegnin (**8**) [20], viomellein (**9**) [21], cycloanthranilylproline (**10**) [22], circumdatins F (**11**) [23], G (**12**) [23], E (**13**) [24], H (**14**) [25], B (**15**) [26], and L (**16**) [27], ochratoxins A (**17**) [28] and B (**18**) [29], and stephacidin A (**19**) [30].

Different cultivation experiments with organic or inorganic supplements were performed in order to diversify the metabolite pattern. Addition of inorganic salts to the rice medium mainly influenced the accumulation of these secondary metabolites causing either an increase or decrease of their concentrations of compounds when compared to cultivation of the fungus on solid rice medium containing sea salt (Table 1).

Table 1. Concentrations of selected compounds (in mAU*min at 235 nm) in cultures of *A. ochraceus* grown on solid rice medium (control) vs. cultures grown in the presence of different inorganic salts (n = 2 in each case).

compound	control	3.5% NaCl	3.5% NaBr	3.5% NaI	1% NH4Cl	1% NaNO3	1% NaNO2
4	28.8	29.4	42.0	21.6	22.2	61.3	28.1
5	576.7	257.1	633.1	314.1	447.6	149.0	152.6
6	242.6	28.7	83.7	360.5	20.7	122.0	69.1
7	115.6	38.7	30.0	61.5	11.8	23.6	33.8
8	97.9	81.7	21.0	76.9	n.d.	163.2	23.6
9	112.1	116.8	633.1	63.9	28.8	329.0	152.6
11	23.4	51.8	77.3	8.6	128.0	51.1	5.3
12	8.7	49.7	69.8	9.7	39.6	66.6	12.6
13	n.d. [a]	24.9	n. d.	n.d.	n.d.	n.d.	n.d.
14	n.d.	n.d.	92.7	n.d.	148.5	n.d.	n.d.
15	158.1	296.5	450.4	40.4	527.7	224.2	17.8
16	34.5	154.9	179.5	22.1	80.6	83.1	13.7
17	275.6	237.1	30.0	59.5	25.9	180.4	33.8
18	105.8	11.4	144.8	n.d.	n.d.	n.d.	5.5
19	123.8	140.3	190.4	14.6	174.6	116.9	5.4

[a] n.d. = not detected in the HPLC chromatogram of the crude extract.

When the fungus was cultivated on white beans instead of rice (both media containing 3.5% NaCl), the alkaloid concentrations (**11**, **12** and **15–18**) remained high in the former extract, while those of all non-alkaloid compounds (**5–9**) were strongly decreased. This made investigation of the

alkaloid fraction easier, resulting in the isolation of a new diketopiperazine, waspergillamide B (**1**), and a known alkaloid, sclerotiamide (**20**) [31] (Table 2).

Table 2. Concentrations of selected compounds (in mAU*min at 235 nm) in cultures of *A. ochraceus* grown on solid rice medium (control) vs. cultures grown on white beans medium (n = 5 in each case).

compound	control	beans
1	n.d.	10.4
4	18.1	16.4
5	767.8	n.d.
6	4.7	n.d.
7	18.3	n.d.
8	103.1	n.d.
9	175.5	11.9
11	12.8	18.2
12	2.3	73.9
15	104.3	105.7
16	16.5	68.2
17	84.7	57.4
18	n.d. [a]	18.5
19	24.8	3.5
20	n.d.	3.5

[a] n.d. = not detected in the HPLC chromatogram of the crude extract.

Comparison of the ^{1}H and ^{13}C NMR data (Table 3) between **1** and waspergillamide A isolated from an Australian mud dauber wasp-associated *Aspergillus* sp. [32] suggested the replacement of the trisubstituted double bond at C-16/C-17 by a methylene group (δ_C 47.2, δ_H 2.01 and 1.54) and an oxygenated quaternary carbon (δ_C 80.5 and signal of a hydroxy group at δ_H 6.24) in **1**. This is further supported by the molecular formula of **1** ($C_{20}H_{26}N_4O_8$) containing an additional H_2O compared to waspergillamide A as evident from the HRESIMS data of **1**. The COSY correlations between H_{ab}-17 and H-18 as well as the HMBC correlation from H_{ab}-17 and 16-OH to C-15 and C-16 confirmed the location of a methylene group at C-17 and the attachment of a hydroxy group at C-16 in **1**. The remaining substructure of **1** was identical to that of waspergillamide A on the basis of detailed analysis of the 2D NMR spectra of **1** (Figure 2). The 3-OH-Val residue in **1** was determined to be present in the D form (*R*) by comparison of retention time of derivatives of acid hydrolysis products of **1** with both enantiomers of Marfey's reagent (D- and L-FDAA) in HPLC [32,33]. In addition, the NOE correlation from 16-OH to Me-14 suggested that these protons were on the same face of diketopiperazine ring, which allowed assignment of the 16*R* configuration for **1**. Thus, the structure of **1**, for which the name waspergillamide B is proposed, was elucidated as shown.
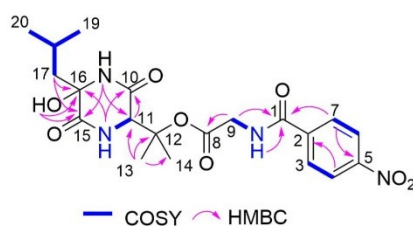
Figure 2. COSY and key HMBC correlations of **1**.

Table 3. ^{1}H and ^{13}C NMR Data for **1**.[a]

No.	δ_C, type	δ_H (*J* in Hz)
1	165.1, C	
2	139.3, C	
3,7	128.7, CH	8.10, d (8.9)
4,6	123.5, CH	8.34, d (8.9)
5	149.1, C	
8	168.6, C	
9	42.3, CH2	4.03, d (5.8)
9-NH		9.21, t (5.8)
10	164.3, C	
11	60.5, CH	4.34, d (2.8)
11-NH		8.17, d (2.8)
12	83.6, C	
13	23.7, CH3	1.60, s
14	22.3, CH3	1.43, s
15	167.6, C	
16	80.5, C	
16-NH		8.73, s
16-OH		6.24, s
17	47.2, CH2	2.01, m
		1.54, m
18	23.9, CH	1.55, m
19	23.4, CH3	0.87, d (6.5)
20	22.5, CH3	0.79, d (6.5)

[a] Measured in DMSO-d_6 (^{1}H at 600 MHz and ^{13}C at 150 MHz).

Co-cultivation experiments of *A. ochraceus* with *S. lividans* caused an increase of the concentrations of PA (**5**) and DHPA (**6**), while co-cultivation of *A. ochraceus* with *B. subtilis* yielded two new penicillic acid derivatives (**2** and **3**) that were absent in axenic fungal or bacterial controls (Table 4).

Compound **2** was isolated as yellowish oil. Based on the HRESIMS data, the molecular formula was established as $C_{15}H_{17}NO_6$. The ^{1}H-NMR spectrum of **2** (Table 5) exhibited four coupling aromatic protons at δ_H 7.88 (dd, H-10), 6.56 (br t, H-11), 7.35 (ddd, H-12) and 6.79 (br d, H-13), suggesting the presence of an *o*-disubstituted benzene ring. An *o*-aminobenzoic acid moiety was established by the COSY correlations between H-10/H-11/H-12/H-13 in addition to the HMBC correlations from H-10 to C-8 at δ_C 152.2 and a carboxy carbon at δ_C 171.1, from H-11 to C-9 at δ_C 111.3, and from H-12 to C-8 (Figure 3). The remaining NMR data of **2** (Table 5) were compatible with those of co-isolated dihydropenicillic acid (**6**), except for the replacement of a methyl group by a methylene group (δ_C 43.8, δ_H 3.75 and 3.09, CH$_2$-6) in **2**. The latter was confirmed by the COSY correlations between H$_{ab}$-6/H-5/Me-7 together with the HMBC correlations from H-2 (δ_H 5.24) to C-1 (δ_C 172.7) and C-4 (δ_C 106.2), from the protons of the methoxy group (δ_H 3.94) to C-3 (δ_C 181.6), and from Me-7 (δ_H 0.96) to C-4. Moreover, the HMBC correlation from H$_{ab}$-6 to C-8 confirmed the linkage between dihydropenicillic acid moiety and *o*-aminobenzoic acid moiety through an amide bond. Thus, the structure of **2** was elucidated as shown. The trivial name ochraspergillic acid A is suggested for this compound. Duplicated signals with a ratio around 5 to 4 observed in the NMR spectra of **2** were caused by tautomerism at C-4, which is common for penicillic acid derivatives [34].

Table 4. Concentrations of selected compounds (in mAU*min at 235 nm) in cultures of *A. ochraceus* grown on solid rice medium (control) vs. co-cultures with *S. lividans* or *B. subtilis* after 4 days (n = 3) or 14 days (n = 2) bacterial pre-incubation.[a]

compound	*A. ochraceus* control 4+14 d	*A. ochraceus* + *S. lividans* 4+14 d	*A. ochraceus* + *B. subtilis* 4+14 d	*A. ochraceus* control 14+14 d	*A. ochraceus* + *S. lividans* 14+14 d	*A. ochraceus* + *B. subtilis* 14+14 d
2	n.d. [b]	n.d.	0.4	n.d.	n.d.	36.2
4	19.2	21.3	60.4	n.d.	n.d.	n.d.
5	350.7	215.1	213.7	452.1	2128.7	745.8
6	691.6	144.8	144.1	349.5	1015.2	268.3
7	131.5	18.1	63.1	56.3	105.6	122.7
8	n.d.	n.d.	n.d.	379.9	193.9	102.2
9	1.9	0.4	0.4	406.3	164.4	110.8
11	16.1	17.0	13.5	125.8	54.8	60.4
12	19.6	19.2	18.5	44.6	16.7	n.d.
15	8.6	13.2	13.3	826.7	273.9	339.7
16	4.0	2.5	1.9	118.8	67.0	39.5
17	37.6	16.7	18.0	28.9	9.6	23.6
19	n.d.	n.d.	n.d.	707.9	239.4	209.7

[a] Compound **3** overlaps other compounds in the HPLC chromatogram and thus is not quantifiable. [b] n.d. = not detected in the HPLC chromatogram of the crude extract.

Table 5. ^{1}H and ^{13}C NMR Data for **2**.[a]

No.	**2** (Ma)[b] δ_C, type [c]	δ_H (*J* in Hz)	**2** (Mi)[b] δ_C, type [c]	δ_H (*J* in Hz)
1	172.7, C		173.0, C	
2	89.9, CH	5.24, s	89.9, CH	5.20, s
3	181.6, C		181.7, C	
4	106.2, C		105.7, C	
5	38.8, CH	2.33, m	39.8, CH	2.38, m
6	43.8, CH$_2$	3.75, dd (13.4, 3.9)	44.8, CH$_2$	3.35, m
		3.09, dd (13.4, 8.8)		3.06, dd (13.7, 7.1)
7	12.6, CH$_3$	0.96, d (6.9)	12.3, CH$_3$	1.13, d (6.9)
8	152.2, C		152.2, C	
9	111.3, C		111.1, C	
10	133.0, CH	7.88, dd (7.7, 1.8)	133.0, CH	7.88, dd (7.7, 1.8)
11	115.3, CH	6.56, br t (7.7)	115.3, CH	6.56, br t (7.7)
12	135.5, CH	7.35, ddd (8.4, 7.7, 1.8)	135.5, CH	7.34, ddd (8.4, 7.7, 1.8)
13	111.9, CH	6.79, br d (8.4)	111.8, CH	6.67, br d (8.4)
3-OMe	60.3, CH$_3$	3.94, s	60.2, CH$_3$	3.88, s
9-COOH	171.7, C		171.7, C	

[a] Measured in CD$_3$OD (^{1}H at 600 MHz and ^{13}C at 150 MHz). [b] Ma and Mi denote the major and minor epimers, respectively. [c] Data extracted from the HSQC and HMBC spectra.
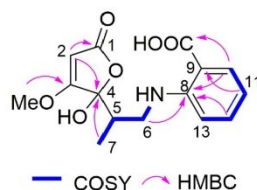
Figure 3. COSY and key HMBC correlations of **2**.

Ochraspergillic acid B (**3**) shared the same molecular formula with **2** on the basis of the HRESIMS data. The ^{1}H-NMR data of **3** (Table 6) were similar to those of **2** and also exhibited two sets of signals with a ratio of 4:3. However, signals of a *p*-disubstituted benzene ring at δ_H 7.78 (d, H-10/12) and 6.62 (d, H-9/13) were observed for **3**. The HMBC correlation from H-9/13 to C-11 (δ_C 118.0) and from H-10/12 to C-8 (δ_C 153.9) and a carboxy carbon (δ_C 170.4) confirmed the presence of a *p*-aminobenzoic acid moiety in **3**. Detailed analysis of the 2D NMR data of **3** revealed that the remaining substructure of **3** was identical to that of **2**.

Table 6. ^{1}H and ^{13}C NMR Data for **3**.[a]

No.	3 (Ma)[b]		3 (Mi)[b]	
	δ_C, type [c]	δ_H (*J* in Hz)	δ_C, type [c]	δ_H (*J* in Hz)
1	172.7, C		173.0, C	
2	90.0, CH	5.26, s	90.1, CH	5.22, s
3	181.4, C		181.3, C	
4	106.2, C		105.7, C	
5	38.4, CH	2.32, m	39.8, CH	2.37, m
6	44.3, CH$_2$	3.71, dd (13.6, 3.8)	44.7, CH$_2$	3.32, m
		3.03, dd (13.6, 9.0)		2.98, dd (13.7, 8.2)
7	12.8, CH$_3$	0.91, d (6.9)	12.1, CH$_3$	1.10, d (6.9)
8	153.9, C		153.9, C	
9,13	112.2, CH	6.62, d (8.8)	112.1, CH	6.55, d (8.8)
10,12	132.6, CH	7.78, d (8.8)	132.6, CH	7.77, d (8.8)
11	118.0, C		118.4, C	
3-OMe	60.3, CH$_3$	3.94, s	60.3, CH$_3$	3.92, s
11-COOH	170.4, C		170.4, C	

[a] Measured in CD$_3$OD (^{1}H at 600 MHz and ^{13}C at 150 MHz). [b] Ma and Mi denote the major and minor epimers, respectively. [c] Data extracted from the HSQC and HMBC spectra.

Most of the identified alkaloids are biogenetically derived from anthranilic acid or from tryptophan. Interestingly, compounds **2** and **3** were only detected during co-cultivation of the fungus with *B. subtilis* but not during co-cultivation with *S. lividans*. Thus, the fungus responds to the presence of different bacteria by accumulation of different metabolites. Similar results were recently reported for co-cultivation of the fungus *Chaetomium* sp. with *Pseudomonas aeruginosa* [35,36] compared to a co-culture of the fungus with *B. subtilis* [37]. Compounds **2** and **3** seem to be biotransformation products of penicillic acid (**5**). Thus, a feeding experiment was performed by adding either anthranilic acid or L-tryptophan to solid rice medium (Table 7). Compound **2** could be unequivocally detected following addition of either 1% or 2% of anthranilic acid or of 2% tryptophan to rice medium. Moreover, the concentration of **2** increased in cultures growing in the presence of 2% anthranilic acid compared to 1% anthranilic acid. These results suggest that anthranilic acid or

tryptophan which are biogenetic building blocks in the formation of **2** and **3** during fungal-bacterial co-cultivation may possibly by traced back to bacterial instead of fungal metabolism as the fungus fails to produce these compounds in absence of added precursors.

Table 7. Concentrations of selected compounds (in mAU*min at 235 nm) in cultures of *A. ochraceus* grown on solid rice medium with pH = 7 or 10 (control) vs. cultures grown in the presence of 1% or 2% anthranilic acid or L-tryptophan (n = 2 in each case).[a]

compound	control pH=7	anthranilic acid 1%	anthranilic acid 2%	control pH=10	tryptophan 1%	tryptophan 2%
2	n.d. [b]	15.4	61.4	n.d.	n.d.	31.6
4	10.8	6.5	n.d.	5.5	10.6	8.9
5	244.1	242.1	90.7	303.3	178.7	145.2
6	77.2	76.8	38.6	92.5	126.7	161.6
7	9.8	4.2	3.2	5.3	11.5	11.0
8	5.0	14.7	26.2	3.7	3.9	24.2
9	44.6	3.5	79.7	28.7	34.8	59.6
11	8.4	1.3	3.3	3.2	5.4	7.0
12	5.9	5.6	7.8	4.3	9.1	12.8
15	6.1	7.9	n.d.	9.1	9.0	n.d.
16	3.1	3.3	n.d.	2.1	3.2	n.d.
17	44.5	46.3	36.6	36.4	43.4	35.4
18	3.6	2.6	3.7	n.d.	12.2	4.5

[a] Compound **3** overlaps other compounds in the HPLC chromatogram and thus is not quantifiable. [b] n.d. = not detected in the HPLC chromatogram of the crude extract.

All isolated compounds were subjected to a cytotoxicity assay against the L5178Y mouse lymphoma cell line and against the A2780 human ovarian carcinoma cell line. Viomellein (**9**) and ochratoxin B (**18**) exhibited strong cytotoxicity against the human ovarian carcinoma cell line A2780 with IC$_{50}$ values of 5.0 and 3.0 μM, respectively. In addition, viomellein (**9**) showed significant cytotoxicity against the mouse lymphoma cell line L5178Y with an IC$_{50}$ value of 5.3 μM. Viomellein (**9**) was further tested against the human Jurkat T and Ramos B cell lines but was shown to be inactive against the latter two cell lines.

3. Discussion

In conclusion, this study on the sponge-derived fungus *A. ochraceus* yielded twenty compounds, which can be classified into peptides (**4, 17, 18**), diketopiperazine alkaloids (**1, 19, 20**), penicillic acid derivatives (**2, 3, 5** and **6**), polyketides (**7–9**) and benzodiazepine alkaloids (**10–16**). The majority of compounds was biogenetically derived from anthranilic acid or tryptophan. Cultivation of the fungus on protein rich media (white beans) yielded the new waspergillamide B (**1**) whereas co-cultivation of *A. ochraceus* with *B. subtilis* yielded two new compounds, ochraspergillic acids A and B (**2** and **3**). The latter two compounds seem to be biogenetically derived from both fungal and bacterial metabolism as indicated by precursor feeding using anthranilic acid or tryptophan.

4. Materials and Methods

4.1. General Experimental Procedures

Specific optical rotations were measured using a JASCO p-1020 polarimeter. High-resolution mass spectra were measured with a UHR-QTOF maXis 4G (Bruker Daltonics) mass spectrometer while low-resolution mass spectra were measured with a Finnigan LCQ Deca mass spectrometer. 1D

and 2D NMR spectra were acquired using Bruker Avance III 300 or 600 spectrometers. Analytical HPLC chromatograms were measured using a DIONEX 3000 system coupled to an Ultimate 3000 diode array UV detector (Thermo Scientific) and a KNAUER Eurospher C18 separation column (125 × 4 mm i.d., 5 μm). HPLC analysis for Marfey's reaction was performed on a Knauer Azura system using a Knauer Smartline UV Detector 2600 and a Macherey-Nagel EC250/4.6 NUCLEOSIL 120-5 C4 separation column. Column chromatography was performed using Sephadex LH20 or silica gel 60M as stationary phases. Thin layer chromatography (TLC) was performed using pre-coated silica gel 60 F254 plates (Merck) with detection under 254 and 365 nm followed by anisaldehyde spray reagent. Semi-preparative HPLC purification was performed using a Lachrom-Merck Hitachi system (L7100 pump and L7400 UV detector) with a Knauer Eurospher C18 column (300 × 8 mm i.d., 10 μm).

4.2. Fungal Material

The sponge-associated fungus was isolated from the tissue of the marine sponge *Agelas oroides*, which was collected at a depth of 10 m in Sığacık-İzmir, Turkey. The fungal strain was identified as *Aspergillus ochraceus* (GenBank accession number MK168605) by amplification and sequencing of the ITS-Region including the 5.8S ribosomal DNA and subsequent BLAST search as previously described [38].

4.3. Fermentation and Extraction

For the initial fermentation 10 1 L Erlenmeyer flasks were filled with solid rice medium (100 g rice from Oryza Milchreis, 3.8 g of sea salt and 110 mL of demineralized water each) and autoclaved at 121°C for 20 min. After cooling to room temperature, the flasks were inoculated, each with a 2–4 cm^2 piece of agar plate, on which the fungus had been growing for one week. The fermentation was continued under static conditions for 14 days at 20°C. At that time the fungus had completely overgrown the medium. Fermentation was terminated by addition of 350 mL of EtOAc. After soaking in EtOAc overnight, the mycelium was cut into pieces with a spatula and shaken continuously for 8 h at 150 rpm, after which the extract was collected via filtration through a paper filter. The residue was washed with 50 mL of EtOAc, filtrated and evaporated to dryness, yielding 17.4 g of an oily substance. A liquid-liquid partitioning was performed between MeOH-H$_2$O (90:10) and *n*-hexane. After evaporation to dryness the *n*-hexane phase weight 13.0 g and the methanolic phase weight amounted to 4.3 g. After HPLC analysis of both phases, only the methanolic phase was further chromatographically investigated.

4.3.1. OSMAC Experiment

To investigate the influences of several inorganic salts or organic supplements to the growth media, cultivation of the fungus was performed on 100 g of solid rice medium with addition of 110 mL of demineralized water and either 3.5% NaCl, 3.5% NaBr, 3.5% NaI, 1% NaNO$_3$, 1% NaNO$_2$, 1% NH$_4$Cl, 1% peptone or 1% yeast extract. The controls consisted of 100 g of solid rice medium with 3.5% sea salt and 110 mL of demineralized water. After autoclaving, the media were inoculated with ~2 cm^2 of overgrown agar plate. The fungus grew on all media at similar growth rates. The experiment was terminated by adding 400 mL of EtOAc to each flask, after which the medium was soaked overnight, cut into pieces, and shaken for 8 h before filtration. After evaporation of EtOAc, the extract was dissolved in 50 mL MeOH and analyzed by HPLC-DAD. Two inoculated flasks were used per experiment. The experiment with white beans medium was conducted using five 100 g flasks of white beans, which were soaked overnight in demineralized water prior to autoclaving.

4.3.2. Co-Cultivation Experiment

Three flasks containing 100 g of autoclaved rice each were inoculated with 10 mL of a bacterial broth (optical density 0.2) and pre-incubated for 4 days at 40°C (*B. subtilis*) or 25°C (*S. lividans*), respectively, before the fungus was introduced. Co-cultivation was performed at 25°C for additional 14 days. The resulting EtOAc extracts were chromatographically compared to the axenic control

cultures of the fungus and the bacteria, which were grown under the same conditions. The experiment was repeated in an identical manner except for an extended pre-incubation period of the bacteria for 14 days.

4.3.2. Feeding Experiment

Cultures were grown on two flasks containing 100 g of solid rice medium each, which was spiked with 1% or 2% of either anthranilic acid (neutralized with 1 M NaOH at pH = 7) or L-tryptophan (set to pH = 10 with 1M NaOH for solubility) before autoclaving. Fungal control cultures were grown under the same conditions and the EtOAc extracts were chromatographically compared.

4.4. Isolation of Compounds

The crude extract of the initial large scale fermentation was subjected to vacuum liquid chromatography (VLC) using silica gel as stationary phase and a gradient of solvent mixtures. The solvent gradient consisted of *n*-hexane-EtOAc (10:0, 8:2, 6:4, 4:6, 2:8), CH_2Cl_2-MeOH (10:0, 90:10, 80:20, 70:30, 60:40, 50:50, 40:60, 30:70, 20:80) and an additional wash step of MeOH with 0.1 % TFA. The resulting 15 fractions (V1 to V15) were analyzed by HPLC. Fractions V7 and V8 were combined (3.1 g) and subjected to another VLC on silica gel using a gradient of EtOAc-DCM (30:70, 40:60, 50:50, 60:40, 70:30, 80:20, 90:10, 100:0) initially and then EtOAc-MeOH (90:10, 85:15, 80:20, 75:25, 70:30, 40:60, 10:90) to yield 14 subfractions (V7/8-V1 to V7/8-V14). Fractions V7/8-V3 and V7/8-V4 were combined amounting to 298 mg and subjected to a Sephadex LH20 column using acetone as mobile phase to yield four subfractions (V7/8-V3/4-SD1 to V7/8-V3/4-SD4). Fraction V7/8-V3/4-SD3 was separated by a silica gel column using CH_2Cl_2-MeOH (98:2) as mobile phase followed by purification using semi- preparative HPLC with a gradient of MeOH-H_2O (55% 0–3 min, 55% to 90% 3–23 min and 90% 23–25 min), yielding **14** (1.1 mg) and **16** (1.6 mg). Fraction V7/8-V3/4-SD4 was further purified by semi-preparative HPLC with a gradient of MeOH-H_2O (50% 0–3 min, 50% to 65% 3–18 min and 100% 18–28 min), yielding **19** (0.7 mg), **13** (0.8 mg), **11** (3.8 mg) and **12** (21.4 mg). Fractions V9 and V10 were combined (282 mg) and further purified by a Sephadex LH20 column using acetone as mobile phase to give **17** (62.9 mg).

The extract (1.8 g) of the 1% NH_4Cl culture was separated by VLC on silica gel as described above to give 14 fractions (V1 to V14). Fraction V4 was subsequently purified on a Sephadex LH-20 column using acetone as eluent to yield **5** (79.8 mg). Fraction V6 was suspended in acetone and centrifuged three times to give **4** (10.0 mg).

The extract (7.5 g) of 1% $NaNO_2$ culture was also fractionated by VLC on silica gel as described for the crude extract of the initial large scale fermentation. Fraction V6 (125 mg) was separated on a Sephadex LH-20 column using MeOH as eluent and subsequently purified by semi-preparative HPLC with a gradient of MeOH-H_2O from 20% to 100% over 25 minutes to yield **7** (10.6 mg).

The EtOAc extract (4.4 g) of the beans culture was subjected to a silica gel VLC column as described above. Fraction V5 was further purified by a silica gel column to yield **15** (33.0 mg) and **16** (61.0 mg). After separation on a Sephadex LH-20 column and subsequent purification by semi-preparative HPLC, fraction V6 yielded **1** (1.6 mg) and **20** (2.6 mg) while fraction V9 yielded **17** (1.0 mg) and **18** (1.1 mg).

The EtOAc extract obtained from the co-culture of the fungus with *B. subtilis* was partitioned between 300 mL *n*-hexane and 400 mL of 90% MeOH-H_2O to give 3.2 g of oily *n*-hexane soluble extract, 4.1 g of methanol soluble dry extract, and 193 mg of an insoluble fraction. The insoluble fraction was dissolved in CH_2Cl_2 and subjected to a Sephadex LH-20 column followed by separation using semi-preparative HPLC with a gradient of CH_3CN-H_2O from 40% to 80% over 20 minutes to yield **9** (2.5 mg) and **8** (3.1 mg). The MeOH soluble fraction was fractionated by a silica gel VLC as described above. Fraction V3 was chromatographed over a Sephadex LH-20 column and subsequently separated by semi-preparative HPLC to yield **5** (80.0 mg) and **6** (59.0 mg). Fraction V5 yielded **7** (24.3 mg), **2** (1.5 mg), **3** (1.3 mg), **10** (3.3 mg), **13** (2.9 mg), **12** (3.7 mg) and **11** (0.4 mg)

following a similar procedure as for fraction V3. Fraction V6 was purified on a Sephadex LH-20 column using acetone as eluent to give **4** (15.0 mg).

Waspergillamide B (**1**): white needles; $[\alpha]_D^{23}$ +22 (c 0.2, MeOH); UV (MeOH) λ_{max} 267 nm; ^{1}H and ^{13}C NMR data, Table 3; HRESIMS *m/z* 451.1824 [M + H]+ (calcd for $C_{20}H_{27}N_4O_8$, 451.1828).

Ochraspergillic acid A (**2**): yellow oil; UV (MeOH) λ_{max} 353, 254 and 221 nm; ^{1}H and ^{13}C NMR data, Table 5; HRESIMS *m/z* 308.1134 [M + H]+ (calcd for $C_{15}H_{18}NO_6$, 308.1129).

Ochraspergillic acid B (**3**): yellow oil; UV (MeOH) λ_{max} 306 and 224 nm; ^{1}H and ^{13}C NMR data, Table 6; HRESIMS *m/z* 308.1127 [M + H]+ (calcd for $C_{15}H_{18}NO_6$, 308.1129).

4.5. Marfey's Reaction for 1

The general procedure was adapted from the C3-method [32,33]. Two aliquots of 100 μg of **1** were hydrolyzed in 200 μL of 6M HCl at 110°C for 12 h in a closed glass vial. Subsequently HCl was removed by drying under a nitrogen stream. The dry residues were treated with 20 μL of 1M aqueous NaHCO₃. Next, 100 μL of a 1% acetone solution of L-FDAA (1-fluoro-2, 4-dinitrophenyl-5-L-alanine amide) was added to the first aliquot of **1**, while 100 μL of a 1% acetone solution of D-FDAA was added to the second aliquot of **1**. The mixtures were kept at 40°C for 1 h and occasionally shaken by hand. To stop the reaction, 20 μL of 1M HCl were added. The mixtures were centrifuged at 13,000 rpm for 10 min and an aliquot of 10 μL was analyzed using a RP-HPLC column with UV detection at 340 nm. The retention times of the L- and D-FDAA product of **1** were compared to each other. A Macherey-Nagel EC250/4.6 Nucleosil 250-5 C4-column (4 × 300 mm, i.d.) was used for HPLC analysis. The gradient of MeOH-H₂O was changed from 15% to 60% MeOH over 55 min at a flow rate of 1 mL/min.

4.6. Cytotoxicity Assay

Cytoxocicity was investigated using the MTT (3-(4,5-dimethylthiazol-2-yl)-2,5-diphenyltetrazolium bromide) method against the mouse lymphoma cell line L5178Y or the human ovarian carcinoma cell line A2780 as previously described [39,40]. As positive controls kahalalide F for L5178Y (IC50 4.3 μM) and cisplatin for A2780 (IC50 2.2 μM) were used. As negative controls 0.1% ethylene glycol monomethyl ether in DMSO was used for L5178Y while 0.9% NaCl, 0.1% DMSO and 1% DMSO were used for A2780.

References

1. Thomas, T.R.A.; Kavlekar, D.P.; LokaBharathi, P.A. Marine drugs from sponge-microbe association—a review. *Mar. Drugs* **2010**, *8*, 1417–1468
2. Debbab, A.; Aly, A.H.; Lin, W.H.; Proksch, P. Bioactive compounds from marine bacteria and fungi. *Microb. Biotechnol.* **2010**, *3*, 544–563.
3. Mayer, A.M.; Glaser, K.B.; Cuevas, C.; Jacobs, R.S.; Kem, W.; Little, R.D.; McIntosh, J.M.; Newman, D.J.; Potts, B.C.; Shuster, D.E. The odyssey of marine pharmaceuticals: a current pipeline perspective. *Trends Pharmacol. Sci.* **2010**, *31*, 255–265.
4. Ebada, S.S.; Proksch, P. Marine-derived fungal metabolites. In *Hb25_Springer Handbook of Marine Biotechnology*; Kim, S.K., Ed.; Springer Berlin Heidelberg: Berlin, Germany, 2015; pp 759–788.
5. Rateb, M.E.; Ebel, R. Secondary metabolites of fungi from marine habitats. *Nat. Prod. Rep.* **2011**, *28*, 290–344.

6. Blunt, J.W.; Carroll, A.R.; Copp, B.R.; Davis, R.A.; Keyzers, R.A.; Prinsep, M.R. Marine natural products. *Nat. Prod. Rep.* **2018**, *35*, 8–53.

7. Hertweck, C. Hidden biosynthetic treasures brought to light. *Nat. Chem. Biol.* **2009**, *5*, 450–452.

8. Brakhage, A.A.; Schroeckh, V. Fungal secondary metabolites - strategies to activate silent gene clusters. *Fungal Genet. Biol.* **2011**, *48*, 15–22.

9. Bayman, P.; Baker, J.L.; Doster, M.A.; Michailides, T.J.; Mahoney, N.E. Ochratoxin production by the *Aspergillus ochraceus* group and *Aspergillus alliaceus*. *Appl. Environ. Microbiol.* **2002**, *68*, 2326–2329.

10. Wang, Y.; Wang, L.; Liu, F.; Wang, Q.; Selvaraj, J.N.; Xing, F.; Zhao, Y.; Liu, Y. Ochratoxin A producing fungi, biosynthetic pathway and regulatory mechanisms. *Toxins* **2016**, *8*, 83.

11. Bacon, C.W.; Sweeney, J.G.; Robbins, J.D.; Burdick, D. Production of penicillic acid and ochratoxin A on poultry feed by *Aspergillus ochraceus*: temperature and moisture requirements. *Appl. Microbiol.* **1973**, *26*, 155–160.

12. Obana, H.; Kumeda, Y.; Nishimune, T. *Aspergillus ochraceus* production of 5,6-dihydropenicillic acid in culture and foods. *J. Food Prot.* **1995**, *58*, 519–523

13. Stack, M.E.; Mislivec, P.B. Production of xanthomegnin and viomellein by isolates of *Aspergillus ochraceus*, *Penicillium cyclopium*, and *Penicillium viridicatum*. *Appl. Environ. Microbiol.* **1978**, *36*, 552–554.

14. Stoev, S.D.; Vitanov, S.; Anguelov, G.; Petkova-Bocharova, T.; Creppy, E.E. Experimental mycotoxic nephropathy in pigs provoked by a diet containing ochratoxin A and penicillic Acid. *Vet. Res. Commun.* **2001**, *25*, 205–223.

15. Stoev, S.D. Balkan endemic nephropathy - still continuing enigma, risk assessment and underestimated hazard of joint mycotoxin exposure of animals or humans. *Chem. Biol. Interact.* **2017**, *261*, 63–79.

16. Liu, J.; Gu, B.; Yang, L.; Yang, F.; Lin, H. New anti-inflammatory cyclopeptides from a sponge-derived fungus *Aspergillus violaceofuscus*. *Front. Chem.* **2018**, *6*, 226.

17. Vansteelandt, M.; Blanchet, E.; Egorov, M.; Petit, F.; Toupet, L.; Bondon, A.; Monteau, F.; Le Bizec, B.; Thomas, O.P.; Pouchus, Y.F.; Le Bot, R.; Grovel, O. Ligerin, an antiproliferative chlorinated sesquiterpenoid from a marine-derived *Penicillium* strain. *J. Nat. Prod.* **2013**, *76*, 297–301.

18. Sassa, T.; Hayakari, S.; Ikeda, M.; Miura, Y. Plant growth inhibitors produced by fungi: part I. isolation and identification of penicillic acid and dihydropenicillic acid. *Agric. Biol. Chem.* **1971**, *35*, 2130–2131.

19. Fuchser, J.; Zeeck, A. Secondary metabolites by chemical screening, 34. – aspinolides and aspinonene/aspyrone co-metabolites, new pentaketides produced by *Aspergillus ochraceus*. *Liebigs Ann.* **1997**, 87–95.

20. Zeeck, A.; Ruß, P.; Laatsch, H.; Loeffler, W.; Wehrle, H.; Zähner, H.; Holst, H. Stoffwechselprodukte von mikroorganismen, 172. isolierung des antibioticums semi-vioxanthin aus *Penicillium citreo-viride* und synthese des xanthomegnins. *Chem. Ber.* **1979**, *112*, 957–978.

21. Sedmera, P.; Volc, J.; Weijer, J.; Vokoun, J.; Musílek, V. Xanthomegnin and viomellein derivatives from submerged cultures of the ascomycete *Nannizzia cajetani*. *Collect. Czech. Chem. Commun.* **1981**, *46*, 1210–1216.

22. Clark, R.L.; Carter, K.C.; Mullen, A.B.; Coxon, G.D.; Owusu-Dapaah, G.; McFarlane, E.; Duong Thi, M.D.; Grant, M.H.; Tettey, J.N.; Mackay, S.P. Identification of the benzodiazepines as a new class of antileishmanial agent. *Bioorg. Med. Chem. Lett.* **2007**, *17*, 624–627.

23. Dai, J.; Carté, B.K.; Sidebottom, P.J.; Sek Yew, A.L.; Ng, S.; Huang, Y.; Butler, M.S. Circumdatin G, a new alkaloid from the fungus *Aspergillus ochraceus*. *J. Nat. Prod.* **2001**, *64*, 125–126.

24. Rahbæk, L.; Breinholt, J. Circumdatins D, E, and F: further fungal benzodiazepine analogues from *Aspergillus ochraceus*. *J. Nat. Prod.* **1999**, *62*, 904–905.

25. López-Gresa, M.P.; González, M.C.; Primo, J.; Moya, P.; Romero, V.; Estornell, E. Circumdatin H, a new inhibitor of mitochondrial NADH oxidase, from *Aspergillus ochraceus*. *J. Antibiot.* **2005**, *58*, 416–419.

26. Rahbæk, L.; Breinholt, J.; Frisvad, J.C.; Christophersen, C. Circumdatin A, B, and C: three new benzodiazepine alkaloids isolated from a culture of the fungus *Aspergillus ochraceus*. *J. Org. Chem.* **1999**, *64*, 1689–1692.

27. Peng, J.; Zhang, X.Y.; Tu, Z.C.; Xu, X.Y.; Qi, S.H. Alkaloids from the deep-sea-derived fungus *Aspergillus westerdijkiae* DFFSCS013. *J. Nat. Prod.* **2013**, *76*, 983–987.

28. Gabriele, B.; Attya, M.; Fazio, A.; Di Donna, L.; Plastina, P.; Sindona, G. A new and expedient total synthesis of ochratoxin A and *d5*-ochratoxin A. *Synthesis* **2009**, 1815–1820.

29. Størmer, F.C.; Kolsaker, P.; Holm, H.; Rogstad, S.; Elling, F. Metabolism of ochratoxin B and its possible effects upon the metabolism and toxicity of ochratoxin A in rats. *Appl. Environ. Microbiol.* **1985**, *49*, 1108–1112.

30. Qian-Cutrone, J.; Huang, S.; Shu, Y.Z.; Vyas, D.; Fairchild, C.; Menendez, A.; Krampitz, K.; Dalterio, R.; Klohr, S.E.; Gao, Q. Stephacidin A and B: two structurally novel, selective inhibitors of the testosterone-dependent prostate LNCaP cells. *J. Am. Chem. Soc.* **2002**, *124*, 14556–14557.

31. Whyte, A.C.; Gloer, J.B.; Wicklow, D.T.; Dowdw, P.F. Sclerotiamide: a new member of the paraherquamide class with potent antiinsectan activity from the sclerotia of *Aspergillus sclerotiorum*. *J. Nat. Prod.* **1996**, *59*, 1093–1095.

32. Quezada, M.; Shang, Z.; Kalansuriya, P.; Salim, A.A.; Lacey, E.; Capon, R.J. Waspergillamide A, a nitro depsi-tetrapeptide diketopiperazine from an Australian mud dauber wasp-associated *Aspergillus* sp. (CMB-W031). *J. Nat. Prod.* **2017**, *80*, 1192–1195.

33. Ueoka, R.; Ise, Y.; Ohtsuka, S.; Okada, S.; Yamori, T.; Matsunaga, S. Yaku'amides A and B, cytotoxic linear peptides rich in dehydroamino acids from the marine sponge *Ceratopsion* sp. *J. Am. Chem. Soc.* **2010**, *132*, 17692–17694.

34. Munday, C.W. Tautomerism of penicillic acid. *Nature* **1949**, *163*, 443–444.

35. Ancheeva, E.; Mándi, A.; Király, S.B.; Kurtán, T.; Hartmann, R.; Akone, S.H.; Weber, H.; Daletos, G.; Proksch, P. Chaetolines A and B, pyrano[3,2-f]isoquinoline alkaloids from cultivation of *Chaetomium* sp. in the presence of autoclaved *Pseudomonas aeruginosa*. *J. Nat. Prod.* **2018**, *81*, 2392–2398.

36. Ancheeva, E.; Küppers, L.; Akone, S.H.; Ebrahim, W.; Liu, Z.; Mándi, A.; Kurtán, T.; Lin, W.; Orfali, R.; Rehberg, N.; Kalscheuer, R.; Daletos, G.; Proksch, P. Expanding the metabolic profile of the fugus *Chaetomium* sp. through co-culture with autoclaved *Pseudomonas aeruginosa*. *Eur. J. Org. Chem.* **2017**, 3256–3264.

37. Akone, S.H.; Mándi, A.; Kurtán, T.; Hartmann, R.; Lin, W.; Daletos, G.; Proksch, P. Inducing secondary metabolite production by the endophytic fungus *Chaetomium* sp. through fungal-bacterial co-culture and epigenetic modification. *Tetrahedron* **2016**, *72*, 6340–6347.

38. Kjer, J.; Debbab, A.; Aly, A.H.; Proksch, P. Methods for isolation of marine-derived endophytic fungi and their bioactive secondary products. *Nat. Protoc.* **2010**, *5*, 479–490.

39. Ashour, M.; Edrada, R.; Ebel, R.; Wray, V.; Wätjen, W.; Padmakumar, K.; Müller, W.E.G.; Lin, W.H.; Proksch, P. Kahalalide derivatives from the Indian sacoglossan mollusk *Elysia grandifolia*. *J. Nat. Prod.* **2006**, *69*, 1547–1553.

40. Engelke, L.H.; Hamacher, A.; Proksch, P.; Kassack, M.U. Ellagic acid and resveratrol prevent the development of cisplatin resistance in the epithelial ovarian cancer cell line A2780. *J. Cancer* **2016**, *7*, 353–363.

5.2 Supporting Information

Cryptic Secondary Metabolites from the Sponge-Associated Fungus *Aspergillus ochraceus*

Marian Frank,[1] Ferhat Can Özkaya,[2] Werner E.G. Müller,[3] Alexandra Hamacher,[4] Matthias U. Kassack,[4] Wenhan Lin,[5] Zhen Liu,[1,*] Peter Proksch[1,*]

[1]Institute of Pharmaceutical Biology and Biotechnology, Heinrich-Heine-Universität Düsseldorf, Universitätsstrasse 1, 40225 Düsseldorf, Germany

[2]Faculty of Fisheries, İzmir Katip Çelebi University, Çiğli, 35620 İzmir, Turkey

[3]Institute of Physiological Chemistry, Universitätsmedizin der Johannes Gutenberg-Universität Mainz, 55128 Mainz, Germany

[4]Institute for Pharmaceutical and Medicinal Chemistry, Heinrich-Heine-Universität Düsseldorf, Universitätsstrasse 1, 40225 Düsseldorf, Germany

[5]State Key Laboratory of Natural and Biomimetic Drugs, Peking University, Beijing 100191, China

*Corresponding authors.
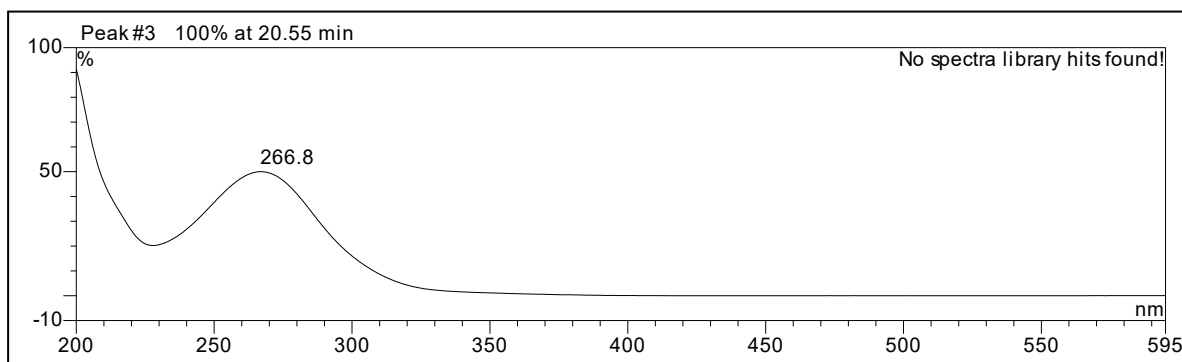
Tel.: +49 211 81 14163; fax: +49 211 81 11923;

e-mail: zhenfeizi0@sina.com (Z. Liu),
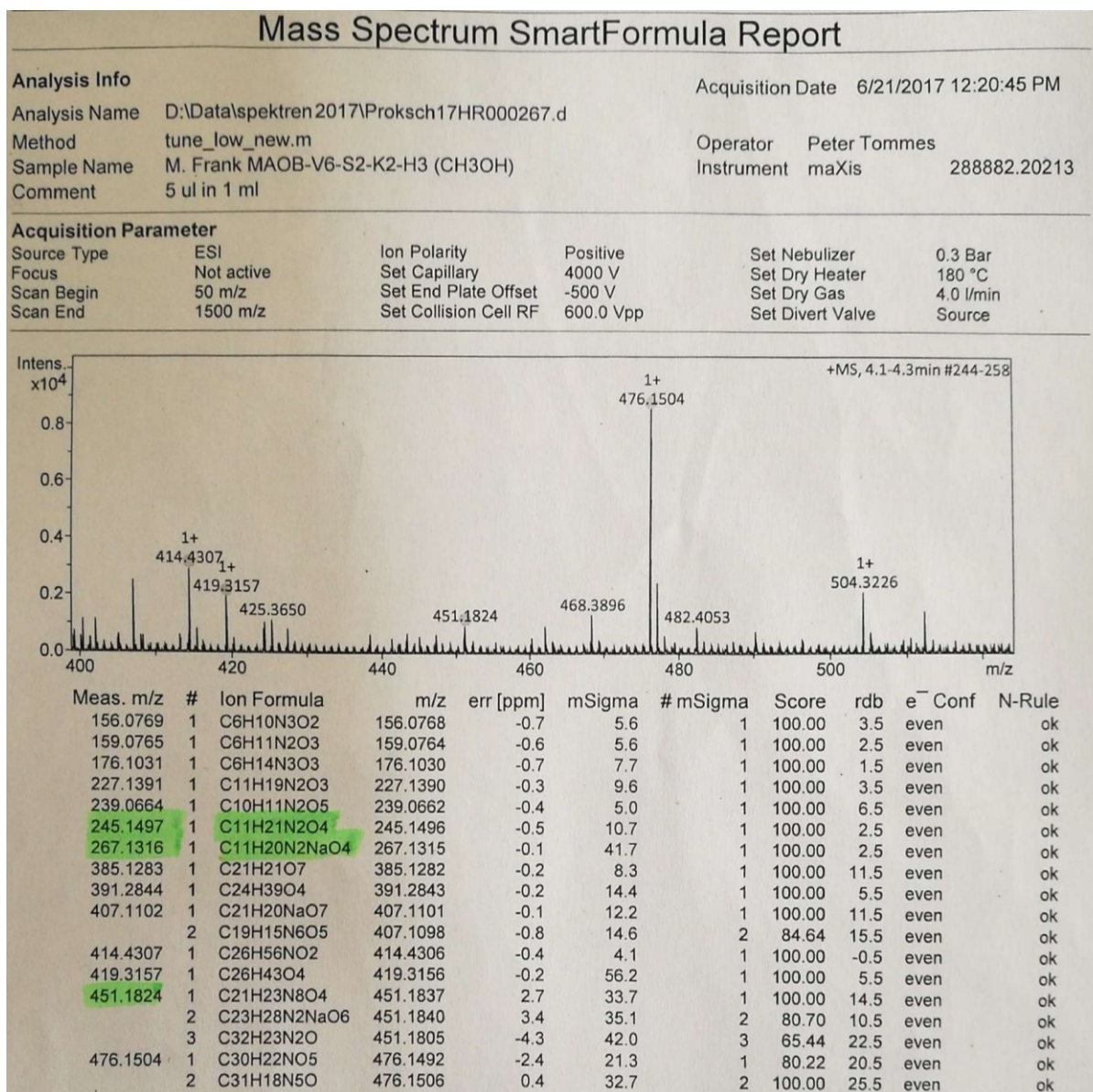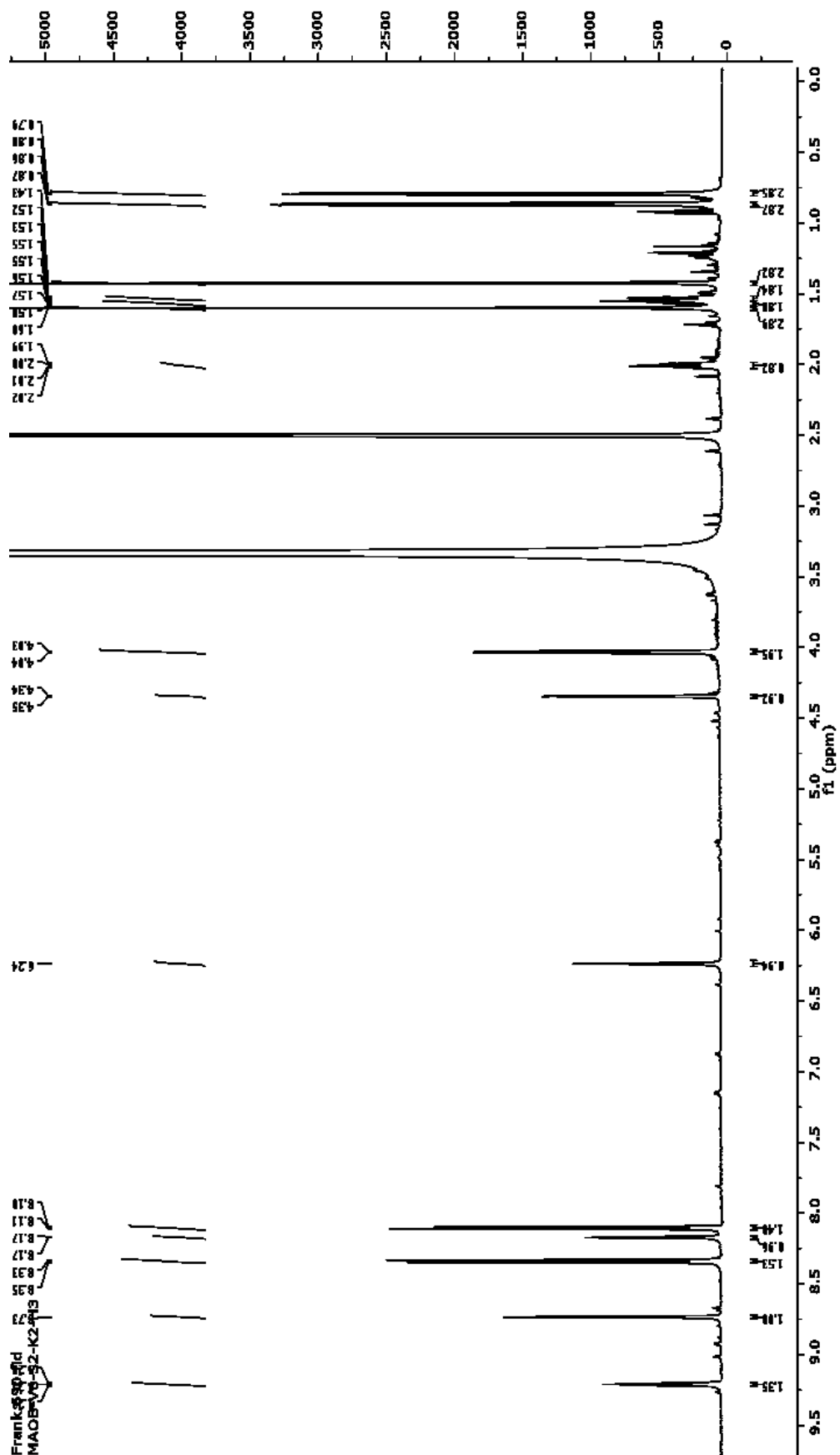
proksch@uni-duesseldorf.de (P. Proksch)

Table of Content

S1. UV spectrum of compound **1**.

S2. HRESIMS of compound **1**.

Mass Spectrum SmartFormula Report

Analysis Info

		Acquisition Date	6/21/2017 12:20:45 PM
Analysis Name	D:\Data\spektren 2017\Proksch17HR000267.d		
Method	tune_low_new.m	Operator	Peter Tommes
Sample Name	M. Frank MAOB-V6-S2-K2-H3 (CH3OH)	Instrument	maXis 288882.20213
Comment	5 ul in 1 ml		

Acquisition Parameter

Source Type	ESI	Ion Polarity	Positive	Set Nebulizer	0.3 Bar
Focus	Not active	Set Capillary	4000 V	Set Dry Heater	180 °C
Scan Begin	50 m/z	Set End Plate Offset	-500 V	Set Dry Gas	4.0 l/min
Scan End	1500 m/z	Set Collision Cell RF	600.0 Vpp	Set Divert Valve	Source

Meas. m/z	#	Ion Formula	m/z	err [ppm]	mSigma	# mSigma	Score	rdb	e⁻ Conf	N-Rule
156.0769	1	C6H10N3O2	156.0768	-0.7	5.6	1	100.00	3.5	even	ok
159.0765	1	C6H11N2O3	159.0764	-0.6	5.6	1	100.00	2.5	even	ok
176.1031	1	C6H14N3O3	176.1030	-0.7	7.7	1	100.00	1.5	even	ok
227.1391	1	C11H19N2O3	227.1390	-0.3	9.6	1	100.00	3.5	even	ok
239.0664	1	C10H11N2O5	239.0662	-0.4	5.0	1	100.00	6.5	even	ok
245.1497	1	C11H21N2O4	245.1496	-0.5	10.7	1	100.00	2.5	even	ok
267.1316	1	C11H20N2NaO4	267.1315	-0.1	41.7	1	100.00	2.5	even	ok
385.1283	1	C21H21O7	385.1282	-0.2	8.3	1	100.00	11.5	even	ok
391.2844	1	C24H39O4	391.2843	-0.2	14.4	1	100.00	5.5	even	ok
407.1102	1	C21H20NaO7	407.1101	-0.1	12.2	1	100.00	11.5	even	ok
	2	C19H15N6O5	407.1098	-0.8	14.6	2	84.64	15.5	even	ok
414.4307	1	C26H56NO2	414.4306	-0.4	4.1	1	100.00	-0.5	even	ok
419.3157	1	C26H43O4	419.3156	-0.2	56.2	1	100.00	5.5	even	ok
451.1824	1	C21H23N8O4	451.1837	2.7	33.7	1	100.00	14.5	even	ok
	2	C23H28N2NaO6	451.1840	3.4	35.1	2	80.70	10.5	even	ok
	3	C32H23N2O	451.1805	-4.3	42.0	3	65.44	22.5	even	ok
476.1504	1	C30H22NO5	476.1492	-2.4	21.3	1	80.22	20.5	even	ok
	2	C31H18N5O	476.1506	0.4	32.7	2	100.00	25.5	even	ok

S3. ^{1}H-NMR (600 MHz, DMSO-d_6) spectrum of compound **1**.

S4. ^{13}C-NMR (125 MHz, DMSO-d_6) spectrum of compound **1**.
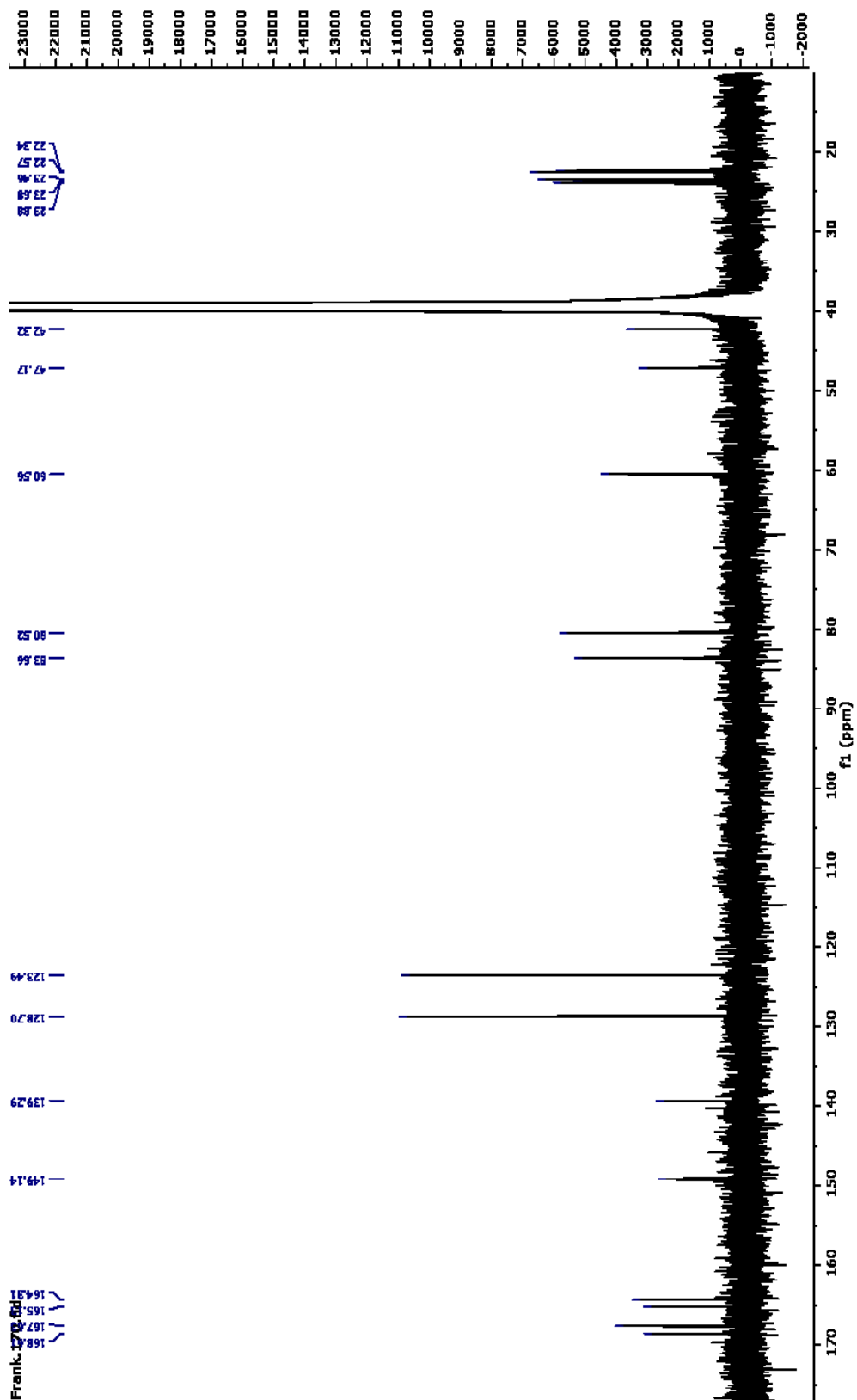
S5. ^{1}H-^{1}H-COSY (600MHz, DMSO-d_6) spectrum of compound **1.**

Frank.711.ser
MAOB-V6-S2-K2-H3
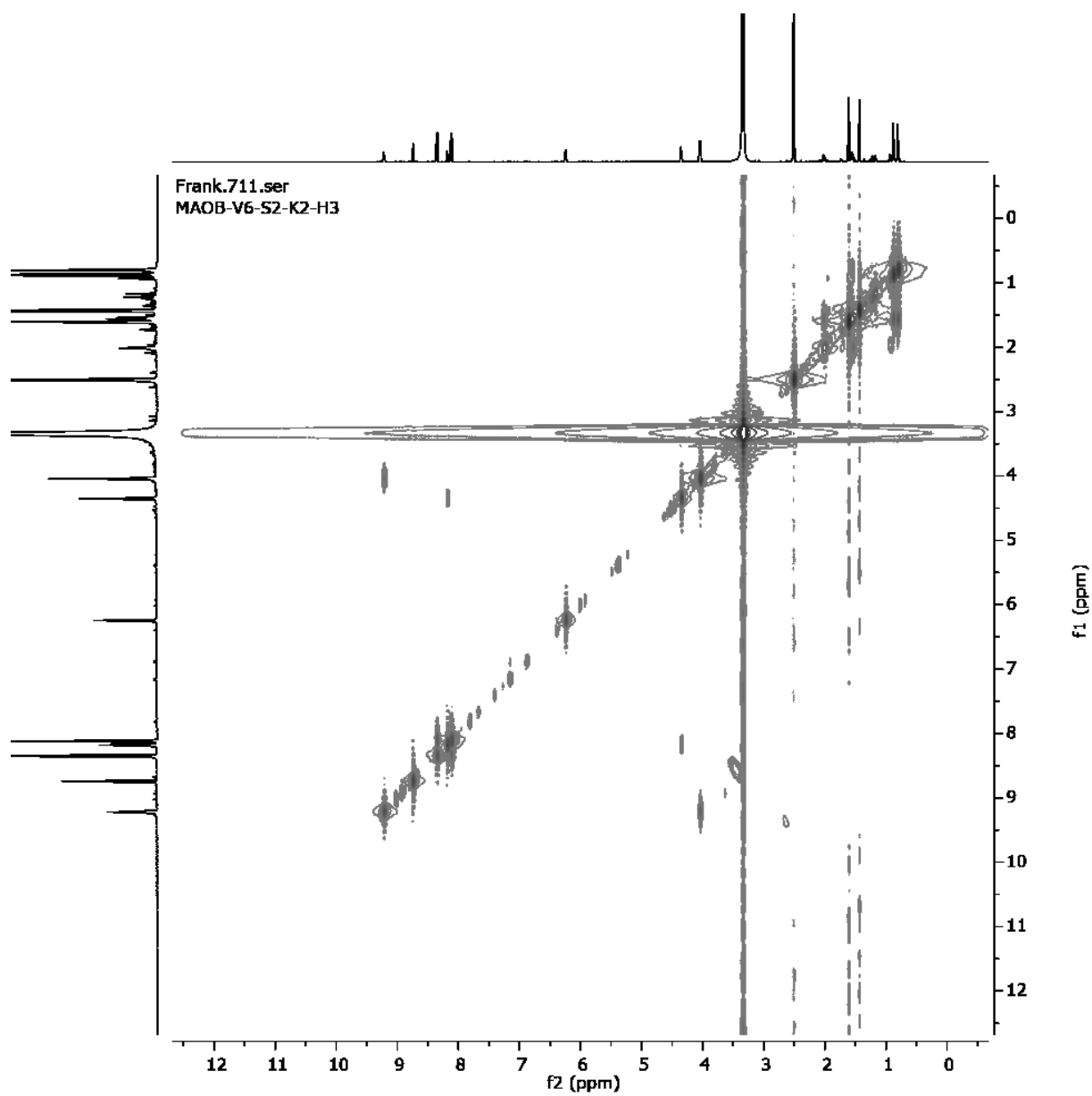
S6. ^{1}H-^{13}C-HSQC (600MHz/150 MHz, DMSO-d_6) spectrum of compound **1**.
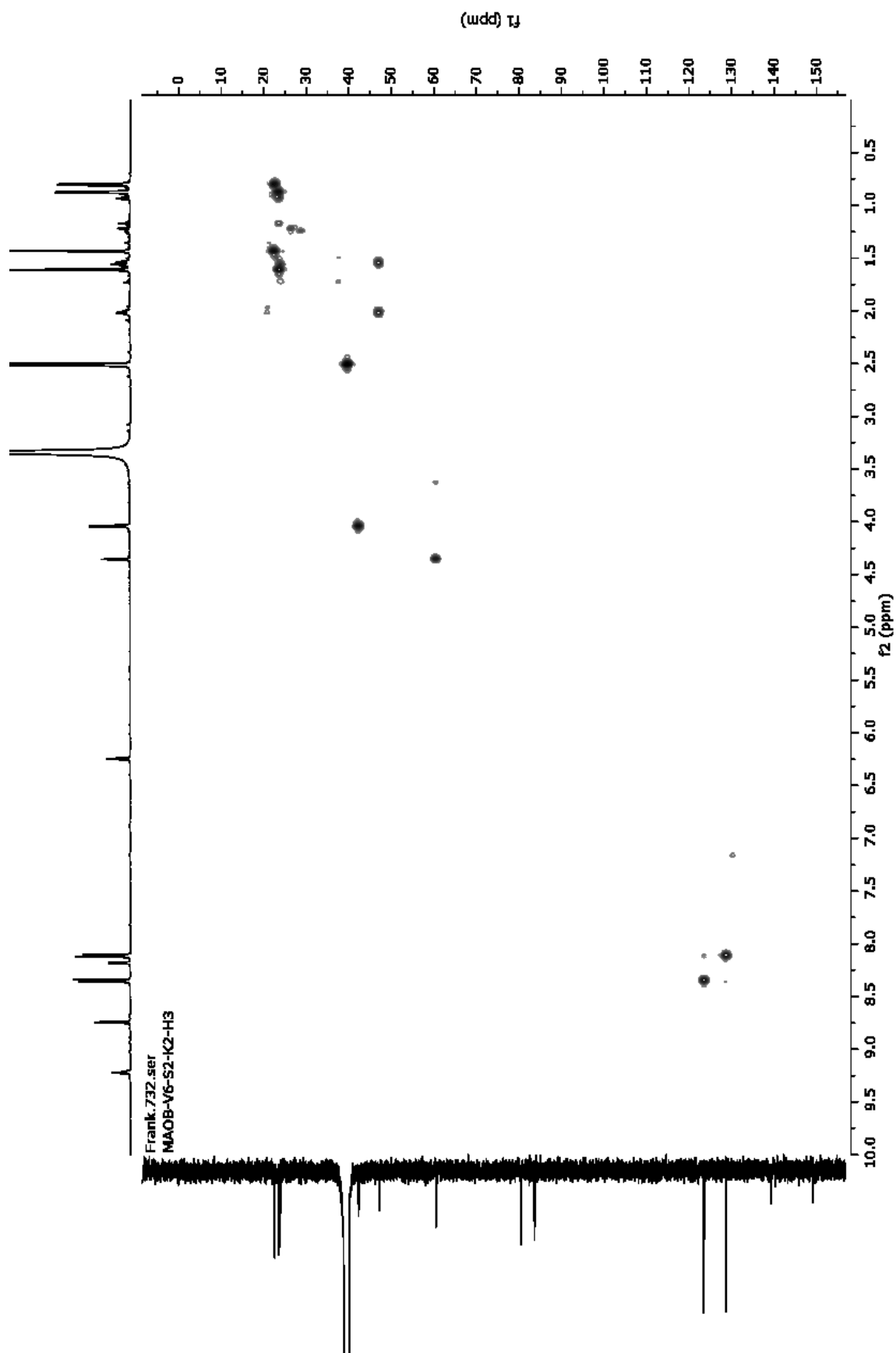
S7. ^{1}H-^{13}C-HMBC (600MHz/150 MHz, DMSO-d_6) spectrum of compound **1**.
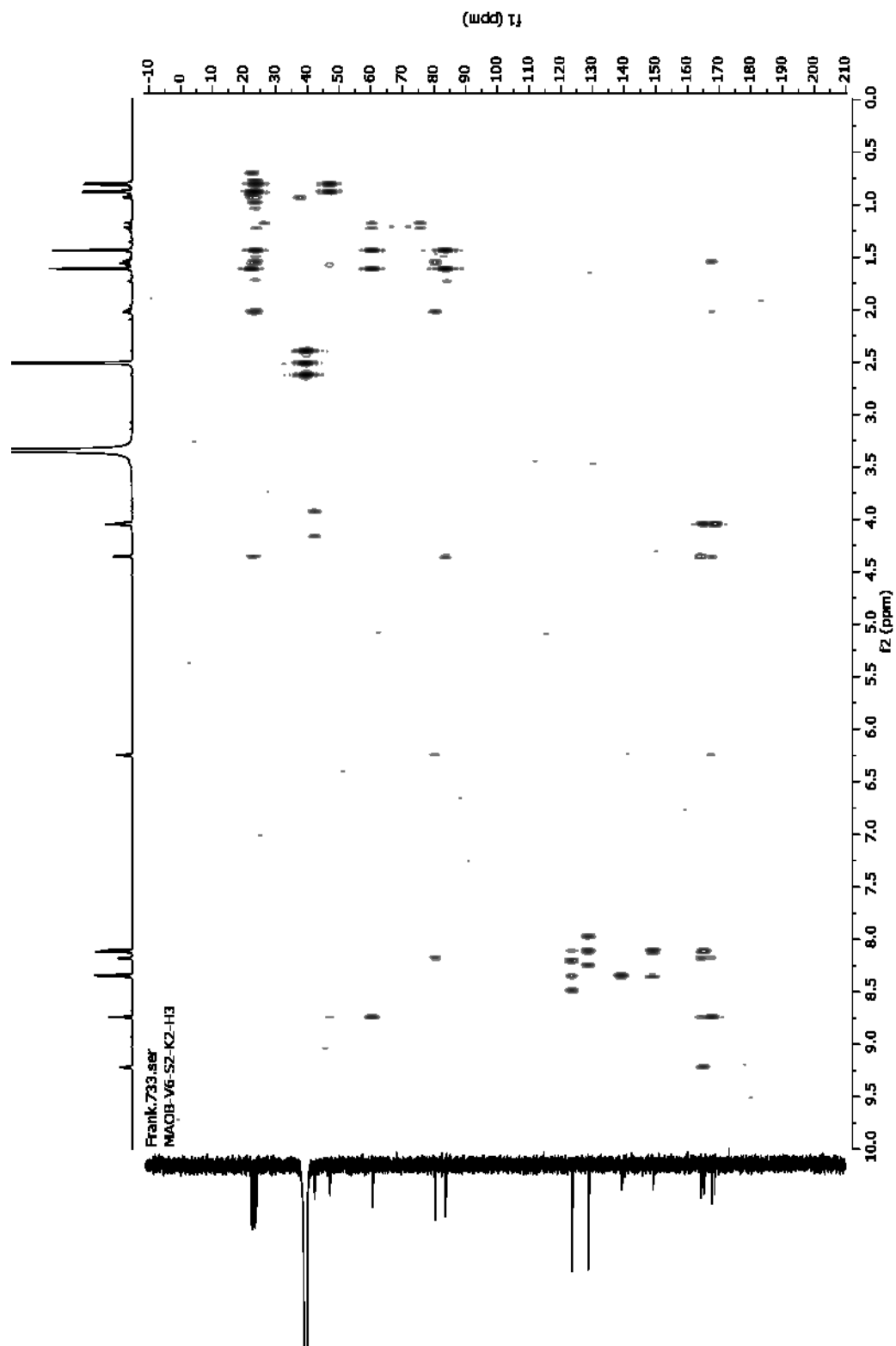
S8. ^{1}H-^{1}H-ROESY (600MHz, DMSO-d_6) spectrum of compound **1**.

Frank.941.ser
Waspergillamide B
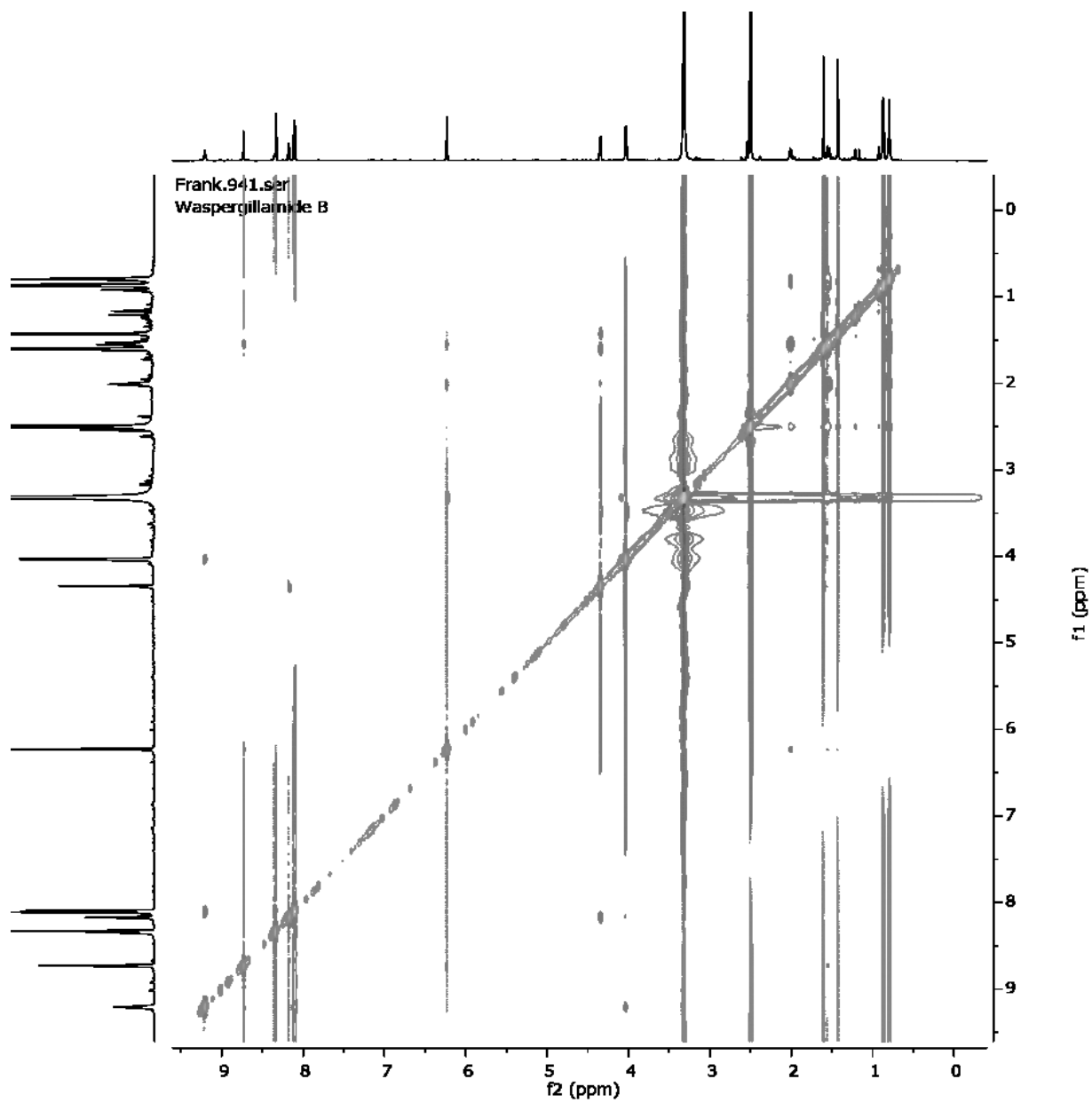
S9. UV spectrum of compound **2**.
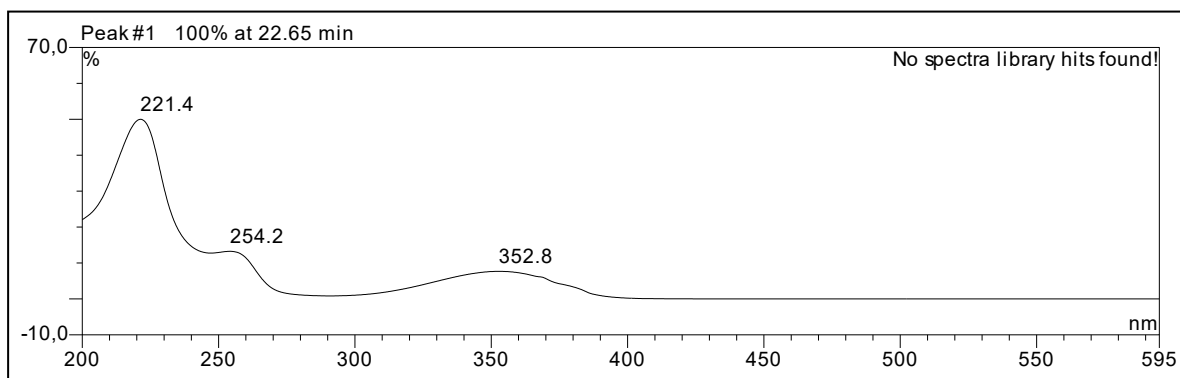
S10. HRESIMS of compound **2**.
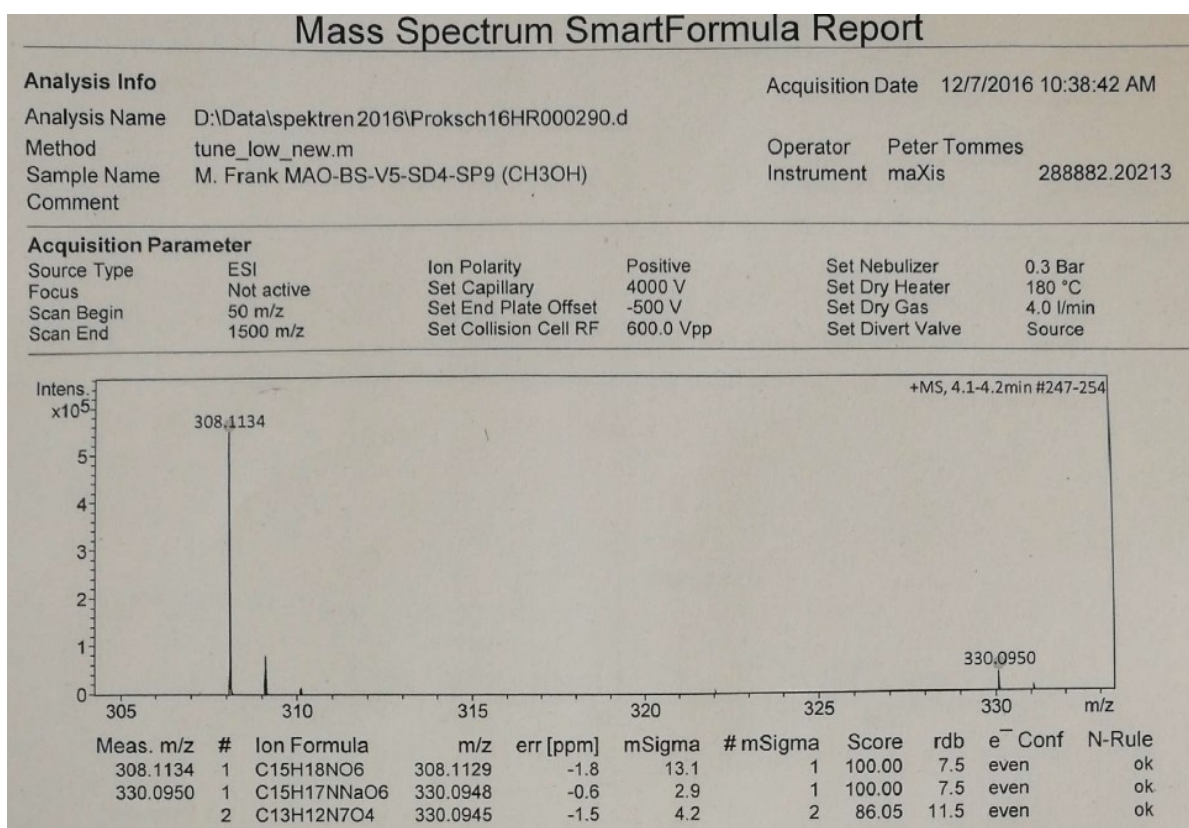
S11. ^{1}H-NMR (600 MHz, MeOH-d_4) spectrum of compound **2**.

S12. ^{1}H-^{1}H –COSY (600 MHz, MeOH-d_4) spectrum of compound **2**.

MoussaMariam.611.ser
MAO-BS-V5-SD4-SP9
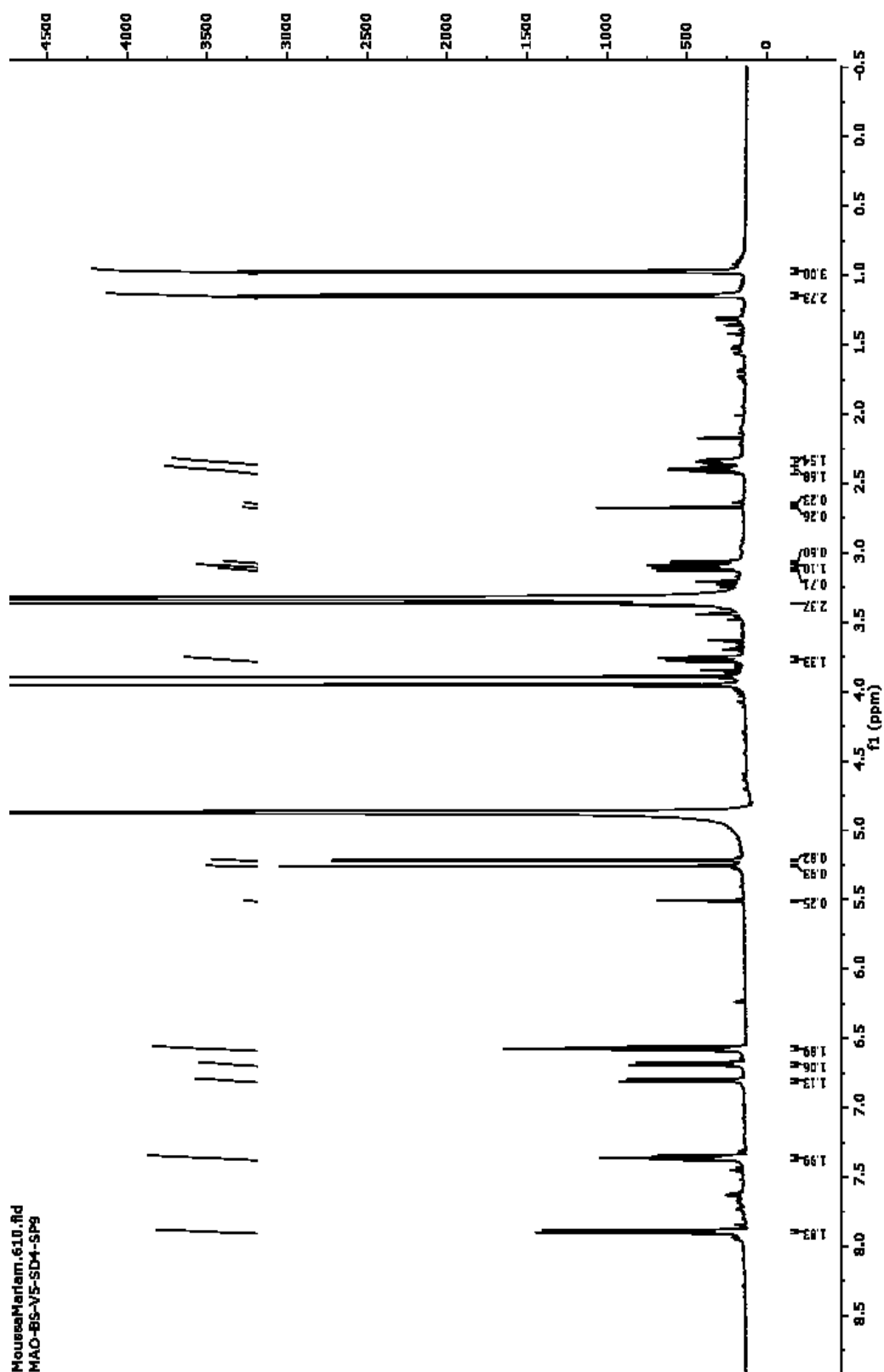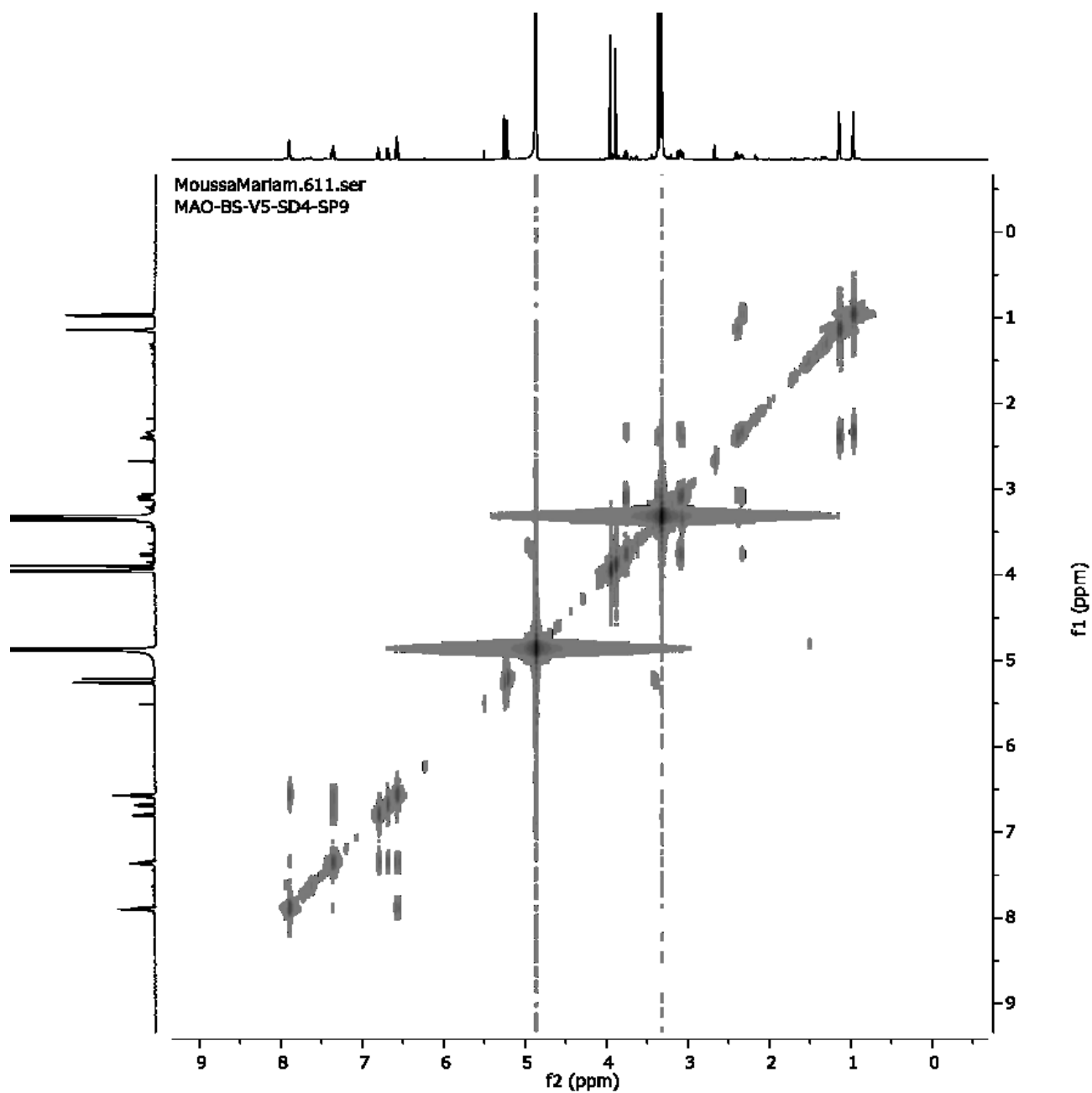
S13. ^1H-^{13}C-HSQC (600MHz/150 MHz, MeOH-d_4) spectrum of compound **2**.
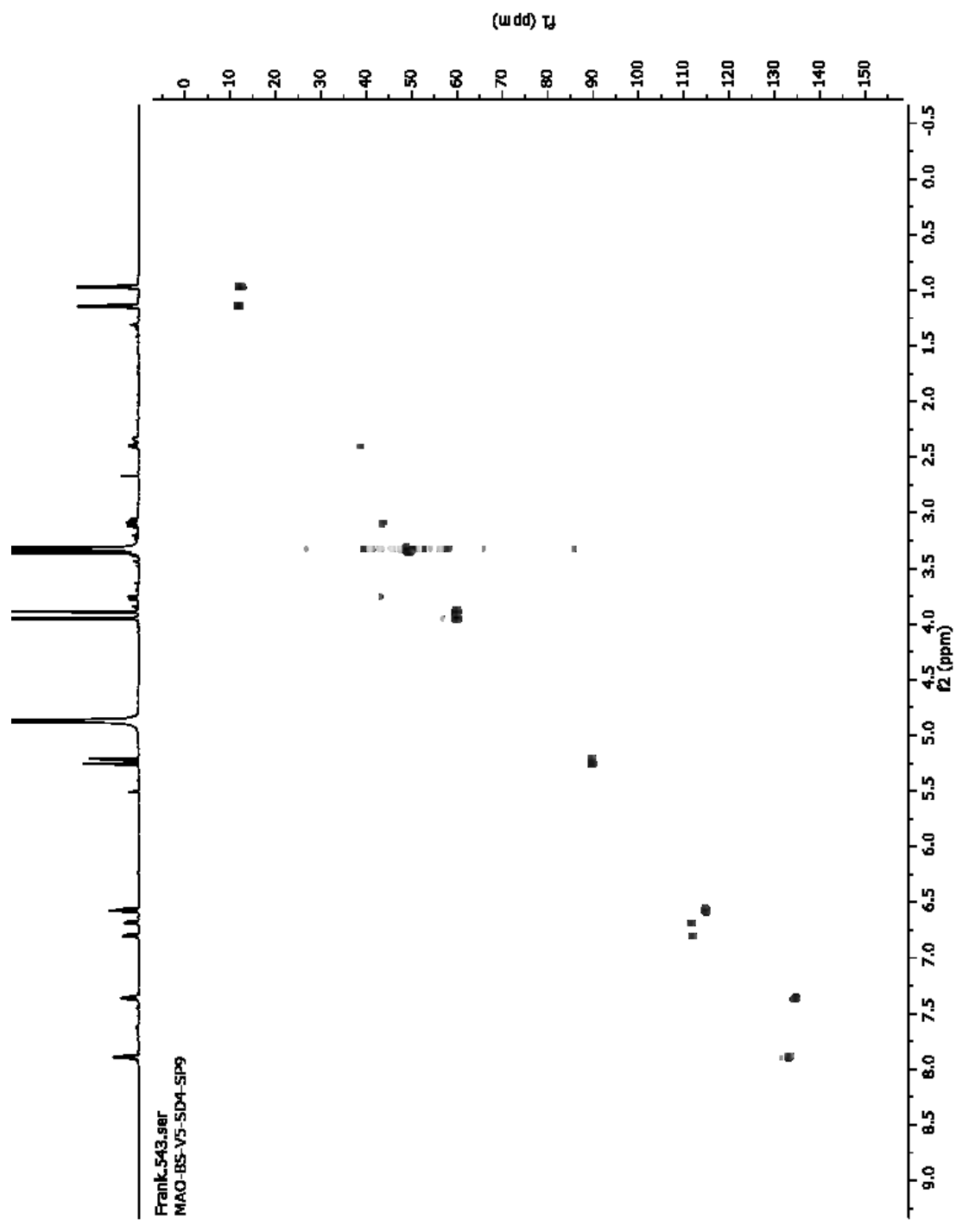
S14. ^{1}H-^{13}C-HMBC (600MHz/150 MHz, MeOH-d_4) spectrum of compound **2**.
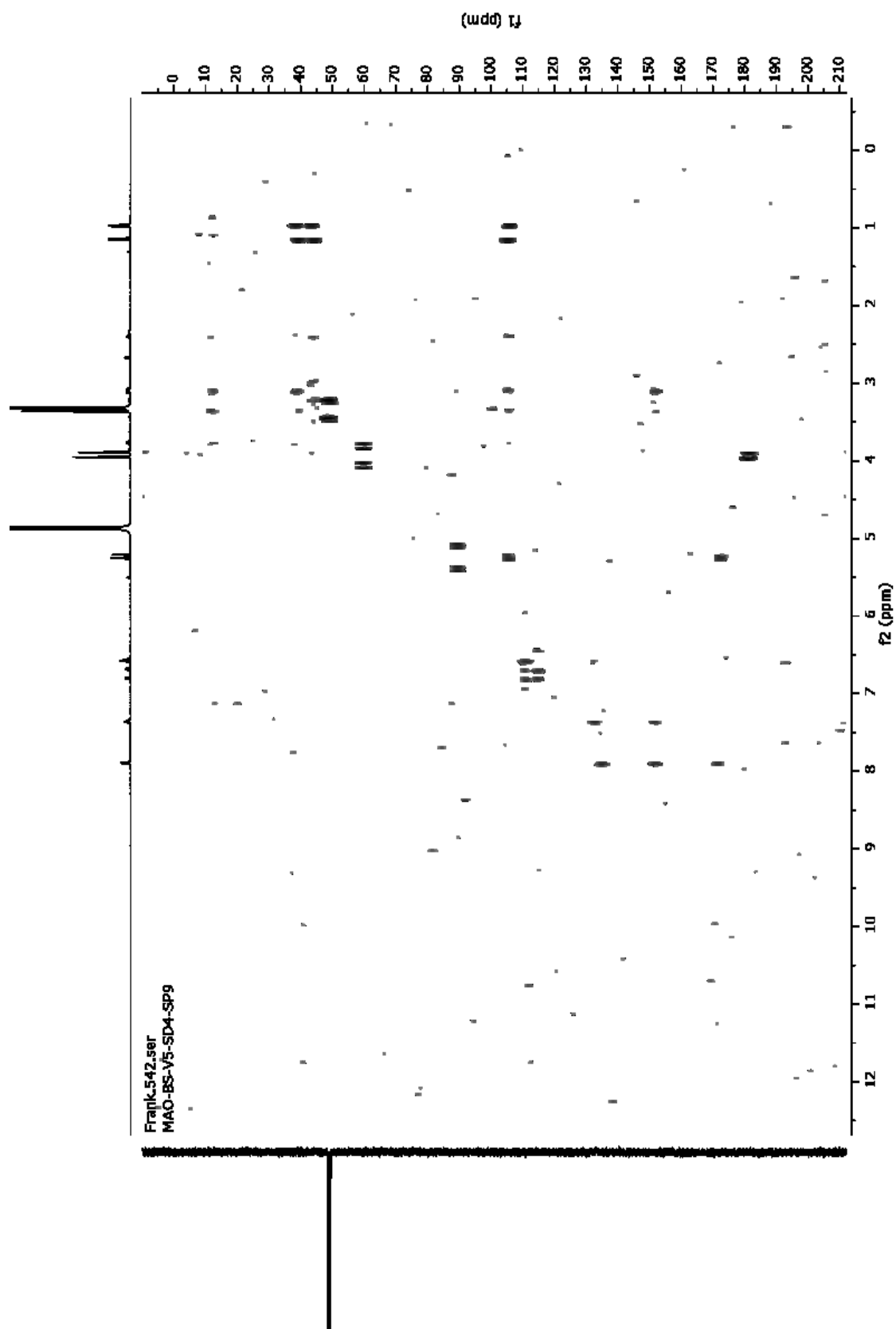
S15. UV spectrum of compound **3**.

S16. HRESIMS of compound **3**.

Mass Spectrum SmartFormula Report

Analysis Info   Acquisition Date   12/7/2016 9:58:56 AM

Analysis Name	D:\Data\spektren 2016\Proksch16HR000289.d		
Method	tune_low_new.m	Operator	Peter Tommes
Sample Name	M. Frank MAO-BS-V5-SD4-SP3 (CH3OH)	Instrument	maXis	288882.20213
Comment			

Acquisition Parameter

Source Type	ESI	Ion Polarity	Positive	Set Nebulizer	0.3 Bar
Focus	Not active	Set Capillary	4000 V	Set Dry Heater	180 °C
Scan Begin	50 m/z	Set End Plate Offset	-500 V	Set Dry Gas	4.0 l/min
Scan End	1500 m/z	Set Collision Cell RF	600.0 Vpp	Set Divert Valve	Source

Meas. m/z	#	Ion Formula	m/z	err [ppm]	mSigma	# mSigma	Score	rdb	e⁻ Conf	N-Rule
150.0549	1	C8H8NO2	150.0550	0.3	3.8	1	100.00	5.5	even	ok
308.1127	1	C15H18NO6	308.1129	0.5	5.9	1	100.00	7.5	even	ok
330.0947	1	C15H17NNaO6	330.0948	0.3	3.7	1	100.00	7.5	even	ok
	2	C13H12N7O4	330.0945	-0.5	5.4	2	94.52	11.5	even	ok
391.2841	1	C24H39O4	391.2843	0.5	12.9	1	100.00	5.5	even	ok
413.2661	1	C24H38NaO4	413.2662	0.3	9.6	1	100.00	5.5	even	ok
	2	C22H33N6O2	413.2660	-0.4	11.0	2	96.76	9.5	even	ok
419.3151	1	C26H43O4	419.3156	1.2	13.8	1	100.00	5.5	even	ok
	2	C25H40N4Na	419.3145	-1.4	18.2	2	87.96	7.5	even	ok

S17. ^{1}H-NMR (600 MHz, MeOH-d_4) spectrum of compound **3**.

S18. ^{1}H-^{1}H –COSY (600 MHz, MeOH-d_4) spectrum of compound **3**.
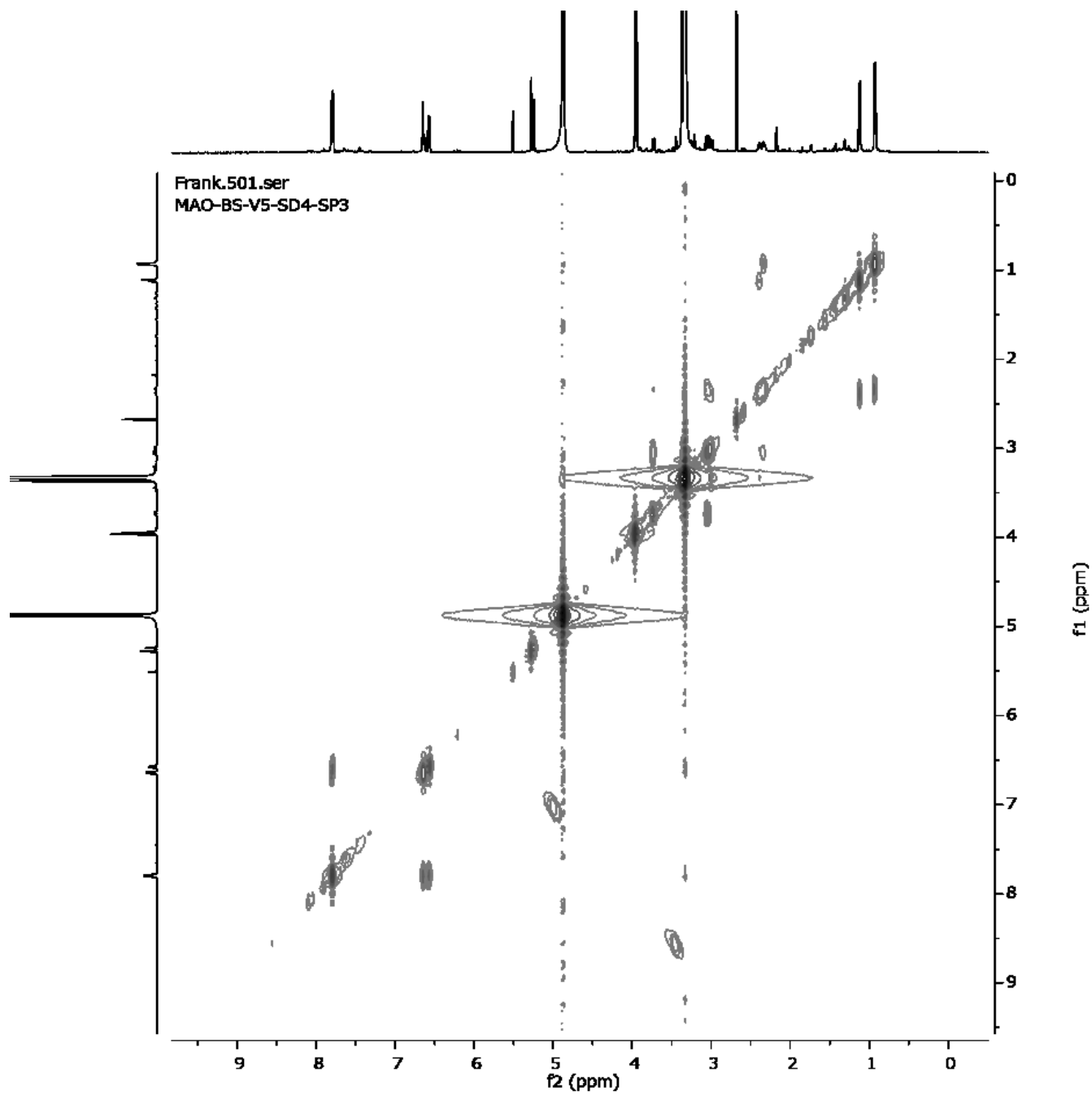
S19. ^{1}H-^{13}C-HSQC (600MHz/150 MHz, MeOH-d_4) spectrum of compound **3**.
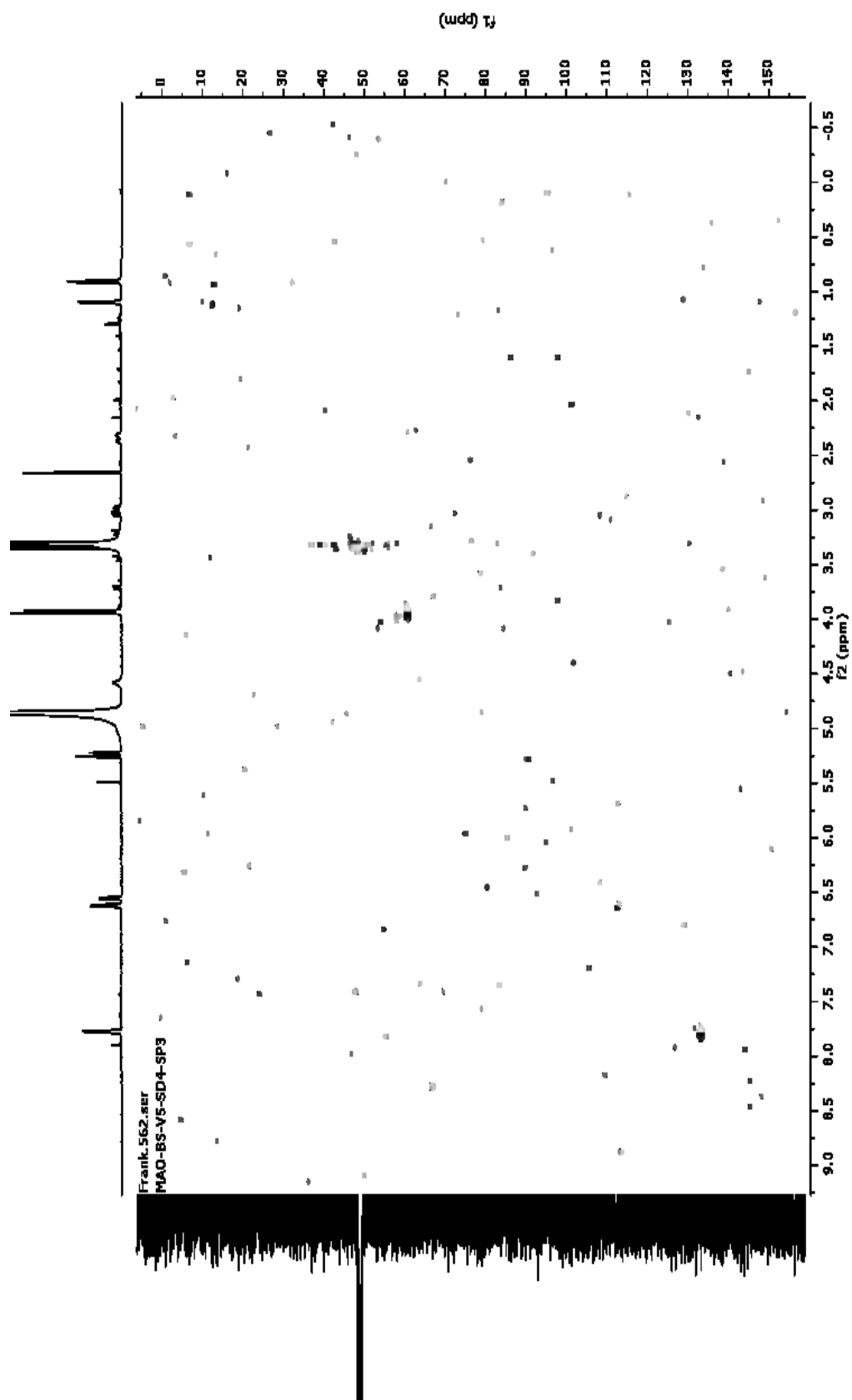
S20. ^{1}H-^{13}C-HMBC (600MHz/150 MHz, MeOH-d_4) spectrum of compound **3**.
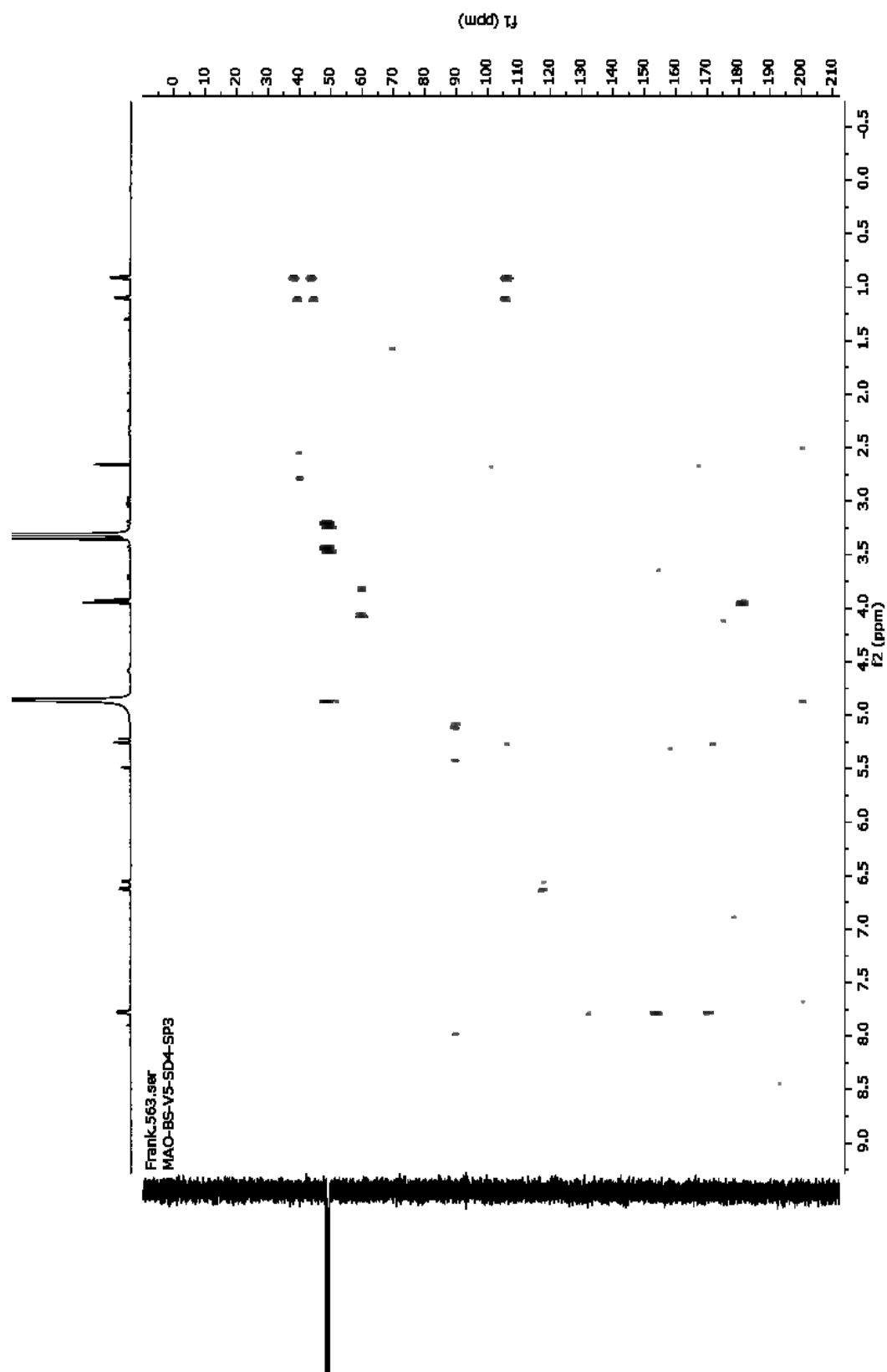
S21 Chromatogram of C$_4$-Marfey's method of compound **1** L-FDAA adduct (short program).
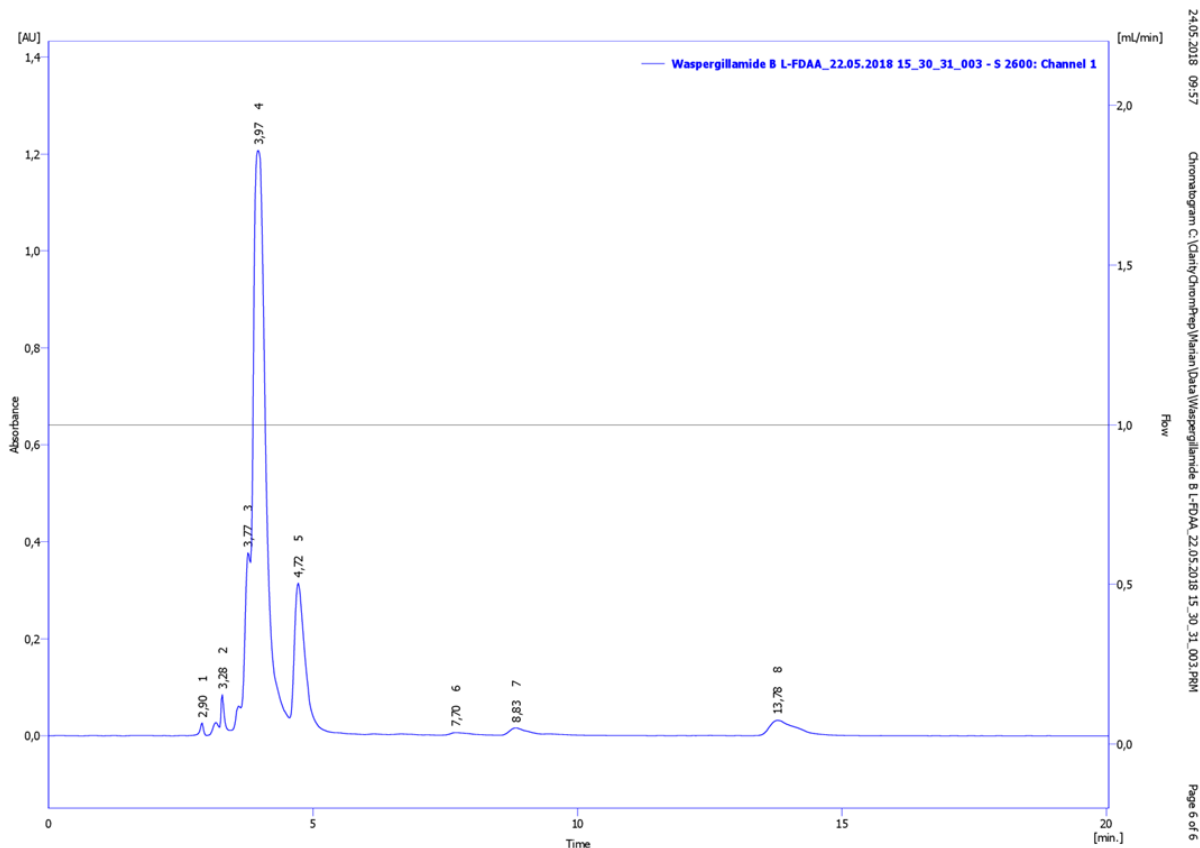
ClarityChrom Prep - Chromatography SW
www.knauer.net

Result Table (Uncal - Waspergillamide B L-FDAA_22.05.2018 15_30_31_003 - S 2600: Channel 1)

	Reten. Time [min]	Area [mAU.s]	Height [mAU]	Area [%]	Height [%]	W05 [min]	Compound Name
1	2,900	135,973	26,424	0,3	1,1	0,08	
2	3,283	1145,408	84,701	2,8	3,6	0,08	
3	3,767	2414,781	377,567	5,9	16,2	0,12	
4	3,967	20250,710	1207,398	49,4	51,9	0,27	
5	4,717	5092,600	314,807	12,4	13,5	0,22	
6	7,700	189,340	6,085	0,5	0,3	0,47	
7	8,833	476,293	15,608	1,2	0,7	0,42	
8	13,783	1122,615	31,767	2,7	1,4	0,58	
9	59,550	808,084	19,902	2,0	0,9	0,68	
10	63,567	6232,356	227,542	15,2	9,8	0,10	
11	64,917	3088,156	15,603	7,5	0,7	5,75	
	Total	40956,318	2327,404	100,0	100,0		

Column	: Machery-Nagel EC250/4.6 Nucleosil 250-5 C4 4x300mm	Detection	: 340nm	
Mobile Phase	: A: Water B: MeOH C: ACN+1%Formic Acid	Temperature	: 50°C	
Flow Rate	: 1 ml/min	Pressure	: max 400bar	
Note	: This method is necessary to separate Allo-Aminoacids!			
Autostop	: 70,00 min	External Start	: Start - Restart, Down	
Detector 1	: S 2600: Channel 1	Range 1	: Bipolar, 10000 mAU, 1 Samp. per Sec.	
Subtraction Chromatogram	: (None)	Matching	: No Change	
Standby Flow	: 1,00 mL/min	Idle State	: Initial	
Time to Standby	: 0,00 min.	Standby Time	: 0,00 min.	
Min. Pressure	: 0,00 bar	Max. Pressure	: 0,00 bar	

Gradient Table

Time [min]	A [%]	B [%]	C [%]	Flow [mL/min]
Initial	85	15	0	1,000
55,00	40	60	0	1,000
55,10	0	100	0	1,000
60,00	0	100	0	1,000
60,10	85	15	0	1,000
70,00	85	15	0	1,000

S22 Chromatogram of C$_4$-Marfey's method of compound **1** D-FDAA adduct (short program).

ClarityChrom Prep - Chromatography SW
www.knauer.net

Result Table (Uncal - Waspergillamide B D-FDAA_22.05.2018 16_40_54_004 - S 2600: Channel 1)
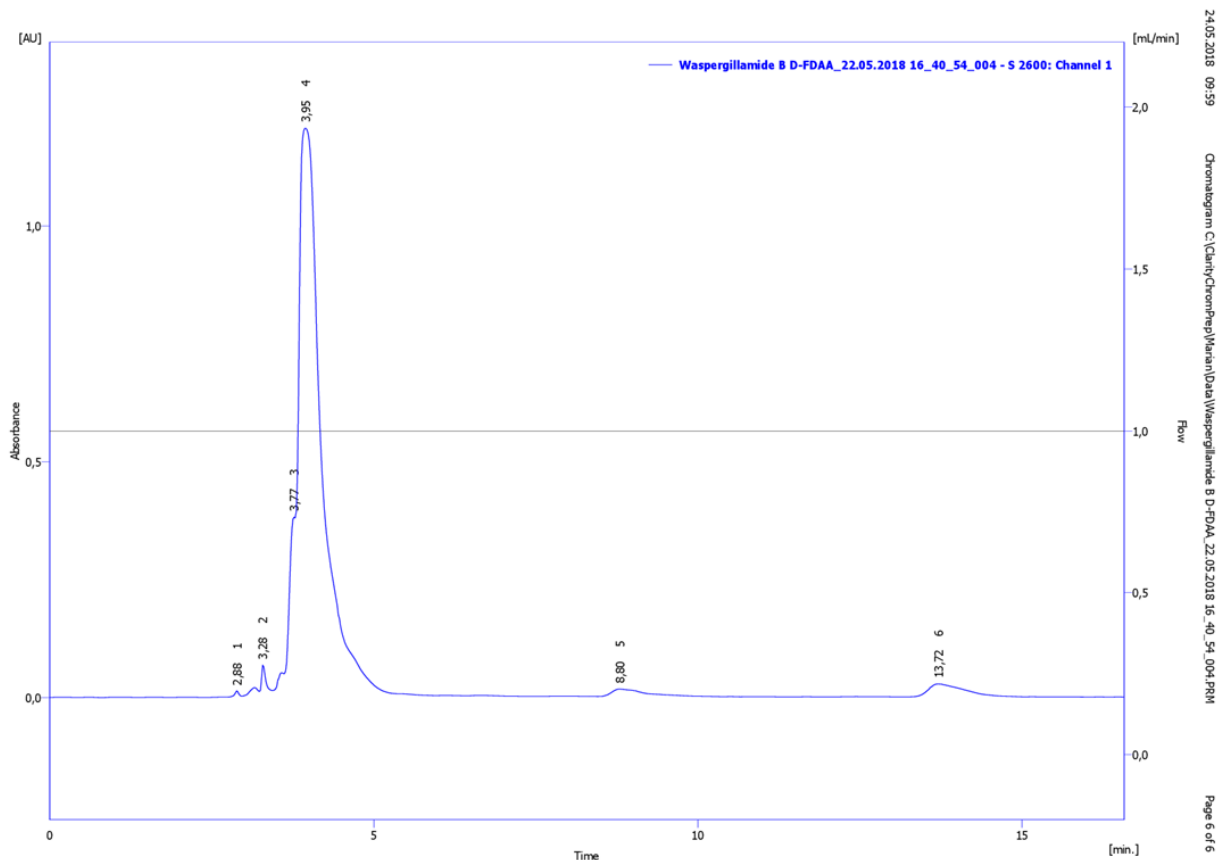
	Reten. Time [min]	Area [mAU.s]	Height [mAU]	Area [%]	Height [%]	W05 [min]	Compound Name
1	2,883	74,995	13,843	0,2	0,7	0,08	
2	3,283	562,189	68,014	1,3	3,5	0,08	
3	3,767	3253,202	381,733	7,2	19,4	0,13	
4	3,950	29635,530	1206,049	65,9	61,2	0,35	
5	8,800	596,916	15,536	1,3	0,8	0,50	
6	13,717	1062,263	27,396	2,4	1,4	0,62	
7	59,567	868,983	23,073	1,9	1,2	0,70	
8	63,567	6388,335	230,922	14,2	11,7	0,08	
9	68,400	2516,890	3,345	5,6	0,2	4,73	
	Total	44959,303	1969,912	100,0	100,0		

Column	: Machery-Nagel EC250/4.6 Nucleosil 250-5 C4 4x300mm	Detection	: 340nm
Mobile Phase	: A: Water B: MeOH C: ACN+1%Formic Acid	Temperature	: 50°C
Flow Rate	: 1 ml/min	Pressure	: max 400bar
Note	: This method is necessary to separate Allo-Aminoacids!		

Autostop	: 70,00 min	External Start	: Start - Restart, Down
Detector 1	: S 2600: Channel 1	Range 1	: Bipolar, 10000 mAU, 1 Samp. per Sec.
Subtraction Chromatogram	: (None)	Matching	: No Change

Standby Flow	: 1,00 mL/min	Idle State	: Initial
Time to Standby	: 0,00 min.	Standby Time	: 0,00 min.
Min. Pressure	: 0,00 bar	Max. Pressure	: 0,00 bar

Gradient Table

Time [min]	A [%]	B [%]	C [%]	Flow [mL/min]
Initial	85	15	0	1,000
55,00	40	60	0	1,000
55,10	0	100	0	1,000
60,00	0	100	0	1,000
60,10	85	15	0	1,000
70,00	85	15	0	1,000

Chapter 6 - General Discussion

6.1 Activation of silent biogenetic gene clusters through OSMAC experiments

OSMAC cultivation experiments have proven themselves as an adequate method to increase the diversity of fungal secondary metabolites (Daletos *et al.* 2017). During this study, *Aspergillus ochraceu*s and *Penicillium canescens* were subjected to numerous OSMAC experiments to explore their unused biosynthetic potential. *P. canescens* produced mainly griseofulvin and its intermediates during a solid rice fermentation. A 5% NaBr OSMAC experiment was performed to investigate whether bromo-analogs of the naturally occuring chlorinated compounds could be produced. The 5% NaBr OSMAC experiment performed on *P. canescens* yielded two new brominated azaphilones, bromophilones A and B. When compared to similar experiments only one reported case of bromination in azaphilones occurred during a cultivation of *Penicillium multicolor* with 3% KBr spiked medium yielding 5-bromoochrephilone (Matsuzaki *et al.* 1998). Halogenation in azaphilones is highly specific to position C-5 and is performed after the assembly of the polyketide core (PKS) through a combination of four redox enzymes, one of them being a flavine dependent halogenase with high regio-selectivity (Sato *et al.* 2016). It has been shown, that flavine dependent halogenases from marine organisms not only accept bromide salt as a substrate, but also may even prefer it in the abundance of competing chloride ions (Neubauer *et al.* 2018). Because the control fermentation of *P. canescens* yielded no azaphilones at all and the color of the medium changed to red on 5% NaBr spiked rice medium it is safe to assume that the gene cluster for the production of bromophilone A and B is silent in the absence of bromide. The experiment did not yield any bromo analogs of griseofulvin and its precursors, the bromination step of bromophilone A and B seems to be performed by a different flavine dependent halogenase, which is presumably stored in a silent gene cluster together with azaphilone specific polyketide synthases (Zabala *et al.* 2012). Effects on the amounts of xanthones and benzophenone pattern of *P. canescens* are better explained when brought into context with the biosynthetic pathway to griseofulvin, which is discussed separately in **chapter 6.4**.

bromophilone A 9α
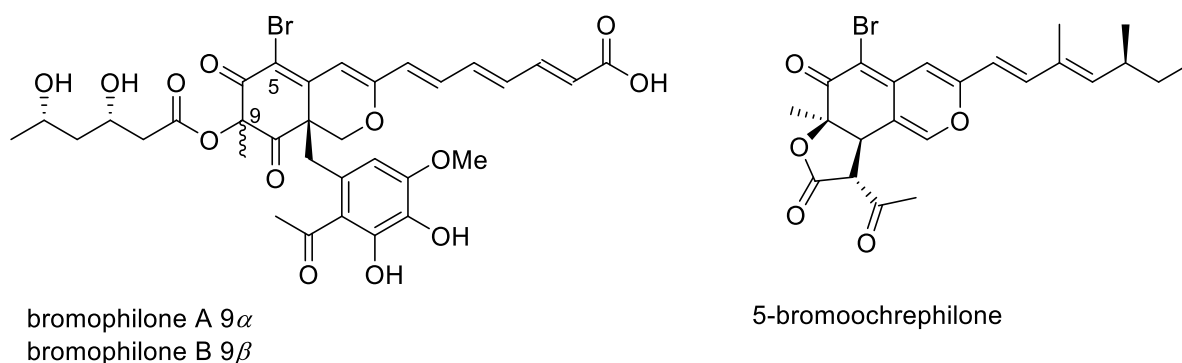bromophilone B 9β

5-bromoochrephilone

Figure 10: Brominated azaphilones from OSMAC experiments.

A. ochraceus produced mainly ochratoxin A (OTA), penicillic acid and several circumdatins during the solid rice control fermentation. OSMAC experiments with *A. ochraceus* with sodium halides and several inorganic nitrogen salts had an influence on the amount of several metabolites, but did not induce any new compounds. However, it is interesting to note, that 3.5% NaBr decreased the amount of OTA, while increasing the amount of the dechlorinated ochratoxin B (OTB). It has been suggested, that OTA synthesis is an adaptation of fungi to thrive on high salt stress medium and that fungi actively transport chloride and bromide ions into their cells and efficiently incorporate it into OTA (Schmidt-Heydt *et al.* 2012). Nevertheless, the halogenation process did not seem to work with bromide ions in this study. While bromoochratoxin A has been reported in a KBr fermentation of *A. ochraceus*, the authors state, that the fungus was far less versatile with the production of bromo-analogs compared to other fungi (Stander *et al.* 2000), which is in agreement with the findings from this study. Cultivation on 1% NH$_4$Cl spiked rice medium decreased the amount of OTA by 90% and OTB to non-detectable levels, suggesting, that chloride concentration is not the only factor during OTA production. OTA might be influenced by catabolite stress; its concentration was decreased during co-cultivation and through the presence of ammonium ions. Biosynthetically OTA is built from the polyketide mellein and a phenylalanine unit.

ochratoxin A

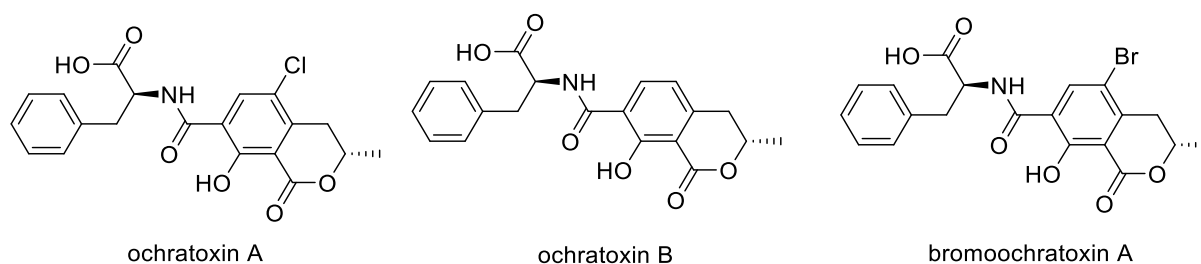ochratoxin B

bromoochratoxin A

Figure 11: Ochratoxin A derivatives.

When changing the medium to protein rich (~21%) white beans medium, *A. ochraceus* produced almost no polyketides, but accumulated a similar amount of alkaloids as compared to the rice control culture. Additionally, one new diketopiperazine alkaloid, waspergillamide B was produced. Diketopiperazine alkaloids are among the most common inducible non-polyketide compounds during OSMAC experiments. Other examples include the phytotoxic tryptostatins from *Aspergillus fumigatus* (Zhang *et al.* 2013) or the penicibrocazines from *Penicillium brocae* (Meng *et al.* 2017). Fungal natural products with nitro-moieties, while very rare, do occur such as in the examples of pyriculamide (Parry *et al.* 2011) or waspergillamide A (Quezada *et al.* 2017).
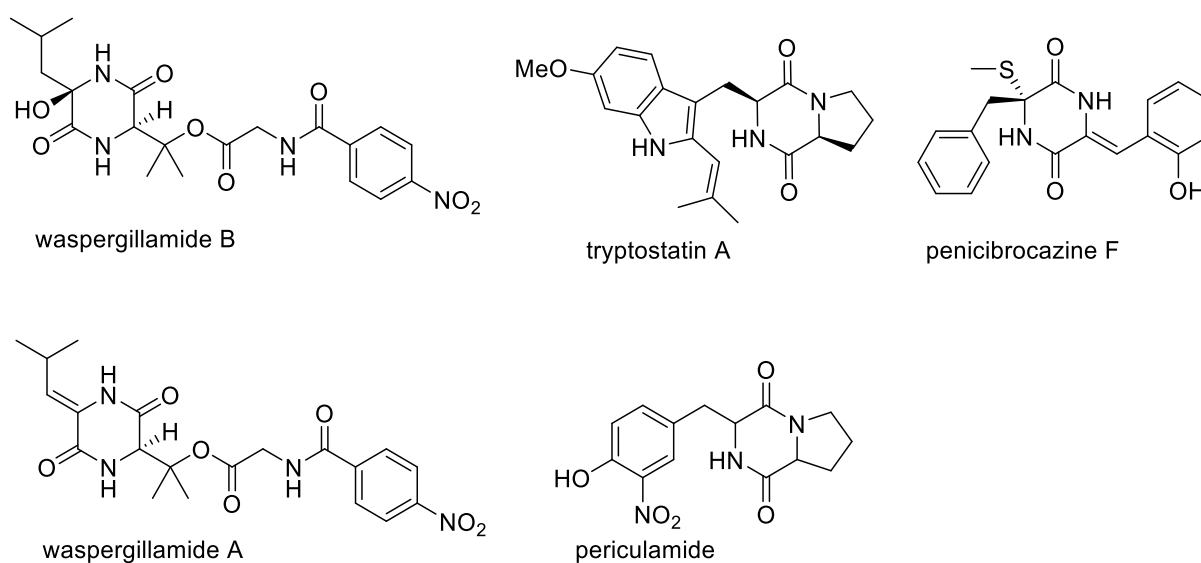
Figure 12: Fungal diketopiperazines from OSMAC experiments and fungal nitro-compounds.

In summary, the OSMAC experiments with *A. ochraceus* and *P. canescens* were able to produce new metabolites from different biogenetic pathways. Bromophilone A and B are derived from polyketide synthases and flavine dependent halogenases, while waspergillamide B is assumed to be formed by non-ribosomal peptide synthases. All results fit into the context of similar research papers and agree with the findings of other research groups. The new compounds are structurally novel and unusual.

6.2 Activation of silent biogenetic gene clusters through co-cultivation

The mixed fermentation approach has been shown to be an adequat method to increase not only the yield, but also the diversity of fungal secondary metabolites numerous times (Daletos *et al.* 2017; Marmann *et al.* 2014). The use of solid rice medium is advantageous for the co-cultivation of fungi with bacteria, because the hyphens of filamentous fungi can be co-opted by the bacteria to reach new nutritional resources (Prosser and Tough 1991) and result in a close spatial relationship of the microorganism for microbial crosstalk to take place (Frey-Klett *et al.* 2011). The microbial interactions of two different microorganisms have been proven to invoke the induction of fungal silent gene clusters through intimate physical contact (König *et al.* 2013; Schroeckh *et al.* 2009). During the last few years, several types of silent gene clusters were reported to be activated by co-cultivation. Common examples include polyketide synthases (PKS), non-ribosomal peptide synthetases (NRPS), terpenoids and biogenetic hybrid compounds (Reen *et al.* 2015).

During the course of this doctoral thesis, the co-cultivation of *A. ochraceus* and *Bacillus subtilis* on solid rice medium afforded the non-ribosomal cyclic tetrapeptide violaceomide A. The compound was recently published from a potato dextrose agar (PDA) fermentation study of the marine sponge derived fungus *Aspergillus violaceofuscus* (Liu *et al.* 2018). During the OSMAC experiments of this study the peptide was also isolated from a 1% NH_4Cl solid rice fermentation of *A. ochraceus*. It could be interpreted as a response to catabolite stress (ter Schure *et al.* 2000), which is either caused by competition for resources during co-cultivation or by an access of the catabolite waste product ammonia during the OSMAC. Additionally, two new penicillic acid derivatives ochraspergillic acids A and B were isolated from the co-cultivation of *A. ochraceus* and *B. subtilis*, which are assumed products of a mixed fungal/bacterial biosynthesis (see **chapter 6.3**). During the co-cultivation of *A. ochraceus* and *Streptomyces lividans*, the production of penicillic acid and dihydropenicillic acid was strongly increased. These examples further demonstrate an increase of orsA gene related PKS activity during co-cultivation, because penicillic acid is derived from orselinic acid (Netzker *et al.* 2015; Sekiguchi *et al.* 1987). When comparing the isolated compounds to the result of other recent co-cultivation attempts, the occurrence of new penicillic acid derivatives was described during the fungal-fungal mixed fermentation of *Fusarium solani* and *Talaromyces sp.*. It yielded the compound coculnol (Nonaka *et al.* 2015), which shows that even though PA has been investigated since the first half of the twentieth century, co-cultivation can still produce new derivatives. While

fungal cyclic tetrapeptides are quite rare, two such peptides were discovered in a mixed fermentation of the mangrove endophytic fungi *Phomopsis sp.* and *Alternaria sp.* (Huang *et al.* 2014).
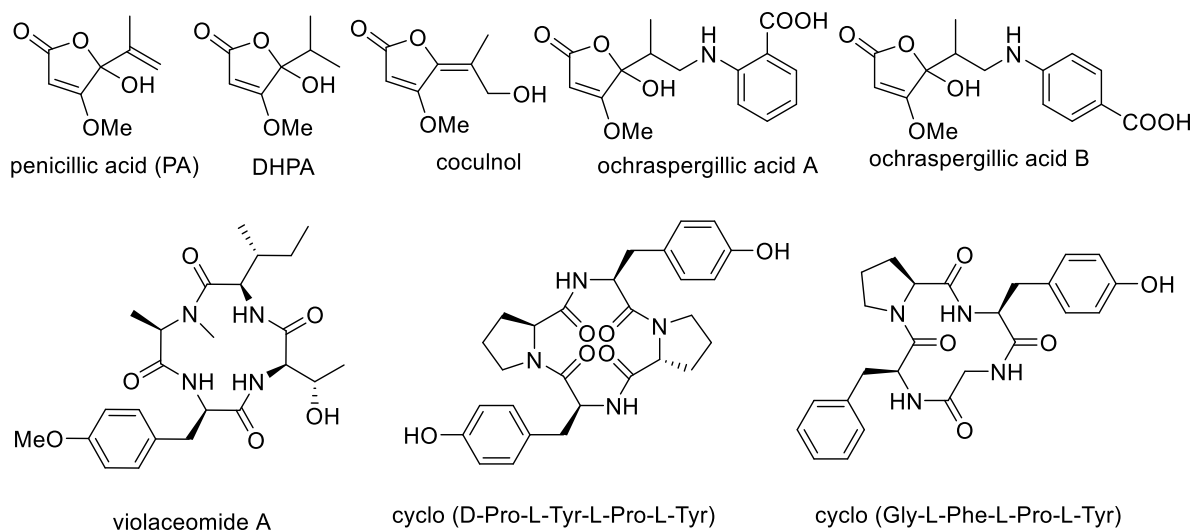

Figure 13: Fungal penicillic acid derivatives (PKS) and cyclic tetrapeptides (NRPS) discovered during co-cultivation experiments

While the compounds did not show observable antibacterial or cytotoxic effects against the tested strains and cell lines, biological activity should not be outright excluded, because non toxic effects of compounds during co-cultivation are well documented, such as non toxic quorum sensing inhibitors like penicillic acid (Sharma and Jangid 2015). Since most of the produced compounds from the co-cultivation of *A. ochraceus* and *B. subtilis* lacked antibiotic activity, the effect on bacterial biofilms of *Staphylococcus aureus* was investigated. However, no compound showed relevant biofilm inhibiting effects. The main quorum sensing (QS) mechanisms by which *S. aureus* organizes its biofilm formation consists of two auto inducer peptides (Kong *et al.* 2006). However, other QS systems such as the *N*-acyl homoserine lactones (AHL) exist, which are known to be inhibited by penicillic acid (Rasmussen and Givskov 2006), but those are more specific to gram-negative bacteria such as *Pseudomonas aeruginosa* (Swift *et al.* 1994). In the future, the presumably inactive metabolites from *A. ochraceus* should be investigated for the inhibition of gram-negative biofilms. The disruption of biofilm formation without lethality to the gram-negative bacteria could prove useful to decrease the likelihood of emerging resistances through natural selection (Hentzer and Givskov 2003). An example of a natural non-toxic, non-bactericidal compound which disrupt bacterial biofilms is the

semisynthetic sponge compound dibromohemibastadin (DBHB), which was able to inhibit the formation of bacterial biofilms in an attempt to decrease microfouling on sea water submerged surfaces (Le Norcy *et al.* 2017), but could in the future be extended to medical applications (Percival *et al.* 2015). This is especially interesting for *A. ochraceus* as several of its secondary metabolites, e.g. circumdatin F, have been reported for antifouling activity (Zhang *et al.* 2014), but were non-toxic in cytotoxity and antibacterial assays during this study.
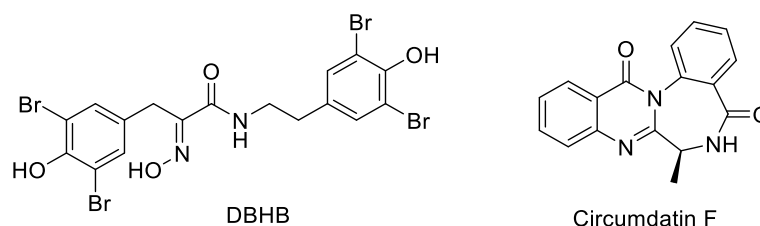
Figure 14: Non-toxic antifouling compounds.

6.3 Induction of mixed fungal-bacterial metabolites

When employing the technique of co-cultivation, the question of the origin of metabolites is always difficult to answer. Such is the case with derivatives of anthranilic acid. While anthranilic acid derivatives have been described from axenic fungal cultivation experiments, as in the case of penipacids A–E (Li *et al.* 2013), circumdatins A-F (Rahbæk *et al.* 1999; Rahbæk and Breinholt 1999) or several other anthranilic acid conjugates (Teponno *et al.* 2017), there are a number of anthranilic acid metabolites that are only occurring during fungal bacterial co-cultivation and not in their axenic controls, such as *N*-carboxymethylanthranilic acid (Chen *et al.* 2015) and *N*-acylanthranilic acid derivatives (Liu *et al.* 2017a).

Figure 15: Fungal anthranilic acid derivatives.

The biosynthetic approach of these alkaloids has been linked to non-ribosomal peptide synthases (Ames and Walsh 2010) and although the crucial anthranilic acid building block is a typical bacterial metabolite, the synthesis does occur in fungi (Hütter and DeMoss 1967) as a salvage pathway of tryptophan (Badawy 2017). The experiments described in **chapter 5** exemplify an attempt to prove a fungal origin of the metabolites ochraspergillic acids A and B, through precur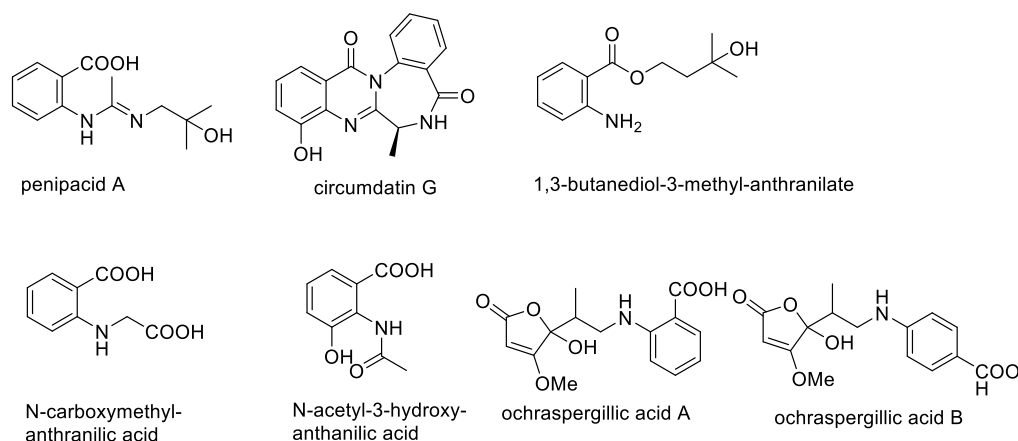sor feeding experiments. Both compounds were isolated from the mixed fermentation of *A. ochraceus* and *B. subtilis* and show distinct features of fungal and bacterial metabolism. The biosynthesis of (dihydro)penicillic acid, which is derived from the polyketide orsellinic acid (Sekiguchi *et al.* 1987), is fungal in nature, while anthranilic acid and para-aminobenzoic acid can be either fungal or bacterial in nature (Slock *et al.* 1990; Tang *et al.* 1994). Both compounds are formed by a Michael-addition of aminobenzoic acid to the penicillic acid keto-form. The resulting enol then changes to the keto-form and the lactolring is formed again. This tautomerism was described for penicillic acid (Munday 1949) and is also visible from the duplication of NMR signals in the spectra of ochraspergillic acids A and B.
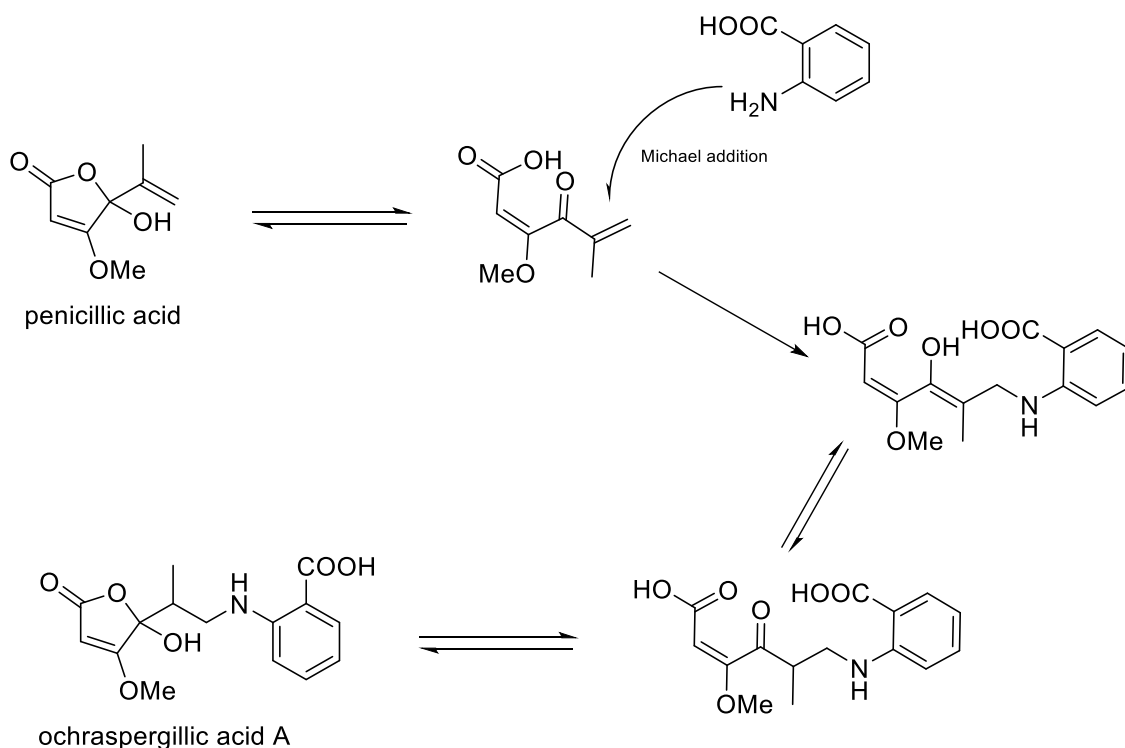

Figure 16: Proposed formation of ochraspergillic acid A.

To clarify the origin of the aminobenzoic acid subunit, feeding experiments with axenic *A. ochraceus* and 1% and 2% supplements of L-tryptophan and anthranilic acid were performed,

in which ochraspergillic acid A was formed at comparable concentrations (as compared to co-cultivation with *B. subtilis*) in a dose-dependent manner. This can be seen as proof, that *A. ochraceus* not only accepts external anthranilic acid, which could be bacterial in nature, but also synthesizes anthranilic acid through the tryptophan salvaging kynurenine pathway at sufficient levels of tryptophan. As such, ochraspergillic acid A can be seen as a true fungal metabolite, which is likely dependent on the abundance of bacterial building blocks, but can also be formed by fungal biosynthesis alone. Ochraspergillic acid B could not be quantified from the crude extract of the feeding experiment, but cannot be excluded because it shares molecular weight and HPLC retentiontime with the constitutively produced fungal alkaloid circumdatin G. The absence of other pABA derived alkaloids from the axenic cultivation experiments in contrast to the anthranilic acid derived alkaloids suggest a bacterial origin of the pABA subunit, making ochraspergillic acid B a mixed fungal and bacterial metabolite. While both compounds fail to show significant cytotoxic or antibacterial effects when tested against several clinically relevant strains, the bioactive properties of *N*-substituted anthranilic acid derivatives have been demonstrated before (Li *et al.* 2013; Thorarensen *et al.* 2007) and these metabolites could still play a role as a fungal defense mechanism during co-cultivation.

6.4 Manipulation of the griseofulvin biosynthesis through NaBr

Under standard solid rice fermentation, conditions the fungus *Penicillium canescens* produced an array of polyketide compounds. The main compound was griseofulvin, which is in concordance with earlier reports (Nicoletti *et al.* 2007). Most other compounds were reported intermediates or products of an alternatively branching pathway, such as the xanthones (Roullier *et al.* 2016). When investigating the EtOAc extract of *P. canescens*, grown on solid rice medium, the compounds norlichexanthone, griseoxanthone C, griseophenones B, C and G, dechlorogriseofulvin and griseofulvin were isolated and identified. Griseofulvin was by far the most abundant compound, crystallizing from the crude extract, totaling at ~6 g out of the 12 g of crude extract. When looking at the biosynthesis of griseofulvin (Roullier *et al.* 2016), the array of isolated intermediates matches the literature. The absence of griseophenone D is explained by the formation of griseoxanthone C by a spontaneous intramolecular dehydration reaction of griseophenone D (Le Pogam and Boustie 2016), while the methylated griseophenone C and all its subsequent derivatives are protected from such reactions. The absence of chlorinated xanthones such as 4-chloronorlichexanthone (Qin *et al.* 2015a) supports

this statement, as a demethylating step would have to occur after the formation of griseophenone B. The formation of griseophenone G is assumed to be from griseophenone B by the flavine dependent halogenase Gsfl, as the rotation of the benzophenone axis results in an open position preferabily targeted for a second chlorination. The new chlorinated diphenylether penicanether and its co-isolated desmethylderivative are assumed to be derived from griseophenone B. They are formed from the intermediate desmethyldehydrogriseofulvin, in an analogous mechanism to the biosynthesis of pesthetic acid from sulochrin through a similar spiran intermediate (Xu *et al.* 2014). The resulting diphenylether is then esterificated to the co-isolated desmethylderivative and *O*-methylated to penicanether.The employed OSMAC approach used 5% NaBr to target the bromination step from griseophenone C to griseophenone B and tried to force bromination through the flavine dependent halogenase Gsfl. However, the observed effect showed a clear inhibition of the chlorinationstep instead of a bromination. The accumulation of griseophenone C by 1300% and the decrease of griseofulvin by 92% clearly marks the exact step at which the synthesis was disrupted. The Gsfl-catalysed chlorination step was inhibited. The amount of dechlorogriseofulvin did not notably change, implying that the formation of the spiro-system is not completely dependent on the chlorination step. The xanthones norlichexanthone, griseoxanthone C and 1,3,5,6 tetrahydroxy-8-methylxanthone also strongly accumulated implying that the formed intermediates take a different pathway if the griseofulvin synthesis becomes blocked. The biosynthesis of 1,3,5,6 tetrahydroxy-8-methylxanthone is not yet known, as it is the only known lichexanthone with a hydroxyl moiety in position 5 (Masters and Bräse 2012), but it is assumed to be derived from norlichexanthone through cytochrome dependent aryl-epoxidation similar to the mechanism involved in the biosynthesis of ravenelin, secalonic acid and geodin (Henry and Townsend 2005). Although the production of bromogriseofulvin by *Penicillium* species has been decribed during KBr feeding experiments on Czapek medium (MacMillan 1954), no bromo analogs were detected during this experiment. This implies that factors other than the halide concentration have to be considered when drawing conclusions about the halide-promiscuity of the responsible halogenase. While the OSMAC experiment ultimately succeeded in producing new brominated compounds, the bromophilones described in **chapter 6.1** are obviously derived from a different polyketide synthase gene cluster and are as such no suitable targets for the highly specialized Gsfl halogenase. These results are still useful for connecting the majority of isolated compounds to a single network of related natural products, where the central intermediate griseophenone C can be converted into different bioactive secondary metabolites

such as the antifungal (and cytotoxic) griseofulvin (Zhong *et al.* 2010) or the antibacterial biofilm inhibitor norlichexanthone (Baldry *et al.* 2016). The blocking of the main metabolic pathway led to an accumulation of intermediates and a push into different biosynthetic directions. Strictly speaking, this is not an induction of cryptic secondary metabolites on the transcription level, but it led to the isolation of previously overlooked metabolites such as 1,3,5,6 tetrahydroxy-8-methylxanthone nonetheless. For future OSMAC experiments, the alternative pathways that intermediate secondary metabolites can take, should be taken into consideration when planning cultivation parameters to ensure that lesser produced compounds are not missed during extract investigation.
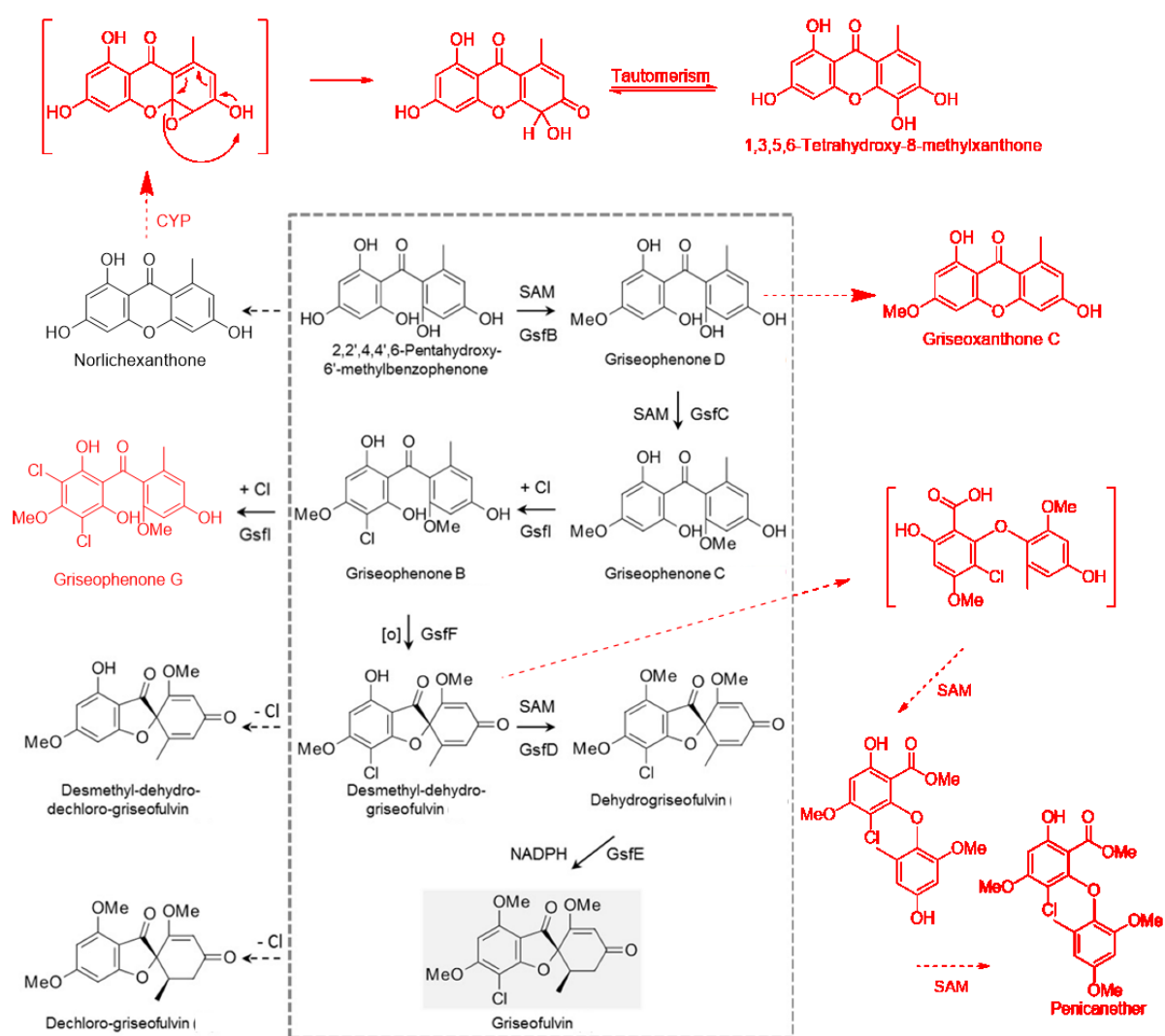

Figure 16: Griseofulvin biosynthesis and branching pathways to other related compounds. Newly proposed paths are shown in red (modified after Roullier *et al.* 2016).

6.5 Investigation of phomoxanthone A

The fungal mycotoxin phomoxanthone A (PXA) has been investigated extensively, because it shows promising cytotoxicity, paired with immuno modulating effects and a remarkable selectivity against cancer cells (Pavão *et al.* 2016; Rönsberg *et al.* 2013). When cooperating with the working group of Sebastian Wesselborg, Matthias Kassack and Stefanie Scheu (Böhler *et al.* 2018; Frank *et al.* 2015; Rönsberg *et al.* 2013), several problems had to be overcome to meet the demand for pure PXA. The fungal strains *Phomopsis longicolla* (Rönsberg *et al.* 2013) and *Phomopsis sp.* (Elsässer *et al.* 2005) (supplied by Barbara Schulz, TU Braunschweig) were cultivated on a large scale on solid rice (5 kg) medium. Both strains showed comparable productive capacities, so the EtOAc extracts were combined and the crude PXA was purified by silica gel vacuum liquid chromatography, followed by recrystallization from a mixture of EtOAc and *n*-hexane. This way pure PXA was produced on a multigramm scale and a steady supply was made possible to meet the demand for mode of action studies by the cooperation partners. During repeated freeze-thaw-cycles of PXA-stock solutions (in DMSO), the cytotoxic activity against Jurkat T- and Ramos B-lymphocytes decreased over time. This disturbing observation was investigated chromatographically and a second compound with identical molecular weight was discovered via LCMS. Both compounds were isolated via semipreparative HPLC from combined DMSO stocks and identified by NMR-spectroscopy as PXA (main compound) and dicerandrol C (impurity). This explained the decreasing cytotoxicity, as dicerandrol C is far less active than PXA (Rönsberg *et al.* 2013). When investigating this rearrangement reaction, PXA was dissolved in several organic solvents at a concentration of 1 mg/mL and left in the lab at ambient conditions of 24 h and 48 h. Conversion to dicerandrol C was observed in DMSO, MeOH and EtOH, but not in EtOAc and DCM. For all further experiments, a protocol was developed to divide PXA volumetrically into 200 nmol aliquotes by dissolving dry PXA in EtOAc and immediately drying the aliquots under a nitrogen stream, followed by removing moisture by freeze-drying. This allowed for one-time use samples, which showed very stable cytotoxic activity and were thus suitable for all further mechanistic investigations (Böhler *et al.* 2018). This way the instability of PXA during biological tests was overcome and it was brought one-step closer to becoming a promising future drug candidate. The method was readily shared with other cooperation partners of the GRK2158 to investigate the bioactive properties of PXA even further. When proposing a plausible reaction mechanism for the rearrangement of PXA to dicerandrol C, the work of Quin *et al.* with secalonic acid described a very similar rearrangement problem. The proposed

retro-oxa Michael reaction led to a linkage shift of secalonic acid A from 4. 4' to 2, 4' and 2, 2' in polar solvents (DMSO) at a thermodynamic equilibrium of 3.2:2:1 (Qin *et al.* 2015b). The proposed mechanism was thus adapted for the rearrangement of PXA (4, 4') to dicerandrol C (2, 2'). Preliminary investigations of the ratio of PXA to dicerandrol C in DMSO containing buffer solutions revealed a similar time dependent equilibrium trend, however the 2, 4' linked derivative (phomoxanthone B) was never detected and is suspected to be unstable under these conditions, however it has been reported as a natural product before co-isolated with PXA (Isaka *et al.* 2001). The proposed mechanism fits with the observation, because unlike a hydrolytic ring opening, it is independent of the presence of water molecules. This explains why the rearrangement is also observed in dry methanol. It also explains, why acid hydrolysis of the esters leaves the dimeric xanthone core intact (Isaka *et al.* 2001), while basic hydrolysis leads to a catalytic opening of the core and several described rearrangement products (Rönsberg *et al.* 2013). During the preparation of PXA-acetyl derivatives, the rearranging effects were also observed after 24 h of pyridine exposure.
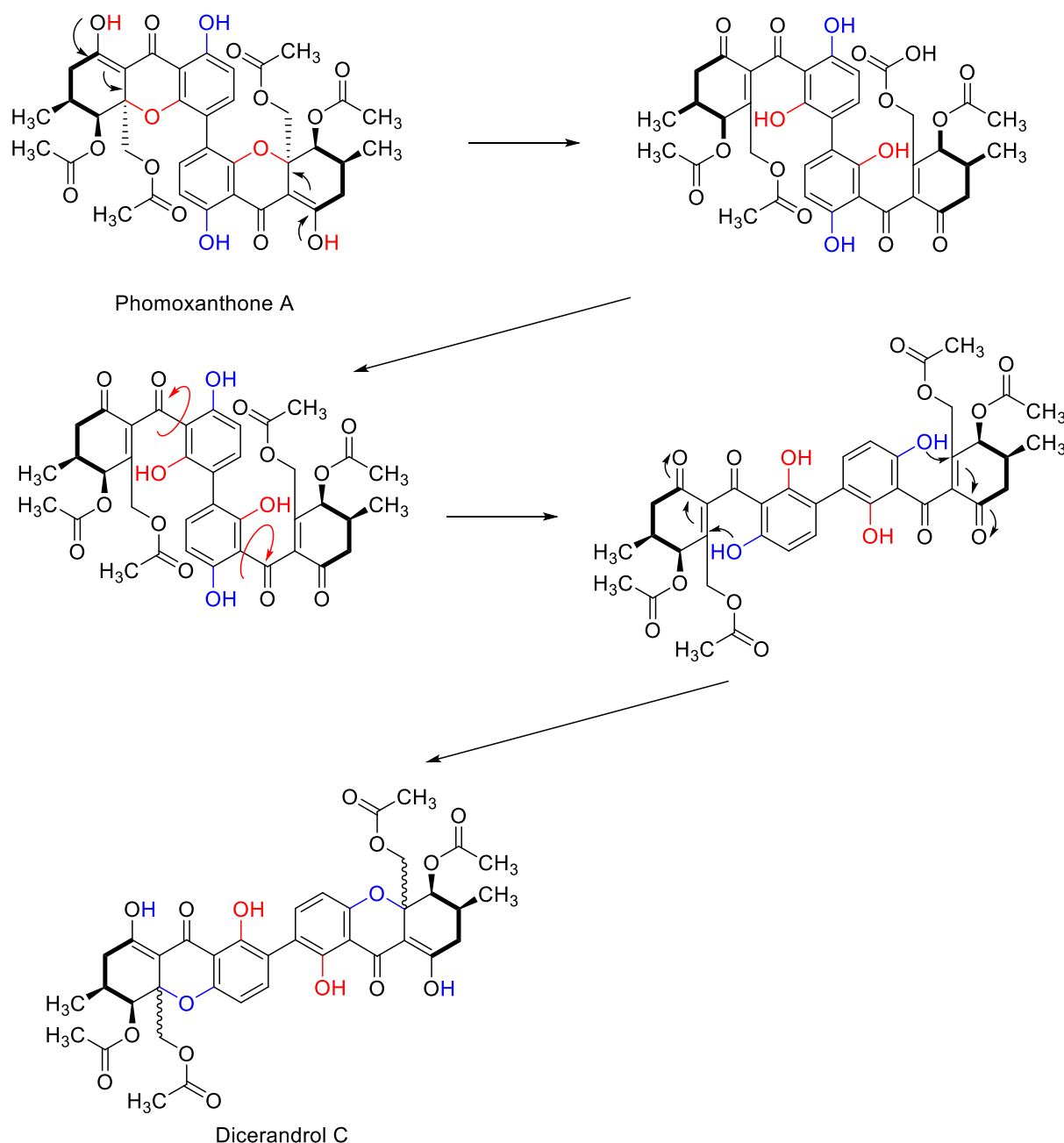
Figure 17: Putative rearrangement of PXA to dicerandrol C by retro-oxa-Michael reaction.

When investigating the structure activity relationship of PXA and its derivatives first steps were taken, after it was discovered, that acid hydrolysis leads to a fully deacetylated dimeric xanthone core with no cytotoxic activity (Isaka *et al.* 2001; Rönsberg *et al.* 2013). Through the process of incomplete acidic hydrolysis, 12- and 12, 12'-deacetyl PXA were produced. Both compounds were considerably less active against Ramos B- and Jurkat T-lymphocytes than PXA, but still retained some cytotoxic activity, while the 5,5',12,12' deacetyl PXA showed no

activity, implying that the 5- and 5'-acetyl moeity must be essential for the cytotoxic mode of action. To investigate the importance of the four hydroxyl moieties, acetylderivatives were prepared and tested. To generate different derivatives, an acetylation method using acetic anhydride and dry pyridine was used at room temperature (Bonner and McNamara 1968). The reaction was investigated after 1 h, 2 h, 6 h and 24 h via LCMS, showing mono- and di-acetylated products after 1 h and tri- and tetra-acetylated products after 2 h. Longer reaction times accumulate additional chromatographic peaks with identical molecular ion peaks, suggesting that rearrangement reactions take over. This was also observed without acetic anhydride by just subjecting PXA to pyridine for 24 hours. 1-Acetyl-, 1,1'-acetyl-, 1,1',8-acetyl- and 1,1,8,8'-acetyl-PXA were isolated and their cytotoxicity was determined. Interestingly, while no compound was more active than PXA, the cytotoxic activity only dropped by a factor of 3-4 for the various acetylated derivatives, regardless of the position of acetylation.This suggests that the free hydroxyl moieties only play a subordinate role, if any in PXA's mode of action. The possibility of *in vitro* ester hydrolysis was considered, however, standard methylation protocols with CH_3I and K_2CO_3 (Swaroop *et al.* 2012) failed due to compound decomposition and were thus abandoned. The dimeric structure is essential for the bioactivity (Cao *et al.* 2012) and rearangement of PXA (4, 4') to dicerandrol C (2, 2') decreases the activity considerably (Rönsberg *et al.* 2013). In conclusion, the 5/5'-acetyl moiety and the 4, 4' linkage are the most important structural parameters regarding the cytotoxicity of PXA, while hydroxyl moieties at positions 1,1',8 or 8' are chemically modifiable. The 12/12' acetyl moieties decrease cytotoxicity considerably, but may be modifiable. These findings may help in the future during target finding and drug optimization, because tracer or tag molecules may be linked to the less important hydroxyl moieties (Lomenick *et al.* 2011), or they may be substituted to improve overall stability of the xanthone core and to protect the biaryl linkage from rearrangement.
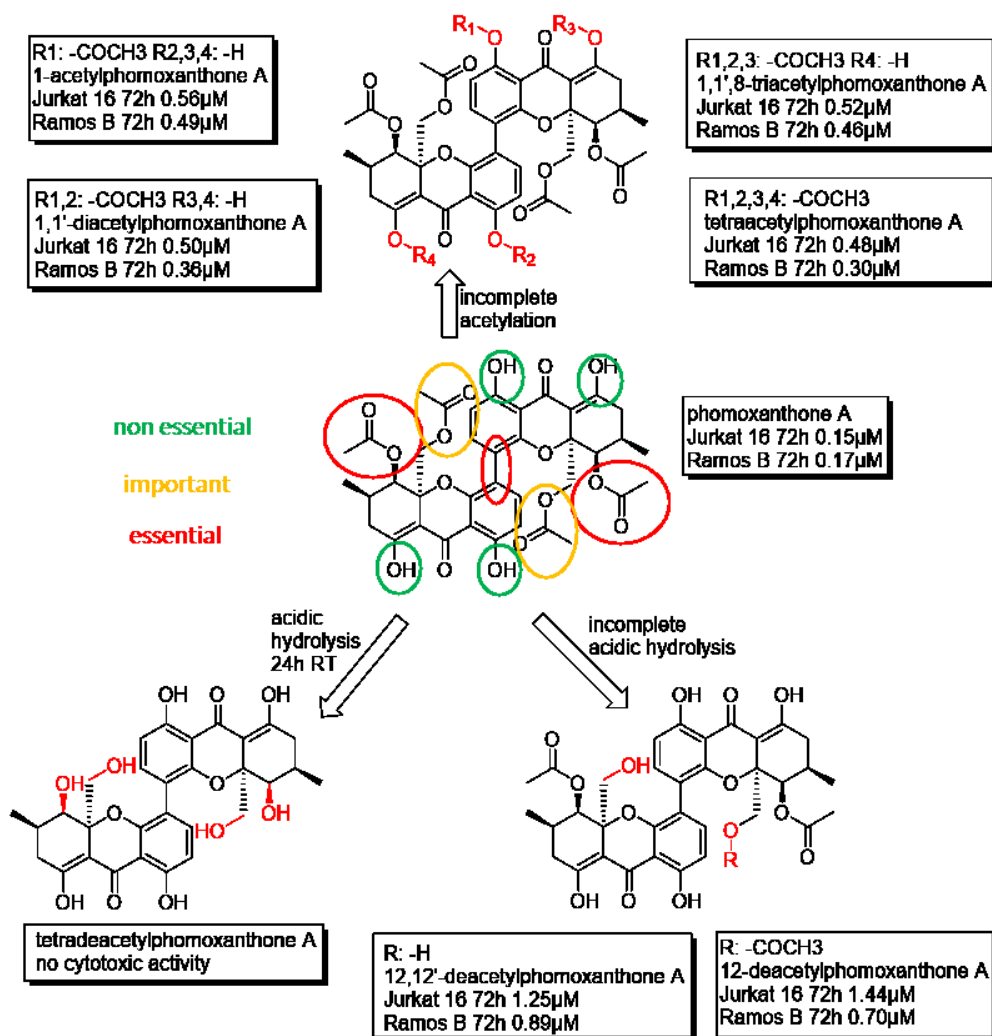
Figure 18: SAR of PXA-derivatives (modified after Frank *et al.* 2015).

Although the mode of action of the cytotoxic activity of PXA was studied extensively by our cooperation partners, the exact molecular targets remain elusive. However, due to its novel mode of action as a mitochondrial toxin (described in **chapter 3**), it could be used as a molecular tool in the study of mitochondrial ion homeostasis and membrane dynamics in the future (Böhler *et al.* 2018). By improving the instability and rearrangement issues and discovering a proper way to understand and deal with these issues, such problems can be avoided in the future and experiments and applications for this interesting natural compound can be planned accordingly. The selectivity for cancer cells will ensure that further investigations will be conducted and the SAR studies may inspire semisynthetic or synthetic analogs with better stability and traceability. With its toxicological and immunological properties, PXA represents an interesting candidate for the discovery of a new fungal anticancer drug.

Conclusion and Prospect

The results of this dissertation research show that it is still worthwhile to investigate marine fungi, even if a large collection of related research papers has already been published. The modification of culturing conditions (OSMAC and co-cultivation) diversified the metabolic profile, leading to the induction and the discovery of new bioactive secondary metabolites. The effects of simple changes in culturing conditions have yielded very specific results and thus future research on the same or similar fungal strains should not be discouraged, but should rather be encouraged to discover cryptic metabolites. The demand for new antibiotics and anticancer drugs is high and natural products have met that demand in the past. The investigation of cytotoxic fungal compounds, regarding mode of action, SAR and stability represents important work on the way to develop new anticancer drugs. Since fungal anticancer drugs are still underrepresented in the current drug market, they show great potential in the search for new lead compounds.

References (for Chapter 1 and 6)

Adachi, K. and Chiba, K. (2007) FTY720 story. Its discovery and the following accelerated development of sphingosine 1-phosphate receptor agonists as immunomodulators based on reverse pharmacology. *Perspectives in Medicinal Chemistry* **1**, 11–23.

Ahrens, E. H. (1976) The management of hyperlipidemia: whether, rather than how. *Annals of internal medicine* **85**, 87–93.

Alberts, A. W., Chen, J., Kuron, G., Hunt, V., Huff, J., Hoffman, C., Rothrock, J., Lopez, M., Joshua, H., Harris, E., Patchett, A., Monaghan, R., Currie, S., Stapley, E., Albers-Schonberg, G., Hensens, O., Hirshfield, J., Hoogsteen, K., Liesch, J. and Springer, J. (1980) Mevinolin: a highly potent competitive inhibitor of hydroxymethylglutaryl-coenzyme A reductase and a cholesterol-lowering agent. *Proceedings of the National Academy of Sciences of the United States of America* **77**, 3957–3961.

Allison, A. C. and Eugui, E. M. (2000) Mycophenolate mofetil and its mechanisms of action. *Immunopharmacology* **47**, 85–118.

Ames, B. D. and Walsh, C. T. (2010) Anthranilate-activating modules from fungal nonribosomal peptide assembly lines. *Biochemistry* **49**, 3351–3365.

Aminov, R. (2017) History of antimicrobial drug discovery: major classes and health impact. *Biochemical pharmacology* **133**, 4–19.

Aminov, R. I. (2010) A brief history of the antibiotic era: lessons learned and challenges for the future. *Frontiers in microbiology* **1**, (134) 1-7.

Amna, T., Puri, S. C., Verma, V., Sharma, J. P., Khajuria, R. K., Musarrat, J., Spiteller, M. and Qazi, G. N. (2006) Bioreactor studies on the endophytic fungus Entrophospora infrequens for the production of an anticancer alkaloid camptothecin. *Canadian journal of microbiology* **52**, 189–196.

Ancheeva, E., El-Neketi, M., Song, W., Lin, W., Daletos, G., Ebrahim, W. and Proksch, P. (2017) Structurally unprecedented metabolites from marine sponges. *Current Organic Chemistry* **21**, 426–449.

Ancheeva, E., Mándi, A., Király, S. B., Kurtán, T., Hartmann, R., Akone, S. H., Weber, H., Daletos, G. and Proksch, P. (2018) Chaetolines A and B, pyrano[3,2-f]isoquinoline alkaloids from cultivation of Chaetomium sp. in the presence of autoclaved Pseudomonas aeruginosa. *Journal of Natural Products* **81**, 2392–2398.

Anderson, R., Higgins Jr, H. M. and Pettinga, C. D. (1961) Symposium: how a drug is born. *Cincinnati Journal of Medicine* **42**, 49–60.

Badawy, A. A.-B. (2017) Kynurenine pathway of tryptophan metabolism: regulatory and functional aspects. *International Journal of Tryptophan Research* **10**, 1-20.

Baldry, M., Nielsen, A., Bojer, M. S., Zhao, Y., Friberg, C., Ifrah, D., Glasser Heede, N., Larsen, T. O., Frøkiær, H., Frees, D., Zhang, L., Dai, H. and Ingmer, H. (2016) Norlichexanthone reduces virulence gene expression and biofilm formation in Staphylococcus aureus. *PloS one* **11**, (e0168305) 1-16.

Balkovec, J. M., Hughes, D. L., Masurekar, P. S., Sable, C. A., Schwartz, R. E. and Singh, S. B. (2014) Discovery and development of first in class antifungal caspofungin (CANCIDAS®)--a case study. *Natural Product Reports* **31**, 15–34.

Barreiro, E. J., Fraga, C. A. M. and Lima, L. M. (2012) Natural products as lead compounds in medicinal chemistry. In *Plant Bioactives and Drug Discovery*; Cechinel-Filho V. (ed); Hoboken, NJ, USA: John Wiley & Sons Inc, **2012**, 81–126. ISBN 9780470582268

Beekman, A. M. and Barrow, R. A. (2014) Fungal metabolites as pharmaceuticals. *Australian Journal of Chemistry* **67**, 827-843.

Bergmann, S., Funk, A. N., Scherlach, K., Schroeckh, V., Shelest, E., Horn, U., Hertweck, C. and Brakhage, A. A. (2010) Activation of a silent fungal polyketide biosynthesis pathway through regulatory cross talk with a cryptic nonribosomal peptide synthetase gene cluster. *Applied and environmental microbiology* **76**, 8143–8149.

Bergmann, W. and Feeney, R. J. (1950) The Isolation of a new thymine pentoside from sponges. *Journal of the American Chemical Society* **72**, 2809–2810.

Biggs, B. W., Lim, C. G., Sagliani, K., Shankar, S., Stephanopoulos, G., Mey, M. de and Ajikumar, P. K. (2016) Overcoming heterologous protein interdependency to optimize P450-mediated taxol precursor synthesis in Escherichia coli. *Proceedings of the National Academy of Sciences of the United States of America* **113**, 3209–3214.

Blayney, D. W., Bazhenova, L., Lloyd, G. K., Huang, L. and Mohanlal, R. (2016) Plinabulin, a novel small molecule that ameliorates chemotherapy-induced neutropenia, is administered on the same day of chemotherapy and has anticancer efficacy. *Blood* **128**, 2508.

Blunt, J. W., Carroll, A. R., Copp, B. R., Davis, R. A., Keyzers, R. A. and Prinsep, M. R. (2018) Marine natural products. *Natural product reports* **35**, 8–53.

Bode, H. B., Bethe, B., Höfs, R. and Zeeck, A. (2002) Big effects from small changes: possible ways to explore nature's chemical diversity. *ChemBioChem* **3**, 619-627.

Böhler, P., Stuhldreier, F., Anand, R., Kondadi, A. K., Schlütermann, D., Berleth, N., Deitersen, J., Wallot-Hieke, N., Wu, W., Frank, M., Niemann, H., Wesbuer, E., Barbian, A., Luyten, T., Parys, J. B., Weidtkamp-Peters, S., Borchardt, A., Reichert, A. S., Peña-Blanco, A., García-Sáez, A. J., Itskanov, S., van der Bliek, A. M., Proksch, P., Wesselborg, S. and Stork, B. (2018) The mycotoxin phomoxanthone A disturbs the form and function of the inner mitochondrial membrane. *Cell death & disease* **9**, 286–302.

Bok, J. W., Chiang, Y.-M., Szewczyk, E., Reyes-Dominguez, Y., Davidson, A. D., Sanchez, J. F., Lo, H.-C., Watanabe, K., Strauss, J., Oakley, B. R., Wang, C. C. C. and Keller, N. P. (2009) Chromatin-level regulation of biosynthetic gene clusters. *Nature chemical biology* **5**, 462–464.

Bonner, T. G. and McNamara, P. (1968) The pyridine-catalysed acetylation of phenols and alcohols by acetic anhydride. *Journal of the Chemical Society B: Physical Organic*, 795.

Brotzu, G. (1948) Research on a new antibiotic. *Publications of the Cagliari Institute of Hygiene*, 5–19.

Bugni, T. S., Richards, B., Bhoite, L., Cimbora, D., Harper, M. K. and Ireland, C. M. (2008) Marine natural product libraries for high-throughput screening and rapid drug discovery. *Journal of Natural Products* **71**, 1095–1098.

Bye, A. and King, H. K. (1970) The biosynthesis of 4-hydroxycoumarin and dicoumarol by Aspergillus fumigatus Fresenius. *Biochemical Journal* **117**, 237–245.

Cao, S., McMillin, D. W., Tamayo, G., Delmore, J., Mitsiades, C. S. and Clardy, J. (2012) Inhibition of tumor cells interacting with stromal cells by xanthones isolated from a Costa Rican Penicillium sp. *Journal of Natural Products* **75**, 793–797.

Castilla-Guerra, L., Del Carmen Fernandez-Moreno, M. and Colmenero-Camacho, M. A. (2016) Statins in stroke prevention: present and future. *Current pharmaceutical design* **22**, 4638–4644.

Chávez, R., Fierro, F., García-Rico, R. O. and Vaca, I. (2015) Filamentous fungi from extreme environments as a promising source of novel bioactive secondary metabolites. *Frontiers in microbiology* **6**, (903) 1-7.

Chen, H., Daletos, G., Abdel-Aziz, M. S., Thomy, D., Dai, H., Brötz-Oesterhelt, H., Lin, W. and Proksch, P. (2015) Inducing secondary metabolite production by the soil-dwelling fungus Aspergillus terreus through bacterial co-culture. *Phytochemistry Letters* **12**, 35–41.

Chong, P. H., Seeger, J. D. and Franklin, C. (2001) Clinically relevant differences between the statins: implications for therapeutic selection. *The American journal of medicine* **111**, 390–400.

Chun, J. and Hartung, H.-P. (2010) Mechanism of action of oral fingolimod (FTY720) in multiple sclerosis. *Clinical neuropharmacology* **33**, 91–101.

Cooper, B., Meyer, J., and Euler, K. (1995). *Production of anthranilic acid by a strain of Bacillus subtillis resistant to sulfaguanidine and fluorotryptophan*, United States, BASF Aktiengesellschaft (Ludwigshafen, DE), US Patent 5422256.

Cormier, A., Knossow, M., Wang, C. and Gigant, B. (2010) The binding of vinca domain agents to tubulin. In: *Microtubules, in vitro;* Wilson L. and Correia J. J. (eds); Academic Press: London, UK, **2010**, 373–390. ISBN 9780123748157.

Dabydeen, D. A., Burnett, J. C., Bai, R., Verdier-Pinard, P., Hickford, S. J. H., Pettit, G. R., Blunt, J. W., Munro, M. H. G., Gussio, R. and Hamel, E. (2006) Comparison of the activities of the truncated halichondrin B analog NSC 707389 (E7389) with those of the parent compound and a proposed binding site on tubulin. *Molecular pharmacology* **70**, 1866–1875.

Daletos, G., Ebrahim, W., Ancheeva, E., El-Neketi, M., Lin, W. H. and Proksch, P. (2017) Microbial coculture and OSMAC approach as strategies to induce cryptic fungal biogenetic gene clusters. In: *Chemical biology of natural products;* Newman, D. J., Cragg, G. M., Grothaus, P. G. (eds); CRC Press: Boca Raton, FL, USA, **2017**, 233–284. ISBN 9781439841945.

Deivanai, S., Bindusara, A. S., Prabhakaran, G. and Bhore, S. J. (2014) Culturable bacterial endophytes isolated from mangrove tree (Rhizophora apiculata Blume) enhance seedling growth in rice. *Journal of natural science, biology, and medicine* **5**, 437–444.

Dolk, F. C. K., Pouwels, K. B., Smith, D. R. M., Robotham, J. V. and Smieszek, T. (2018) Antibiotics in primary care in England: which antibiotics are prescribed and for which conditions? *The Journal of antimicrobial chemotherapy* **73**, ii2-ii10.

Dreyfuss, M., Härri, E., Hofmann, H., Kobel, H., Pache, W. and Tscherter, H. (1976) Cyclosporin A and C. *European journal of applied microbiology and biotechnology* **3**, 125–133.

Duplessis, C. and Crum-Cianflone, N. F. (2011) Ceftaroline: A new cephalosporin with activity against methicillin-resistant Staphylococcus aureus (MRSA). *Clinical medicine reviews in therapeutics* **3**, (a2466) 1-24.

El-Neketi, M., Ebrahim, W., Lin, W., Gedara, S., Badria, F., Saad, H.-E. A., Lai, D. and Proksch, P. (2013) Alkaloids and polyketides from Penicillium citrinum, an endophyte isolated from the Moroccan plant Ceratonia siliqua. *Journal of Natural Products* **76**, 1099–1104.

Elsässer, B., Krohn, K., Flörke, U., Root, N., Aust, H.-J., Draeger, S., Schulz, B., Antus, S. and Kurtán, T. (2005) X-ray Structure Determination, Absolute Configuration and Biological Activity of Phomoxanthone A. *European Journal of Organic Chemistry* **2005**, 4563–4570.

Endo, A., Kuroda, M. and Tsujita, Y. (1976) ML-236A, ML-236B, and ML-236C, new inhibitors of cholesterogensis produced by Penicillium citrinum. *The Journal of Antibiotics* **29**, 1346–1348.

Erdoğrul, Ö. and Azirak, S. (2004) Review of the studies on the red yeast rice (Monascus purpureus). *Turkish Electronic Journal of Biotechnology* **2**, 37–49.

Evidente, A., Kornienko, A., Cimmino, A., Andolfi, A., Lefranc, F., Mathieu, V. and Kiss, R. (2014) Fungal metabolites with anticancer activity. *Natural Product Reports* **31**, 617–627.

Fanelli, F., Reveglia, P., Masi, M., Mulè, G., Zonno, M. C., Cimmino, A., Vurro, M. and Evidente, A. (2017) Influence of light on the biosynthesis of ophiobolin A by Bipolaris maydis. *Natural Product Research* **31**, 909–917.

Fleming, A. (1929) On the antibacterial action of cultures of a Penicillium, with special reference to their use in the isolation of B. influenae. *British Journal of Experimental Pathology* **10**, 226–236.

Frank, M., Niemann, H., Böhler, P., Stork, B., Wesselborg, S., Lin, W. and Proksch, P. (2015) Phomoxanthone A - from mangrove forests to anticancer therapy. *Current Medicinal Chemistry* **22**, 3523–3532.

Frey-Klett, P., Burlinson, P., Deveau, A., Barret, M., Tarkka, M. and Sarniguet, A. (2011) Bacterial-fungal interactions: hyphens between agricultural, clinical, environmental, and food microbiologists. *Microbiology and Molecular Biology Reviews* **75**, 583–609.

Fujita, T., Inoue, K., Yamamoto, S., Ikumoto, T., Sasaki, S., Toyama, R., Chiba, K., Hoshino, Y. and Okumoto, T. (1994) Fungal metabolites. Part 11. a potent immunosuppressive activity found in Isaria sinclairii metabolite. *The Journal of Antibiotics* **47**, 208–215.

Gangadevi, V. and Muthumary, J. (2007) Taxol, an anticancer drug produced by an endophytic fungus Bartalinia robillardoides Tassi, isolated from a medicinal plant, Aegle

marmelos Correa ex Roxb. *World Journal of Microbiology and Biotechnology* **24**, 717–724.

Gomes, N. G. M., Lefranc, F., Kijjoa, A. and Kiss, R. (2015) Can Some Marine-Derived Fungal Metabolites Become Actual Anticancer Agents? *Marine drugs* **13**, 3950–3991.

Gosio, B. (1893) Contributo all'etiologia della pellagra; ricerche chimiche e batteriologiche sulle alterazioni del mais. *Giornale della Reale Accademia di Medicina di Torino* **56**, 484–487.

Gu, J., Gui, Y., Chen, L., Yuan, G., Lu, H.-Z. and Xu, X. (2013) Use of natural products as chemical library for drug discovery and network pharmacology. *PloS one* **8**, (e62839) 1-10.

Guo, B., Li, H. and Zhang, L. (1998) Isolation of an fungus producting Vinblastine. *Journal of Yunnan University (Natural Sciences)* **20**, 214–215.

Hardoim, P. R., van Overbeek, L. S., Berg, G., Pirttilä, A. M., Compant, S., Campisano, A., Döring, M. and Sessitsch, A. (2015) The Hidden World within Plants: Ecological and Evolutionary Considerations for Defining Functioning of Microbial Endophytes. *Microbiology and Molecular Biology Reviews* **79**, 293–320.

Henry, K. M. and Townsend, C. A. (2005) Ordering the reductive and cytochrome P450 oxidative steps in demethylsterigmatocystin formation yields general insights into the biosynthesis of aflatoxin and related fungal metabolites. *Journal of the American Chemical Society* **127**, 3724–3733.

Hentzer, M. and Givskov, M. (2003) Pharmacological inhibition of quorum sensing for the treatment of chronic bacterial infections. *The Journal of Clinical Investigation* **112**, 1300–1307.

Hirata, Y. and Uemura, D. (1986) Halichondrins - antitumor polyether macrolides from a marine sponge. *Pure and Applied Chemistry* **58**, 701–710.

Horwitz, S. B. (1994) Taxol (paclitaxel): mechanisms of action. *Annals of Oncology* **5**, (Suppl 6) 3-6.

Huang, S., Ding, W., Li, C. and Cox, D. G. (2014) Two new cyclopeptides from the co-culture broth of two marine mangrove fungi and their antifungal activity. *Pharmacognosy Magazine* **10**, 410–414.

Hussain, A., Rather, M. A., Dar, M. S., Aga, M. A., Ahmad, N., Manzoor, A., Qayum, A., Shah, A., Mushtaq, S. and Ahmad, Z. (2017) Novel bioactive molecules from Lentzea

violacea strain AS 08 using one strain-many compounds (OSMAC) approach. *Bioorganic & Medicinal Chemistry Letters* **27**, 2579–2582.

Husted, S. E., Ziegler, B. K. and Kher, A. (2006) Long-term anticoagulant therapy in patients with coronary artery disease. *European Heart Journal* **27**, 913–919.

Huttanus, H. M., Sheng, J. and Feng, X. (2016) Metabolic engineering for production of small molecule drugs: challenges and solutions. *Fermentation* **2**, (4) 1-16.

Hütter, R. and DeMoss, J. A. (1967) Organization of the tryptophan pathway: a phylogenetic study of the fungi. *Journal of Bacteriology* **94**, 1896–1907.

Isaka, M., Jaturapat, A., Rukseree, K., Danwisetkanjana, K., Tanticharoen, M. and Thebtaranonth, Y. (2001) Phomoxanthones A and B, Novel Xanthone Dimers from the Endophytic Fungus Phomopsis Species. *Journal of Natural Products* **64**, 1015–1018.

Jelić, D. and Antolović, R. (2016) From Erythromycin to Azithromycin and New Potential Ribosome-Binding Antimicrobials. *Antibiotics* **5**, (29) 1-13.

Jeon, J., Choi, J., Lee, G.-W., Park, S.-Y., Huh, A., Dean, R. A. and Lee, Y.-H. (2015) Genome-wide profiling of DNA methylation provides insights into epigenetic regulation of fungal development in a plant pathogenic fungus, Magnaporthe oryzae. *Scientific Reports* **5**, 8567–8577.

Johnson, I. (1983) Human insulin from recombinant DNA technology. *Science* **219**, 632–637.

Jozala, A. F., Geraldes, D. C., Tundisi, L. L., Feitosa, V. d. A., Breyer, C. A., Cardoso, S. L., Mazzola, P. G., Oliveira-Nascimento, L. d., Rangel-Yagui, C. d. O., Magalhães, P. d. O., Oliveira, M. A. d. and Pessoa, A. (2016) Biopharmaceuticals from microorganisms: from production to purification. *Brazilian Journal of Microbiology* **47 Suppl 1**, 51–63.

Junker, B. (2000) Fermentation. In *Encyclopedia of Chemical Technology*; Othmer, K. (ed), Hoboken, NJ, USA: John Wiley & Sons, Inc. **2000**, 11. ISBN 9780471484943

Kahan, J. S., Kahan, F. M., Goegelman, R., Currie, S. A., Jackson, M., Stapley, E. O., Miller, T. W., Miller, A. K., Hendlin, D., Mochales, S., Hernandez, S., Woodruff, H. B. and Birnbaum, J. (1979) Thienamycin, a new beta-lactam antibiotic. I. Discovery, taxonomy, isolation and physical properties. *The Journal of Antibiotics* **32**, 1–12.

Kanoh, K., Kohno, S., Asari, T., Harada, T., Katada, J., Muramatsu, M., Kawashima, H., Sekiya, H. and Uno, I. (1997) (−)-Phenylahistin: A new mammalian cell cycle inhibitor produced by aspergillus ustus. *Bioorganic & Medicinal Chemistry Letters* **7**, 2847–2852.

Kharwar, R. N., Mishra, A., Gond, S. K., Stierle, A. and Stierle, D. (2011) Anticancer compounds derived from fungal endophytes: their importance and future challenges. *Natural Product Reports* **28**, 1208–1228.

Kong, K.-F., Vuong, C. and Otto, M. (2006) Staphylococcus quorum sensing in biofilm formation and infection. *International Journal of Medical Microbiology* **296**, 133–139.

König, C. C., Scherlach, K., Schroeckh, V., Horn, F., Nietzsche, S., Brakhage, A. A. and Hertweck, C. (2013) Bacterium induces cryptic meroterpenoid pathway in the pathogenic fungus Aspergillus fumigatus. *ChemBioChem* **14**, 938–942.

Kornienko, A., Evidente, A., Vurro, M., Mathieu, V., Cimmino, A., Evidente, M., van Otterlo, W. A. L., Dasari, R., Lefranc, F. and Kiss, R. (2015) Toward a Cancer Drug of Fungal Origin. *Medicinal Research Reviews* **35**, 937–967.

Kunert, R. and Casanova, E. (2013) Recent advances in recombinant protein production: BAC-based expression vectors, the bigger the better. *Bioengineered* **4**, 258–261.

Lahlou, M. (2013) The Success of Natural Products in Drug Discovery. *Pharmacology & Pharmacy* **04**, 17–31.

Law, M. R., Wald, N. J. and Rudnicka, A. R. (2003) Quantifying effect of statins on low density lipoprotein cholesterol, ischaemic heart disease, and stroke: systematic review and meta-analysis. *British Medical Journal)* **326**, 1423 - 1427.

Le Norcy, T., Niemann, H., Proksch, P., Linossier, I., Vallée-Réhel, K., Hellio, C. and Faÿ, F. (2017) Anti-Biofilm Effect of Biodegradable Coatings Based on Hemibastadin Derivative in Marine Environment. *International Journal of Molecular Sciences* **18**, 1520–1538.

Le Pogam, P. and Boustie, J. (2016) Xanthones of Lichen Source: A 2016 Update. *Molecules* **21**, 294–324.

Letscher-Bru, V. (2003) Caspofungin: the first representative of a new antifungal class. *Journal of Antimicrobial Chemotherapy* **51**, 513–521.

Li, C.-S., Li, X.-M., Gao, S.-S., Lu, Y.-H. and Wang, B.-G. (2013) Cytotoxic anthranilic acid derivatives from deep sea sediment-derived fungus Penicillium paneum SD-44. *Marine Drugs* **11**, 3068–3076.

Li, J.-L., Sun, X., Chen, L. and Guo, L.-D. (2016) Community structure of endophytic fungi of four mangrove species in Southern China. *Mycology* **7**, 180–190.

Liu, J., Gu, B., Yang, L., Yang, F. and Lin, H. (2018) New Anti-inflammatory Cyclopeptides From a Sponge-Derived Fungus Aspergillus violaceofuscus. *Frontiers in Chemistry* **6**, (226) 1-8.

Liu, S., Dai, H., Heering, C., Janiak, C., Lin, W., Liu, Z. and Proksch, P. (2017a) Inducing new secondary metabolites through co-cultivation of the fungus Pestalotiopsis sp. with the bacterium Bacillus subtilis. *Tetrahedron Letters* **58**, 257–261.

Liu, Y., Chen, S., Liu, Z., Lu, Y., Xia, G., Liu, H., He, L. and She, Z. (2015) Bioactive Metabolites from Mangrove Endophytic Fungus Aspergillus sp. 16-5B. *Marine Drugs* **13**, 3091–3102.

Liu, Y., Stuhldreier, F., Kurtán, T., Mándi, A., Arumugam, S., Lin, W., Stork, B., Wesselborg, S., Weber, H., Henrich, B., Daletos, G. and Proksch, P. (2017b) Daldinone derivatives from the mangrove-derived endophytic fungus Annulohypoxylon sp. *RSC Advances* **7**, 5381–5393.

Lobanovska, M. and Pilla, G. (2017) Penicillin's Discovery and Antibiotic Resistance: Lessons for the Future? *The Yale Journal of Biology and Medicine* **90**, 135–145.

Lomenick, B., Olsen, R. W. and Huang, J. (2011) Identification of direct protein targets of small molecules. *ACS Chemical Biology* **6**, 34–46.

MacMillan, J. (1954) Griseofulvin. Part IX. Isolation of the bromo-analogue from Penicillium griseofulvum and Penicillium nigricans. *Journal of the Chemical Society (Resumed)*, 2585–2587.

Maertens, J. A. (2004) History of the development of azole derivatives. *Clinical microbiology and infection: the official publication of the European Society of Clinical Microbiology and Infectious Diseases* **10**, (Suppl 1) 1–10.

Marmann, A., Aly, A. H., Lin, W., Wang, B. and Proksch, P. (2014) Co-cultivation—a powerful emerging tool for enhancing the chemical diversity of microorganisms. *Marine Drugs* **12**, 1043–1065.

Martins, A., Vieira, H., Gaspar, H. and Santos, S. (2014) Marketed marine natural products in the pharmaceutical and cosmeceutical industries: tips for success. *Marine Drugs* **12**, 1066–1101.

Masters, K.-S. and Bräse, S. (2012) Xanthones from fungi, lichens, and bacteria: the natural products and their synthesis. *Chemical Reviews* **112**, 3717–3776.

Matsuda, S. and Koyasu, S. (2000) Mechanisms of action of cyclosporine. *Immunopharmacology* **47**, 119–125.

Matsuzaki, K., Tahara, H., Inokoshi, J., Tanaka, H., Masuma, R. and Omura, S. (1998) New brominated and halogen-less derivatives and structure-activity relationship of azaphilones inhibiting gp120-CD4 binding. *The Journal of Antibiotics* **51**, 1004–1011.

McGovern, P. E., Zhang, J., Tang, J., Zhang, Z., Hall, G. R., Moreau, R. A., Nuñez, A., Butrym, E. D., Richards, M. P., Wang, C.-S., Cheng, G., Zhao, Z. and Wang, C. (2004) Fermented beverages of pre- and proto-historic China. *Proceedings of the National Academy of Sciences of the United States of America* **101**, 17593–17598.

Meng, L.-H., Li, X.-M., Liu, Y., Xu, G.-M. and Wang, B.-G. (2017) Antimicrobial alkaloids produced by the mangrove endophyte Penicillium brocae MA-231 using the OSMAC approach. *RSC Advances* **7**, 55026–55033.

Montastruc, J. L., Rascol, O. and Senard, J. M. (1993) Current status of dopamine agonists in Parkinson's disease management. *Drugs* **46**, 384–393.

Munday, C. W. (1949) Tautomerism of Penicillic Acid. *Nature* **163**, 443–444.

Najafpour, G. D. (2007) Production of Antibiotics. In *Biochemical Engineering and Biotechnology*; Najafpour, G. D. (ed); Elsevier Science: Amsterdam, NL (2007) 263–279. ISBN 9780444528452

Nelson, M. L. and Levy, S. B. (2011) The history of the tetracyclines. *Annals of the New York Academy of Sciences* **1241**, 17–32.

Netzker, T., Fischer, J., Weber, J., Mattern, D. J., König, C. C., Valiante, V., Schroeckh, V. and Brakhage, A. A. (2015) Microbial communication leading to the activation of silent fungal secondary metabolite gene clusters. *Frontiers in Microbiology* **6**, 299.

Neubauer, P. R., Widmann, C., Wibberg, D., Schröder, L., Frese, M., Kottke, T., Kalinowski, J., Niemann, H. H. and Sewald, N. (2018) A flavin-dependent halogenase from metagenomic analysis prefers bromination over chlorination. *PloS one* **13**, e0196797.

Newman, D. J. and Cragg, G. M. (2007) Natural products as sources of new drugs over the last 25 years. *Journal of Natural Products* **70**, 461–477.

Newman, D. J. and Cragg, G. M. (2016) Natural Products as Sources of New Drugs from 1981 to 2014. *Journal of Natural Products* **79**, 629–661.

Nicoletti, R., Lopez-Gresa, M. P., Manzo, E., Carella, A. and Ciavatta, M. L. (2007) Production and fungitoxic activity of Sch 642305, a secondary metabolite of Penicillium canescens. *Mycopathologia* **163**, 295–301.

Nonaka, K., Chiba, T., Suga, T., Asami, Y., Iwatsuki, M., MASUMA, R., Ōmura, S. and Shiomi, K. (2015) Coculnol, a new penicillic acid produced by a coculture of Fusarium solani FKI-6853 and Talaromyces sp. FKA-65. *The Journal of Antibiotics* **68**, 530–532.

Nützmann, H.-W., Reyes-Dominguez, Y., Scherlach, K., Schroeckh, V., Horn, F., Gacek, A., Schümann, J., Hertweck, C., Strauss, J. and Brakhage, A. A. (2011) Bacteria-induced

natural product formation in the fungus Aspergillus nidulans requires Saga/Ada-mediated histone acetylation. *Proceedings of the National Academy of Sciences of the United States of America* **108**, 14282–14287.

Nyfeler, R. and Keller-Schierlein, W. (1974) Stoffwechselprodukte von Mikroorganismen 143. Mitteilung. Echinocandin B, ein neuartiges polypeptid-antibioticum aus Aspergillus nidulans var. echinulatus: isolierung und bausteine. *Helvetica Chimica Acta* **57**, 2459–2477.

Oh, D.-C., Jensen, P. R., Kauffman, C. A. and Fenical, W. (2005) Libertellenones A-D: induction of cytotoxic diterpenoid biosynthesis by marine microbial competition. *Bioorganic & medicinal chemistry* **13**, 5267–5273.

Okada, B. K. and Seyedsayamdost, M. R. (2017) Antibiotic dialogues: induction of silent biosynthetic gene clusters by exogenous small molecules. *FEMS Microbiology Reviews* **41**, 19–33.

Ola, A. R. B., Thomy, D., Lai, D., Brötz-Oesterhelt, H. and Proksch, P. (2013) Inducing Secondary Metabolite Production by the Endophytic Fungus Fusarium tricinctum through Coculture with Bacillus subtilis. *Journal of Natural Products* **76**, 2094–2099.

Osinga, Tramper and Wijffels (1999) Cultivation of Marine Sponges. *Marine Biotechnology* **1**, 509–532.

Oxford, A. E., Raistrick, H. and Simonart, P. (1939) Studies in the biochemistry of micro-organisms: Griseofulvin, C17H17O6Cl, a metabolic product of Penicillium griseo-fulvum Dierckx. *Biochemical Journal* **33**, 240–248.

Özkaya, F. C., Ebrahim, W., El-Neketi, M., Tansel Tanrıkul, T., Kalscheuer, R., Müller, W. E. G., Guo, Z., Zou, K., Liu, Z. and Proksch, P. (2018) Induction of new metabolites from sponge-associated fungus Aspergillus carneus by OSMAC approach. *Fitoterapia* **131**, 9–14.

Parry, R., Nishino, S. and Spain, J. (2011) Naturally-occurring nitro compounds. *Natural Product Reports* **28**, 152–167.

Patil, A. and Majumdar, S. (2017) Echinocandins in antifungal pharmacotherapy. *The Journal of Pharmacy and Pharmacology* **69**, 1635–1660.

Patridge, E., Gareiss, P., Kinch, M. S. and Hoyer, D. (2016) An analysis of FDA-approved drugs: natural products and their derivatives. *Drug Discovery Today* **21**, 204–207.

Pavão, G. B., Venâncio, V. P., Oliveira, A. L. L. de, Hernandes, L. C., Almeida, M. R., Antunes, L. M. G. and Debonsi, H. M. (2016) Differential genotoxicity and cytotoxicity of

phomoxanthone A isolated from the fungus Phomopsis longicolla in HL60 cells and peripheral blood lymphocytes. *Toxicology in vitro* **37**, 211–217.

Percival, S. L., Suleman, L., Vuotto, C. and Donelli, G. (2015) Healthcare-associated infections, medical devices and biofilms: risk, tolerance and control. *Journal Of Medical Microbiology* **64**, 323–334.

Proksch, P., Ebel, R., Edrada, R., Riebe, F., Liu, H., Diesel, A., Bayer, M., Li, X., Han Lin, W., Grebenyuk, V., Müller, W. E.G., Draeger, S., Zuccaro, A. and Schulz, B. (2008) Sponge-associated fungi and their bioactive compounds: the Suberites case. *Botanica Marina* **51**, 196.

Prompanya, C., Fernandes, C., Cravo, S., Pinto, M. M. M., Dethoup, T., Silva, A. M. S. and Kijjoa, A. (2015) A new cyclic hexapeptide and a new isocoumarin derivative from the marine sponge-associated fungus Aspergillus similanensis KUFA 0013. *Marine Drugs* **13**, 1432–1450.

Prosser, J. I. and Tough, A. J. (1991) Growth mechanisms and growth kinetics of filamentous microorganisms. *Critical Reviews in Biotechnology* **10**, 253–274.

Qin, C., Lin, X., Lu, X., Wan, J., Zhou, X., Liao, S., Tu, Z., Xu, S. and Liu, Y. (2015a) Sesquiterpenoids and xanthones derivatives produced by sponge-derived fungus Stachybotry sp. HH1 ZSDS1F1-2. *The Journal of Antibiotics* **68**, 121–125.

Qin, T., Iwata, T., Ransom, T. T., Beutler, J. A. and Porco, J. A. (2015b) Syntheses of Dimeric Tetrahydroxanthones with Varied Linkages: Investigation of "Shapeshifting" Properties. *Journal of the American Chemical Society* **137**, 15225–15233.

Quezada, M., Shang, Z., Kalansuriya, P., Salim, A. A., Lacey, E. and Capon, R. J. (2017) Waspergillamide A, a Nitro depsi-Tetrapeptide Diketopiperazine from an Australian Mud Dauber Wasp-Associated Aspergillus sp. (CMB-W031). *Journal of Natural Products* **80**, 1192–1195.

Rahbæk, L. and Breinholt, J. (1999) Circumdatins D, E, and F: further fungal benzodiazepine analogues from aspergillus ochraceus. *Journal of Natural Products* **62**, 904–905.

Rahbæk, L., Breinholt, J., Frisvad, J. C. and Christophersen, C. (1999) Circumdatin A, B, and C: Three New Benzodiazepine Alkaloids Isolated from a Culture of the Fungus Aspergillus ochraceus. *The Journal of Organic Chemistry* **64**, 1689–1692.

Rahman, M. (2013) Medical Applications of Fermentation Technology. *Advanced Materials Research* **810**, 127–157.

Ralston, Alma Payne, 1900- (1970). *The cleere observer: a biography of Antoni van Leeuwenhoek; illustrated by Charles Pickard*, London: Macmillan.

Rasmussen, T. B. and Givskov, M. (2006) Quorum-sensing inhibitors as anti-pathogenic drugs. *International Journal of Medical Microbiology* **296**, 149–161.

Rateb, M. E. and Ebel, R. (2011) Secondary metabolites of fungi from marine habitats. *Natural Product Reports* **28**, 290–344.

Ratnaweera, P. B., Silva, E. D. de, Williams, D. E. and Andersen, R. J. (2015) Antimicrobial activities of endophytic fungi obtained from the arid zone invasive plant Opuntia dillenii and the isolation of equisetin, from endophytic Fusarium sp. *BMC Complementary and Alternative Medicine* **15**, (220) 1-7.

Reen, F. J., Romano, S., Dobson, A. D. W. and O'Gara, F. (2015) The Sound of Silence: Activating Silent Biosynthetic Gene Clusters in Marine Microorganisms. *Marine Drugs* **13**, 4754–4783.

Romano, S., Jackson, S. A., Patry, S. and Dobson, A. D. W. (2018) Extending the "One Strain Many Compounds" (OSMAC) Principle to Marine Microorganisms. *Marine Drugs* **16**, (244) 1-29.

Rönsberg, D., Debbab, A., Mándi, A., Vasylyeva, V., Böhler, P., Stork, B., Engelke, L., Hamacher, A., Sawadogo, R., Diederich, M., Wray, V., Lin, W., Kassack, M. U., Janiak, C., Scheu, S., Wesselborg, S., Kurtán, T., Aly, A. H. and Proksch, P. (2013) Pro-apoptotic and immunostimulatory tetrahydroxanthone dimers from the endophytic fungus Phomopsis longicolla. *The Journal of Organic Chemistry* **78**, 12409–12425.

Roullier, C., Bertrand, S., Blanchet, E., Peigné, M., Du Robiou Pont, T., Guitton, Y., Pouchus, Y. F. and Grovel, O. (2016) Time Dependency of Chemodiversity and Biosynthetic Pathways: An LC-MS Metabolomic Study of Marine-Sourced Penicillium. *Marine Drugs* **14**, (103) 1-15.

Sato, M., Winter, J. M., Kishimoto, S., Noguchi, H., Tang, Y. and Watanabe, K. (2016) Combinatorial Generation of Chemical Diversity by Redox Enzymes in Chaetoviridin Biosynthesis. *Organic Letters* **18**, 1446–1449.

Schatz, A., Bugle, E. and Waksman, S. A. (1944) Streptomycin, a Substance Exhibiting Antibiotic Activity Against Gram-Positive and Gram-Negative Bacteria. *Proceedings of the Society for Experimental Biology and Medicine* **55**, 66–69.

Schmidt-Heydt, M., Graf, E., Stoll, D. and Geisen, R. (2012) The biosynthesis of ochratoxin A by Penicillium as one mechanism for adaptation to NaCl rich foods. *Food microbiology* **29**, 233–241.

Schroeckh, V., Scherlach, K., Nützmann, H.-W., Shelest, E., Schmidt-Heck, W., Schuemann, J., Martin, K., Hertweck, C. and Brakhage, A. A. (2009) Intimate bacterial–fungal interaction triggers biosynthesis of archetypal polyketides in Aspergillus nidulans. *Proceedings of the National Academy of Sciences of the United States of America* **106**, 14558–14563.

Sekiguchi, J., Katayama, S. and Yamada, Y. (1987) 6-Methyl-1,2,4-benzenetriol, a new intermediate in penicillic acid biosynthesis in Penicillium cyclopium. *Applied and Environmental Microbiology* **53**, 1531–1535.

Sensi, P., Margalith, P. and Timbal, M. T. (1959) Rifomycin, a new antibiotic; preliminary report. *Il Farmaco; Edizione Scientifica* **14**, 146-147.

Sharma, R. and Jangid, K. (2015) Fungal Quorum Sensing Inhibitors. In *Quorum Sensing vs Quorum Quenching: A Battle with No End in Sight*; Kalia V. C. (ed); New Delhi: Springer India, **2015**, 237–257. ISBN 9788132219828

Shen, B. (2015) A New Golden Age of Natural Products Drug Discovery. *Cell* **163**, 1297–1300.

Silverman Kitchin, J. E., Pomeranz, M. K., Pak, G., Washenik, K. and Shupack, J. L. (1997) Rediscovering mycophenolic acid: A review of its mechanism, side effects, and potential uses. *Journal of the American Academy of Dermatology* **37**, 445–449.

Singh, A. V., Bandi, M., Raje, N., Richardson, P., Palladino, M. A., Chauhan, D. and Anderson, K. C. (2011) A novel vascular disrupting agent plinabulin triggers JNK-mediated apoptosis and inhibits angiogenesis in multiple myeloma cells. *Blood* **117**, 5692–5700.

Slock, J., Stahly, D. P., Han, C. Y., Six, E. W. and Crawford, I. P. (1990) An apparent Bacillus subtilis folic acid biosynthetic operon containing pab, an amphibolic trpG gene, a third gene required for synthesis of para-aminobenzoic acid, and the dihydropteroate synthase gene. *Journal of Bacteriology* **172**, 7211–7226.

Smith, E. B. (1990) History of antifungals. *Journal of the American Academy of Dermatology* **23**, 776–778.

Stancu, C. and Sima, A. (2001) Statins: mechanism of action and effects. *Journal of Cellular and Molecular Medicine* **5**, 378–387.

Stander, M. A., Steyn, P. S., Lübben, A., Miljkovic, A., Mantle, P. G. and Marais, G. J. (2000) Influence of Halogen Salts on the Production of the Ochratoxins by Aspergillusochraceus Wilh. *Journal of Agricultural and Food Chemistry* **48**, 1865–1871.

Stierle, A., Strobel, G. and Stierle, D. (1993) Taxol and taxane production by Taxomyces andreanae, an endophytic fungus of Pacific yew. *Science* **260**, 214–216.

Stone, J. K., Bacon, C. W. and White Jr, J. F. (2000) An overview of endophytic microbes: endophytism defined. In *Microbial endophytes*; Bacon, C. W. and White Jr, J. F. (eds); CRC Press: Boca Raton, FL, USA, **2000**, 17–44. ISBN 9780824788315

Swaroop, P. S., Raut, G. N., Gonnade, R. G., Verma, P., Gokhale, R. S. and Reddy, D. S. (2012) Antituberculosis agent diaportheone B: synthesis, absolute configuration assignment, and anti-TB activity of its analogues. *Organic & Biomolecular Chemistry* **10**, 5385–5394.

Swift, S., Bainton, N. J. and Winson, M. K. (1994) Gram-negative bacterial communication by N-acyl homoserine lactones: a universal language? *Trends in Microbiology* **2**, 193–198.

Sykes, R. B. and Bonner, D. P. (1985) Discovery and development of the monobactams. *Reviews of Infectious Diseases* **7**, (Suppl 4) 579-593.

Tang, C. M., Smith, J. M., Arst, H. N. and Holden, D. W. (1994) Virulence studies of Aspergillus nidulans mutants requiring lysine or p-aminobenzoic acid in invasive pulmonary aspergillosis. *Infection and Immunity* **62**, 5255–5260.

Teponno, R. B., Noumeur, S. R., Helaly, S. E., Hüttel, S., Harzallah, D. and Stadler, M. (2017) Furanones and Anthranilic Acid Derivatives from the Endophytic Fungus Dendrothyrium variisporum. *Molecules* **22**, 1674.

ter Schure, E. G., van Riel, N. A. and Verrips, C. T. (2000) The role of ammonia metabolism in nitrogen catabolite repression in Saccharomyces cerevisiae. *FEMS Microbiology Reviews* **24**, 67–83.

Thorarensen, A., Li, J., Wakefield, B. D., Romero, D. L., Marotti, K. R., Sweeney, M. T., Zurenko, G. E. and Sarver, R. W. (2007) Preparation of novel anthranilic acids as antibacterial agents: extensive evaluation of structural and physical properties on antibacterial activity and human serum albumin affinity. *Bioorganic & Medicinal Chemistry Letters* **17**, 3113–3116.

Tobert, J. A. (2003) Lovastatin and beyond: the history of the HMG-CoA reductase inhibitors. *Nature Reviews Drug Discovery* **2**, 517-526.

Tomlinson, P. B. (2016). *The botany of mangroves*; Tomlinson, P. B. (ed); Cambridge University Press, Cambridge, UK, **2016**. ISBN 1107080673

Vandamme, E. J. (1992) Production of vitamins, coenzymes and related biochemicals by biotechnological processes. *Journal of Chemical Technology and Biotechnology* **53**, 313–327.

Wainwright, M. (1989) Moulds in Folk Medicine. *Folklore* **100**, 162–166.

Wang, F.-Z., Wei, H.-J., Zhu, T.-J., Li, D.-H., Lin, Z.-J. and Gu, Q.-Q. (2011a) Three new cytochalasins from the marine-derived fungus Spicaria elegans KLA03 by supplementing the cultures with L- and D-tryptophan. *Chemistry & Biodiversity* **8**, 887–894.

Wang, H., Eze, P. M., Höfert, S.-P., Janiak, C., Hartmann, R., Okoye, F. B. C., Esimone, C. O., Orfali, R. S., Dai, H., Liu, Z. and Proksch, P. (2018) Substituted l -tryptophan- l -phenyllactic acid conjugates produced by an endophytic fungus Aspergillus aculeatus using an OSMAC approach. *RSC Advances* **8**, 7863–7872.

Wang, Q.-X., Bao, L., Yang, X.-L., Guo, H., Ren, B., Guo, L.-D., Song, F.-H., Wang, W.-Z., Liu, H.-W. and Zhang, L.-X. (2013) Tricycloalternarenes F-H: three new mixed terpenoids produced by an endolichenic fungus Ulocladium sp. using OSMAC method. *Fitoterapia* **85**, 8–13.

Wang, X., Zhang, X., Liu, L., Xiang, M., Wang, W., Sun, X., Che, Y., Guo, L., Liu, G., Guo, L., Wang, C., Yin, W.-B., Stadler, M., Zhang, X. and Liu, X. (2015) Genomic and transcriptomic analysis of the endophytic fungus Pestalotiopsis fici reveals its lifestyle and high potential for synthesis of natural products. *BMC Genomics* **16**, 28.

Wang, Y., Lu, Z., Sun, K. and Zhu, W. (2011b) Effects of high salt stress on secondary metabolite production in the marine-derived fungus Spicaria elegans. *Marine Drugs* **9**, 535–542.

Wijesekera, K., Mahidol, C., Ruchirawat, S. and Kittakoop, P. (2017) Metabolite diversification by cultivation of the endophytic fungus Dothideomycete sp. in halogen containing media: Cultivation of terrestrial fungus in seawater. *Bioorganic & Medicinal Chemistry* **25**, 2868–2877.

Wilkins, J., and Hill, S. (2006). *Food in the ancient world*; Wilkins, J., and Hill, S. (eds); Hoboken, NJ, USA: John Wiley & Sons, Inc. **2006**, ISBN 9780631235514

Wilson, L., Creswell, K. M. and Chin, D. (1975) The mechanism of action of vinblastine. Binding of acetyl-3Hvinblastine to embryonic chick brain tubulin and tubulin from sea urchin sperm tail outer doublet microtubules. *Biochemistry* **14**, 5586–5592.

Xu, X., Liu, L., Zhang, F., Wang, W., Li, J., Guo, L., Che, Y. and Liu, G. (2014) Identification of the first diphenyl ether gene cluster for pestheic acid biosynthesis in plant endophyte Pestalotiopsis fici. *ChemBioChem* **15**, 284–292.

Yamazaki, Y., Tanaka, K., Nicholson, B., Deyanat-Yazdi, G., Potts, B., Yoshida, T., Oda, A., Kitagawa, T., Orikasa, S., Kiso, Y., Yasui, H., Akamatsu, M., Chinen, T., Usui, T., Shinozaki, Y., Yakushiji, F., Miller, B. R., Neuteboom, S., Palladino, M., Kanoh, K., Lloyd, G. K. and Hayashi, Y. (2012) Synthesis and structure-activity relationship study of antimicrotubule agents phenylahistin derivatives with a didehydropiperazine-2,5-dione structure. *Journal of Medicinal Chemistry* **55**, 1056–1071.

Yocum, R. R., Waxman, D. J., Rasmussen, J. R. and Strominger, J. L. (1979) Mechanism of penicillin action: penicillin and substrate bind covalently to the same active site serine in two bacterial D-alanine carboxypeptidases. *Proceedings of the National Academy of Sciences of the United States of America* **76**, 2730–2734.

Zabala, A. O., Xu, W., Chooi, Y.-H. and Tang, Y. (2012) Characterization of a silent azaphilone gene cluster from Aspergillus niger ATCC 1015 reveals a hydroxylation-mediated pyran-ring formation. *Chemistry & Biology* **19**, 1049–1059.

Zain, M. E., El-Sheikh, H. H., Soliman, H. G. and Khalil, A. M. (2011) Effect of certain chemical compounds on secondary metabolites of Penicillium janthinellum and P. duclauxii. *Journal of Saudi Chemical Society* **15**, 239–246.

Zhang, H. W., Song, Y. C. and Tan, R. X. (2006) Biology and chemistry of endophytes. *Natural Product Reports* **23**, 753–771.

Zhang, M. M., Qiao, Y., Ang, E. L. and Zhao, H. (2017) Using natural products for drug discovery: the impact of the genomics era. *Expert Opinion on Drug Discovery* **12**, 475–487.

Zhang, Q., Wang, S.-Q., Tang, H.-Y., Li, X.-J., Zhang, L., Xiao, J., Gao, Y.-Q., Zhang, A.-L. and Gao, J.-M. (2013) Potential allelopathic indole diketopiperazines produced by the plant endophytic Aspergillus fumigatus using the one strain-many compounds method. *Journal of Agricultural and Food Chemistry* **61**, 11447–11452.

Zhang, X.-Y., Xu, X.-Y., Peng, J., Ma, C.-F., Nong, X.-H., Bao, J., Zhang, G.-Z. and Qi, S.-H. (2014) Antifouling potentials of eight deep-sea-derived fungi from the South China Sea. *Journal of Industrial Microbiology & Biotechnology* **41**, 741–748.

Zhao, Y., Liu, D., Proksch, P., Yu, S. and Lin, W. (2017) Angupyrones A - E, α-Pyrone Analogues with ARE-Activation from a Sponge-Associated Fungus Truncatella angustata. *Chemistry & Biodiversity* **14**, (e1700236) 1-7.

Zhong, N., Chen, H., Zhao, Q., Wang, H., Yu, X., Eaves, A. M., Sheng, W., Miao, J., Cui, F. and Wang, J. (2010) Effects of griseofulvin on apoptosis through caspase-3- and caspase-9-dependent pathways in K562 leukemia cells: An in vitro study. *Current Therapeutic Research* **71**, 384–397.

List of Abbreviations

Abbreviation	
$[\alpha]_D$	specific optical rotation at the sodium d-line
A2780	human ovarian cancer cell line
AHL	N-acyl homoserine lactone
COSY	correlated spectroscopy
CsA	Ciclosporin A
CYP3A4	cytochrome P450 3A4
DCM	dichloromethane
DMSO	dimethyl sulfoxide
ECD	electronic circular dichroism
EtOAc	ethyl acetate
FDA	Food and Drug Administration
Gsfl	flavine dependent halogenase of griseofulvin biosynthesis
HAT	histone-acetyltransferase
HDAC	histone-deacetylase
HMBC	heteronuclear multiple bond correlation
HMG-CoA	3-hydroxy-3-methylglutaryl coenzyme A
HPLC	high performance liquid chromatography
HRESIMS	high resolution electrospray ionisation mass spectrometry
HSQC	heteronuclear single quantum correlation
IC_{50}	half maximal inhibitory concentration
ITS	internal transcribed spacer
L5178Y	mouse lymphoma cell line
LC-MS	liquid chromatography-mass spectrometry
LDL	low density lipopreotein
MeOH	methanol
MTT	3-(4,5-dimethylthiazol-2-yl)-2,5-diphenyltetrazolium
NaBr	sodium bromide
NF-AT	nuclear factor of activated T-cells
NFκB	nuclear factor kappa-light-chain-enhancer of activated B cells
NMR	nuclear magnetic resonance

NOE	nuclear Overhauser effect
NRPS	non-ribosomal peptide synthase
orsA	orsellinic acid synthase gene cluster
OSMAC	One Strain Many Compounds
OTA	ochratoxin A
PA	penicillic acid
PKS	polyketide synthase
PS	Penicillinsäure
PXA	phomoxanthone A
QS	quorum sensing
ROESY	rotating-frame nuclear Overhauser effect correlation spectroscopy
S1P	sphingosine-1-phosphat
SAHA	Suberanilohydroxamic acid
SAM	S-adenosyl-methionin
SAR	structure-activity-relation
SREBP	sterol regulatory element binding protein
SWB	Struktur-Wirkungs-Beziehung
μM	Micromolar (10^{-6}mol/L)

Research contributions

Publications and Manuscripts

(1) Frank, Marian; Niemann, Hendrik; Böhler, Philip; Stork, Björn; Wesselborg, Sebastian; Lin, Wenhan; Proksch, Peter (**2015**): Phomoxanthone A - From Mangrove Forests to Anticancer Therapy. In: *Current Medicinal Chemistry* 22 (30), 3523–3532.

Overall contribution to this publication: 70%, first author, production of phomoxanthone A, synthesis and purification of new derivatives, structure elucidation, interpretation of SAR data and preparation of the manuscript.

(2) Böhler, Philip; Stuhldreier, Fabian; Anand, Ruchika; Kondadi, Arun Kumar; Schlütermann, David; Berleth, Niklas; Deitersen, Jana; Wallot-Hieke, Nora; Wu, Wenxian; **Frank, Marian**; Niemann, Hendrik; Wesbuer, Elisabeth; Barbian, Andreas; Luyten, Tomas; Parys, Jan B.; Weidtkamp-Peters, Stefanie; Borchardt, Andrea; Reichert, Andreas S.; Peña-Blanco, Aida; García-Sáez, Ana J.; Itskanov, Samuel; van der Bliek, Alexander M.; Proksch, Peter; Wesselborg, Sebastian; Stork, Björn (**2018**): The mycotoxin phomoxanthone A disturbs the form and function of the inner mitochondrial membrane. In: *Cell death & disease* 9 (3), 286-302.

Overall contribution to this publication: 10%, tenth author, producer and supplier of phomoxanthone A (PXA), analytical investigation of PXA instability and development of PXA handling protocol.

(3) Frank, Marian; Hartmann, Rudolf; Plenker, Malte; Can Özkaya, Ferhat; Müller,Werner E.G.; Kassack, Matthias U.; Hamacher, Alexandra; Lin, Wenhan; Liu, Zhen; Proksch, Peter Proksch.(**2019**): Brominated Azaphilones from the Sponge-Associated Fungus *Penicillium canescens*. Manuscript ready for submission.

Overall contribution to this manuscript: 70%, first author, laboratory work includes cultivation and extraction, compound isolation and structure elucidation and preparation of the manuscript.

(4) Frank, Marian; Özkaya, Ferhat C.; Müller, Werner E.G.; Hamacher, Alexandra; Kassack, Matthias U.; Lin, Wenhan; Zhen Liu,1, Liu, Zhen; Proksch, Peter. (**2019**) Cryptic Secondary Metabolites from the Sponge-Associated Fungus *Aspergillus ochraceus.* Manuscript submitted to *Marine Drugs* in 12/2018.

Overall contribution to this manuscript: 70%, first author, laboratory work includes cultivation and extraction, compound isolation and structure elucidation and preparation of the manuscript.

Declaration of Academic Honesty

Hiermit erkläre ich ehrenwörtlich, dass ich die vorliegende Dissertation mit dem Titel „Bioactive Secondary Metabolites from Endophytic and Marine Fungi" selbst angefertigt habe. Außer den angegebenen Quellen und Hilfsmitteln wurden keine weiteren verwendet. Diese Dissertation wurde weder in gleicher noch in abgewandelter Form in einem anderen Prüfungsverfahren vorgelegt.

Düsseldorf, den 09.01.2019

Marian Frank

Acknowledgement

First, I want to thank my supervisor Prof. Dr. Dres. h.c. Peter Proksch for offering me the opportunity to join his research group at the "Institut für Pharmazeutische Biologie und Biotechnologie" at the "Heinrich-Heine-Universität Düsseldorf" and earn my doctoral degree. During all this time, he always supported me and made sure that I had numerous opportunities to perform my research, collaborate with other research groups, visit national and internatiol conferences, visit foreign research groups and present and publish my own research work. I am especially grateful for the trust and respect I was treated with and for the good professional and personal relationship that has developed over the years. Further, I want to thank him for his continueous encouragement and his keen sense for good collaborative work, from which many fruitful projects have arisen and new friendships were formed.

> I want to thank Dr. Zhen Liu for helping to improve my manuscripts, rechecking my data, suggesting experiments and always making the time to help me inspite of his very tight schedule.

> I am grateful to my mentor Prof. Dr. Matthias U. Kassack (Institut für Pharmazeutische und Medizische Chemie, HHU Düsseldorf) for co-reviewing my thesis and for our nice collaboration, performing cytotoxicity screenings against human ovarian carcinoma cell line A2780.

> My appreciation goes to Prof. Dr. Werner E.G. Müller (Institut für Physiologische Chemie und Pathobiochemie, Universität Mainz) for performing cytotoxicity screenings against mouse lymphoma cell line L5178Y.

> I want to thank Prof. Dr. Sebastian Wesselborg and Prof. Dr. Björn Stork (Institut für Molekulare Medizin I, HHU Düsseldorf) for years of good collaboration and for performing cytotoxicity assays against Ramos B- and Jurkat-T-lymphocytes.

> I want to express my gratitude to Prof. Dr. Rainer Kalscheuer (Institut für Pharmazeutische Biologie und Biotechnologie, HHU Düsseldorf) for performing anti-tubercular screenings and antimicrobial assays.

> I want to thank Prof. Dr. Tibor Kurtán (Department of Organic Chemistry, University of Debrecen) for performing CD measurements and ECD calculations, helping me with complex stereochemical questions.

➢ My special thanks goes to me colleagues and friends who made my trips to China possible and enjoyable: Haiqian Yu, Yunhua Shi, Dr. Huiqin Chen, Dr. Hao Wang, Imke Form, Nam Tran-Cong, Kim Le, Dr. Yanbo Zeng, Chenyin Wang and Dr. Yang Liu

➢ My appreciation goes to Claudia Eckelskemper and our team of technicians Katja Friedrich, Simone Miljanovic, Simone Mönninghoff-Pützer, Linda Wiegand and Waltraud Schlag for all the support and advice they provided.

➢ For spending a great time with and exchanging scientific ideas I want to thank Dr. Rini Muharini, Dr. Rudi Rudiyansyah, Dr. Amin Mokhlesi, Arta Kuci, Dr. Mohamed Elnaggar, Dr. Ferhat Oezkaya, Feng Pan, Lisa Küppers, Xiaoqin Yu, Harwoko, Ni Putu Ariantari, Dina El-Kashef, Ying Gao, Dr. Shuai Liu, Dr. Lena Hammerschmidt, Sebastian Dumröse, Dr. Daowan Lai and Dr. Sherif Elsayed.

Outside of the institute, I want to thank the following people:

➢ Dr. Alexandra Hamacher, Chenyin Wang, Philip Böhler and Fabian Stuhldreier for performing various MTT-assays and for being terrific collaboration partners.

➢ Malte Plenker for performing the NMR experiments at the FZ Jülich.

➢ Dr. Stefanie Hagenow, Jens Hagenow and David Reiner for having a very nice lunch group and always providing sound advice for chemical synthesis and pharmacological considerations.

➢ My wife Annika Frank for endless love and support, for cheering me up during this stressful time and for prove reading this thesis.

➢ My close family members Volker Frank, Silke Braun, Kira Frank and Cindy Frank for providing non-workrelated emotional support.

➢ My good friends Alexander Cadeddu, Lucas Braun, Tobias Frentzen, Laura Schäkel, Stefan Seufert, Sandra Gedrat, Immo Weber, Marcin Golkowski, Dr. Nils Wentzell, Patrick Lau, Georg Meggiolaro, Karl Meggiolaro, Adam Görtz, Margarethe Görtz, Julia Schakow, Nicola Sellinger, Susanne Bähtz, Michele Bonus, Roland Otte, Christian Müller, Stefan Mädel, Marc Heßling, Norbert Geller, Mike Bruns, Jessica Schuhwerk, Tobias Dolls, Birgit Jordan, Lieter Alvarez, Bastian Wimmer and Tanja Tänzer for spending holidays and leasure time with me and keeping my spirits up.